8th INTERNATIONAL 100% RENEWABLE ENERGY CONFERENCE

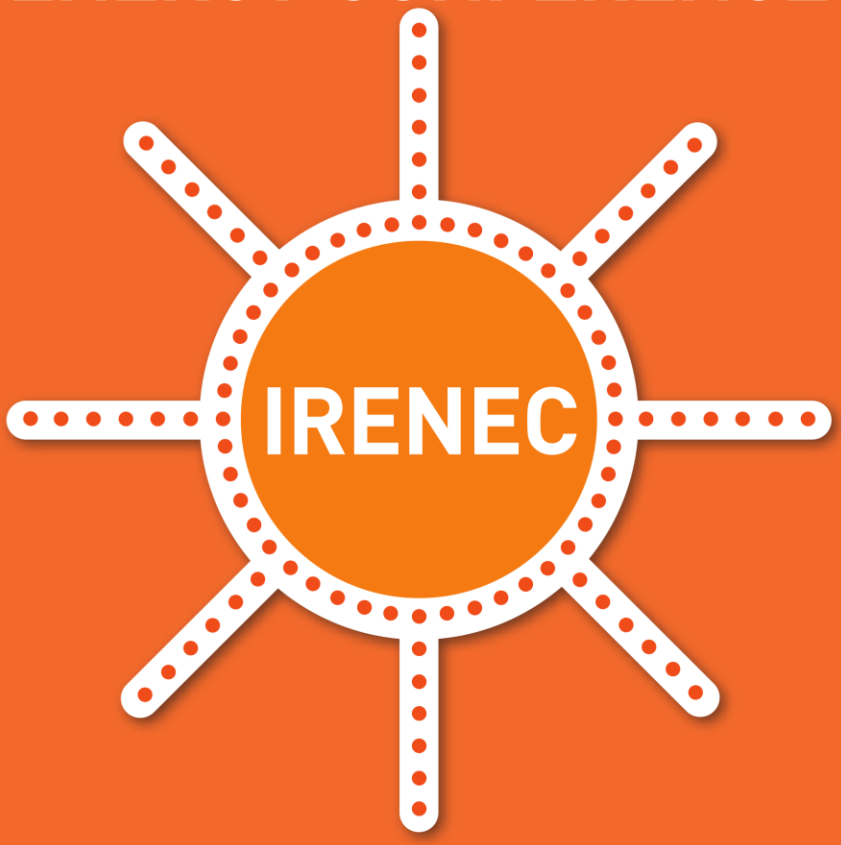

IRENEC 2018

PROCEEDINGS

7-9 MAY 2018

RENEWABLE ENERGY ASSOCIATION

EUROSOLAR Turkey

Editors

Tanay Sıdkı Uyar

Alper Saydam

Publishing Date June 2018

ISBN 978-605-62511-3-9

Tanay Sıdkı Uyar

Conference Chair,
IRENEC2018

Dear Participants,

In our journey of promoting 100% Renewable Energy, we have arrived the 8th stop where we shall again share our research results and other achievements.

Every day we are discovering and practicing the good quality of renewable energies. The genie is out of the bottle. It is time to use the good quality of human beings to guide this opportunity effectively to the destination. The qualities of human beings can play its role if the individuals and countries talk together and define problems correctly and find solutions that can be implemented.

Renewable energy resources at each corner of the atmosphere are ready to be converted to electricity and process heat locally when needed. Kinetic energy of the moving air, chemical energy stored in biomass, heat and light of the sun and geothermal resources are available all over our planet earth free of charge. As the main energy source of living space on earth, sun and its derivatives were available before, are available today and will be available in the future.

Global support provided for the renewable energy made the market penetration of renewables possible. Today wind and solar energy became the cheapest way of producing electricity in many parts of the World.

Cities and countries who are trying to reach 100% renewable energy mix are working on preparing the infrastructure necessary to be able to supply more renewable energy for industry, transportation and buildings by smart grids and renewable energy storage systems.

Since renewable energy is available at every corner of our atmosphere, Community Power (the involvement of the local people individually or through their cooperatives and municipalities in the decision making process and ownership of their energy production facilities) is becoming the most effective approach for transition to 100% renewable energy future.

During IRENEC2018 we shall share and learn from the global experiences on difficulties, barriers, opportunities and solutions for transition to 100 % renewable energy societies and make our contribution to Global Transition to 100% Renewable Energy.

Best Regards,

Tanay Sıdkı Uyar

Conference Chair, IRENEC2018

President, Renewable Energy Association of Turkey

(EUROSOLAR Turkey)

Organization

Organizing Committee

Conference Chair

Tanay Sıdkı Uyar	Marmara University, TR

Conference Co-Chairs

İbrahim Dinçer	University of Ontario Institute of Technology, CA
Friedrich Klinger	Innowind Forschungsgesellschaft mbH, DE
Preben Maegard	Senior Vice President, EUROSOLAR, DK
Remigijus Lapinskas	President of World Bioenergy Association, LT
Wolfgang Palz	EU Commission Official (ret.)

Local Organizing Committee (Administrative)

Erhan Çakar

Başak Gündüz

Ahmet Özer Kaliber

Turgut Okkaya

Serdar Tan

Işıl Uyar

Local Organizing Committee (Academic)

Alper Saydam

Doğancan Beşikci

Uğur Baş

Ahmet Erkoç

Ozan Özmen Eren Şat

Anıl Türkünoğlu

Tanay Sıdkı Uyar

Program Committee (Research Papers)

Caglayan, Dilara Gulcin	Forschungszentrum Juelich GmbH, DE
Pezzola, Lorenzo	Yanmar R&D Europe, IT
Bingöl, Ferhat	Izmir Institute of Technology, TR
Kurt, Gül	Kocaeli University, TR
El-Mohamad, Abdallah	Cyprus International University, LB
Abuşoğlu, Ayşegül	Gaziantep University, TR
Sulukan, Egemen	National Defense University, TR
Beşikçi, Doğancan	Marmara University, TR
Bakırcı, Seçkin	Marmara University, TR
Yılmaz, Mustafa Alper	National Defense University, TR
Köker, Utku	Süleyman Demirel University, TR
Elbaz, Abdurazaq	Karabuk University, LY
Ruwa, Tonderai Linah	Cyprus International University, ZW
Gungor, Sercan Gulce	Fırat University, TR
İçel, Yasin	Adıyaman University, TR
Özgöztaşı, Mehmet Burak	Dr. Lütfi Kırdar Research and Practice Hospital, TR
Seçkin, Candeniz	Marmara University, TR
Çelik. Mustafa Cem	Marmara University, TR
Haydargil, Derya	Gaziantep University, TR

Scientific Advisory Committee

Houri, Ahmad F.	Lebanese American University, LB
Miguel, Antonio Ferreira	University of Evora, PT
Ragnarsson, Árni	Iceland GeoSurvey, IS
Dinçer, İbrahim	University of Ontario, CA
Yıldız, İlhami	Dalhousie University, CA
Abbasoğlu, Serkan	University of Nebraska Lincoln, USA
Tamura, Yukio	Beijing Jiaotong University, CN
Sulukan, Egemen	National Defense University, TR
Sağlam, Mustafa	Marmara University, TR

Contents

Full Research Papers

Full Research Papers

Impact of Wind Year Selection on the Design of Optimized Energy Systems Based on Variable Renewable Energy Sources

Dilara Gulcin Caglayan[1], Heidi Heinrichs[1], Jochen Linssen[1], Martin Robinius[1], Detlef Stolten [1,2]

***Abstract*—** When analyzing highly renewable energy scenarios, a detailed spatial and temporal representation of the electricity generation is essential. For this, representative weather data are required. Most analyses performed in this context use historical data of either one specific reference year or a single-year aggregate of multiple years. This study analyzes the impact of employing 36 different reference years on the design of an exemplary future energy system. This exemplary energy system consists of wind energy for power-to-hydrogen via electrolysis including the hydrogen pipeline transport for most south-western European countries. The applied optimization model determines capacities and operation as well as costs of the technologies to meet the assumed future hydrogen demand. The results reveal that the cost of the system changes by up to 20% between wind years. Furthermore, significant variation in installed capacities per region with respect to the choice of wind years can be observed.

***Keywords*—** Optimization, power-to-hydrogen, variable renewable energy, wind years.

I. Introduction

FOSSIL based energy systems cause high greenhouse gas (GHG) emissions in which carbon dioxide from combustion of fossil fuels has the highest share. Increase in GHG emissions and decrease in fossil fuels have triggered a shift towards renewable energy systems over the last years. For instance, globally between the years 2000 and 2016 installed capacity of renewable energies has increased by by 1256 GW, whereas, increase in wind and solar energy is 745 GW [1]. To compare the impact on GHG emissions of different energy system designs, Veziroglu and Sahin [2] discussed three systems: an existing fossil fuel system, a coal/synthetic fossil fuel system and a solar-hydrogen energy system. The coal/synthetic fossil fuel system is found to be the worst option concerning emissions, whereas the solar-hydrogen system is found to be the best. Although variable renewable energies (VRE) are environmentally-friendly, available across the world and rapidly descending in cost, their intermittency remains the main obstacle to a VRE based energy system. To address this issue, excess power, which occurs when power production is more than demand, produced via VRE during peak power production times can be transformed to a chemical energy carrier. This can be used later in the energy system for either grid balancing or direct use in other processes. Considering its high energy density, low storage cost and being carbon-free, hydrogen is a promising chemical energy carrier. It can be produced by splitting water via electrolyzers, stored in vessels or caverns and finally utilized in fuel cells to produce electricity in the power sector, in fuel cell electric vehicles in the transport sector or in industry as a feedstock and enables the so called “sector coupling” [3]. The process, where hydrogen is produced as a chemical energy carrier at peak power production is called “Power to Hydrogen (P2H)”. Schiebahn et al. [4] discuss multiple uses of hydrogen from P2H within three scenarios in Germany. In their conclusion, it is asserted that utilization of hydrogen in the transportation sector could be a business case owing to the comparative high efficiency of fuel cell vehicles.

In the literature, various studies can be found on the design of energy systems including VRE with different spatial and temporal resolution as well as various reference wind years. Samsatli et al. [5] used weather data of 2014 for the optimal design and operation of a wind-hydrogen-electricity network in Great Britain to supply hydrogen demand for transportation sector by using a spatio-temporal optimization model. Duigou et al. [6] investigated the techno-economic feasibility for large scale hydrogen underground storage in France considering hydrogen for transportation sector in the year 2050. For this analysis, wind production time series data were obtained by using wind profile of 2005. Robinius et al. [7] analyzed linking German power and transport sectors by using a highly detailed spatial and temporal model in which parameters of Weibull distribution is obtained by using measured wind speeds between 1981 and 2000. Welder et al. [8] looked into a wind-based energy system to supply hydrogen demand for the transportation sector and industry by using a spatio-temporal optimization model for Germany. Among the available data collected from weather stations between 2010 and 2013, 2012 was chosen since 205 of 403 weather stations had a complete data set.In the model documentation of EnergyPLAN [9] consideration of different wind years is mentioned for 1996, 2000 and 2001. In their analysis across Europe, Heide et al. [10] considered years between 2000 and 2007 by taking

Dilara Gulcin Caglayan[1] is with Institute of Energy and Climate Research - Electrochemical Process Engineering (IEK-3) Forschungszentrum Juelich GmbH, 52425 Juelich, Germany (phone: +492461615396 ; e-mail: d.caglayan@fz-juelich.de).

Heidi Heinrichs[1], (e-mail: h.heinrichs@fz-juelich.de).

Jochen Linssen[1], (e-mail: j.linssen@fz-juelich.de).

Martin Robinius[1], (e-mail: m.robinius@fz-juelich.de).

Detlef Stolten [1,2], is Chair for Fuel Cells, RWTH Aachen University, c/o Institute of Energy and Climate Research - Electrochemical Process Engineering (IEK-3)Forschungszentrum Juelich GmbH, 52425 Juelich, Germany (e-mail: d.stolten@fz-juelich.de).

monthly average over 96 months for total European wind power generation. Bogdanov et al. [11] used data for 2005 with 0.45° x0.45° spatial resolution for their investigations on the electricity, gas and heat supply options across northeastern Asia. The same dataset and year is included in the study of Gulagi et al. [12] for India and the region of South Asian Association for Regional Cooperation (SAARC) claiming that installed capacities of renewables would not be affected drastically by the choice of wind year. For the analysis of an 100% renewable electricity scenarios in Australia, 2010 is chosen by Elliston et al. [13]. Budischak et al. [14] examine an electricity system with 90-99.9% renewable energy in eastern United States by using 4 wind years between 1999 and 2002. Fripp [15] employs 2004 for an investigation on California with high shares of renewables. From these studies, it is apparent that wind years are chosen due to data available to the investigators. Moreover, it is seen that in some studies, the applied wind year or source of the data are not specified [16]–[22].

Although variation in wind power production is recognized in the context of wind energy and its potential by an EEA report [23] and Banuelos-Ruedas et al. [24], the impact of this variation in energy system design has not been fully discussed. Until now, most studies in this realm focus on one year for wind power production in the context of energy system design without explaining the reason behind choosing that specific year. However, possible changes in the energy system design due to different wind year have not been investigated systematically, which is necessary for a robust design. This study presents an analysis based on 36 weather years ranging between 1980 and 2015 in order to investigate the impact in the final design of an exemplary energy system which utilizes wind energy to produce hydrogen for the transportation sector. In order to observe the influence of wind power production time series data, a spatio-temporal optimization model is employed for a case study including Germany, Netherlands, Belgium, Luxemburg, Switzerland, France and Italy.

II. Methodology

In order to study the effects of the wind year selection on energy system design results, a mixed integer linear program is used in this analysis which minimizes the total annual cost (TAC) of the energy system under consideration.The details about the optimization methodology are thoroughly discussed by Welder et al. [8]. The framework which is used to build the model is called “Framework for Integrated Energy Systems Assessment (FINE)” will be soon published as open source [25]. In order to achieve reasonable model run times, time series aggregation [26], [27] is applied to aggregate the hourly resolution of one year for all demand and VRE generation time series data to 30 representative days each with 24 hourly values. To observe the influence of wind years, the system is optimized when keeping all input parameters constant except onshore and offshore wind energy time series. Total installed capacities of onshore and offshore wind turbines, electrolyzer and storage technologies are compared for each wind year in order to observe the variations in the system to supply hydrogen demand for passenger cars.

Determination of input parameters such as wind production time series data, regional availability of storage technologies, hydrogen demand for passenger cars and connection of the regions for hydrogen transmission are explained in the following paragraphs. Capital expenditure (CAPEX), operational expenditure (OPEX) and economic lifetime of technologies used in the analysis are given Table I.

TABLE I

COST PARAMETERS USED IN THE ANALYSIS

Technology	CAPEX	OPEX (% CAPEX)	Economic Lifetime	Source
Pipeline	2740 €/m	5.0	40	[28]
Salt Cavern	520 €/MWh	2.5	30	[29], [30]
Vessel	8250 €/MWh	2.0	30	[31]
Electrolyzer	500 €/kW	1.5	10	[32]
Onshore WT	1000 €/kW	5.0	20	[33], [34]
Offshore WT	2300 €/kW	5.0	20	[33]

Electricity produced by wind turbines is converted to hydrogen to supply the demand at any time. Yearly hydrogen demand of a country is calculated by multiplying population, car ownership, average annual driving distance of passenger cars (cf. Table II), fuel consumption of fuel cell electric vehicles (FCEV) of 0.0071 kg H_2/km [4] and market penetration of FCEV which is assumed to be 75% [35]. Overall hydrogen demand is distributed spatially by population density which is also used to determine demand center by weighted centroid. Yearly hydrogen demand for each region is projected onto an hourly demand profile of a reference fueling station. Hydrogen pipelines are considered for the connection of the regions, since pipelines are most often the cost-optimal solution to transport hydrogen for large distances and capacities [32]. Fig.1 shows the region of interest with possible pipeline connections as well as regions including salt caverns as a storage technology. The pipeline connection can be built between two adjacent regions. Formulation of pipeline routes is performed by finding the shortest path between two centroids amongst combined existing natural gas pipelines [36] and railways [37]. Corsica and Sardinia are disconnected from other regions in order to observe the effect of wind year selection independent from hydrogen transportation.

TABLE II

PARAMETERS USED IN CALCULATION OF HYDROGEN DEMAND [38]–[40]

Country	Population (Million)	Car Ownership (%)	Annual Driving Distance (km/a)
Belgium	11.21	50.86	12941
France	66.42	51.09	14942
Germany	81.20	54.07	12397
Italy	60.80	64.70	11429
Luxemburg	0.56	71.30	12167
Netherlands	16.90	48.62	12453
Switzerland	8.24	54.86	12882

Regarding storage technology, existing salt caverns that are currently used to store natural gas are assumed to be suitable for hydrogen storage as well [41]. These caverns are employed

here without altering their maximum allowable capacity. However since there is no available salt cavern in Corsica and Sardinia, gaseous hydrogen storage vessels are introduced as storage in the islands. High pressure PEM-electrolysis is used to produce hydrogen with 70% efficiency [4], [42].

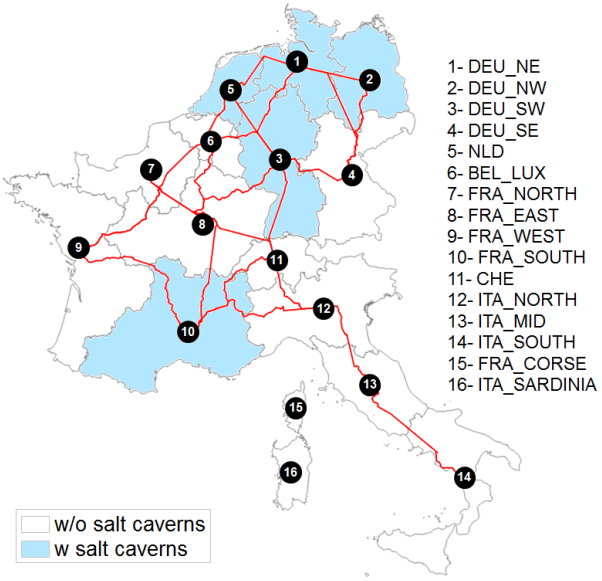

Fig. 1 Region of Interest with Possible Pipeline Connections and Salt Caverns

For wind energy simulations, wind speeds at 50 m are obtained by using the Modern-Era Retrospective analysis for Research and Applications (MERRA) dataset [43]. This dataset has a spatial resolution of 0.65°x0.50° covering the regions of interest and an hourly temporal resolution. It is available for years starting from 1980, which enables the investigation of 36 years. Wind speeds at 50 m are projected to the hub height of wind turbines by using roughness lengths suggested by Silva et al. [44] in response to location specific land cover as defined by the Corine Land Cover (CLC) dataset [45]. Power curves of wind turbines are used to determine power output of the corresponding wind speeds calculated at the hub heights. Convolution of the power curve similar to that employed by Staffel and Green [46] is applied, as well as an additional holistic loss of 5%. This algorithm for wind turbine simulations is employed both for onshore and offshore wind turbines.

Onshore wind energy: A set of typical exclusion criteria with buffer distances applied to the regions by using the GLAES model [47]. Vestas V136-3.45MW [48] at a hub height of 82 m is chosen as the onshore wind turbine model. Assuming a separation distance of 850 m, which is approximately six times the rotor diameter [49], wind turbines are placed across the available area as a result of the exclusion criteria. For each wind year, turbines placed within a region are simulated by using the algorithm described above. For each region, the average time series data of all turbines is calculated and used as onshore wind energy production.

Offshore wind energy: Location, wind turbine model, hub height and overall capacity of offshore wind park projects for Germany, Netherlands, Belgium, France and Italy are obtained [50]. Due to lack of power curves for offshore wind turbines, wind turbine model for offshore wind energy is chosen as Senvion 6.2M152 [51]. If a hub height is specified in the wind park project, that height is used in the simulations. In cases where hub height is not available, 80 m is assumed. Since there is only one location for each wind park, each individual park is simulated by using the wind energy simulation algorithm separately. An average time series is calculated for each region by using the time series data of the wind parks within that region.

III. Results

Fig.2 shows the average full load hours (FLH) of onshore wind turbines in each region with respect to the underlying wind year. FLH are calculated for each region by using corresponding wind years' time series data by simply dividing overall production by the capacity of the wind turbine. In general, it can be seen that the Netherlands has a good potential for electricity production by onshore wind energy amongst the considered regions, whereas Northern Italy has the worst. From year to year, however, it is seen that onshore FLH varies from region to region. For instance, variation in the average FLH in the Netherlands is between 1900 to 2750 hours, whereas it is 950 to 1550 hours for Southeastern Germany. This variation is pronounced especially in the years between 1985 and 1990. Having a deeper look into average FLH of regions in each year, it can be seen that there is not one year in which all the regions have low power production. For instance, wind power production in most of the regions is relatively low in 1996 and 2010; however, Southern Italy and Sardinia (and France in 2010) have higher average FLH compared to their production with other years. In other words, a summarily low or high wind production year cannot be identified for all regions.

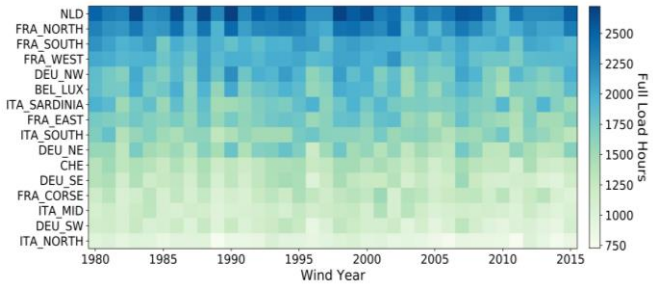

Fig. 2 Average Full Load Hours of Onshore Wind Energy in the Regions Considered

Pipeline connections between regions as a result of the optimization differ with respect to wind years. The number of repetitions of pipeline connections between regions is presented in Fig.3. It is noticed that there are some connections being built once to four times among the 36 wind years; for instance the connection between Southern France and Switzerland, as well as between Western and Southern France. However, it is evident that there are some pipeline connections repeatedly built. Especially pipelines connecting Italian regions are consistently built due to their lower potential for wind power. Because of this, hydrogen demand in Switzerland

and Italy are met by transporting hydrogen from high wind power production regions for all wind years.

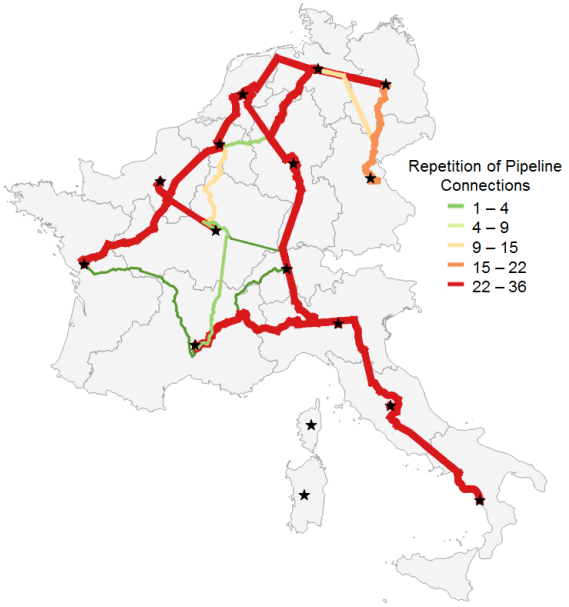

Fig. 3 Repetition of pipeline connection built as a result of optimization of each year

The change in the share of components in Total Annual Cost (TAC) of a result of the optimization with respect to wind years can be seen in Fig.4. A major portion of the TAC comes from wind turbine and electrolyzer costs, while contributions of technologies such as pipeline, salt caverns and vessels are relatively small. The TAC of the system alters between 41 Billion €/a to 50 Billion €/a. The most significant variation in the TAC occurs between 1997 and 1998 with approximately a 20% change. In 1997, it is seen that there is almost no onshore wind turbine installed while, for 1998, a significant portion of the hydrogen demand is supplied by onshore wind energy. The change in the installed capacities of onshore and offshore wind energy is due to the nature of the optimization problem. Considering the objective of TAC minimization, the cheapest generation option to supply demand is always chosen. Therefore, while building a technology in a region, FLH of technologies and their cost play a significant role. In other words, which technology to install within a region is decided by comparing the cost of each technology and its FLH. In relatively cheaper systems, such as for 1980, 1983, 1988 and 1998, installed capacities of onshore and offshore wind turbine ratios are different in each year although the TAC of systems are comparable. Therefore, neither higher onshore or offshore installed capacities cause higher TAC. Significant variation in the TAC is caused by the wind year chosen, since total installed capacity increases with lower power production to supply the demand which is the same for all years. Years in which higher TAC is observed correspond to lower onshore FLH in the context of promising onshore wind energy regions. For instance, wind years such as 1987, 1997 and 2003 are the years in which promising regions like Netherlands, some regions in France and Northern Germany have relatively low average onshore FLH.

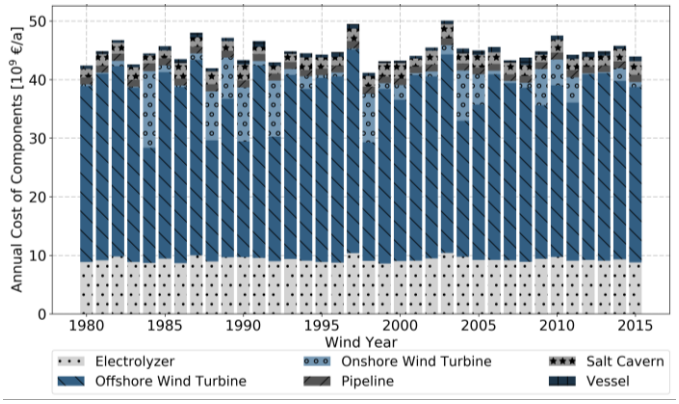

Fig. 4 Change in Total Annual Cost of System with respect to Wind Year

IV. Conclusion

Influence of historical wind years between 1980 and 2015 on an exemplary multi-national wind-based energy system to supply hydrogen demand for passenger cars is investigated. Average full load hours (FLH) of wind power production reveal that there is not a precise year in which all regions have low or high power production. Variation in the average FLH results in different system design parameters such as installed capacities of onshore and offshore wind turbines, and pipeline connections. Although some regions are occasionally connected, perpetual pipeline connections are distinguished. Fluctuation in optimal systems design is evident between years. This is seen in both the TAC as well as in the ratio between installed capacities of onshore and offshore wind. By looking at these variations, it can be concluded that using one wind year to design an energy system is not robust. As a result, it can be said that in order to have robust results capturing the future energy systems behavior multiple years should be considered; although robust pipeline design can be attained.

Acknowledgments

This work was supported by the Helmholtz Association under the Joint Initiative “EnergySystem 2050—A Contribution of the Research Field Energy.”

References

[1] International Renewable Energy Agency, “Capacity and Generation.” [Online]. Available:http://resourceirena.irena.org/gateway/dashboard/. [Accessed: 22-Jan-2018].

[2] T. N. Veziroğlu and S. Şahin, “21st Century’s energy: Hydrogen energy system,” Energy Convers. Manag., vol. 49, no. 7, pp. 1820–1831, Jul. 2008.

[3] M. Robinius et al., “Linking the Power and Transport Sectors—Part 1: The Principle of Sector Coupling,” Energies, vol. 10, no. 7, 2017.

[4] S. Schiebahn, T. Grube, M. Robinius, V. Tietze, B. Kumar, and D. Stolten, “Power to gas: Technological overview, systems analysis and economic assessment for a case study in Germany,” Int. J. Hydrogen Energy, vol. 40, no. 12, pp. 4285–4294, Apr. 2015.

[5] S. Samsatli, I. Staffell, and N. J. Samsatli, “Optimal design and operation of integrated wind-hydrogen-electricity networks for decarbonising the domestic transport sector in Great Britain,” Int. J. Hydrogen Energy, vol. 41, no. 1, pp. 447–475, Jan. 2016.

[6] A. Le Duigou et al., “Hydrogen pathways in France: Results of the HyFrance3 Project,” Energy Policy, vol. 62, pp. 1562–1569, Nov. 2013.

[7] M. Robinius et al., “Linking the Power and Transport Sectors—Part 2:

Modelling a Sector Coupling Scenario for Germany," Energies, vol. 10, no. 7, 2017.
[8] L. Welder, D. S. Ryberg, L. Kotzur, T. Grube, M. Robinius, and D. Stolten, "Spatio-Temporal Optimization of a Future Energy System for Power-to-Hydrogen Applications in Germany," Energy, submitted for publication.
[9] H. Lund, "EnergyPLAN: Advanced Energy Systems Analysis Computer Model Documentation Version 11.4," 2014.
[10] D. Heide, M. Greiner, L. von Bremen, and C. Hoffmann, "Reduced storage and balancing needs in a fully renewable European power system with excess wind and solar power generation," Renew. Energy, vol. 36, no. 9, pp. 2515–2523, Sep. 2011.
[11] D. Bogdanov and C. Breyer, "North-East Asian Super Grid for 100% renewable energy supply: Optimal mix of energy technologies for electricity, gas and heat supply options," Energy Convers. Manag., vol. 112, pp. 176–190, Mar. 2016.
[12] A. Gulagi, D. Bogdanov, and C. Breyer, "The role of storage technologies in energy transition pathways towards achieving a fully sustainable energy system for India," J. Energy Storage, Nov. 2017.
[13] B. Elliston, I. MacGill, and M. Diesendorf, "Least cost 100% renewable electricity scenarios in the Australian National Electricity Market," Energy Policy, vol. 59, pp. 270–282, Aug. 2013.
[14] C. Budischak, D. Sewell, H. Thomson, L. Mach, D. E. Veron, and W. Kempton, "Cost-minimized combinations of wind power, solar power and electrochemical storage, powering the grid up to 99.9% of the time," J. Power Sources, vol. 225, pp. 60–74, Mar. 2013.
[15] M. Fripp, "Switch: A Planning Tool for Power Systems with Large Shares of Intermittent Renewable Energy," Environ. Sci. Technol., vol. 46, no. 11, pp. 6371–6378, Jun. 2012.
[16] S. Ashok, "Optimised model for community-based hybrid energy system," Renew. Energy, vol. 32, no. 7, pp. 1155–1164, Jun. 2007.
[17] J. Jung and M. Villaran, "Optimal planning and design of hybrid renewable energy systems for microgrids," Renew. Sustain. Energy Rev., vol. 75, pp. 180–191, Aug. 2017.
[18] E. M. Nfah, J. M. Ngundam, and R. Tchinda, "Modelling of solar/diesel/battery hybrid power systems for far-north Cameroon," Renew. Energy, vol. 32, no. 5, pp. 832–844, Apr. 2007.
[19] H. Lund and B. V. Mathiesen, "Energy system analysis of 100% renewable energy systems—The case of Denmark in years 2030 and 2050," Energy, vol. 34, no. 5, pp. 524–531, May 2009.
[20] M. Haller, S. Ludig, and N. Bauer, "Decarbonization scenarios for the EU and MENA power system: Considering spatial distribution and short term dynamics of renewable generation," Energy Policy, vol. 47, pp. 282–290, Aug. 2012.
[21] H. Dagdougui, A. Ouammi, and R. Sacile, "Modelling and control of hydrogen and energy flows in a network of green hydrogen refuelling stations powered by mixed renewable energy systems," Int. J. Hydrogen Energy, vol. 37, no. 6, pp. 5360–5371, Mar. 2012.
[22] B. Pfluger and M. Wietschel, "Impact of renewable energies on conventional power generation technologies and infrastructures from a long-term least-cost perspective," 9th International Conference on the European Energy Market, 2012, pp. 1–10.
[23] European Energy Agency, "Europe's Onshore and Offshore Wind Energy Potential: An Assessment of Environmental and Economic Constraints.," 2009.
[24] F. Bañuelos-Ruedas, C. Ángeles Camacho, and S. Rios-Marcuello, "Methodologies Used in the Extrapolation of Wind Speed Data at Different Heights and Its Impact in the Wind Energy Resource Assessment in a Region," in Wind Farm - Technical Regulations, Potential Estimation and Siting Assessment, G. O. Suvire, Ed. InTech, 2011.
[25] Juelich Forschungszentrum IEK-3, "Framework for Integrated Energy Systems Assessment (FINE)," 2018. [Online]. Available: https://github.com/FZJ-IEK3-VSA/FINE
[26] L. Kotzur, P. Markewitz, M. Robinius, and D. Stolten, "Impact of different time series aggregation methods on optimal energy system design," Renew. Energy, vol. 117, pp. 474–487, Mar. 2018.
[27] L. Kotzur, P. Markewitz, M. Robinius, and D. Stolten, "Time series aggregation for energy system design: Modeling seasonal storage," Appl. Energy, vol. 213, pp. 123–135, Mar. 2018.
[28] J. Mischner, Gas2energy.net : systemplanerische Grundlagen der Gasversorgung, 2., Überar. München: DIV, Deutscher Industrieverlag, 2015.
[29] K. Stolzenburg, "Integration von Wind-Wasserstoff-Systemen in das Energiesystem," 2014.
[30] P. Elsner, D. Uwe, and S. Hrsg, "Energiespeicher Technologiesteckbrief zur Analyse „Flexibilitätskonzepte für die Stromversorgung 2050"," 2015.
[31] M. Beccali, S. Brunone, P. Finocchiaro, and J. M. Galletto, "Method for size optimisation of large wind-hydrogen systems with high penetration on power grids," Appl. Energy, vol. 102, pp. 534–544, 2013.
[32] M. Reuß, T. Grube, M. Robinius, P. Preuster, P. Wasserscheid, and D. Stolten, "Seasonal storage and alternative carriers: A flexible hydrogen supply chain model," Appl. Energy, vol. 200, pp. 290–302, Aug. 2017.
[33] C. Lacal Arantegui, Roberto; Jaeger-Waldau, Arnulf; Vellei, Marika; Sigfusson, Bergur; Magagna, Davide; Jakubcionis, Mindaugas; Perez Fortes, Maria Del Mar; Lazarou, Stavros; Giuntoli, Jacopo; Weidner Ronnefeld, Eveline; De Marco, Giancarlo; Spisto, Amanda;, "ETRI 2014 - Energy Technology Reference Indicator projections for 2010-2050," 2014.
[34] European Climate Foundation, "Roadmap 2050. A practical guide to a prosperous, low carbon Europe(volume I)," 2010.
[35] M. Robinius, "Strom- und Gasmarktdesign zur Versorgung des deutschen Straßenverkehrs mit Wasserstoff," RWTH Aachen, 2015.
[36] WorldMap, "Natural Gas Pipelines in Europe, Asia, Africa & Middle East."[Online].Available:https://worldmap.harvard.edu/data/geonode:natural_gas_pipelines_j96. [Accessed: 04-Apr-2017].
[37] N. Earth, "1:10 m Cultural Vectors." [Online]. Available: http://www.naturalearthdata.com/downloads/10m-cultural-vectors/. [Accessed: 04-Apr-2017].
[38] United Nations, "World population prospects: The 2015 Revision," 2015. [Online]. Available: https://esa.un.org/unpd/wpp/. [Accessed: 09-Dec-2016].
[39] European Comission, "EU Transport in figures: Statistical Pocketbook 2015," 2015.
[40] G. Papadimitriou et al., "Transport data collection supporting the quantitative analysis of measures relating to transport and climate change Project acronym: TRACCS," 2013.
[41] Gas Infrastructure Europe, "GIE Storage Map," GIE Storage Map Dataset in Excel-Format, 2016. [Online]. Available: http://www.gie.eu/index.php/maps-data/gse-storage-map. [Accessed: 11-Jun-2017].
[42] S. Baufumé et al., "GIS-based scenario calculations for a nationwide German hydrogen pipeline infrastructure," Int. J. Hydrogen Energy, vol. 38, no. 10, pp. 3813–3829, Apr. 2013.
[43] M. M. Rienecker et al., "MERRA: NASA's Modern-Era Retrospective Analysis for Research and Applications," J. Clim., vol. 24, pp. 3624–3648, 2011.
[44] J. Silva, C. Ribeiro, and R. Guedes, "Rougness Length Classification of Corine Land Cover Classes," 2000. [Online]. Available: http://citeseerx.ist.psu.edu/viewdoc/download;jsessionid=5553BF237EA27088446BF89B39E2CA6E?doi=10.1.1.608.2707&rep=rep1&type=pdf. [Accessed: 14-May-2017].
[45] Copernicus Land Monitoring Service, "Corine Land Cover (Version 18.5.1)," 2012.
[46] I. Staffell and R. Green, "How does wind farm performance decline with age?," Renew. Energy, vol. 66, pp. 775–786, Jun. 2014.
[47] D. S. Ryberg, M. Robinius, and D. Stolten, "Methodological Framework for Determining the Land Eligibility of Renewable Energy Sources," arXiv preprint arXiv:1712.07840, 2017. [Online]. Available: https://arxiv.org/abs/1712.07840.
[48] Vestas, "4 MW Platform." [Online]. Available: https://www.vestas.com/en/products/turbines/v136-_3_45_mw#!at-a-glance. [Accessed: 12-May-2017].
[49] SQWE, "Renewable and Low-carbon Energy Capacity Methodology," 2010.
[50] 4COffshore, "Offshore Wind Farms." [Online]. Available: http://www.4coffshore.com/windfarms/. [Accessed: 10-Dec-2016].
[51] Senvion, "Technical data 6.2M152." [Online]. Available: https://www.senvion.com/global/en/products-services/wind-turbines/6xm/62m152/. [Accessed: 15-May-2017].

Effect of air inlet geometry on raw gas composition and tar content in a fuel flexible small scale downdraft gasifier

Lorenzo Pezzola[1], Valerio Magalotti[1], Roberto Mussi[1], Patuzzi Francesco[2], Marco Baratieri[2], Hiroaki Wakizaka[3]

***Abstract*—** Biomass gasification technology has a key role among renewable sources for micro scale bioenergy production in terms of programmability, carbon neutrality and integration with rural community needs. Yanmar Company, engine and machinery Japanese manufacturer, has developed a novel fuel flexible downdraft gasifier system capable of valorizing multiple biomass sources such as rice husk, woodchips and pellets from agricultural waste. The system has been installed in 2014 in Italy and includes a wet gas purification equipment and two Yanmar CP25VBZ cogeneration units. The system generates 40kW$_e$ and 66kW$_{th}$ and has cumulated an overall amount of more than 2500 operating hours.

Biomass gasification process is the result of complex interactions among several thermochemical reactions and therefore reactor designing must take several variables into consideration. Equivalent ratio is one of the most relevant parameters together with air inlet geometry. The scope of this study is to assess the effect of a secondary air nozzle along the reactor, added to the conventional reactor configuration. The adopted methodology aims to experimentally understand the impact of different air flowrates on the gas quality. The secondary air section is located below the reduction zone and it is calibrated in order to increase the temperature and keep reactions stability into the reactor. The feedstock used consists of woodchips with moisture content equal to 8%w/w.

The raw gas is sampled at the reactor outlet and contaminants content is assessed through a sampling system according to UNI CEN/TS 15439:2008. An online micro gas chromatography system is used to measure the gas composition. A first experimental campaign has been carried out during conventional operation mode and a second one modifying the secondary to primary air flow ratio.
Results are provided in terms of temperature distribution along the reactor, gas composition, tar content, conversion efficiency and mass balance.

Keywords— Biomass gasification, Open core downdraft, Tar cracking, Raw gas analysis, Cogeneration.

I. INTRODUCTION

THE world primary energy consumption is recording nowadays a gradual transition towards renewable sources [1]. Nevertheless, among the yearly global consumption of 168.5 TWh in 2015 [2], oil, gas and coal remain the main energy source powering the world accounting a primary energy share of 85% [2] compared with the 3% share of the renewable energy sources. On the other hand, renewable energy (not considering hydro power) is the fastest growing source of energy with a global rate of 7.1 % per year and is expected to cover 10% of the world energy share by 2035[2]. Focusing on European area, the context changes significantly: the whole EU achieved a 16.4% share of renewable energy following the European energy directive that sets a binding target of 27% of renewable energy share by 2030 as a part of EU's energy climate goals for 2030 [3].

Among renewable energy sources (RES), biomass plays a key role with an energy production share (considering thermal and electrical power) of 64% in the EU-28 in 2015[4] composed by solid biofuels such as wood or charcoal (45%), Biogas and biofuels (15%) and municipal waste (5%)[5]. Thanks to this peculiar framework, woody biomass gasification is considered as one of the most promising technology to produce simultaneously heat and electric power in combination especially with micro-scale (lower than 200 kW$_{el}$) dislocated production. According to the industry guide [6], in 2016 the EU total installed electric capacity of wood gasifiers is around 78 MW$_{el}$ distributed over more than 950 power plants.

Gasification of solid biomass refers to a thermochemical process that converts solid fuel into a combustible producer gas which is mainly composed by CO, H_2, CO_2, CH_4, , N_2 (in case of air as gasification agent) plus some condensable contaminants known as tars[7]. Tars mixture consist in a group of organic compounds that is mostly generated during biomass pyro gasification reaction. In particular, it is largely composed by aromatic hydrocarbons, Naphthalene, Toluene, Phenolic compounds and other heterocyclic compounds.

Despite the positive statistics, gasification technology is still facing some difficulties to break into the market because of lack of reliability mainly connected with tar contamination in producer gas. In fact, it is considered to be one of the main bottlenecks for the industrialization of the gasification technology [8] especially for micro scale application that generate electric power through reciprocating internal

Lorenzo Pezzola[1], Valerio Magalotti[1], Roberto Mussi[1] are with Yanmar R&D Europe s.r.l., Viale Galileo 3/a, 50125 Florence (Italy) (corresponding author's phone: +39 055-5121693 ; e-mail:lorenzo_pezzola@yanmar.com).

Patuzzi Francesco[2], Marco Baratieri[2], are with the Free University of Bolzano, Piazza Università, 1, 39100 Bolzano (Italy).

Hiroaki Wakizaka[3] is with Yanmar Energy Solutions, Umegahara, Maibara, Shiga (Japan).

combustion engines (ICE). Tar condensation can be observed starting from temperatures of 400°C [9] but most of the compounds have a condensation temperature of less than 200-150 °C [10]. For these reasons, ICE technology is particularly sensitive to tar content into the fuel gas because of the gas mixture tendency to condensate under standard operating condition. According to Basu [11], the acceptable upper limit of tar content into the wood gas mixture is estimated to be in the range of 50-100 g/Nm3 for ICE application. The methodology adopted to decrease the tar concentration can be divided into two main groups: primary methods, that reduce the tar production employed into the gasifier reactor, and secondary treatment methods, that aim to reduce the tar content by cleaning techniques after the reactor [10]. Among the first category, many research works have obtained promising results focusing on optimization of operating parameters (such as air input ratio and nozzle geometry) and multi stage reactor approach [12], [13], [14], [15].

This work presents the methodology and the results of an assessment of wood gasification into an open top downdraft gasifier with a nominal power of 200 kW_{th}. The experiment reports the gasification efficiency of the reactor under a double air configuration in comparison with the single air open top operation. The focus or the work is to understand the effect of the new air inlet nozzle into the system in term of controllability, gas quality, tar contamination and carbon conversion efficiency.

V. EXPERIMENTAL PLANT

The biomass gasification system adopted to perform the present study has been installed thanks to a partnership between Yanmar R&D Europe (YRE) and by Yanmar Research Japan (YRJ). The plant has been installed in May 2014 in northern Italy (Milano area) by a factory of the Yanmar group as a demonstration power plant. The feedstock of the plant consists in local wood chips characterized by variable moisture content (WMC) of 35-45 %, ash content of 0.8-1.5% and bulk density of 240-270 kg/m^3. The biomass is firstly fed into a storing-dryer facility that is capable of decrease the biomass water content to a lower value of 14-8%. The dried biofuel is fed into the fixed bed open core downdraft reactor that is capable to produce 126 Nm^3/h of produced gas with a Cold Gas Efficiency (CGE) of approximately 80% (depending on the heating value of the fuel used). The innovative reactor design coupled to a large number of sensors and high automation degree, allows high flexibility and auto-adaptability of the system, furthermore, low temperature profile makes possible to process high ash content biomass like rice husk or agricultural residues [16]. The producer gas flow is filtered through a cyclone and bag filters and then reaches the wet cleaning section composed by gas coolers, water scrubber, and a charcoal filter. The cleaned and cooled gas is supplied to a couple of Yanmar cogeneration units (CP25VB3 natural gas engine) capable of 40 kW_e of electric power and 68 kW_{th} of thermal power at 84°C [17]. The heat is dispatched through the heat network to end local users, for either direct use inside the factory during winter time, or indirect use, via an absorption chiller, to supply 46 Kw_c of cooling power [18]. When neither cooling or heating power is required, the heat is used to dry the biomass into the stratified woodchip dryer that can store up to 20 m^3 of biomass.

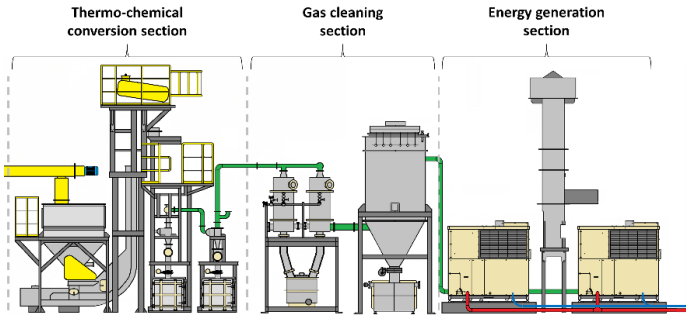

Fig. 1 Experimental plant layout overview (dryer not included)

VI. EXPERIMENTAL PROCEDURE

A schematic of the reactor and the installed instruments are showed in Fig.2. The gasifier reactor is an open top, down draft, fixed bed gasifier, developed and patented by YRJ [19]. The biomass and the gasification agent are fed into the reactor (standard case) from the upper part with a rate of 48 kg/h of wood and 70 Nm^3/h of air. The main chemical reactions taking place along the reactor can be summarized from the top to the bottom with: biomass drying, pyrolysis, combustion and char reduction. The unconverted charcoal is disposed from the bottom of the gasifier with a rate of 4.5 kg/h while 127 Nm^3/h of producer gas are diverted to a cyclone for fine char removal. A secondary air nozzle has been installed in the bottom part of the gasifier, below the reduction zone of the reactor, in the same duct of the biochar extraction. The purpose of the second air nozzle is to enhance the carbon conversion efficiency by increasing reaction temperatures and understand the effect of the dual air stage on the tar content into the producer by means of a partial oxidation on unconverted carbon and temperature increase.

The transmitters located along the reactor consist into three thermocouples located in the upper part of the reactor, in the bottom part and at the gasifier outlet, and two pressure sensors located at the inlet and outlet of the reactor. Temperature sensor help to control the position of the combustion front and to maintain a correct feeding rate. On the other hand, pressure sensors are adopted to avoid the problem of channeling. The phenomena consist into the creation of preferential gas channels during the reduction process mainly along the bottom part of the reactor that allow the producer gas to rapidly cross the reduction zone preserving a high tar content and decreasing the conversion efficiency.

The concept of the dual air reactor wants to take beneficial effect from the effect of a partial oxidation and high T° at the outlet of the reactor [20], [21]. In fact, thanks to higher temperature, some heavy tar molecules can be converted into lighter tars, refractory tars (coke and condensable tar) and

steam [22], minimizing the detrimental effect of tar condensation along the gas line.

The producer gas flowrate is maintained at a constant value by an induced draft fan (IDF) whose power is controlled through an inverter. For this reason, by acting on the second air valve opening rate, it is possible to balance the second air to primary air ratio defined as (1)

$$SAR = \frac{\text{sec}ondary\ air\ \ flowrate}{primary\ air\ \ flowrate} \quad (1)$$

The optimal SAR is obtained experimentally with the target to increase the gasifier outlet temperature and maintaining a chemical stability during the operations. Once the operation parameters have been experimentally set, two different tests have been carried out as follows: the first test is the standard layout gasification (STND) that consisted in 1 hour and 51 minutes of operation when the secondary air valve has been kept completely shut. Under this layout the optimal Equivalent ratio (ER) is equal to 0.271. ER was calculated as explained in (2).

$$ER = \frac{actual\ air\ to\ fuel\ mass\ ratio}{stoichiometric\ air\ to\ fuel\ mass\ ratio} \quad (2)$$

The second test is the dual air (DA) test and consists into 2 hours and 8 minutes of stable gasification condition when the secondary air valve has been calibrated to allow 21 % SAR. Into the second layout the ER is set be 0.287. During both test the producer gas flowrate is maintained at a constant value of 126.6 Nm_3/h by controlling the inverter frequency of the IDF. The hot sampling port is located at the cyclone outlet (Fig.2). The producer gas has been sampled at a maximum temperature of 320 °C during the first test and of 370°C during the second one. The sampling line consisted of a heated filter, housing a quartz thimble kept at 200 °C, and a tar sampling system. The tar collection has been performed following the producer gas through a series of six impinger bottles, according to the technical specification UNI CEN/TS 15439; the first impinger bottle acts as a moisture collector; all the bottles except the last one is filled with isopropanol, an organic solvent suitable for tar capture. Except the first and the fourth, all the bottles are equipped with G0 frits (i.e., sintered glass filters with a nominal pore size in the range 160-250 μm); the first, the second and the fourth bottle are kept at 35/40 °C with water as cooling liquid, while the others are cooled at -15/-20 °C with a mixture of salt/ice/water. The gas suction device consists of a drying tower, a rotameter, a membrane vacuum pump and a dry gas volume meter (measurement range: 0.4-6.0 m^3h^{-1}; accuracy: 0.09% at 1.2 m^3h^{-1}, -0.2% at 0.4 and 6.0 m^3). In each test, at least 0.5 Nm^3 of producer gas has been flown through the system. After the tar sampling system, the producer gas has been analyzed by means of a micro Gas Chromatography (GC) Agilent 490 equipped with a Molsieve 5A column able to detect H_2, O_2, N_2, CH_4 and CO and a PoraPLOT U column able to detect CO_2, C_2's, C_3's and H_2S. The system was previously calibrated for H_2, O_2, N_2, CH_4, CO, CO_2 and ethane by means of a multi points calibration.

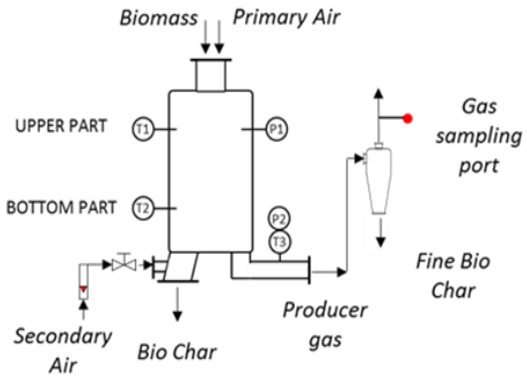

Fig. 2 Process flowchart and installed instruments

VII. Results

Fig.3 reports the average temperature profile variation along the reactor during the second test (DA test). The results are standardized to the reference case of the standard condition recorded during the first test (STND test). During the DA test, the reactor shows an increased exothermic condition compared with the standard case. In fact, the outlet temperature exceeds by a factor of 17% the one recorded in standard condition. The upper part of the gasifier as well increases its temperature by 38 % while on the other hand the lower part of the gasifier, where mainly the char reduction reaction takes place, decreases its temperature by 8%. The profile clearly identifies the fact than during the DA test the main combustion front moves upwards since the primary air flowrate, that is suctioned from the top of the reactor, decreases in favor of the second air inlet flowrate. The lower ER supported by the primary air, decreases the amount of heat released by the primary combustion and, as a consequence, the reduction temperature decreases as well.

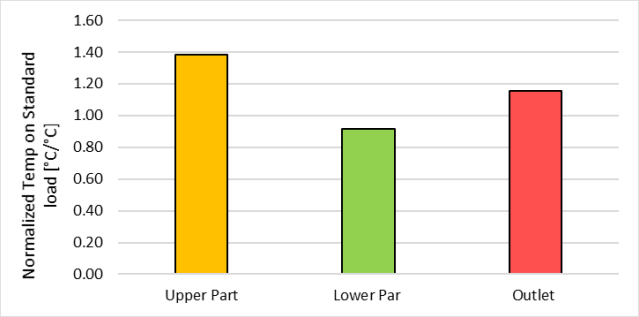

Fig. 3 Normalized temperature variation. STND test is assumed as reference case.

The tradeoff among the lower and outlet reactor temperature is motivate by means of a partial combustion in the proximity of the gasifier outlet that might be positive in terms of tar reaction at higher temperature but can be detrimental for the conversion efficiency of the char bed as well for the catalytic behavior of the bed during the tar cracking.

In order to define the overall air mass flow rate, the key parameter to consider is the N_2 content in the producer gas (Fig.4) with the assumption that the whole N_2 crossing the reactor acts as an inert element and that Nitrogen contribution from the biomass to the gas is null. The woodchip and char mass flowrate is measured through a weight measure across the tests. Results of the mass balance are reported in Table I.

TABLE I
MASS BALANCE COMPARISON

Name	Unit	STND	DA
Wood chip mass flowrate	kg/h	47.9	49.9
Secondary Air Ratio (SAR)	$\%_{mol}$	0	21
Char production	kg/h	4.4	4.9
Char to wood ratio (CWR)	$\%_w$	9.3	9.9
Producer gas flowrate	Nm^3/h	126.6	126.6
Carbon Conversion (CC)	$\%_w$	83.7	82.5
Producer gas flowrate	kg/h	138.5	145.2
Air overall flowrate	Nm^3/h	69.5	76.8

The DA test is characterized by an increase in the fuel consumption by 4% followed by an increase of char production of 11%. The char to wood ratio, defined in (3), rises from 9.3% to 9.9% showing a decrease into the char to gas conversion. As a confirm, the gasifier Carbon Conversion (CC), calculated with (4), drops by a factor of 1.4%. This comparison among CWR and CC describes the fact that the production of char increases in the DA test and, according with the carbon mass balance, its composition is characterized by a higher carbon content. This fact can be mainly related to the effect of a slower carbon reduction along the char bed, due to lower temperatures in the char reduction phase, and to non-uniformity of the air flow path in the bottom part of the reactor that cannot guarantee a sufficient charcoal oxidation.

$$CWR = \frac{char\ production\ rate}{biomass\ \ feeding\ rate} \tag{3}$$

$$CC(\%) = \frac{\dot{m}_{gas}\ (y_{CO_2}\frac{12}{44} + y_{CO}\frac{12}{28} + y_{CH_4}\frac{12}{16})}{\dot{m}_{fuel}\ y_C} \times 100 \tag{4}$$

Where m_{gas} is the producer gas flowrate [kg/h], y_x is the volume percentage of a component in the gas (Fig.4), m_{fuel} is the woodchip flowrate [kg/h] and y_C is the mass percentage of carbon in ultimate analysis of biomass feedstock.

Fig.4 reports the comparison among the gas composition, the low heating value and tar content during the STND test and the DA test. The higher content of N_2 during DA test confirms the fact that, by fixing the outlet producer gas flowrate with inverter controlled IDF, a major amount of oxidation agent crosses the reactor because of the lower pressure drop related with the reactor sub section where the secondary air input nozzle is located.

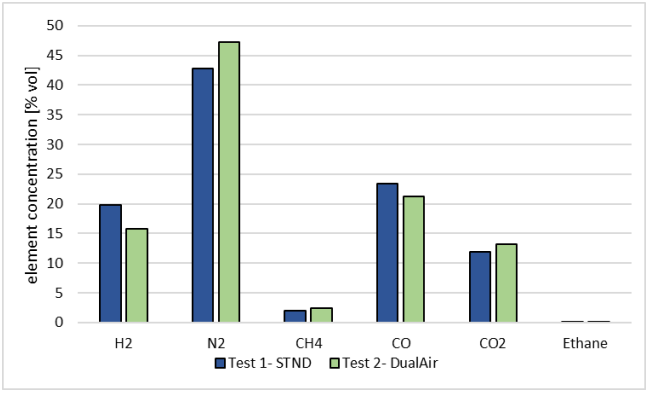

Fig. 4 Gas composition from micro GC

The lower content of CO (-10%) and the higher amount of N_2 (+20%) and CO_2 (+11%) identify the fact that in the outlet section of the gasifier oxidation takes place, as expected by the increased outlet temperature (Fig.3). The exothermic reaction causes the LHV to decrease from 5.87 to 5.33 MJ/Nm^3 by oxidation of the combustible elements such as H_2 and CO (Fig.5a). The uncontrolled combustion of the producer gas derives to the fact that, because of the nozzle geometry into the reactor and the short contact time between air and charcoal, the oxidation of the charcoal is scarce and the residual oxygen oxidizes the producer gas.

$$CGE = \frac{gas\ \ flowrate \cdot LHV_{gas}}{biomass\ \ flowrate \cdot LHV_{biomass}} \tag{5}$$

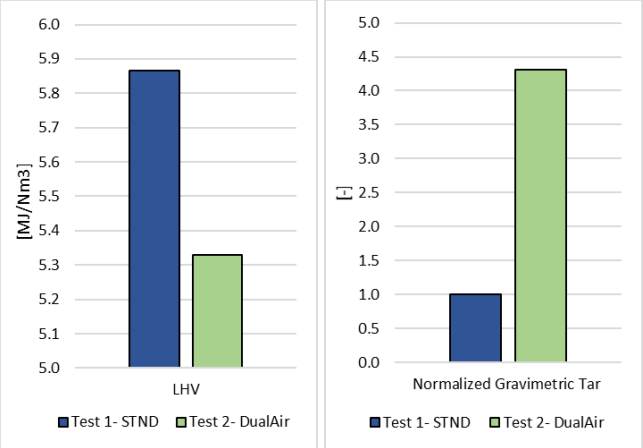

Fig. 5 (a) Prod gas LHV dry basis (b) Normalized gravimetric tar content. Reference case is STND test.

The tar concentration increases (Fig.5b) by a factor of 4.3 from the STND test to the DA test. This result underline the fact that, despite the positive effect that the partial combustion might have on tar concertation in proximity to the reactor outlet, the temperature of lower part of the gasifier (where mainly the char bed reduction reaction is located) plays a greater role in tar conversion efficiency. As a conclusion, the cold gas efficiency (CGE) (5) of the STND operation is 84% while during the DA test it drops to the value of 73.1 %.

VIII. CONCLUSION

A full scale biomass gasification plant with an open core, downdraft reactor has been tested with two alternative air input geometry design. The second test (SA test) differs from the reference standard test (STND), by the addition of a secondary air nozzle in proximity of the char discharge area of the reactor. During the SA test the secondary air flow is optimized in order to maintain reactor stability and to enhance the gasifier outlet temperature. For this reason, in comparison with the STND case, the ER increased by 6%, the gasifier outlet temperature increased by 17% while the temperature recorded at the lower part of the gasifier decreases by 8%. The mass balance shows an increase in woodchip consumption of 4% and a gain of the char to wood ratio of 7%.

The analysis of the producer gas components and the tar contamination shows a reduction of the $LHV_{dry\ basis}$ from 5.87 to 5.33 MJ/Nm^3 and a tar concertation enhancement of 4.3 times. As a conclusion the SA test is characterized by several criticalities: the additional nozzle located below the reduction zone of the charcoal does not allow a sufficient oxidation and brings to uncontrolled combustion of the producer gas. Even if the outlet temperature is sensibly higher in comparison with the standard case, it does not counterbalance the loss of catalytic capability of the char into the reduction zone caused by a temperature decrease into the lower part of reactor. The result is a relevant increase of tar contamination into the producer gas and an increase in unconverted carbon content in the charcoal.

REFERENCES

[1] British Petroleum. 2017. " BP Energy Outlook 2017 edition"
[2] U.S Energy Information Administration. EIA.2017. "International Energy Outlook 2017"
[3] European Commission. Renewable energy, moving towards low carbon economy. Available on: https://ec.europa.eu/energy/en/topics/renewable-energy [accessed: 02/03/2018]
[4] Eurostat. Energy from biomass. Available on: http://ec.europa.eu/eurostat/web/environmental-data-centre-on-natural-resources/natural-resources/energy-resources/energy-from-biomass [accessed: 02/03/2018]
[5] Eurostat. Gross inland consumption of renewable energy, EU-28, 2005 and 2015. Available on: http://ec.europa.eu/eurostat/statistics-explained/index.php/Wood_as_a_source_of_energy
[6] Industry guide 2018. Thermochemical biomass gasification. FEE das Innovationsnetzwerk. Available on: http://fee-ev.de/11_Branchenguide/2018_Industry_Guide_Biomass_Gasification_EN.pdf
[7] T B. Reed ,A. Das; Handbook of Biomass Downdraft Gasifier Engine Systems, SERIISP-271-3022 DE88001135 March 1988 UC Category: 245
[8] Chen Y, Luo Y-H, Wu W-G, Su Y. Experimental investigation on tar formation and destruction in lab-scale two stage reactor. Energy and Fuels 2007;21:3028-35
[9] Bram van der Drift; Tar Dew Point and the great extrapolation show; Presentation held in occasion of IEA-Istanbul- 18 April 2012
[10] R.N. Singh, S.P. Singh and J.B. Balwanshi Devi Ahilaya Vishwavidhlya, Tar Removal from Producer Gas: A review. Research Journal of Engineering science; Vol 3(10),16-22, October (2014).
[11] Prabir Basu; 2010; Biomass gasification and Pyroilysis: practical design and theory; Academic press.
[12] S.C Bhattacharya, A.H.Md. Mizanur Rahman Siddique, Hoang-Luong Pham; A study on wood gasification for low-tar gas production; Energy 24/1999) 285-296.
[13] Kitipong J., Sompop J., Kathrina M., Gratuito B., Wongsuwan H., Homhual S., Experimental study of wood downdraft gasification for an improved producer gas quality through an innovative two-stage air and premixed air/gas supply Approach, Bioresource Technology, 102, 4834–4840 (2011).
[14] Peder brandt, Elfinn Larsen, Ulrik Henriksen; High tar Reduction in a Two-Stage Gasifier,Energy & Fuels 2000, 14, 816-819
[15] S. C. Bhattacharya and Animesh Dutta; Two-stage gasification of wood with preheated air supply:a promising technique for producing gas of low tar content.
[16] R. Mussi, L. Pezzola, A. Bellissima, A.M. Rizzo, H. Wakizaka, D. Chiaramonti; Gasification of grapevines pruning residues into a fuel flexible gasification system: experimental investigation; 2017 European Biomass Conference & Exhibition (EUBCE), Oral presentation.
[17] Toru Nakazono, Yuta Watanabe; A Study of Stoichiometric Bio-Mass Gas Engine 2015-32-0831; JSAE/SAE 2015 Small Engine Technologies Conference & Exhibition.
[18] L. Pezzola, V. Magalotti, R. Mussi, A. Bellissima, M. Colaiemma, M. Benenati, T. Tolda; Beyond combined heat and power: poligenerative small scale renewable plant. MCE 2018 exposition presentation, Milano.
[19] EPO, European Patent Application, EP 2767576 A1.
[20] Peder Brandt, Elfinn Larsen, Ulrik Henriksen. "High Tar Reduction in a Two-Stage Gasifier". Energy & Fuels 2000, 14, p. 816-819.
[21] Ruta Khonde, Ashis S. Chaurasia; Tar cracking of rice husk in biomass gasifier: Reactor design and experimentation, Indian Journal of Chemical Technology 24(1):55-60 · January 2017
[22] Fjellerup, Jan Søren; Ahrenfeldt, Jesper; Henriksen, Ulrik Birk; Gøbel, Benny; Formation, Decomposition and Cracking of Biomass Tars in Gasification; DTU Library 2015

Large Scale Wind Turbine Installation for Offshore Gas Platforms; Is It Feasible?

Ferhat Bingöl[1]

Abstract **-** In early days of wind energy, due to the cost and difficulties of developing offshore wind farms, several ideas were tested by scientist/engineers in aim to utilize known offshore wind resources. One of them was to use numerous USA oil/gas platforms which are no longer in use as an offshore platform to erect single wind turbine; because of the limited space. It was studied and concluded that one turbine was not feasible and could not compete with the market when LCOE is much higher. After nearly two decades, now the new wind turbine technologies for offshore have reached 12MW. In this study, the use of oil/gas platform idea is revisited for wind turbine installation with a combined production and cost. The results show highly possible feasibility for wind turbine installation with medium wind class wind resources. The study puts together an initial feasibility methodology based on state-of-the-art energy yield software and latest cost models combined for such purpose.

Keywords— offshore, wind, platforms, LCOE

I. Introduction

Offshore oil and gas platforms are a standard part of the energy industry where extracting these energy reserves of cost efficient sources. There had been several oil/gas platforms all around the world in last century [1]. Although, there are new platforms are erected every day, the use of abandoned platforms is a question since the beginning. One of many ideas was to erect wind turbines on the platform and use the rest of the life time of the platform for clean energy production. This will lower the carbon footprint of the total operation and make use of the maximum of the platform.

The idea is being discussed since 1993 mostly for California offshore locations and Mexican Gulf installations of USA where the first oil rig was decommissioned in 1996 [2]. Several environmental and economic studies are made to understand if the idea is feasible. The discussion for such possibility was ended negative due to several reasons. Main reason was the production capacity. Platforms are rather small areas and the separation between turbines should be at least 2 rotor diameters not to get effected from each other. In such case, one can only allocate single turbine on the platform which is not sufficient enough to make profit from the investment at the begging of the millennium where turbine capacities were around 2 MW. In 2009 there was an attempt to convert several offshore rigs into wind energy platforms [3] around Scotland which shows the return of the interest on the subject with the new generation wind turbines up to 10MW capacity.

II. Method And theory

Site Description

In Turkey, Turkish Petroleum Cooperation[1] (TPAO) which is a state investment with public shareholders. TPAO is focused on gas and oil investments and has license for offshore exploration and production. The company has erected 5 platforms in last 60 years. The first TPAO platform was built in the North Marmara hence got the same name as a platform[2] in 1993 to extract gas resources from a relatively close shore location around Silivri (Fig. 1). The platform is situated at 45m sea depth and almost 2.5-3km from the shore of Silivri village of the city of Istanbul and the height of the platform is nearly 20m (Fig. 2). The platform has worked until 1999 with success. The platform was being under consideration of decommissioning due to high cost of rigging, but the platform has several years more lifespan in general conditions. Therefore, a final decision is made by the company to build a gas storage platform and the conversion is successfully applied in 1999 with a recent extension in 2015 [4]. Nevertheless, since the platform is still functional it is believed by the author that it can also be used to erect a wind turbine.

Fig. 1 Location of the Marmara Sea and the North Marmara gas platform (red star)

1 Ferhat Bingöl: Department of Energy Systems Engineering / Izmir Institute of Technology
Gulbahce Campus, ME Building Room:128 Urla, 35430, Izmir TURKEY
ferhatbingol@iyte.edu.tr

[1] In Turkish - Türkiye Petrolleri Anonim Ortaklığı http://www.tpao.gov.tr
[2] "Kuzey Marmara" in Turkish and official documentation

Fig. 2 Recent picture of the North Marmara platform [4-Slide 4]

Reference Wind Turbines

In recent years, several institutes and companies are published their conceptional design wind turbine equal or bigger than 5MW capacity. The aim of the studies are to overcome common problems of the wind turbines due to the growing sizes. The design criteria of these turbines are for offshore due to the three positive points listed in the introduction of this article thus reducing the number of challenges to deal with at the same time. Most well-known concept wind turbines are designed by National Renewable Energy Laboratories (NREL) of USA [5], FP7 funded EU project Logistic Efficiencies And Naval architecture for Wind Installations with Novel Developments - LEANWIND (based on Vestas V164) [6] and Technical University of Denmark (DTU) of Denmark [7,8] design capacities of 5MW, 8MW and 10MW respectively. Power and thrust curves of these turbines are publicly available and used in previous studies (Figure 3).

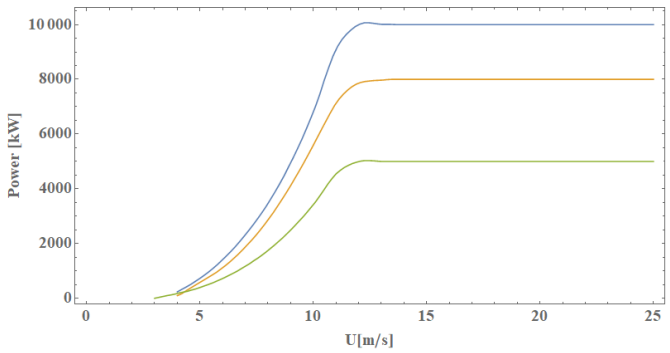

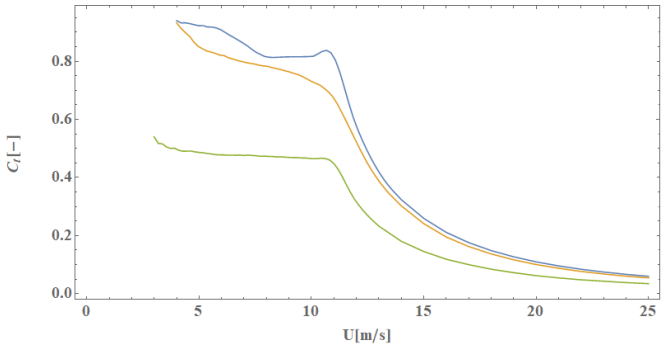

Figure 3 Power (top) and thrust coefficient (bottom) curves of 3 reference turbines [8]

III. Wind Resources

In-situ meteorological mast measurements are needed in any wind farm project development process. A minimum yearly dataset gives a good average of the wind energy density at the location and that can be used to predict annual energy production (AEP) with industry standard applications. It should also be stated at this stage that current international wind farm development standards only suggest in-situ measurement with conventional mast. Therefore, the TPAO was invited to this study to give access to the platform and its structural information but the company did not show any interest of erecting a mast on the platform or participating in the study. When in-situ measurements are ruled out, one other trustworthy option for wind resources, the Global Wind Atlas (GWA) version 2 is finalized in November 2017 is used in the study.

In GWA the whole globe is modelled with 1/12º resolution [9]. The study uses long term re-analysis dataset as input and state-of-the-art down-scaling methodologies to create a global atlas. Therefore, GWA version 2 has been chosen as the yield assessment model input as the wind characteristics in the region. The North Marmara gas platform is located at 41º3'4.34"N and 28º11'6.98"E. Closest three GWA calculation nodes are shown in Fig. 4-LEFT with red circles. Three nodes are used to make an atlas interpolation to the platform (Fig. 4). The interpolation result of the atlas Leading wind direction is between 30º to 60º as it is very common at the region. Power density at 100m also shows an average for Turkey.

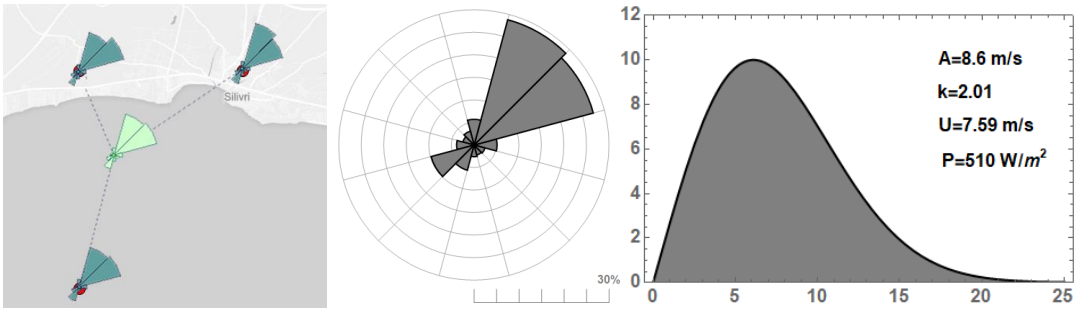

Fig. 4 LEFT: Sectoral frequencies of the closest 3 nodes and
MIDDLE: their interpolation to the platform location at around center of triangle,
RIGHT: Weibull fit for the 100m a.s.l. at the interpolation location.

The atlas data has been downscaled by means of industry standard software WAsP[3] which uses Wind Atlas Methodology [10] and requires elevation and roughness information of the area. Digital elevation model dataset, SRTM version 4.1[4] [11], is used for the elevation information above sea level and coastline (Figure 5). The roughness of the surroundings is characterized by open area, short trees into the land, and patches of forest with trees of approximately 5-12 m height at some coastline locations. There is also a village at the main wind direction 30°. Aerodynamic roughness of the area has been split into 8 different classes and the CORINE Land Cover 2012 dataset[5] polygons have been used to identify the borders of each class; nevertheless the polygons are altered based on aerial imagery findings (Figure 6). The wind atlas is applied to the platform location and three reference turbine AEP are calculated and shown in

[3] WAsP Version 11.6 is used. http://www.WAsP.dk

[4] Available from the CGIAR-CSI SRTM 90m Database (http://srtm.csi.cgiar.org).

[5] The Copernicus programme (https://land.copernicus.eu/pan-european/corine-land-cover/clc-2012/view).

Table 1. The growth of AEP is not linear to the turbine size as expected. The capacity factor (CF) of each turbine reaches up to almost 40%.

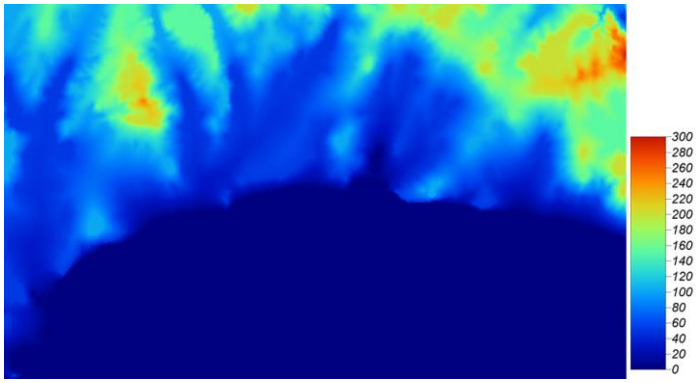

Figure 5 Elevation map of the area. Highest location a.s..l. is 300m.

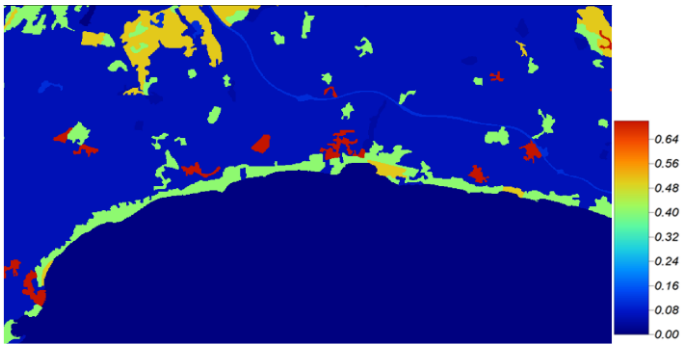

Figure 6 Roughness classes of area. Highest roughness is at a city of 0.7m.

Table 1 AEP for each turbine for the same platform location based on GWA2 information.

Turbine	A[m/s]	k[-]	U[m/s]	P[W/km2]	AEP[MWh]	CF[%]
NREL (5MW)	8.0	2.13	7.07	388	15010	34.3
LW (8MW)	8.4	2.14	7.47	456	26595	38.0
DTU (10MW)	8.6	2.15	7.66	491	34761	39.7

Figure captions and table headings should be sufficient to explain the figure or table without needing to refer to the text. Figures and tables not cited in the text should not be presented. Styles Heading Table and Caption Figure are available in this template for tables and figures.

IV. COST MODEL

After getting the AEP values, it is possible to predict the income of the power plant and the transmission costs. The other cost units are applied from the study of Ebenhoch et. al, from 2015. The study breaks down the cost into operational expenditure (OPEX) and capital expenditure (CAPEX) parts with linear equations as a function of the relative variable of each case (e.g. sea depth, distance to shore, installed capacity). Assumptions and adjustments is listed as follows:

- It has been assumed that the platform does not need extra supporting structure to place any of the reference turbines, so the cost on turbine and installation of it kept as onshore costs in CAPEX but with offshore O&M in OPEX. This assumption is further discussed in Section Results.
- No substation is planned because the platform is 2 km from the shore and the cabling can easily reach to an onshore substation with minimal transportation loss.
- Standard Turkish transmission cost have been applied to the cost model because the suggested European cost was significantly higher than the national prices. The cost per kWh is set yearly by the state which depends on the installed capacity and the energy production which are around €3600/MW and € 0.02/kWh, respectively, for the year 2018.
- Production loses due to the maintenance and electrical array are common in any wind turbine and 10% of total loss is added to the calculation but no any other losses are applied to the final numbers.

V. RESULTS

When the cost model is applied to the three different cases, the 20 years OPEX costs are seen to be around 30%-35% of the CAPEX cost for each turbine but the revenue increases linearly (Figure 7). 8MW seems to be the minimum turbine capacity to make revenue from such a project. Furthermore ROI of each scenario are also calculated and the minimum 8 years is the best case even with the assumption of no extra structural upgrade is needed for the platform. This raise the minimum capacity limit for a feasible project to a 10MW wind turbine (**Error! Reference source not found.**).

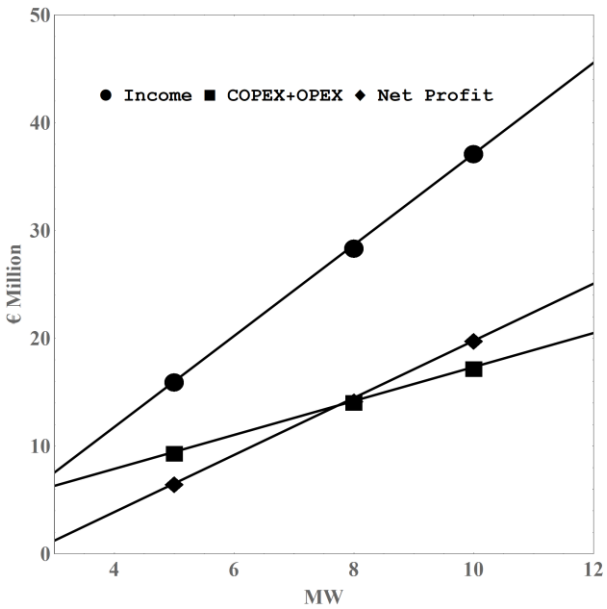

Figure 7 Life time expenditure for different size wind turbines (points) and linearized trends for each parameter.

Table 2 CAPEX and OPEX figures of the three reference turbines with return of investment (ROI) and Levelized Cost of Energy (LCOE) per kWh.

Turbine	**NREL**	**LW**	**DTU**
Size [MW]	5	8	10
CAPEX			
Project Development	€ 1 076 438	€ 1 076 438	€ 1 076 438
Turbine	€ 4 734 366	€ 7 746 636	€ 9 826 336
Cables and Installation	€ 1 170 000	€ 1 872 000	€ 2 340 000
TOTAL	€ 6 980 804	€ 10 695 074	€ 13 242 774
OPEX (20 years)			
Project Management	€ 1 101 072	€ 1 101 072	€ 1 101 072
O&M	€ 266 250	€ 347 520	€ 369 000
Transmission	€ 1 117 089	€ 2 049 363	€ 2 625 429
TOTAL	€ 2 484 411	€ 3 497 955	€ 4 095 501
PRODUCTION (20 years)			
AEP [GWh]	300.2	531.9	695.2
Income	€ 16 075 710	€ 28 483 245	€ 37 229 031
Capacity Factor [%]	34.3	37.9	39.7
Net Profit	€ 6 610 495	€ 14 290 216	€ 19 890 756
ROI	10.3 years	8.6 years	8 years
LCOE [cent/kWh]	2.2	2.69	2.86

VI. Conclusion

Feasibility of offshore gas platform conversion is made with combined calculation method of up-to-date energy yield assessment and inconsequentially adapted cost model. WAsP software with digital elevation and roughness model are used with wind characteristic of the location taken from GWA version 2. The cost model for offshore and onshore installations developed in a previous study is adapted for the unique case of the study and altered for Turkish market where it is necessary.

There are important points to be considered before making any conclusions. First, in this study, there are two important and unknown costs are present; (i) the necessary upgrade cost of the platform (ii) the financial cost due to the commercial loan. It was not possible to take these two important costs to the calculation because there was no information was shared by the owner about the platform and it is not certain what can be the interest rate for such a project where it has been tried in Turkey. On the other hand, current calculation gives the figure for best case scenario and indication of what should be investigated for further improvement.

Acknowledgment

Wind Atlas Data is obtained from the Global Wind Atlas 2.0, a free, web-based application developed, owned and operated by the Technical University of Denmark (DTU) in partnership with the World Bank Group, utilizing data provided by Vortex, with funding provided by the Energy Sector Management Assistance Program (ESMAP). For future information: https://globalwindatlas.infoConclusion

A conclusion section is not required. Although a conclusion may review the main points of the paper, do not replicate the abstract as the conclusion. A conclusion might elaborate on the importance of the work or suggest applications and extensions.

References

[1] Howe RJ (1986) Evolution of offshore drilling and production technology. In: Offshore Technology Conference. DOI:10.4043/5354-MS.

[2] Dokken Q (1993) Flower Gardens Ocean Research-Project - Using Offshore Platforms As Research Stations. Marine Technology Society Journal 27(2): 45–50.

[3] Media (2009) When oil rig met wind turbine. Online. URL https://www.greentechmedia.com/articles/read/when-oil-rig-met-wind-turbine-5692 Last Visited: 1 October 2017

[4] Türkiye Petrolleri, Doğal Gaz Depolama Müdürlüğü (2017), Silivri Doğalgaz Deoplama Tesisleri ve Depolama Tesisleri Kapasite Arttırımı Çalışmaları. Istanbul 22nd World Petroleum Congress URL http://slideplayer.biz.tr/slide/1928545/ Last Visited 1 March 2018

[5] Schwartz M, Heimiller D, Haymes S and Musial W (2010) Assessment of Offshore Wind Energy Resources for the United States. Technical Report NREL/TP-500-45889, National Renewable Energy Laboratory. Prepared under Task No.WE10.1211.

[6] LEANWIND (2017) Logistic Efficiencies and Naval Architecture for Wind Installations with Novel Developments. Technical report, European Union Funded Project.

[7] Bak C, Zahle F, Bitsche R, Kim T, Yde A, Henriksen L, Hansen M, Blasques J, Gaunaa M and Natarajan A (2013) The dtu 10-mw reference wind turbine.

[8] Desmond C, Murphy J, Blonk L and Haans W (2016) Description of an 8 mw reference wind turbine. Journal of Physics: Conference Series 753(9): 092013. URL http://stacks.iop.org/1742-6596/753/i=9/a=092013.

[9] Jake Badger (2017) Global Wind Atlas 2. Online. URL https://globalwindatlas.info/.

[10] Troen I and Lundtang Petersen E (1984) Windatlas for the European Communities. La Loupe, pp. 561–573.

[11] Jarvis A, Reuter H, Nelson A and Guevara E (2008) Hole-filled srtm for the globe version 4, available from the cgiar-csi SRTM 90m database http://srtm.csi.cgiar.org. Technical report.

[12] *Ebenhoch R, Matha D, Marathe S, Muoz PC and Molins C (2015) Comparative levelized cost of energy analysis. Energy Procedia 80(Supplement C): 108 – 122. DOI: https://doi.org/10.1016/j.egypro.2015.11.413. 12th Deep Sea Offshore Wind R&D Conference, EERA DeepWind'2015.*

Grid Code Survey on Frequency Control for Wind Power System

Gül KURT[1]

Abstract— The power ststem frequency is an indicator of balance between power generation and load consumption. Any deviation from planned production or consumption moves the system frequency away from its nominal value. Wind powered generators have limited ability to vary their output. Grid codes requıre that wind farms must be capable of operating continously within frequency variation limits. Also, large penetration rate of wind power into conventional generation can have significiant impacts on stability of grid frequency. Some grid codes require the capability to vary active power output in response to changes in system frequency. According to some of them, wind power plants are required to provide power reserves like conventional generating units do. This paper focuses the review of the requirments set by grid codes and participation of wind power plants in the system frequency control.

Keywords—Wind power, Grid Code, Frequency Regulation

I. INTRODUCTION

Wind energy is becoming a larger portion of the global energy profile. According to European Wind Association (EWEA) that the worldwide generation capacity of electricity by using wind turbine will become 12 % and 20 % in 2020 and 2030, respectively. Several countries such as Denmark (44%), Portugal (24%), Irland (24%), Spain (18,6%), Germany (20%), UK (%13.5) have relatively high percentage of their electrical energy are produced by wind power [1].

Total generated power must be equal to consumed power and electrical losses in the grid. Otherwise, if power generation exceeds load, grid frequency will go up; if load exceeds power generation, grid frequency will fall down. Balance between generation and load have to maintain in order to regulate the grid frequency as soon as possible.

In general, grid frequency regulation application, after a large disturbance, grid frequency is stabilized by two control regimes as shown in Fig.1. These are;

- inertia response and primary frequency control
- secondary frequency control or automatic generation control

Grid regulation rules named as grid codes are used by transmission system operators (TSO) to ensure for maintaining grid stability and performance. One of the grid codes is frequency regulation in utility grid.

Gül Kurt[1] is with Kocaeli University, Electrical Engineering Department, Kocaeli, Turkey (e-mail: gulenderkurt@hotmail.com, gul.kurt@kocaeli.edu.tr).

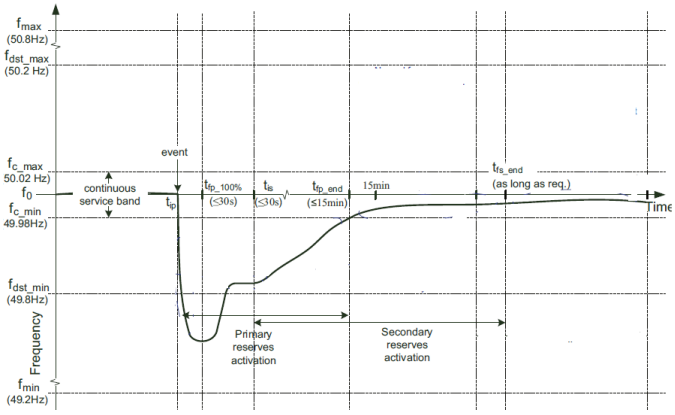

Fig.1 Concepts definition (particular values of time frames and frequencies are according to their commendations of ENTSO-E [2])

TABLE I
PARAMETERS EXTRACTED FROM ENTSO-E'S RECOMMENDATIONS AND SOME EUROPEAN GRID CODES FOR CONVENTIONAL GENERATING UNITS PARTICIPATING IN SYSTEM FREQUENCY CONTROL [2].

Parameter	ENTSO-E	German Grid Code	Spanish Grid Code	Irish Grid Code	UK Grid Code
f_0	50 Hz	50 Hz	50 Hz	50 Hz	50 Hz
f c_min;	49.98;	49.98;	49.98;	49.985;	49.985;
f c_max	50.02 Hz	50.02 Hz	50.02 Hz	50.015 Hz	50.015 Hz
f dst_min;	49.8;	49.8;	49.8;	49.5;	49.5;
f dst_max	50.2 Hz	50.2 Hz	50.2 Hz	50.5 Hz	50.5 Hz
f min;	49.2;	49.2;	49.2;	49.0;	49.2;
f max	50.8 Hz	50.8 Hz	50.8 Hz	51.0 Hz	50.8 Hz
tip;	After a few seconds after detecting a frequency deviation of ±20 mHz	After a few seconds after detecting a frequency deviation of ±20 mHz	After a few seconds after detecting a frequency deviation of ±20 mHz	0 seconds (or with frequency deviation of ±15mHz)	0 seconds (or with frequency deviation of ±15mHz)
tfp_50%;	≤ 15 s	-	≤ 15 s	-	-
tfp_100%;	≤ 30 s	≤ 30 s	≤ 30 s	-	≤ 30 s
tfp_end	≥ 15 min	≥ 15 min	As long as required	≥ 30 s	≥ 30 min
tis;	≤ 30 s	≤ 30 s	-	≤ 5 s	-
tfs_100%;	≤ 15 min	≤ 15 min	≤ 500 s	≤ 15 s	-
tfs_end	As long as required	As long as required	≥ 15 min	10 min	-

Same grid codes for different countries are summarized in Table 1 Thermal or hydraulic power units with conventional synchronous generators have to provide grid frequency regulation service. Unlike conventional generators, wind power generators have not been required to provide grid frequency regulation service.

Integration of wind energy into power systems on such a large scale is not straightforward. Increasing of wind power generation in utility grid has led to regulating new grid codes.

In order to explain behavior of wind turbine after frequency deviation, this paper organized as follows: section II provides inertial response, primary frequency response of wind power generation and gives contribution of wind turbine generator

unite to secondary frequency control; section II reviews grid codes of frequency regulation for different countries which have high wind penetration level.

II. Frequency Regulation

Inertia is the stored rotating energy in the system. The sudden disconnection of generators in the grid will produce rotor swings between generator and grid. Kinetic energy stored on turbine rotor is consumed; generators slow down so that frequency tends drop. Inertia of rotating mass of synchronous machines limits the rate of change of frequency after a large disturbance such as generation loss. Less inertia will give faster change in frequency, rotor angle and instability. High inertia provides great system stability. Conventional synchronous generators contribute directly to the system inertia.

Modern converter based wind turbine generator such as double-fed induction generator with partial-rated converter and permanent magnet synchronous generator with full-rated converter are integrated with the grid through voltage source converter. The grid-side converter can control real and reactive power independently. The speed of a wind turbine is not synchronous with grid and is controlled maximize active decoupled from grid by converter. Thus, the turbine does not contribute to system inertia. Replacing conventional power plants with converter-based wind plants will lead to decrease of physical kinetic energy in the power system. Operation with large amount of wind power and small amount of synchronous generation, frequency would drop so fast that, the system stability endangered [3].

Inertia response is important to maintain grid stability and can be added synthetically as a function of synthetic inertia control function to avoid frequency instability. Synthetic inertia control temporarily provides additional amount of power in response to significant under-frequency events. Initial frequency droop is limited after loss of large generation and system is kept stable until primary frequency control takes over [4], [6],

Primary frequency response is automatic and begins within seconds after the frequency change, rather than minutes. Control is achieved by speed governors within all conventional synchronous generators driven by turbines with valve-controlled gas or gate controlled fluid flow units in hydro power or thermal power system. Governor sense a change in speed and adjust the energy input into the generator's prime mover. Governor will attempt to adjust a generator's MW output in accordance with droop setting. All conventional generating units are participated primary control as speed droop characteristics. The grid frequency deviation will be stabile in a steady state value within acceptable error limits from nominal frequency while the generation or load change is compensated by the prime mover power change.

The primary frequency control by wind turbines can be integrated into the rotor-side active power control loop and demonstrate behavior similar to conventional synchronous generators. The wind turbine must operate in curtailed mode to provide reserve for primary response when frequency drops. Wind turbine generators can reduce their power outputs very effectively, so nonsymmetrical droop characteristics similar to one shown in Fig. 2 can be implemented in wind power plants [4], [5], [3].

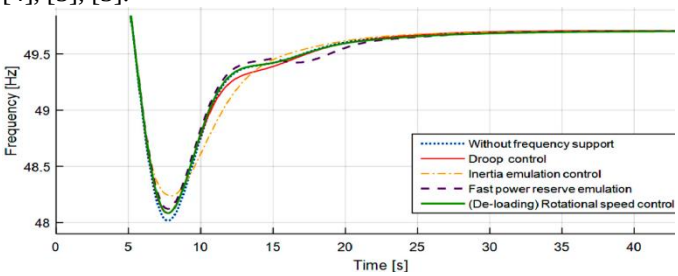

Fig.2 Frequency response for different controllers after disturbance [5]

Secondary frequency control named as automatic generation control (AGC), are activated to restore the rated frequency of the grid. Selected power plants raise or lower power generation in response to command signal from TSO. Also, AGC control can be realized by active power interchanges by tie-line between control areas.

AGC capable wind turbines and plants receive TSO's command signals. Wind power participate secondary control as power level available from wind.

The most popular methods for reference power tracking by wind turbines appear to be pitch angle control and rotor speed control. Pitch angle method preferably applied to above rated wind speed, pitch angle regulation could affect fatigue life of the blades as it affects their dynamic loads. Rotor speed controls method preferably applied to below rated wind speed levels. Danger of excessive mechanical stress in the rotor shaft due to the fast de-loading through the fast torque control for speed regulation. Due to the inertia of the rotor, the power ramping is not linear. These are effective methods for primary and secondary controls of wind turbines [2], [7].

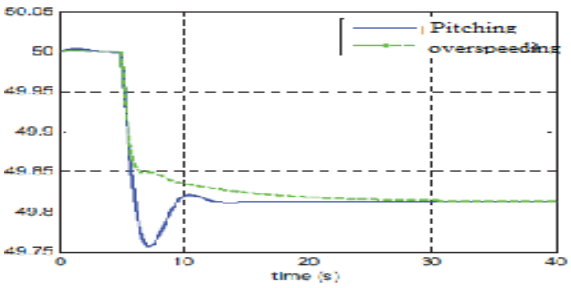

Fig. 3

III. GRID CODES FOR FREQUENCY REGULATION IN WIND POWER GENERATION

Grid Codes of islanded European networks, such as those for the networks of Ireland and the UK, set specific requirements for renewable generating units regarding the provision of primary reserves in both directions of frequency deviations. In contrast, in other continental European networks with a high penetration of renewable based power plants, as in the case of Germany and Spain, current grid codes do not require renewable generating units to provide.

Fig.2 Duration of wind farm must remain connected in different grid codes [6],[10]

primary reserves for their participation in frequency control related tasks. The frequency ranges grid codes for wind power are presented in Fig. 2. In the green frequency required by the various ranges, the wind turbines must remain connected and operate continuously at full power output. In the white ranges, they must remain connected at least for the minimum time specified, usually at a lower power output, in order to support the grid during frequency restoration. In many cases the active power reduction must be controlled proportionally with the frequency deviation from the nominal. In the extreme grey frequency ranges, wind turbines are allowed to disconnect from the grid. The active power requirements at different frequencies, if specified in the grid code, are also shown in Fig. 2

The German Grid Code indicates that renewable generators should, following instruction from the operators, be able to reduce its power output to a signalled value at a ramp rate of at least 10% of the connection capacity per minute without tripping. For frequencies above 50.5 Hz power output should be reduced at a rate of 5% per second. When the frequency deviation decreases, power output must be increased again output per minute.

The Irish Wind Grid Code requires that the WF shall be capable of controlling the ramp rate of its active power output with a maximum MW per minute ramp rate set by the

TSO.There are two maximum ramp rate settings. The first ramp rate setting applies to the MW ramp rate average over one minute whereas the second ramp rate setting is applicable to the MWper minute ramp rate average over ten minutes

Denmark is currently one of the countries in the world that have high wind penetration to the power system. Wind power plants with a power output range of 11 kW to 25 kW have no requirements outside of normal production area, while wind power plants with power output greater than 25 kW must stay connected to the grid for a limited period of time with reduced active power production [10]

England and Wales put no limit on the ramp rate for wind farms capacity below 300MW. For wind farms capacity between 300 and 1000MW, the maximum ramp rate is 50MW per minute. In contrast, wind farms with capacity over 1000MW should be limited with ramp rate of 40MW per minute.

For wind farms in China, the ramp rates for power increase and power reduction are limited depending on the size of the wind farms. Large wind farms with capacity over 150 MW penetration level. have to limit their ramp rates to 100MW every 10 minutes average and 30MW per 1-minute average [5], [8].

In Italy, in the frequency range between 47.5 Hz and 50.3 Hz, the WPP equipped with static converters are generally requested to produce their maximum rated active power.When the frequency value exceeds 50.3 Hz they are requested to linearly reduce the value of the active power production, with a droop constant between 2% and 5% so that a reduction of the entire rated power is obtained within 10 s in MV and 30 s in HV, where the reduction of half the power should be achieved within 15 s [10].

Turkish Grid Code; each wind farm connected to Turkish transmission system must be capable of accepting farms an active power set-point signal from TSO and implementing the necessary changes. If necessary; the output power of wind farms will be controlled in the range of 20-100% of rated powers by TSO. The ramp rate for wind over 100 MW rated power: 4% in a minute; the farms less than 100 MW rated power: 5% in a minute [11], [12].

Spain Grid Code; the wind generators must disconnect if the frequency is below 48Hz during more than 3 seconds or above 51Hz.

IV. Conclusion

As wind energy continues to reach higher penetration levels, the role of wind turbines and wind plants in grid frequency regulation is becoming more important. Wind energy might be viewed as an enabling resource for grid regulation objectives, aiding in wind energy penetrations higher than 20%.

When comparing the frequency operating ranges, the stiffness of the network has to be considered. Small systems, like Irland and UK are more prone to deviate from nominal frequency in case of unbalance between load and generation than large systems, like UCTE in European.

References

[1] https://windeurope.org ; Wind in power 2017 report

[2] F. Díaz González, M. Hau, A. Sumper, and O. Gomis Bellmunt, "Participation of wind power plants in system frequency control: Review of grid code requirements and control methods", *Renewable and Sustainable Energy Reviews.*, vol. 34, pp. 551–564, 2014.

[3] J. Aho, A. Buckspan, J. Laks, P. Fleming, Y. Jeong, F. Dunne, M. Churchfield, L. Pao, K. Johnson, "A Tutorial of Wind Turbine Control for Supporting Grid Frequency through Active Power Control ," *American Control Conference Montreal, Canada June 27-29, 2012*

[4] C. Sourkounis, P. Tourou, "Grid Code Requirements for Wind Power Integration in Europe," Conference Papers in Energy Volume 2013

[5] G.C.Tarnowski,, "Coordinated Frequency Control of Wind Turbines in Power Systems with High Wind Power Penetration," PhD Thesis, Technical University of Denmark, November 2011

[6] R. Leelarujı, M. Bollen, "Synthetic inertia to improve frequency and how often it is needed", Report 2015:224, ISBN 978-91-7673-224-3, Stockholm, September 2015.

[7] Moutis, S. Papathanosious, "Primary load frequency control from pitch controlled wind turbines," Renewable and Sustainable Energy Reviews., 34(2014)551–564, vol. ED-11, pp. 34–39, Jan. 1959.

[8] Z.Yong, D. Zhengang, L. Xuelian, "Comparison of Grid Code Requirements with Wind Turbine in China and Europe," *Power and Energy Engineering Conference (APPEEC)*, Asia-Pacific, 2010

[9] E. Muljadi, V. Gevorgian, M. Singh, S. Santos, "Understanding Inertial and Frequency Response of Wind Power Plants," IEEE Symposium on Power Electronics and Machines in Wind Applications Denver, Colorado July 16-18, 2012.

[10] http://www.marinet2.eu/wp-content/uploads/2017/04/D2.26-Collation-of-European-grid-codes_final_report-1.pdf

[11] S. A. Alsharafi, A. H. Besheer, H. M. Emara, "Primary Frequency Response Enhancement for Future Low Inertia Power Systems Using Hybrid Control Technique," Energies 2018,11,699

[12] http://www.resmigazete.gov.tr/eskiler/2013/01/20130103-10.htm

[13] https://w3.usa.siemens.com/smartgrid/us/en/newsletters/Documents/WindEnergyGenerationRegulationTurkey.pdf

The Thermodynamic analysis of a Solar-Wind Hybrid System in Lebanon- A case study in Deir Ammar El Baddawi

Abdallah El Mohamad[1], Meliz Hastunc[2], and Muhammad Abid[3]

Abstract—Lebanon is a country dependent on mostly fossil fuels. To the author's knowledge there is no installed renewable energy systems connected to the grid. The situated region of Lebanon is in the Middle-East. Due to this reason the country is affected in terms of political issues and electricity shortages. The place of this power plant was chosen due to the presence of enough land space plus its location which is near the power station for distribution.

Therefore, the aim of this study is to present an idea about an alternative solution to minimize this shortage especially taking into consideration that Lebanon has the potential to generate electricity via renewable energy. The analysis was carried out using MATLAB Simulink software. The energy analysis of the system was conducted. The results obtained showed the advantage of using such a system in Lebanon. This study shows that adding more capacity to the grid by connecting a hybrid system will help Lebanon overcome its energy situation

Keywords— Renewable energy, Hybrid power plant, Solar, Wind, MATLAB.

I. INTRODUCTION

Lebanon is a country situated in the middle-east with an area of 10452 Km^2. In terms of population, it has approximately 5,882,562 capita on its land. In addition to this, there is the presence of the refugees (1.5 million Palestinian and 2 million Syrian). The current GDP (Gross Domestic Product) of the country is more than 48 Billion USD (United State Dollar) and there is and estimation of increment of 1.7% by the end of 2018. The location of Lebanon is in the middle of the regional conflicts. All of these and more has enlarged the existing problem of Lebanon which is the lack of energy production. Lebanon, as will be mentioned in detail in the following sections, has a shortage in electricity with an average of 18 hours per day in electricity. The reason for such shortage in electricity is due to many aspects. One of the main problems is the increasing population, mainly refugees, in the country [6]. If certain measures are not taken considering this aspect, the amount of electricity production will slowly decrease with in time. This will also decrease the number of hours of electricity supplied to cities. Another important issue is the lack of equipment in the power stations. The current equipment is old; this majorly affects the efficiency of the systems. Compared to new technologies around the world, the equipment in Lebanon are not so new. Due to the pre-mentioned reasons and many more, this study will observe the advantages of a hybrid PV-wind system in a certain area of the country. This system is proposed as a solution for the lack of electricity production. The energy analysis of the system will be calculated. This study will help propose a solution for Lebanon, for the transition from 100% fossil fuel to switch to renewable energy. The organization of the proposed paper is as follows; Section II explains the current energy situation of Lebanon. The following section, Section III, will present the energy production of the country. Followed by Section IV, which revises production cost and tariffs used in the country. Section V will discuss the renewable energy potential and which renewable energy sources are more abundant in Lebanon. Section VI will express the chosen location and the benefits of this location.

Section VII includes the description of the power plant simulation. Section VIII will show the simulation and discussion of the simulated power plant. Section IX, the energy calculations are carried out for both energy sources. The barriers for implementing this power plant are revised in Section X. Finally, Section XI is the conclusion.

II. BACKGROUND AND CURRENT SITUATION

Lebanon needs between 2000 and 2100 MW energy production in average. This increases during summer, it reaches a peak at around 2450 MW. The total capacity currently available in Lebanon in terms of production and imports is at its maximum, which is 1500 MW (Fig.2). This leaves a huge divergence between the demand and supply of approximately 500 to 600 MW. The demand is more than 15 000 GWh and the total of purchase and production is more than 12 000 GWh. Due to this, the energy supplied will be deficit for nearly 3000 GWh as seen in Fig. 3. The energy supplied that is delivered is split into 3 major sections and distributed to three different areas as follows [4]:

Abdallah El Mohamad[1] Energy systems engineering, PhD student, El-Mina, Tripoli, Lebanon, Zaylaa-bldg (phone:+905428893157; amohamad@ciu.edu.tr).

Meliz Hastunc[2], Energy systems engineering, PhD student, Cyprus International University (e-mail: mhastunc@ciu.edu.tr).

Muhammad Abid[3] asst.Prof, Pakistan, (e-mail: mabid@ciu.edu.tr).

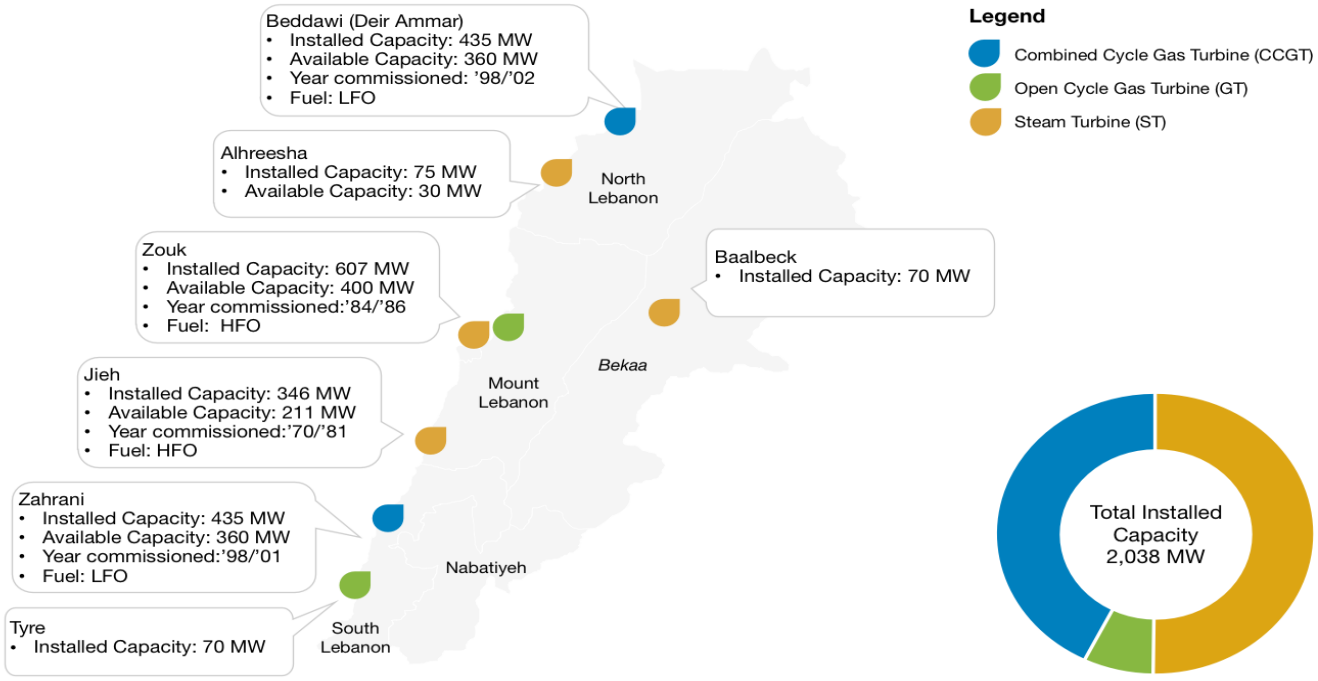

Fig.1. Installed capacity of Lebanon

- 22.11h is supplied to the greater Beirut
- 15.79 h is supplied to Southern Lebanon
- 15.82 h is supplied to Northern Lebanon

So as an average the total supply is approximately 18 h for the whole country. The most available renewable energy sources in the country are mainly, solar energy and wind. This is due to the geographical location of the country. The renewable energy sector in Lebanon is not fully developed. Only 4.5 % of the total production is generated from renewable energy resources and the rest of 95.5% is imported in form of fossil fuels [1]. Fig.1 illustrates the installed capacity of Lebanon.

III. Energy Production

The production of energy in Lebanon can be divided into three major parts:

- Purchase: In the past, Lebanon purchased electric energy from Syria and Egypt with an amount of 589 GWh and 527 GWh respectively.
- Hydraulic power plants: these power plants are available on the main four rivers in Lebanon, which are; Litani, Nahr Ibrahim and Nahr el bared, with a capacity of 274 MW and an actual value of 190 MW.
- Thermal Power Plants: the thermal power plants are composed of HFO-fired (Heavy Fuel Oil) steam turbines (zouk jieh and hraycheh), diesel fired combined cycle gas turbine (baddawi and zahrani) and diesel fired open cycle gas turbine (sour and Baalbek). The amount of production should be 2038 MW but the actual capacity is 1590 MW.

IV. Production Cost And Tariff

A. Costs and tariff

The average cost of electricity that will include the fixed cost of EDL (Electricité du Liban) is 0.1714 USD/kWh which is decomposed of 0.1077 USD/kWh as fuel cost and 0.0637 USD/kWh for the generation, transmission and distribution costs. The fluctuation of fuel cost will vary but as an average the cost of fuel bills are between 1200 M$ and 1500 M$ [9] .

The distribution system has 18,182 transformers and 1,206,499 as low voltage customers. This is in addition to 82 000 customers within concessions. Each of these customers has meters rated between 5 and 20 amps. In terms of monthly consumption, the average is less than 500 kWh. The tariff and charge of electricity varies as follows [9]:

TABLE I
ELECTRICITY TARIFFS FOR LOW VOLTAGE [9]

Electricity Tariffs low voltage	
Consumption(kWh/month)	Tariff(LL/kWh)
<100	35
101-300	55
301-400	80
401-500	120
>500	200
Small to Medium Industy	115
Agriculture	115
Public sector	140

B. Losses and Non-technical losses and collection rates:

There is a presence of 40 % losses, which is more than 300 million USD. This is distributed as 15% technical losses, 20% non-technical losses and 5% uncollected bills. The worth of the uncollected bills is more than 1.3 billion USD, 75% of them are from the private sector and 25% is from the public sector, villages and refugees camps [8].

The non-technical losses are not uniform; it varies between the provinces from 9.6 % to 58% and between regions between 15 % and 78 %. The same thing is for the collection rates, which vary from 83% to 97% in provinces and 62% to 97.5% within the regions [8].

C. Concessions:

The number of subscribers is 82,000 and it is distributed as 56% in Zahle, 28% in Jbeil, 12% in Alieh and 4% in Bhamdoun as EDL provides these spots by reducing prices from 50 to 75 LBP (Lebanese pound)/kWh. In addition to this, the cost of production is 255 LBP/kWh that leads to accumulation losses of approximately 185 million USD in the last eight years compared to the price of energy wheeled from Syria and Egypt [5].

D. Losses due to the national economy:

The estimated cost of the unsupplied energy is estimated by EDF (Electricite de France) and the World Bank in the public expenditure review. It varies between 200 and 2000 USD/MWh. Due to this, there will be an average of 700 USD/MWh that is not supplied including the cost of the private generation. This leads to a total sum of the losses that equals to 2.5 billion USD for the Lebanese economy. This is distributed as 1.3 billion for private generation and 1.2 billion USD for direct customer losses [5].

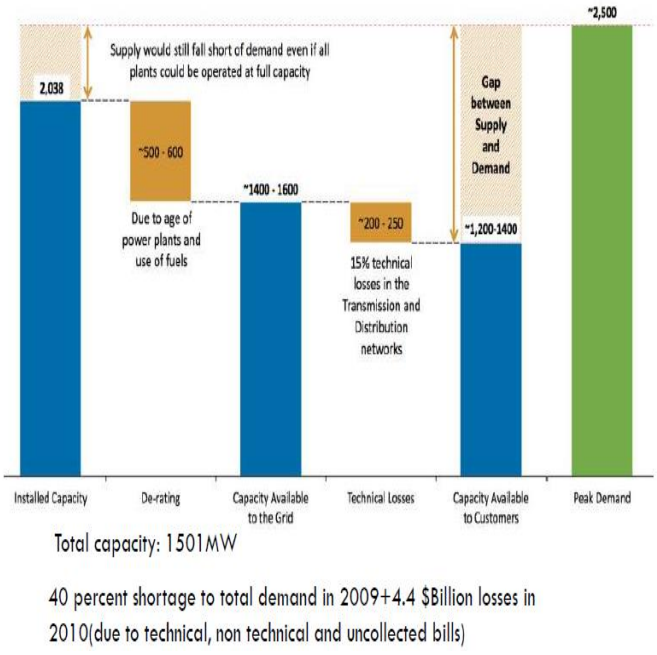

Fig. 2 Installed Capacity vs. Needed Capacity

V. Lebanon Potential of Renewable Energy

The geography as well as the position of Lebanon on the middle-eastern shore of the Mediterranean Sea is useful and it has a potential for renewable energy production. In order to decide whether to integrate renewable energy generation there are certain constraints such as;

- Geographical constraints
- Urban constraints
- Agricultural constraints
- Financial constraints

The total amount of possible generation of renewable energy will be presented as follows:

- Wind and wind farms: 5408 MW which is 12139 GWh
- Distributed PV of 170 MW which is 280 500 GWh
- PV farms 87 600 MW which is 146 130 GWh
- CSP 8056 MW which is 18 275 GWh
- Hydro 368 MW which is 1363 GWh

In addition to this, geothermal generates 109 GWh and Biomass that generates 605.5 GWh. As a total the renewable energy potential is worth more than 460 TWh.

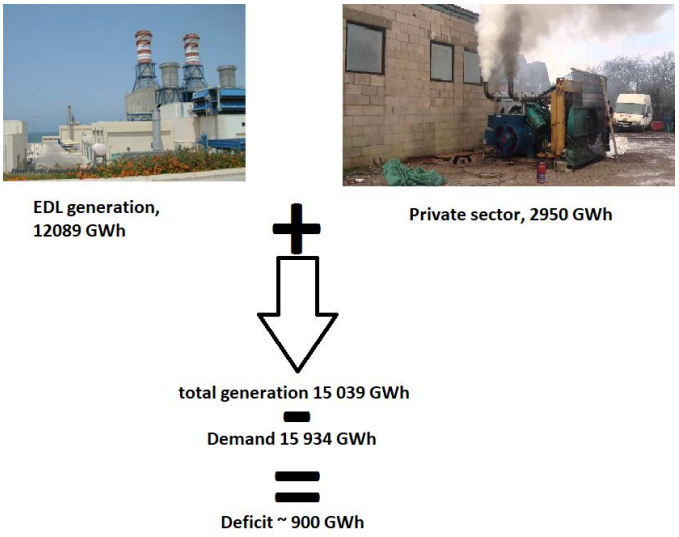

Fig. 3 The Amount of Deficit

VI. Deir Ammar

Deir Ammar is located in the northern part of Lebanon with an area of approximately 4.51 Km^2. Its location is far from Tripoli, about 7.5 km distance. The distance from the capital Beirut is about 84 km.

The location of Deir Ammar is near to one of the biggest power plants available in Lebanon which is a CCGT (Combined Cycle Gas Turbine) generating 435 MW. The surrounding area geographically is available to install the proposed hybrid system. The system is shown in Fig. 3.

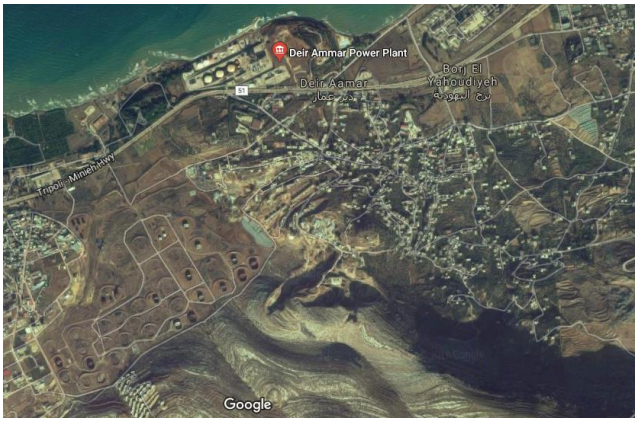

Fig. 4: Deir Ammar Power-Plant (1/500) [3]

The reason behind choosing this area is the availability of a sub-station that will facilitate the transmission of the generated power.

VII. Hybrid System Description

The system is composed of PV farm and Wind Farm, the PV farm is placed in zone A as shown in Fig. 5 with a land size of 0.4 km^2 that is planted with 200,000 panels with a capacity of 250 W each. The total capacity of the PV farm is 50 MW.

The wind farm is composed of 14 wind turbines distributed along the valley of Terbol, in zone B, as shown in Fig. 6. It has a distance of 6.5 km and the difference between two turbines is 500m [2]. This value is according to the rule of spacing for turbines, which requires a minimum distance which equals to 2 rotor diameters between the turbines.

The turbine used in the system is a 6.15 MW and has a diameter of 126 m. The total capacity of the wind farm is 84 MW in total.

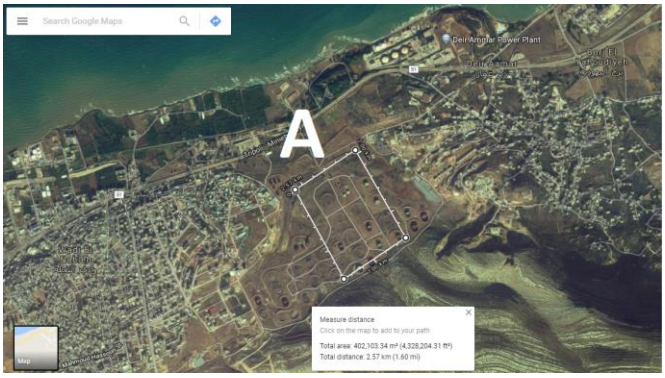

Fig. 5: Zone A [3]

Fig. 6: Zone B [3]

VIII. Simulation

In the simulation a residential load of 150 MW with a PV farm and wind farm that would simulate the power generated for 24 hours was assumed.

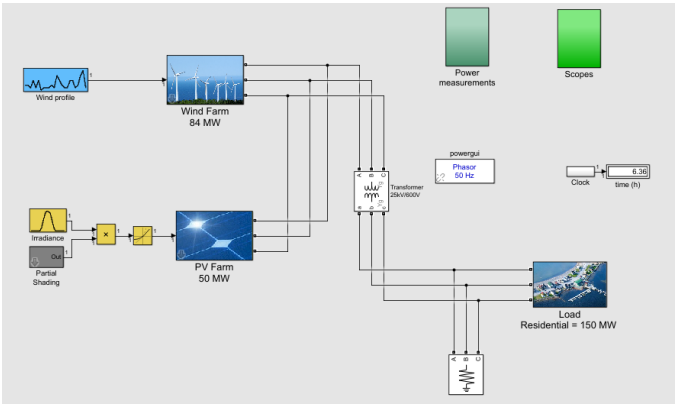

Fig. 7: Hybrid Power Plant simulation [3]

The data for Wind speed and for solar irradiation was taken from the data supplied by NASA using Ret-screen.

As mentioned before the total usable amount of generation in Lebanon is 1501 MW, and the total consumption of Lebanon is 2500 MW at its peak.

The total deficit is nearly 1000 MW; reducing this value by adding a renewable power plant that will supply 134 MW will definitely reduce the cut-off duration. Planning a similar or same power plant in Lebanon will definitely allow Lebanon to pass its electricity crisis and it will be one great step to transact to 100% Renewable.

IX. Energy Calculations

To calculate the annual energy output of a PV system the global formula (1) was used to obtain the electricity generated.

$$E = A * r * H * PR \quad (1)$$

Where E is the energy (kWh), A is the total solar panel area (m^2), H is the annual average of solar radiation on tilted panels, and PR is the performance ratio or the coefficient for losses.

In the proposed project, the total solar panel area is 324000 m^2, the solar panel yield is 15.37% and the annual average irradiation on tilted panels is 2007.5 kWh/m^2.yr; so the results of the calculation can be seen in (2) and (3):

$$E=324000*15*2007.5*0.75 \quad (2)$$

$$E=74.932769 \text{ GWh/yr} \quad (3)$$

To calculate the power of a wind turbine the formula (4) is used as:

$$P=k*C_p*1/2*\rho*A*V^3 \quad (4)$$

Where P is the output power, Cp is the maximum power coefficient, ρ is the air density (1.1 kg/m^3 in Lebanon), A is the rotor swept area, V is the wind speed and k is a constant to yield power in kilowatts. The results can be seen below in (5) and (6);

$$P=1.33*0.4*0.5*1.1*(3.14*126/4)*16.7^3 \quad (5)$$

$$P=6.134 \text{ MW} \quad (6)$$

X. Barriers for Implementing

There are a lot of barriers facing the development of renewable energy in Lebanon. The absence of a clear contracting procedure (PPA) as well as the absence of a clear taxation policy. The policies used by the government of Lebanon never offers an open market neither a licensing schemes for installers or investors. According to the law 426, the right is only given for EDL to control, generate and distribute electricity in Lebanon [10]. EDL is also suffering from aging staff and administration. This forms a severe financial deficit.

The absence of the licenses under the law 288 is also a barrier in front of the development of renewable energy sector in Lebanon [10]. Any proposal that comes from any investor needs to be confirmed from 2 ministries (ministry of energy and water and ministry of finance). Finally and most importantly, the absence of a clear grid code for renewable energy is a very important concern.

XI. Conclusion

The Lebanese electricity crisis could be solved by implementing renewable energy power plants in a way that Lebanon can become a self-dependent country by generating electricity using 100% renewable sources. Similar power plants could be implemented in Zahrani as well as Zouk and Jiyeh where old fossil fuel power plants exist. A transaction like this will help Lebanon decrease emissions extracted to the environment and most importantly solve the lack of electricity in the country.

References

[1] Ahmad Hourin, Samira Ibrahim-Korfali," Residential energy consumption patterns: the case of Lebanon", Natural Science Division, Lebanese American University, Beirut 1102 2801, Lebanon, 14 March 2005

[2] Draft PPS 18: Renewable Energy Annex 1 Wind Energy: Spacing of Turbines planning portal (UK)

[3] Google maps (2018), Deir Ammar, www. Googlemaps.com

[4] Hadi Ayoub, Mohammad & Assi, Ibrahim & Mohammad Hammoud, Abdallah & Assi, Ali. (2013). Renewable energy in Lebanon Status, problems and solutions. 1-4. 10.1109/ICM.2013.6734950.

[5] Jouni, A., Najjar, R., & Mourtada, A. (2016). Evaluation of national energy action plan: The case of the Lebanese NEEAP (2011–2015). 2016 3rd International Conference on Renewable Energies for Developing Countries (REDEC). doi:10.1109/redec.2016.7577564

[6] Marc Ziade, " Technical Challenges to 24/7 electricity in Lebanon" , Sept 2012

[7] Ministry of Energy and Water. (2012). The National Energy Efficiency Action Plan for the Republic of Lebanon-NEEAP 2011-2015. Beirut, Lebanon: Ministry of Energy and Water and Lebanese Center for Energy Conservation.

[8] Ministry of Energy and Water. (2016). The Second National Energy Efficiency Action Plan for the Republic of Lebanon-NEEAP 2016-2020. Beirut, Lebanon: Ministry of Energy and Water and Lebanese Center for Energy Conservation.

[9] Policy paper for the Electricity Sector, Gebran bassil ,ministry of energy and water, 2014

[10] Renewable Energy Policy Network for the 21st Century. (2015). Renewables 2015 Global status Report.

[11] The National Renewable Energy ActionPlan for the Republic of Lebanon 2016-2020. LCEC November 2016.

A Portrait of Municipal Wastewater Treatment Systems in Turkey as Self-sustaining Renewable Energy Producers

Ayşegül Abuşoğlu[1]

***Abstract*—**This study aimed to review detailed potential analysis of sustainable energy generation using the municipal wastewater and sewage sludge present in the current municipal wastewater treatment systems in Turkey. The study considered three interconnected systems in energy recovery from municipal sewage sludge: (1) anaerobic digestion of sewage sludge for biogas production; (2) use of the produced biogas in a gas engine powered cogeneration system for combined heat and power generation; (3) disposal of sewage sludge cake by drying and burning in a fluidized bed incineration plant, using the actual sewage sludge treatment operation data of an active municipal wastewater treatment plant in Gaziantep. This plant treats nearly 200,000 m^3 of domestic wastewater per day and generates 10,000-18,000 m^3 biogas daily. Total electricity generated by the biogas fuelled gas engine is 1,000 kWh, which is used for the wastewater treatment on site.

***Keywords*—**Wastewater treatment, sewage sludge, biogas, combined heat and power generation.

I. INTRODUCTION

THE topic of energy was and is both individual, social and cultural in the past and in the present. Today *sustainability* is the ultimate goal for all countries and almost everyone agrees on this, however still the concept is defined with certain flexibilities that can vary among countries. In the most objective perspective *sustainability* will depend on our ability to increase our current energy sources and create a portfolio that can cope with many challenges from transportation demand to national security. Understanding the idea of sustainability in a doctrinal manner, such as prohibiting fossil fuels or large-scale energy systems prevents developing a realistic perspective on opportunities that can be provided by renewable and clean energy sources suggested by this idea. World population is increasing rapidly and cities are growing to huge sizes. According to United Nations data [1] it is estimated that by 2050, 66% of world population will be living in cities, this ratio is 54% today. This being the case, it becomes difficult to imagine that the energy of mega

metropolitan cities can be supplied merely with solar and wind power. The ultimate lesson history teaches us is that relying on a single fuel or technology and regarding it as the promised savior would be a mistake.

Wastewaters are classified as industrial and domestic according to their pollution types. Industrial wastewaters are waters produced by the industry and containing high concentrations of metals and chemicals, with a capacity to inflict devastating damage on the environment. On the other hand, domestic wastewaters are waters of human origin, containing approximately 99% water with the rest consisting of organic and inorganic substances and which are - although not to the extent of industrial wastewaters - harmful for the environment [2]. Wastewater treatment methods consist of primary treatment methods - also called basic operations - and secondary treatment methods, named as biological operations. As a result of physical and chemical treatment methods, wastewater achieves a structure which has no inconvenience for discharge into natural receiving environments such as rivers and lakes. In the biological treatment part, after physical and chemical methods, the collected wastewater sludge is improved using aerobic and anaerobic methods and used in the generation of renewable fuel such as biofilm or biogas. After the biological treatment process the wastewater sludge is disposed using various methods. However, the disposal process of the sludge is not as easy as told and is one of the most complex environmental problems encountered by engineers, researchers and managers working on the wastewater treatment. The main reason for this is that usually, depending on the type of operation implemented, the sludge obtained from wastewater treatment operations is usually a very dilute suspension containing low rates of solid substances [3].

Wastewater treatment systems consume high amounts of electricity due to the steps and complexity of the treatment process. In spite of this, there are advantages such as the fact that the biogas acquired during the anaerobic sludge digestion process can be used in power generation via combined heat and power generation coupled with the treatment facility, and the fact that the sludge cake to be disposed after the digestion process is first dried by combustion in fluidized bed combustion facilities and then burned for second possible energy generation. The wastewater sludge can thus not only be

Ayşegül Abuşoğlu[1] is with the Department of Mechanical Engineering, Gaziantep University, 27310, Gaziantep, Turkey (e-mail: ayabusoglu@gantep.edu.tr).

fully disposed, but the electricity generation within the wastewater treatment system can also be achieved from a by-product of the system itself, in other words, from sludge. Therefore, we can describe wastewater treatment systems as "self-sustaining" systems due to their operations to dispose of environmental pollutants and their ability to solve these operations by obtaining power from the by-products of the treatment process.

There are many studies in the open literature, most of which make future projections about the renewable energy potential of Turkey based on the country's statistical wastewater treatment data. The current values of the data used in these studies can easily be accessed from the relevant official websites of the state [4, 5]. However, still it would be suitable to take a look at the important studies conducted during the last two years regarding the energy potential of wastewater treatment facilities. In his study reviewing Turkey's biomass energy potential, Toklu [6] specified the usable biomass energy potential of the country as 17 Mtoe and this value roughly corresponds to 73 MWh of power generation potential. According to their study examining and comparing the biomass and bioenergy based development potentials of Turkey and Malaysia, Ozturk et al. [7] predicted that Turkey's total biomass potential would be 52.5 Mtoe by 2030. Eksi and Karaosmanoglu [8] stated that as of 2016 there were five active and licensed biogas engine powered cogeneration facilities operating within wastewater treatment facilities in Turkey and that they operated with a total 7,600 kWh operation capacity.

This study examines the energy generation potential using the actual operational data of the municipal wastewater treatment facility located in the Gaziantep region. For this purpose, first the energy consumptions of the sub-systems within the facility were calculated. As an example of a "self-sustaining" wastewater treatment facility, the mentioned facility is separated into three sections starting with the *anaerobic sludge digestion system* which is the biogas production stage, then the *biogas engine powered cogeneration system* and the *fluidized bed sludge combustion system*, developed for disposing sludge. Each section has been examined in detail in the context of energy consumption and generation potentials in the light of current operating data.

II. ENERGY CONSUMPTION OF WASTEWATER TREATMENT OPERATIONS

In the Gaziantep central municipal wastewater treatment facility, daily 200,000 m^3 domestic wastewater equivalent to 1,000,000 population is discharged into a local stream after primary and secondary treatment systems where physical and chemical treatment operations are performed in the treatment facility. The sludge collected after the treatment operations is first subject to flotation and thickening operations, then stored in anaerobic tanks for biogas generation via anaerobic bacteria, then the sludge cake taken from the anaerobic digestion tanks are subject to dewatering operation and the dryness is increased to 27% and the disposal operation is initiated. Table 1 shows the energy consumption amounts calculated based on the operating data of the Gaziantep municipal wastewater treatment facility.

TABLE 1
ELECTRICITY CONSUMPTIONS OF THE SUB-SYSTEMS OF THE GAZIANTEP WASTEWATER TREATMENT FACILITY

Sub-system	Electricity consumption (kW)
Primary Treatment	191.83
Secondary Treatment	1394.34
Flotation and Thickening System	350.78
Anaerobic Digestion Process	31.78
Sludge Dewatering System	160.0
Overall Treatment System	2083.73

III. RENEWABLE ENERGY PRODUCTION IN A "SELF-SUSTAINING" WASTEWATER TREATMENT FACILITY

Anaerobic Sludge Digestion System

The sludge digestion operation in wastewater treatment systems is performed in high-efficiency anaerobic sludge digestion reactors. The reactors consist of hermetically sealed closed tanks. The sludge in the rector is mechanically mixed constantly to ensure that the organic structure and the microorganisms mix thoroughly and the sludge is heated by constant cycles through heat exchangers to increase the metabolic rates of the microorganisms and thus speed-up the digestion process. Average sludge temperature in the reactors is approximately 35°C and sludge with 35–55 g/liter density is loaded with a daily flow of 800–1,200 tons into four reactors with a total volume of 32,000 m^3. Daily 8000–15,000 m^3 of biogas is generated as a result of the anaerobic digestion process in the rectors. The biogas produced in anaerobic environment using bacteria that are active in the mesophilic (20-40°C) temperature range, contains 55-75% methane (CH_4), 25-45% carbon-dioxide (CO_2), 0,1-1,5% hydrogen-sulfide (H_2S) and 0.01-0.05% ammonia (NH_3). Before being burnt in the gas motors to generate electricity, the biogas produced in the anaerobic digestion tanks is sent to the desulfurization unit to lower its sulfur amount to below legal limits. The upper and lower heat values of the biogas acquired from the waste water sludge vary between 22-30 MJ/m^3 and 19-26 MJ/m^3 [9] respectively. Table 2 shows the official content of the biogas produced in the facility, prepared by the administration of the Gaziantep wastewater treatment facility. The dryness ratio of the sludge cake taken from the anaerobic digestion tanks is increased to 27% by through subjection to dewatering process.

B. Biogas engine powered cogeneration system

The biogas engine powered cogeneration system operating as coupled with the wastewater treatment facility consists of a four-stroke, spark-ignited, 12-cylinder, V-configuration Deutz TCG 2020 diesel engine and other auxiliary equipment (see Fig. 1).

TABLE 2
CONTENT OF THE BIOGAS PRODUCED IN THE GAZIANTEP WASTEWATER TREATMENT FACILITY

Content	Volumetric value (%)
Methane (CH_4)	60.0
Carbon-dioxide (CO_2)	35.0
Nitrogen (N_2)	1.5
Hydrogen (H_2)	0.3
Oxygen (O_2)	0.5
Hydrogen Sulfide (H_2S) (ppm)	2,500-3,000
LHV (kJ/kg)	17.892
HHV (kJ/kg)	21.250

The biogas produced through stabilization of the sewage sludge of the wastewater treatment facility is used as the system fuel. Detailed explanation of the biogas engine-powered cogeneration facility operation can be found in reference no. [10].

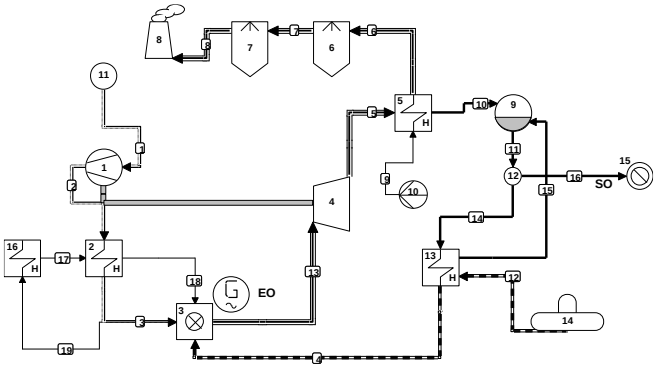

Fig. 1 Flowchart of the biogas engine powered cogeneration system

The annual electricity generation of the cogeneration facility is 8,760 GWh and the biogas consumption corresponding to such generation was calculated to be 3,400,000 m^3. The cogeneration system consumes 61% of the biogas produced in one year in the anaerobic sludge digestion tanks. As 0.387 m^3 biogas containing 60% methane is consumed for each 1 kWh electricity generated in the system, the total consumption cost of the biogas required for generating 1,000 kWh was calculated as TRY 241.78 TL (USD 60.22). In Turkey, the cost of natural gas required for generating 1,000 kWh was stated to be TRY 166.62 (41.50 USD) on average [11]. However, as biogas is produced as a fully useful and sustainable system output in the wastewater treatment facility that also includes the cogeneration system, the cost of consuming the biogas as fuel actually also includes the stabilization cost of the wastewater sludge. 1 kWh of the electricity generated in the cogeneration system costs 36.14 kurus (9 cent). The cost of generating a total of 1,000 kWh electricity was found to be TRY 361.4 TL (USD 90). Considering that the tariff applied by TEDAŞ to industrial enterprises is 41.4 kurus/kWh (10.3 cent/kWh) [12], it can clearly be seen that the electricity generated from the biogas in the cogeneration system in the wastewater treatment facility costs less.

C. Fluidized bed sludge incineration system

There is a fluidized bed sewage sludge incineration and drying facility inside the Gaziantep central wastewater treatment system used to dispose a large section of the sludge dewatered to 27% dry substance content, whose volume is reduced at a certain rate through digestion with anaerobic process. The capacity of this unit is 180 tons/day and is based on burning the sludge in a boiler according to fluidized bed principle after sludge with 27% dry substance content is dried and turned into a 40% dry structure. The function of the thermal drier is achieved by transferring the heat within the 20 tons of heat transfer oil - whose closed-circuit circulation is achieved by heating in fluidized bed sludge combustion boiler - to the sludge with 27% dry matter content that is spread over the drier surface. The 121.5 tons/day of sludge cake - whose dry substance content is increased at the output of the thermal drier - is supplied into the fluidized bed boiler. The upper heat value of this biomass sent to the fluidized bed boiler was determined as 2,833 kcal/kg and fine grain coal with calorific value 2,750 kcal/kg is also supplied to the boiler. The exhaust gas released after the combustion system in the fluidized bed boiler is passed through the economizer unit operating in serial connection with the boiler output. The exhaust gas that enters the economizer - which is a heat-exchange unit - at 550°C temperature, transfers its heat to the ambient air that enters the unit in reverse direction and increases the temperature of the air to 450°C; the heated air enters the hot air chamber of the fluidized bed boiler and ensures that the temperature of its sand bed does not decrease. The exhaust gas on the other hand continues its path and first goes through the cyclone and membrane dust filter unit in serial connection with the economizer unit and then through the wet chimney and is released into the atmosphere. Exhaust gas temperature at the chimney entrance is around 120°C. At this temperature, in other words a relatively low temperature, it is possible to generate electricity from the waste through an organic cycle. As burning around 180 tons of sludge every day requires high amount of heat energy and also, as the waste heat is used to keep the fluidized bed material at high temperature, it is not possible to use higher-temperature exhaust gas to generate electricity. However, feasibility studies are being conducted to generate 1,000-1,500 kWh electricity using Organic Rankine Cycle in the facility.

IV. TURKEY'S BIOPOWER GENERATION POTENTIAL FROM WASTEWATER TREATMENT SLUDGE

The total number of municipal wastewater treatment plants in Turkey reached 881 by the end of 2016 with an approximate capacity of 5,491 Mm^3/year and the annual amount of wastewater treated in these plants was reported approximately as 3,842 Mm^3 [13]. As of 2016, a total of 881 wastewater treatment plants with the following breakdown of physical (55), biological (492), advanced (135) and natural (199)

treatment were in operation serving 581 municipalities. Of the total amount of wastewater that was processed in Turkey, 44.5% was processed via advanced treatment, 31.6% via biological treatment, 23.6% via physical treatment and 0.33% via natural treatment. The ratio of the Turkey population that was serviced by sewage network managed by a municipality was 84% in 2016 and this corresponds to 90% of the total municipality population. The ratio of the Turkey population that would be serviced by a municipality that has a wastewater treatment system is 70% and this corresponds to 75% of the total population that would be registered within a municipality. The average wastewater discharged into the receiving environment per person in the municipalities via the sewage network was determined as 183 litres per day in 2016. The analysis of the year 2016 data collected from the municipalities indicated that municipal wastewater plants produced 1,471,680 tons wastewater sludge, annually [13]. The environmental data in 2016 as reported by the Turkish Statistical Institute (TSI) [14] indicated that the daily production of 60 g of sewage sludge per person should be considered in calculations based on 25% dry material content.

Although the daily wastewater treatment and wet sewage sludge capacities of municipal wastewater treatment facilities in Turkey are known, there is no comprehensive inventory about the total quantities and features of the net sludge produced in these facilities. Therefore, it is urgently necessary to prepare regional treatment sludge inventories, prepare archives for their quantitative and qualitative features and determine alternative methods for suitable sludge disposal. According to 2016 TurkStat data [13], approximately 300,000 tons of domestic/urban treatment sludge was produced in our country and 31.4% of this was burned in fluidized bed incineration systems to dry and dispose of the sludge. 27.6% of the sludge produced in the facilities was disposed of in regular storage areas while 21% was sent to municipality solid-waste facilities. 2.3% of the sewage sludge was randomly discharged on land while 6.5% was consciously applied to land for ecologic improvement purposes. 3.1% of domestic sewage sludge was regularly demanded and used in agriculture, while 11% of the sludge was disposed by burning in production such as cement etc. In a study [15] we conducted in 2012 based on 2010 TurkStat data, we had made a projection on the sludge and biogas production potential of our country by taking into consideration the number and capacities of urban wastewater treatment facilities operating actively in our seven geographical regions and the average features of their domestic wastewater sludge. Accordingly, the annual biogas production potentials of municipal wastewater treatment systems in Turkey is above 200 million m^3 and furthermore, this amount can be increased if the efficiency of anaerobic sludge digestion tanks can be increased with new sludge stabilization techniques. Considering that the all the produced biogas will be used in electricity generation within the wastewater treatment facility, it can be predicted that 530 GWh electricity can be generated by burning the whole biogas potentially obtained from Turkey's domestic wastewater sludge. Considering the increased number of wastewater treatment facilities as of 2016, biogas production has almost exceeded 230 million m^3. Assuming that the corresponding amount of electrical generation is annually approximately 600 GWh, then when we use the whole domestic sewage sludge potential effectively and efficiently, it becomes possible to meet 1% of the total annual power need of our country through treatment facilities. This value will rise to 2% considering the electrical potential that can be generated in sludge incineration facilities that operate very efficiently and to which secondary electricity generation systems (such as ORC) can be coupled.

V. SUGGESTIONS AND CONCLUSION

The biomass energy industry has been the locomotive of the renewable energy industry throughout the world and is increasing maintaining this status. I can list some of my opinions and suggestions as follows for more efficient and effective utilization of Turkey's biogas resources:

- Preparations should be made as soon as possible for waste and energy master plan, which are the common problems of the ministries of agriculture, energy and environment and regional strategies should be developed by receiving consultancy from both domestic and overseas experienced scholars and institutions.
- Separate renewable energy pricing should be provided for large and small-scale biogas systems.
- Biogas investments should be made attractive for both domestic and foreign investors.
- Grants should be given to waste and renewable energy projects through the development agencies of the ministry of energy in Turkey and the rural development programs of Ipard [16], in other words the "instrument for pre-accession assistance" established to provide assistance to candidate and potential candidate countries (Ipard 1 for 2007-2013 and Ipard 2 for 2014-2020). Small producers can be informed of these assistances through municipalities, development agencies and media organizations. There is of course an important handicap here: grant bureaucracy.
- Viewing biogas facilities only as power generation facilities would be to miss the point; they are one of the unique facilities that require no imports, reduce pollution by disposing environmentally hazardous waste and meanwhile generate renewable energy.
- Particularly through the operations performed in wastewater treatment facilities, which constitute the main topic of our study, biogas facilities seem - through their electricity and heat generation - to be capable of solely meeting the power need of the systems they operate as coupled. In Table 1 the total power consumption of the Gaziantep municipal wastewater treatment facility is given as 2,083.73 kWh. 1,000 kWh electricity is generated with the biogas engine powered cogeneration system. This generation meets 48% of the facility's need. If an Organic Rankine Cycle is established before chimney in the fluidized bed sewage sludge incineration facility it shall be possible to generate up to 1,000 kWh of electricity. Thus, all of the wastewater treatment facility's power need will be met

from itself. Considering that the final product output of the sludge combustion facility is ash, with the possibility of producing an organic ink that has no harm to the environment, wastewater treatment facilities can be considered as unique facilities with zero-waste principle and generation of 100% renewable and sustainable energy.

- As the biogas produced in the facilities are fully burnt and turned into electrical power, there is no methane release into the nature, which paves the way for countries to make large gains from carbon markets.
- There is no need for R&D studies that require large investments regarding power generation from biogas. This is because biogas production technology through anaerobic digestion of domestic wastewater sludge is almost traditionally known for years, therefore establishing a biogas facility consists merely of mechanical assembly through accurate project development with suitable capacity. However, effective entry of biogas into the power generation in Turkey will be possible through regular and systematic preparation of waste inventory and submission thereof to generation companies with continuous updating.

REFERENCES

[1] http://www.un.org/en/development/desa/news/population/world-urbanization-prospects-2014.html (Accessed on March 01, 2018).
[2] H. S. Peavy, D. R. Rowe, and G. Tchobanoglous, *Environmental Engineering*. Singapore: McGraw-Hill, 1985.
[3] J. Werther and T. Ogada, ″ Sewage sludge combustion″, Prog Energ Combust, vol. 25, pp. 55-116, 1999.
[4] http://www.tuik.gov.tr
[5] http://www.eie.gov.tr
[6] E. Toklu, ″ Biomass energy potential and utilization in Turkey″, Renew Energ, vol. 107, pp. 235-244, 2017.
[7] M. Ozturk, N. Saba, V. Altay, R. Iqbal, K. R. Hakeem, M. Jawaid, et al.,″ Biomass and bioenergy: An overview of the development potential in Turkey and Malaysia″, Renew Sust Energ Rev, vol. 79, pp. 1285-1302, 2017.
[8] G. Eksi and F. Karaosmanoglu, ″ Combined heat and biopower: A technology review and assessment for Turkey″, Renew Sust Energ Rev, vol. 73, pp. 1313-1332, 2017.
[9] Netherland Agency for Energy and Environment, *Biomethane and Biohydrogen*, pp. 58-102, 2003.
[10] A. Abusoglu, S. Demir, and M. Kanoglu, ″ Thermoeconomic analysis of a biogas engine powered cogeneration system″ J Therm Sci Tech (in Turkish), vol. 33, pp.09-21, 2013.
[11] www.epdk.org.tr
[12] www.tedas.gov.tr
[13] www.tuik.gov.tr
[14] www.turkstat.gov.tr
[15] A. Abusoglu, S. Demir, and M. Kanoglu, ″ Assessment of sewage sludge potential from municipal wastewater treatment plants for sustainable biogas and hydrogen productions in Turkey″, as a book chapter in *Causes, Impacts and Solutions to Global Warming*. New York: Springer, 2012.
[16] www.ipard.gov.tr

A Country-Based Assessment of the Economic Growth and Energy Interaction

Egemen Sulukan[1], Mumtaz Karatas[2]

Abstract— Energy is the major input nearly in every process in national economies. Recent studies and empirical analyses show that the relationship between the economic growth and energy consumption level of the industrialized countries has a tendency to decrease in the last few decades. In this study, we aim to analyze this relationship on an analytic basis by determining the correlation coefficients for the gross domestic product (GDP), primary energy production, and primary energy consumption parameters of selected nine OECD countries, viz. UK, Germany, Japan, France, Italy, Spain, Greece, Canada, and Turkey. In our analysis, we use the open-source data obtained from the United States Energy Information Administration and World Bank.

The analysis results reveal that there is a strong positive relation for Turkey, Canada and Greece in terms of the pair combinations of the selected three parameters, i.e. GDP & energy production, GDP & energy consumption and energy production & energy consumption levels. Nonetheless, for Japan, Germany and UK energy production & energy consumption levels encompass a positive correlation, while the GDP is decoupled from energy production and consumptions addressing to negative correlation results.

***Keywords*—**GDP, Primary Energy Production, Primary Energy Consumption, Pearson Correlation Coefficient.

I.INTRODUCTION

SINCE the industrial revolution, energy appears as the most influential factor in national economies. The increasing concerns in productivity of the industries, residential demands, agriculture and the transport sectors mainly depend on the energy production in a country, while the balance between energy production-consumption finally results in the import level in terms of energy supply security.

From the financial perspective; the world's nations currently specify their ultimate economic target in terms of Gross Domestic Product (GDP). GDP is the total market value of all final goods and services produced in a country in a given year. In 2017, GDP varied from $19 trillion for the US, and $12 trillion for China, $5 trillion for Japan, to $793 billion for Turkey. In a broader perspective, 15 economies would have GDP above $1 trillion, 62 have above $100 billion and 177 have above $1 billion. Top five economies account for approximately 54%, whereas top ten accounts for approximately 67%. Top 20 economies add up to over 80%. 92 smallest economies only contribute 1 % to global wealth and 154 lowest ranked constitute only 10 % of total [2]. As a significant financial indicator, GDP per capita is mainly known as a proxy of the level of standard of living in the literature and is calculated by dividing GDP by midyear population, based on market exchange rates [2].

Speaking of the energy profile of a national economy, Total Primary Energy Supply (TPES) gets to the foreground as a key parameter. TPES is made up of the indigenous production with imports, minus exports and stock changes according to energy balance tables produced by International Energy Agency [3].

The energy balance table provides data on the supply and demand flow of all energy products as well as on the production, import, export, transformation, and consumption within the national territory. It is also widely used in the estimation of total energy supply, forecasting, and the study of substitution and conservation.

The energy production-consumption situation primarily depends on the domestic energy potentials, installed energy production capacity, and the total demand within the country. As a specific sample; the key indicators are given for Turkey in Table I of the year 2015.

TABLE I KEY INDICATORS FOR TURKEY (2015) [3].

Population	Millions	77.45
GDP	Billion $	1087.55
GDP PPP		1779.24
Energy production	Mtoe	31.65
Net imports		103,62
TPES		123.81
Electricity cons.	TWh	229.20
CO_2 emissions	Mt of CO_2	317.22

In 2005, net imports have been 103.62 Mtoe, more than three-fold of energy production in Turkey. Naturally, the general energy outlook in Turkey is highly based on compulsory imports in order to maintain the economy. Total Primary Energy Production is considered one of the key parameters affecting the general energy outlook together with total primary energy consumption, which basically measures the total energy demand of a country. Primary energy

Egemen Sulukan[1] is lecturer in the Mechanical Engineering Department of the Naval Academy, National Defense University, 34940 Tuzla-Istanbul/TURKEY (corresponding author's phone: +905424359142; e-mail: esulukan@dho.edu.tr).

Mumtaz Karatas[2] is an Associate Professor in the Industrial Engineering Department of the Naval Academy, National Defense University, 34940 Tuzla-Istanbul/TURKEY (mkaratas@dho.edu.tr)

consumption refers to the direct use at the source, or supply to users without transformation, of crude energy, that is, the energy that has not been subjected to any conversion or transformation process [4].

The relationship between the economic growth, energy production, and energy consumption levels has always been one of the major discussions. In the recent literature; Bakirtas and Akpolat [5] analyzed the relationship between energy consumption, urbanization and economic growth using Dumitrescu-Hurlin panel Granger causality test for the period 1971–2014 in New Emerging-Market Countries (Colombia, India, Indonesia, Kenya, Malaysia, and Mexico). In another study, Shahbaz et al [6] searched the interconnections between energy consumption and economic growth in top ten energy-consuming countries i.e. China, the USA, Russia, India, Japan, Canada, Germany, Brazil, France and South Korea by the quantile-on-quantile (QQ) approach of Sim and Zhou. Pinzón [7] applied the Granger-causal relationship between EC and economic growth (EG) in Ecuador by analyzing aggregated and disaggregated data for 1970–2015. Mahmood and Ahmad [8] analyzed the impact of economic growth on energy intensity in European countries in terms of energy-growth relationship. Kahouli [9] examined the short and long-run causal link between economic growth, energy consumption, and financial development by using data set of six South Mediterranean Countries for the 1995–2015 periods.

In this study, GDP per capita is determined as the decisive coefficient for the financial field, while TPES and TPEC reveal the energy interaction within the national economy. In particular, we use the Pearson correlation coefficients to measure how strong the relationship between the variable pairs: (1) GDP per capita & Total Primary Energy Production, (2) GDP per capita & Total Primary Energy Consumption, and (3) Total Primary Energy Production & Total Primary Energy Consumption of the selected nine OECD countries, viz. UK, Germany, Japan, France, Italy, Spain, Greece, Canada, and Turkey.

The organization of this paper is as follows: The data used in the study and the preliminary information on the Pearson correlation coefficients are briefly introduced in Section II. Section III includes the results and discussion of our country-wise analysis. We conclude in Section IV.

II. DATA AND METHODOLOGY

Problem Data

The data used in this study is obtained from the United States Energy Information Administration and World Bank websites for the selected nine OECD countries between years 2001 and 2016. The GDP per capita, Total Primary Energy Production, and Total Primary Energy Consumption data are given in Tables III, IV, and V, respectively. The same data is used in [10] for assessing Turkey's energy management performance with the help of a hybrid multi-criteria decision-making methodology.

Methodology

As previously mentioned, in this study we employ the well-known Pearson's correlation coefficient to perform our analysis. The Pearson's correlation (sometimes, called as Pearson's *R*) is commonly used in linear regression and it basically measures the linear correlation between two variables, say *X* and *Y*. Let x_i and y_i be the i^{th} terms of the vectors *X* and *Y*, where $\overline{x}$ and $\overline{y}$ denote the averages of those vectors, respectively. Then the correlation coefficient *r* can be calculated as:

$$r = \frac{\sum_i (x_i - \overline{x})(y_i - \overline{y})}{\sqrt{\sum_i (x_i - \overline{x})^2}\sqrt{\sum_i (y_i - \overline{y})^2}} \qquad (1)$$

The strength and direction of the relationship between *X* and *Y* are determined with respect to the value of *r*, which has a value between +1 and −1. In particular, a correlation coefficient of 1 means that the relationship between the variables is perfect and for every increase in one variable, there is an increase in the other. For a correlation coefficient of -1, the relationship is said to be perfect, although, for every increase in one variable, there is a decrease the other. Zero means the variables are not related and for every increase or decrease in one of the variables, there is no change in the value of the other. The properties and history of Pearson's correlation coefficient are discussed in references Pearson [11-13]. The intervals of correlation coefficient and the scale used to measure the relationship strength used in this study are given in Table II.

TABLE II CORRELATION COEFFICIENT INTERVAL AND CORRESPONDING RELATIONSHIP DEGREE & DIRECTION

Interval	(-1.0) – (-0.5)	(-0.5) – (-0.3)	(-0.3) – (-0.1)	(-0.1) – (-0.1)	(0.1) – (0.3)	(0.3) – (0.5)	(0.5) – (1.0)
Relationship level and direction	strong negative	moderate negative	weak negative	no linear relationsh ip	weak positive	moderate positive	strong positive

TABLE III GDP PER CAPITA FOR NINE OECD COUNTRIES IN SCOPE BETWEEN YEARS 2001-2016 (USDx10^3)

	2001	2002	2003	2004	2005	2006	2007	2008	2009	2010	2011	2012	2013	2014	2015	2016
Canada	23.35	23.78	27.84	31.69	35.95	40.14	44.26	46.44	40.94	47.81	52.27	52.50	52.27	50.19	43.34	**42.18**
France	22.44	24.21	29.66	33.89	34.95	36.64	41.70	45.52	41.71	40.76	43.84	40.84	42.57	42.55	36.53	36.86
Germany	23.66	25.18	30.33	34.13	34.66	36.41	41.78	45.66	41.70	41.79	46.05	44.01	45.60	47.77	41.32	**42.16**
Greece	12.85	14.40	18.97	22.51	23.22	25.57	29.76	33.07	30.72	27.87	26.84	22.24	21.84	21.63	18.07	17.89
Italy	20.07	21.82	26.92	30.64	31.39	32.79	36.96	39.81	36.16	35.01	37.34	34.81	35.37	35.18	30.17	30.66
Japan	32.73	31.25	33.73	36.46	35.80	34.11	34.09	37.95	39.43	43.07	46.33	46.70	38.55	36.15	34.47	**38.90**
Spain	15.25	16.93	21.43	24.87	26.48	28.46	32.72	35.61	32.38	30.78	31.97	28.65	29.37	29.72	25.79	26.62
Turkey	2.87	3.35	4.29	5.48	6.65	7.20	8.66	9.64	8.00	9.40	9.83	10.54	10.80	10.30	10.98	10.86
UK	25.75	28.09	32.49	38.22	39.88	42.45	48.38	45.29	37.24	38.62	41.34	41.29	42.29	46.28	44.31	**40.37**

TABLE IV TOTAL PRIMARY ENERGY PRODUCTION FOR THE NINE OECD COUNTRIES IN SCOPE BETWEEN YEARS 2001-2016 (QUADRILLION BTU)

	2001	2002	2003	2004	2005	2006	2007	2008	2009	2010	2011	2012	2013	2014	2015	2016
Canada	18.02	18.36	18.27	18.66	18.87	19.22	19.54	19.04	18.32	18.36	18.83	19.13	19.71	20.53	20.55	**18.68**
France	5.15	5.13	5.15	5.17	5.12	5.16	5.09	5.16	4.82	5.10	5.11	5.09	5.17	5.25	5.12	**5.12**
Germany	5.29	5.31	5.28	5.36	5.25	5.29	5.24	5.08	4.83	4.86	4.75	4.86	4.48	4.44	4.53	**4.68**
Greece	0.39	0.40	0.42	0.42	0.42	0.40	0.38	0.39	0.41	0.39	0.38	0.42	0.38	0.34	0.34	0.34
Italy	1.30	1.22	1.18	1.26	1.19	1.16	1.08	1.15	1.17	1.29	1.36	1.43	1.59	1.66	1.50	1.35
Japan	4.47	4.17	3.74	4.16	4.15	4.36	4.00	3.75	3.95	4.20	2.96	1.65	1.63	1.64	1.83	1.51
Spain	1.51	1.34	1.51	1.46	1.30	1.40	1.39	1.39	1.43	1.73	1.54	1.55	1.69	1.67	1.49	1.39
Turkey	0.90	0.94	0.92	1.00	1.06	1.15	1.17	1.19	1.23	1.35	1.39	1.40	1.23	1.10	1.22	1.51
UK	11.16	11.00	10.48	9.40	8.54	7.77	7.29	6.94	6.55	6.18	5.34	4.94	4.61	4.63	5.12	**4.76**

TABLE V TOTAL PRİMARY ENERGY CONSUMPTION FOR THE NINE OECD COUNTRIES IN SCOPE BETWEEN YEARS 2001-2016 (QUADRILLION BTU)

	2001	2002	2003	2004	2005	2006	2007	2008	2009	2010	2011	2012	2013	2014	2015	2016
Canada	12.82	13.05	13.43	13.77	13.81	13.72	13.70	13.52	13.06	12.98	13.40	14.04	14.41	14.55	14.36	**10.83**
France	11.09	11.02	11.11	11.31	11.38	11.40	11.22	11.32	10.75	11.03	10.84	10.61	10.62	10.21	10.26	**9.64**
Germany	14.62	14.31	14.17	14.33	14.09	14.31	13.80	14.10	13.21	14.02	13.48	13.57	13.49	13.07	12.21	**12.33**
Greece	1.36	1.36	1.44	1.43	1.44	1.48	1.50	1.47	1.40	1.35	1.31	1.21	1.11	1.08	1.10	1.07
Italy	7.62	7.65	7.90	8.09	8.13	8.07	7.97	7.90	7.35	7.66	7.50	7.23	6.82	6.60	6.67	6.03
Japan	22.20	22.11	22.11	22.76	22.57	22.89	22.70	21.81	20.60	21.79	20.91	20.49	19.56	19.10	18.74	**17.33**
Spain	5.75	5.83	6.13	6.34	6.52	6.57	6.74	6.53	6.11	6.24	6.12	6.02	5.67	5.59	5.55	4.80
Turkey	2.88	3.13	3.30	3.49	3.71	4.04	4.35	4.24	4.24	4.49	4.84	5.09	5.16	5.18	5.72	5.51
UK	9.88	9.75	9.79	9.85	9.82	9.71	9.37	9.26	8.73	8.92	8.43	8.70	8.48	8.02	8.11	7.06

III. RESULT AND DISCUSSION

In this section, we present our main results and findings of our analysis for the selected datasets. To analyze and illustrate the impact of GDP per capita on electricity production and consumption, we utilize data from the nine selected of OECD Countries for the period 2001-2016. This period is wide enough to justify the use of these data for the determination of the relationship between GDP and electricity production and consumption in these nine countries.

Comparative analyses are performed with respect to the three-pairs; namely, (a) GDP and energy production, (b) GDP and energy consumption and (c) energy production and energy consumption, respectively. The correlation coefficients referring to the relationship between these parameters are illustrated in Fig. 1 and Table VI and interpreted as follows:

GDP & Energy Production

Canada and Turkey draw a strong positive correlation in this domain. It means that the relationship between the economic growth and the energy production in these countries are highly coupled and for every increase in GDP refers to energy production in Canada and Turkey, while Italy shows no linear relationship and UK and Germany results in a strong negative relationship in terms of these two parameters.

GDP & Energy Consumption

GDP and energy consumption correlations follow similar trends with that of the GDP & Energy production correlations where Turkey has strong and Canada has a weak positive correlation, while Italy shows no linear relationship and Germany results in strong negative and UK has a moderate negative relationship in terms of these two parameters.

Energy Production & Energy Consumption

The situation in energy production and energy consumption starts with strong positive correlation for Japan, UK, Germany, Turkey, Greece, and Canada; while France has no linear relationship, Italy has a strong negative

and Spain has a weak negative correlation. This situation addresses that, energy production and consumption is highly coupled in most of these countries.

TABLE VI CORRELATION COEFFICIENTS FOR PAIRWISE COMPARISON

Country	GDP & energy production		GDP & energy consumption		energy production & energy consumption	
	Correlation coefficients	Relation level	Correlation coefficients	Relation level	Correlation coefficients	Relation level
UK	-0.753	strong negative	-0.452	moderate negative	0.851	strong positive
Germany	-0.746	strong negative	-0.602	strong negative	0.820	strong positive
Japan	-0.377	moderate negative	-0.281	weak negative	0.891	strong positive
France	-0.156	weak negative	-0.193	weak negative	0.013	no linear relationship
Italy	0.070	no linear relationship	-0.052	no linear relationship	-0.748	strong negative
Spain	0.162	weak positive	0.330	moderate positive	-0.241	weak negative
Greece	0.171	weak positive	0.421	moderate positive	0.714	strong positive
Canada	0.571	strong positive	0.290	weak positive	0.622	strong positive
Turkey	0.844	strong positive	0.958	strong positive	0.806	strong positive

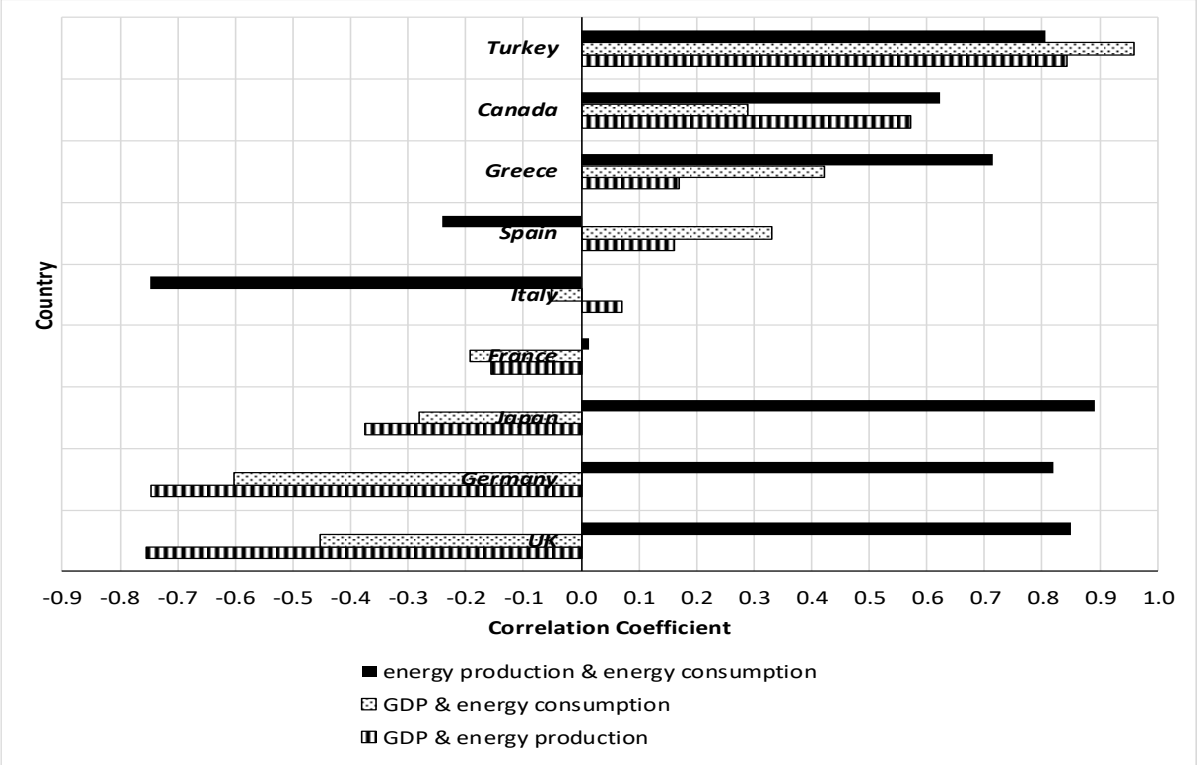

Fig. 1 A comparison of correlation coefficients for the nine OECD countries

Figure 1 gives a general outlook in terms of the correlation coefficient results in a broader perspective. In general terms; Turkey, Canada, and Greece, show a direct relationship with each other in GDP, energy production and consumptions. It can be assessed that economic growth grows along with the same direction with energy production and consumption in these countries. In Japan, Germany and UK energy production-consumption draw a coupled positive pattern, while GDP-energy production-consumptions encompass a negative correlation.

The situation in Spain, Italy, and France differs than the abovementioned countries in a way that; Spain keeps the correlation between GDP-energy production and consumption, but energy production-consumption trends turn to a negative side as seen in Italy.

IV. CONCLUSION

The relationship between the economic growth and the energy interactions in national economies attract great attention in the literature and the researchers conducted various analyses to indicate if these parameters affect each other in a positive or negative direction. In this study, the well-known Pearson's correlation coefficient is deployed on the data from nine of OECD Countries for the period 2001-2016 is used to analyze and illustrate the impact of GDP per capita on electricity production and consumption levels.

Our analysis shows that there is a strong positive correlation for Turkey, Canada, and Greece in terms of selected three parameter pairs, i.e. GDP & energy production, GDP & energy consumption and energy production & energy consumption levels. But this situation differs for Japan, Germany, and UK in a diverse manner while energy production & energy consumption levels encompass in a positive correlation, while GDP is decoupled from energy production and consumptions addressing to negative correlation results. Spain, Italy, and France gave hybrid results mainly caused by their economic sectoral structures and the differentiation in supply/demand balances.

REFERENCES

[1] GDP data from International Monetary Fund World Economic Outlook (April-2017), http://www.imf.org, (Retrieved in March 2018).

[2] P. E. Diacon, L. G. Maha, "The Relationship between Income, Consumption and GDP: A Time Series, Cross-Country Analysis," *Procedia Economics and Finance*, vol. 23, pp. 1535-1543, 2015, https://doi.org/10.1016/S2212-5671(15)00374-3

[3] International Energy Agency (IEA) website, https://www.iea.org/statistics/resources/balancedefinitions/#tpes, (Retrieved in March 2018).

[4] Glossary of Environment Statistics,"Studies in Methods," Series F, No. 67, United Nations, New York. https://stats.oecd.org/glossary/detail.asp?ID=2112, (Retrieved in March 2018), 1997

[5] T. Bakirtas, A. G. Akpolat, "The Relationship between Energy Consumption, Urbanization, and Economic growth in New Emerging-Market countries," *Energy*, vol. 147(5), pp. 110-121, 2018, https://doi.org/10.1016/j.energy.2018.01.011.

[6] M. Shahbaz, M. Zakaria, S. J. D. Shahzad, M. K. Mahalik, "The Energy Consumption and Economic Growth Nexus in Top Energy- Consuming Countries: Fresh Evidence from Using the Quantile-on-Quantile Approach," *Energy Economics*, vol. 70, pp. 282-301, 2018, https://doi.org/10.1016/j.eneco.2018.02.023.

[7] K. Pinzón , "Dynamics between Energy Consumption and Economic Growth in Ecuador: A Granger Causality Analysis*," Economic Analysis and Policy*, vol. 57, pp. 88-101, 2018, https://doi.org/10.1016/j.eap.2017.09.004.

[8] T. Mahmood, E. Ahmad, "The Relationship of Energy İntensity with Economic Growth: Evidence for European Economies," *Energy Strategy Reviews*, vol. 20, pp. 90-98, 2018, https://doi.org/10.1016/j.esr.2018.02.002.

[9] B. Kahouli, "The Short and Long Run Causality Relationship among Economic Growth, Energy Consumption and Financial Development: Evidence from south Mediterranean Countries," (SMCs), *Energy Economics*, vol 68, pp. 19- 30, 2017, https://doi.org/10.1016/j.eneco.2017.09.013.

[10] M. Karatas, E. Sulukan, I. Karacan, "Assessment of Turkey's Energy Management Performance via a Hybrid Multi-criteria Decision-Making Methodology," *Energy*, to be published.

[11] K. Pearson, "Mathematical Contributes to the Theory of Evolution. III. Regression, Heredity, and Panmixia," *Philosophical Transactions of the Royal Society of London*, vol. 187, pp 253-318, 1896

[12] K. Pearson, "Mathematical Contributions to the theory of Evolution. VIII. On the Correlation of Characters not Quantitatively Measurable," *Proceedings of the Royal Society of London*, vol. 66(424-433), pp. 241-244, 1900

[13] K. Pearson, "Notes on the History of Correlation," *Biometrika*, vol. 13(1), pp. 25-45, 1920.

Urban Scaled Reference Energy System Development with a Sectoral Focus

Doğancan Beşikci[1], Egemen Sulukan[2], and Tanay Sıdkı Uyar[3]

Abstract— Energy demand takes shape in a diversified manner depending on the natural resources, socio-economic profile, industrial sectors and the income level in cities. The demand level also influences the energy consumption, coupled with its environmental effects.

This study aims to analyze and determine the potential of the marble sector, which is a significant part of the energy model developed for Burdur, Turkey. Burdur, the selected city as the analysis domain, is located in the West Mediterranean region of Turkey. Burdur province makes most of its revenue from marble sector, because of the rich marble veins and region-specific marble types. Other than the marble, Burdur also makes income from livestock breeding, agriculture and dairy products. As a result, high capacity marble quarries also attract local and foreign companies to Burdur province and stimulate the establishment of various marble processing plants.

Marble sector in Burdur is analyzed in energy system structure perspective as two main segments; quarrying and processing of the marble. The entire equipment and machinery inventory was determined from a middle sized marble quarry and processing plant. Reference Energy System is based on the year 2016, extending to 2031 by Answer-TIMES energy-economy-ecology model generator. Energy demand of the sector in the years 2021-2026-2031 were calculated and Burdur-TIMES model is designed and developed on urban scale, based on rich energy technology and sector based data.

Keywords— Burdur, Turkey, Answer-TIMES, Energy Modeling, Reference Energy System, Renewable Energy.

I. INTRODUCTION

MARKAL (Market Allocation) is a cost optimization model to make energy model in any kind of domain by using technology focused approach.

In this approach, MARKAL evaluates three kinds of data that can be classified in energy-economy-ecology aspects. Energy side basically contains annual production or consumption of energy, economy side contains economic data of the technology such as installation or maintenance costs, tax or subsidies and ecology side contains all kind of emissions caused by any energy technology [1].

Cities with relatively low populations need various industrial sectors to develop. These industries develop in accordance with the city's natural reserves and potentials, and the focus for Burdur is the marble sector.

The most cost-effective industries for Burdur have been marble quarrying and marble processing. Unique marble colors found in the landscape helped the development of the industry. The potential of the marble attracted national and foreign investors to the city, as China is the leading investor.

Employment in the marble industry exceeded 8800 and harnessed the 25% of the total employment of the city, as of 2016. There are 378 marble quarries and marble processing establishments in and around the city. The total export of marble of the city has reached 132 million dollars as of 2015 [2].

The importance of the marble industry of the city also points out that it is the most energy intensive industry among the city's industrial structure.

Increasing the energy efficiency of the electricity consumption and efficient utilization of the potential of the developing marble industry is very significant in the development of the city. Therefore, modelling the marble industry in Burdur by MARKAL method and developing a road plan in accordance with the needs of the industry will play an important role in development of the marble industry.

Doğancan Beşikci1 is MSc candidate in Marmara University, İstanbul, Turkey (Corresponding author's phone:+905386320519; email:dogancanbesikci@outlook.com).

Egemen Sulukan2, is lecturer in Turkish Naval Academy of National Defense University, İstanbul, Turkey. (e-mail:esulukan@dho.edu.tr).

Tanay Sıdkı Uyar3 is a faculty member in Mechanical Engineering Department, Marmara University, Turkey, (email:tanaysidkiuyar@outlook.com).

II. METHODOLOGY

First step in the study has been the creation of a reference energy system, wile the time horizon of this model study is structured from 2016 to 2031 with 5-year periods. The base scenario is based on the year 2016. Then, the reference energy system was integrated using Answer interface to TIMES software and relevant energy sources was related to the system. On this step, an initial template is developed for the year 2016, which presents the current situation of the energy system of Burdur in details. As the next step, specified parameters for the technologies related to the industry were calculated accordingly.

Background on ANSWER- TIMES

TIMES (an acronym for The Integrated MARKAL-EFOM System) is an economic model generator for local, national or multi-regional energy systems; which provides a technologyrich basis for estimating energy dynamics over a long-term, multi-period time horizon. It is usually applied to the analysis of the entire energy sector, but may also be applied to study in a single industrial sector (e.g. the electricity and district heat sector). Reference case estimates of end-use energy service demands (e.g., car road travel; residential lighting; steam heat requirements in the paper industry; etc.)

are provided by the user for each region. In addition, the user provides estimates of the existing stock of energy related equipment in all sectors, and the characteristics of available future technologies, including the present and future sources of primary energy supply and their potentials. Using these as inputs, the TIMES model aims to supply energy services at minimum global cost (more accurately at minimum loss of surplus) by simultaneously making equipment investment and operating, primary energy supply, and energy trade decisions, by region. For example, if there is an increase in residential lighting energy service relative to the reference scenario (perhaps due to a decline in the cost of residential lighting, or due to a different assumption on GDP growth), either existing generation equipment must be used more intensively or new - and possibly more efficient- equipment must be installed. The choice by the model of the generation equipment (type and fuel) is based on the analysis of the characteristics of alternative generation technologies, on the economics of the energy supply, and on environmental criteria. TIMES is thus a vertically integrated model of the entire extended energy system.

ANSWER-TIMES is a Windows interface developed by Noble-Soft Systems, for working with the TIMES family of energy system models. ANSWER-TIMES provides the energy analyst with facilities for data entry/edit/browse, for model run generation and for result handling [3].

III. INDUSTRIAL SECTOR AND SECTORAL FOCUSING ON MARBLING

According to energy balance tables, industrial sectors are the most energy intensive areas in Turkey. Marble industry is known as one of the most energy intensive sectors among the industry.

Turkey has five billion m^3 marble reserves (observable, possible and considered reserves) reported, which equals to 40% of total world marble reserves according to MTA (General Directorate of Mineral Research and Exploration of Turkey). With 13.9 billion tonnes (approx. 5.1 billion m^3) of total reserves and 1.6 billion tonnes observable reserves, Turkey alone can provide the world's marble needs for up to 80 years with the current consumption trends. In Turkey, 80 different structures and 120 different colors of textures of marble reserves was identified. The most recognized marbles in international markets of Turkey are Süpren, Elazığ Cherry, Akşehir Black, Manyas White, Bilecik Beige, Tiger Hide, Denizli Traverten, Ege Maroon, Milas Lilac, Karacasu Green (Firuze), Kütahya Chocolate Traverten, Gemlik Diyabaz and Afyon Sugar [4].

A. Marble Industry in Burdur

Burdur is located in the south-west part of Turkey, as shown in Figure 1 and currently a developing city. Energy intensive industries among the city are cement, marble and milk industries.

Industry sector has the highest energy consumption share in Burdur, while there are 378 marble quarries and processing establishments, providing 25% of the total employment of the city, which have a major portion in energy consumption.

Fig. 1 Marble potential map of Turkey

Marble industry commonly utilizes electricity and diesel fuels as the energy sources. Marble industry consists two parts; first, mining and coarse cutting of the marble and the second part is processing of the marble and reduction to the desired finer dimensions.

BURDUR	City Illumination	2.335,79
	Household	21.237,53
	Industry	50.042,09
	Agricult. Irrigation	729,33
	Commercial	18.194,88

Fig. 2 Electricity consumption of Burdur (MWh) [5]

IV. REFERENCE ENERGY SYSTEM FOR BURDUR AND MARBLE SECTOR

The proposed reference energy system consists of six main pillars. These components are resources, primary energy carriers, process and conversion technologies, final energy carriers, demand technologies and demands. According to relation between these pillars, the sub-parts were linked with arrows, representing the energy flow accordingly.

As seen in Figure 3, electricity is generated through different energy sources and consumed for different demands by demand technologies. This structure is called reference energy system. Resources pillar shows if the energy sources which are used to provide the city's energy needs are generated in the city or imported from outside of the city.

Primary energy carriers identified in Burdur energy network are; coal, natural gas, electricity, hydro power, solar power, gasoline, diesel and LPG.

The technologies given under the process and conversion technologies pillar convert the primary energy carriers to secondary or final energy carriers. There are three different process technologies in Burdur, namely, natural gas power station, hydro electric power plants and solar PV.

Final energy carriers are the main inputs to the demand technologies and mainly provide energy for demand pillar. The demands are structured in five primary bodies, namely, housing and trading, industry, public services, transportation and agriculture.

Each cell illustrates the related energy technologies and/or energy carriers. Each generation or consumption of any energy carrier is linked to relevant technologies through arrows, shaping as a complete energy network flow.

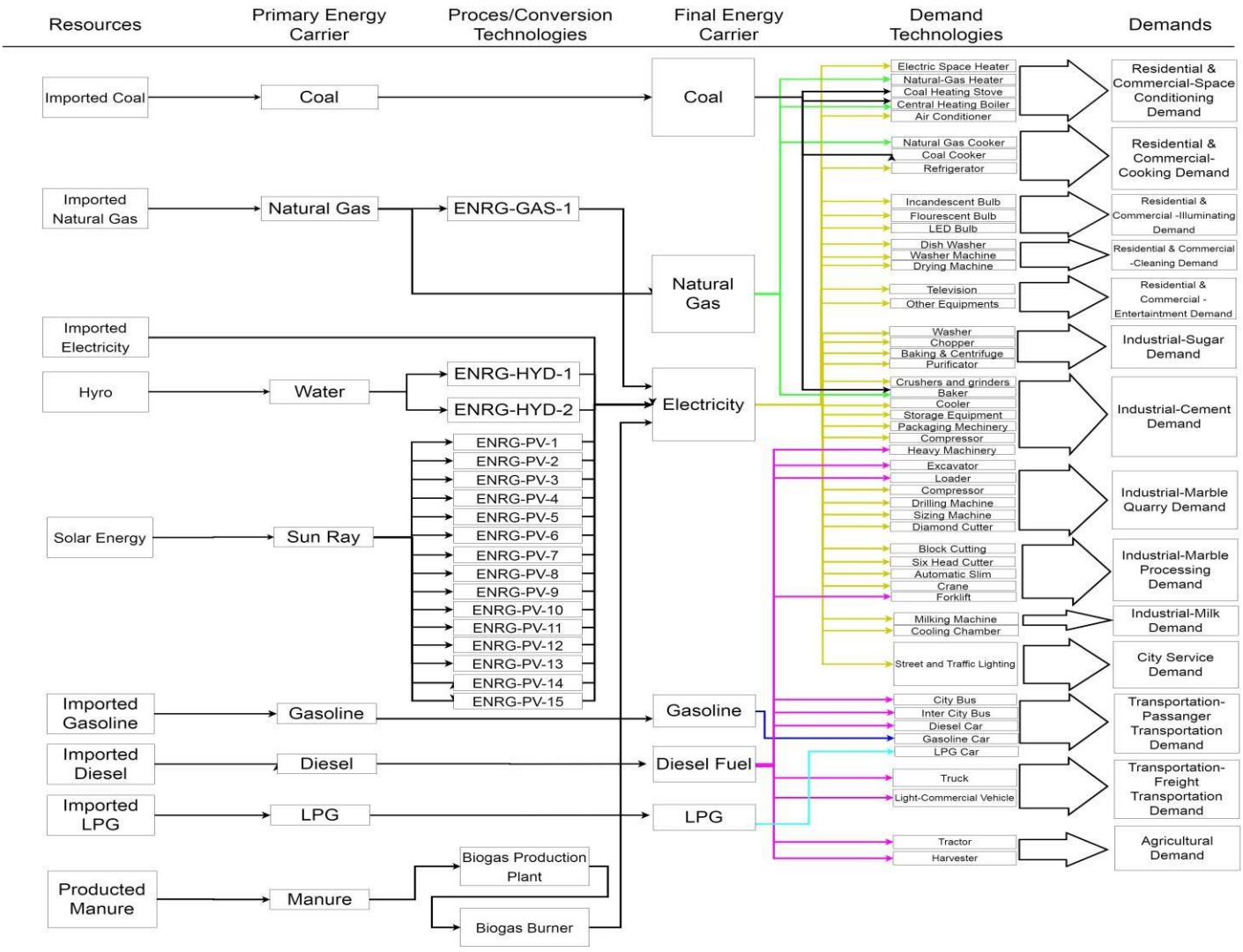

Fig. 3 Reference energy system of Burdur

A. Marble Sector in Burdur and RES

Marble industry of the Burdur is overviewed under two parts. First part, the technologies used in marble mines, provides for the demands of the marble mining. These technologies providing for the needs of the industry are identified and determined by the interviews with the companies working for the marble industry.

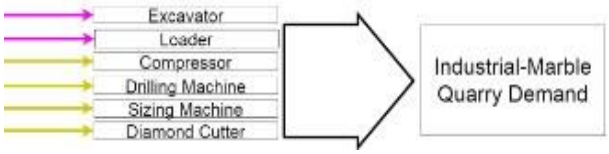

Fig. 4 Marble quarry technologies and demand

The technology options for the marble mining mainly based on six different technologies as shown in Figure 4:

• Excavator: Employed in transportation of coarse cut marble from marble quarries to the loading points.

• Loader: Employed in loading of coarse cut marbles to trucks or carriers.

• Compressor: Employed in providing energy for compressors used for marble breakers from the quarries.

• Drilling Machine: Employed in drilling the 3 corners of the marble slab to remove the slab from the quarry.

• Sizing Machine: Employed in rough partition of the marble slab.

• Diamond Cutter: Employed in removing the marble slab from the quarry.

On the fuel data used for six technologies of the marble mining, pink arrow is linked to the diesel fuel, representing that excavator and loader use diesel fuel, while yellow arrow

indicates the electricity and the compressor, drilling machine, sizing machine and diamond cutter use electricity.

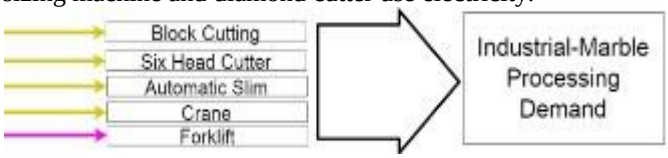

Fig. 5 Marble processing technologies and demand

As seen in Figure 5, we urged on five different technologies for the providing of marble processing demand. These are;

• Block Cutter: Employed in rough separation of marble slab to smaller parts,

• Six Head Cutter: Employed in separation of smaller parts to specific finer dimensions using multiple cutting head.

• Automatic Slim: Employed in sandpapering and polishing of the finer marble pieces.

• Crane: Employed in transportation of the fine marbles to next processing station or the storage.

• Forklift: Employed in loading of fine marbles to the trucks.

		Efficiency of Technology	Annual Availability of Capacity	Bound on Activity of Process	Demand		Technical Life Time of Process	Start Year of New Investment
Excavator (Diesel)	TIME DEPENDANT DATA	0.4	0.69	0.01341	0.00370	TIME INDEPENDENT DATA	8	2010
Loader (Diesel)		0.4	0.49	0.01259	0.00247		8	2010
Compressor		0.9	0.79	0.00975	0.00693		8	2010
Drilling machine		0.9	0.69	0.00638	0.00396		8	2010
Sizing machine		0.9	0.69	0.00638	0.00396		8	2010
Diamond cutter		0.9	0.69	0.00797	0.00495		8	2010
Block cutter	TIME DEPENDANT DATA	0.9	0.79	0.02215	0.0158	TIME INDEPENDENT DATA	10	2010
Six head cutter		0.9	0.69	0.02174	0.0135		10	2010
Automatic slim		0.9	0.69	0.01812	0.0113		10	2010
Crane		0.9	0.49	0.01020	0.0045		10	2010
Forklift (Diesel)		0.4	0.49	0.03878	0.0076		10	2010

Fig. 6 Demand technologies and parameters

V.DATA SETS AND PARAMETERS

Demand-driven and technology based data sets have been created and developed in order to calculate each demand. Then, these data sets have been constructed under two main groups, as (i) time-dependent and (ii) time independent and given as follows:

• ACT_BND (Bound on Activity of Process): Total energy can be consumed by the technology related to this data is calculated in PJ unit.

• ACT_EFF (Efficiency of Technology): This data shows the efficiency percent of the related data.

• NCAP_AFA (Annual Availability of Capacity): This data shows the annual utilization percent of the related technology.

The second group is time independent data, which is specified as follows:

• NCAP_START (Start Year for New Investment): This data shows the establishment year of the related technology.

• NCAP_LIFE (Technical Life Time of Process): This data shows the active period of the related technology.

After the establishment of the reference energy system, the related data of the technologies are taken from the active companies working in marble sector and the reports of Energy Market Regulatory Authority (EPDK) of Turkey and then, the demands are calculated accordingly.

As seen on the table, the average efficiency of the diesel fuel consuming technologies is determined as 40% according to the current diesel technologies. Consumption of diesel fuel consuming technologies is determined from related company officials, based on monthly consumption of the technology. Determined annual fuel consumption is multiplied by the total energy present in unit volume of the fuel and calculated in kWh unit. Finally, the calculated value is converted by kWh-PJ conversion and formed the final data.

Efficiency of the technologies that are consuming electricity are taken as 90% as per the current electric motor efficiency values. Energy consumption of each technology is calculated due to the working loads and the utilization of the related technology is calculated based on the working time intervals of the working team in each shift in the light of the interviews with the company officials. Maximum consumption values that the technologies can utilize are derived from the EPDK data.

The total life time and starting date are determined in accordance with average working time by the interviews with the company officials. The total lifetime of the mining equipment and tools are calculated as 8 years in regards to the hard working conditions of the marble mining and three work shifts per day. The average lifetime of the marble processing equipment and tools are assumed as ten years.

The block cutter has been determined as the most frequently utilized technology in the marble industry with its high usage level and high efficiency of electric motors.

VI. CONCLUSION

In this study, a preliminary industrial analysis is given for the energy planning of Burdur marble industry. Primary steps have been determined as the identification of the reference energy system of the city and the marble industry. Then, the reference energy system is specified by using the TIMES software through its Answer interface. Parameters and the related demands of the industry were calculated based on the data collected from local industry and EPDK reports.

The market share of the marble industry in Burdur is increasing every year with it is high contribution to employment rates. Therefore, the marble industry is determined as the leading sector to be analyzed in detail, to establish longterm energy plans to achieve sustainable development. When establishing long term energy plans, maturing technologies that will be introduced can be involved into the energy system before installation, and the future development of the industry can be estimated. This way, different alternative scenarios can be developed and analyzed, and then cost-effective industrial course of actions can prudently be developed.

REFERENCES

[1] Seebregts A.J., Goldstein G.A., Smekens K. (2002) Energy/Environmental Modeling with the MARKAL Family of Models. In: Chamoni P., Leisten R., Martin A., Minnemann J., Stadtler H. (eds) Operations Research Proceedings 2001. Operations Research Proceedings 2001 (Selected Papers of the International Conference on Operations Research (OR 2001) Duisburg, September 3–5, 2001), vol 2001. Springer, Berlin,
[2] Heidelberg
[3] Turkish Statistics Department, Turkey.
[4] Available at: www.tuik.gov.tr/PreTablo.do?al t_id=1051.
[5] Noble-Soft Systems, "Answer-Times Getting Started Manual", 2014
[6] Erkanol D, Aydındağ A, "Türkiye Geneli Doğaltaş Potansiyel Alanlarının Belirlenmesi Projesi"
[7] Turkish Republic of Energy Market Regulatory
[8] Available at: www.epdk.org.tr/TR/Dokumanlar/ Elektrik/
[9] YayinlarRaporlar/ElektrikPiyasasiGelisimRaporu

A Model Based Analysis on End-Use Energy Efficiency for Çanakkale, Turkey

Seçkin Bakırcı[1], Seyed Pejman Razavi[2], Egemen Sulukan[3], Tanay Sıdkı Uyar[4]

***Abstract*—** World energy demand is increasing due to rapidly increasing population, urbanization, change of lifestyle, technological and industrial development. Although technology has become more efficient in terms of energy consumption by the advances in energy technologies, it seems that this does not affect the total energy consumption as desired.

There is a significant interaction between renewable energy and energy efficiency. The energy saving potential can increase the share of renewable energy in the energy mix and accelerate to become more economical by opening to new markets. This paper primarily focuses on the importance of energy efficiency in the transition of 100% renewable energy in cities. A detailed energy network, namely Reference Energy System is developed for Çanakkale to identify the components and the interrelations between the energy supply, demand and energy technologies as a holistic approach. This framework also aims to analyze end-use efficiency in the electricity consumption in Çanakkale and will allow us to make inferences for large-scale situations from a broader perspective.

It is crucial to increase end-use efficiency in order to meet or even reduce the rising energy demand and then plan a sustainable, environmentally friendly energy system.

***Keywords*—** Renewable energy, End-use efficiency, Energy Modelling.

I. INTRODUCTION

Energy policy has traditionally underestimated the benefits of end-use efficiency for society, the environment, and employment. Achievable levels of economic efficiency depend on a country's industrialization, motorization, electrification, human capital, and policies. But their realization can be slowed by sector -and technology- specific obstacles including lack of knowledge, legal and administrative obstacles, and the market power of energy industries.

Seçkin BAKIRCI[1] is a research assistant in Istanbul Yeni Yüzyıl University and a MSc candidate in Marmara University, İstanbul, Turkey (Corresponding author's phone:+905366767740; email: seckin.bakirci@yeniyuzyil.edu.tr).
Seyed Pejman Razavi[2] is a faculty member in Mechanical Engineering Department, Marmara University, Turkey.
Egemen Sulukan[3], is lecturer in Turkish Naval Academy of National Defense University, İstanbul, Turkey. (e-mail:esulukan@dho.edu.tr).
Tanay Sıdkı Uyar[4] is a faculty member in Mechanical Engineering Department, Marmara University, Turkey, (email:tanaysidkiuyar@outlook.com).

Governments and companies should recognize innovations that can lower these obstacles. The external costs of energy use can be covered by energy taxes, environmental legislation, and greenhouse gas emissions trading. There is also an important role for international harmonization of regulations for efficiency of traded products. Rapid growth in demand provides especially favorable conditions for innovations in developing countries—enabling these countries to leapfrog stages of development if market reforms are also in place. [1]

The economic potentials of more efficient energy use will continue to grow with new technologies and with cost reductions resulting from economies of scale and learning effects. Considerations of the second law of thermodynamics at all levels of energy conversion and technological improvements at the level of useful energy suggest further potential for technical efficiency of almost one order of magnitude that may become available during this century. Finally, structural changes in industrialized and transition economies—moving to less energy intensive production and consumption—will likely contribute to stagnant or lower energy demand per capita in these countries [1].

The list of things that can be done when talking about energy efficiency can be quite long. However, this article focuses on electric energy efficiency in residential buildings. Buildings account for nearly one-third of global total final consumption (TFC), of which almost three-quarters is consumed in residential buildings, with the remainder used in commercial facilities (services) [2].

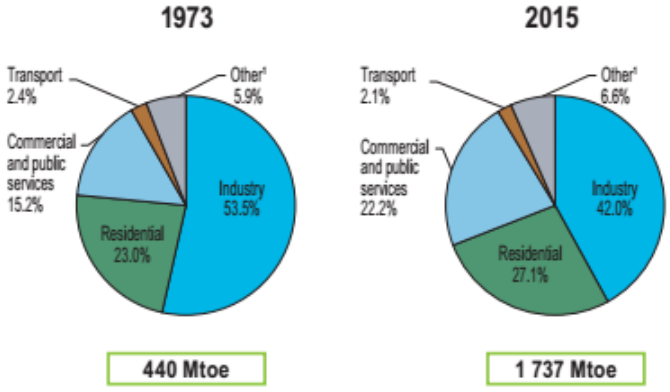

Fig.1 1973 and 2015 shares of world electricity consumption [3] (1 TWh = 0.086 Mtoe)

Efficiency of energy use in buildings is affected by building envelopes, design and orientation, as well as by the efficiency

of energy-consuming devices, including climate control systems, lighting, appliances and office equipment [2].

Fig.2 Average Electricity Consumption per Electrified Household, Selected Regions and World, 2010 and 2014 [3]

II. REFERENCE ENERGY SYSTEM CONCEPT

MARKAL means market allocation. The model's main aim was to assess energy technologies in a large scope and integrated structure. Although it had implementations in 1980s, but MARKAL has evolved in time to a more dynamic scope that focused on energy supply–demand equilibrium. The model involves all phases of energy market; starting from extraction, conversion, or process and end use in each related sector by various technologies that produce or consume energy carriers. These energy technologies compose a reference energy system (RES) with every single energy input and output of the energy system as regional or global level. RES also represents the energy economics of the relevant technologies, which take place in the entire energy system [4].

Figure 3 gives a simplified representation of a typical MARKAL RES showing the five main components usually recognized in each model structure: primary energy resources (SRC), energy conversion into electricity or low-temperature heat (CON), other energy processing (PRC) and energy end uses (DMD), and the demands (DM) for energy services and products [4].

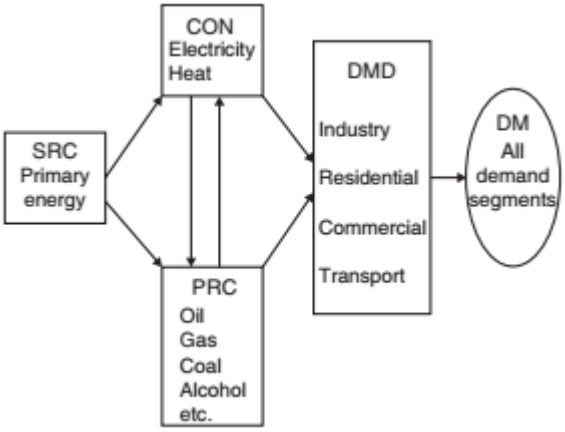

Fig.3 Simplified representation of a typical MARKAL RES [4]

TIMES (an acronym for The Integrated MARKAL-EFOM System) is an economic model generator for local, national or multi-regional energy systems, which provides a technology-rich basis for estimating energy dynamics over a long-term, multi-period time horizon. It is usually applied to the analysis of the entire energy sector, but may also be applied to study in detail single sectors (e.g. the electricity and district heat sector). Reference case estimates of end-use energy service demands (e.g., car road travel; residential lighting; steam heat requirements in the paper industry; etc.) are provided by the user for each region. In addition, the user provides estimates of the existing stock of energy related equipment in all sectors, and the characteristics of available future technologies, as well as present and future sources of primary energy supply and their potentials. Using these as inputs, the TIMES model aims to supply energy services at minimum global cost (more accurately at minimum loss of surplus) by simultaneously making equipment investment and operating, primary energy supply, and energy trade decisions, by region. For example, if there is an increase in residential lighting energy service relative to the reference scenario (perhaps due to a decline in the cost of residential lighting, or due to a different assumption on GDP growth), either existing generation equipment must be used more intensively or new – possibly more efficient – equipment must be installed. The choice by the model of the generation equipment (type and fuel) is based on the analysis of the characteristics of alternative generation technologies, on the economics of the energy supply, and on environmental criteria. TIMES is thus a vertically integrated model of the entire extended energy system [5].

ANSWER-TIMES is a Windows interface developed by Noble-Soft Systems, Australia, for working with the TIMES family of energy system models. ANSWER-TIMES provides the energy analyst with facilities for data entry/edit/browse, for model run generation and for results handling [5].

III. CASE CITY: ÇANAKKALE

Çanakkale is located on the north-western coast of Turkey, like İstanbul, embraces two continents with one arm reaching out to Asia, Biga Peninsula and the other Europe, Gelibolu Peninsula. The transition climate between Black Sea and Mediterranean climates is dominating the city. Winters are mild, windy and rainy and the summers are windy and hot. Çanakkale has population of 530417 people according to 2017 TUIK statistics.

TABLE I
INPUT DATA FOR THE CASE CITY

ÇANAKKALE	
Location (º N)	39° 27' - 40° 45'
Population, million	0.5
Electricity demand, GWh	21.4
GDP per capita ($1000)	14

The city has 2.287,51 MW installed electricity generating capacity and produced 14.670.802,91 MWh electricity in 2016 [6]

TABLE II
DISTRIBUTION OF ELECTRICITY CONSUMPTION BY CONSUMER TYPE IN 2016 ,MWh[6]

ÇANAKKALE	
Illumination	41.956,48 MWh
Household/Residential	324.829,74 MWh
Industry	2.697.231,81 MWh
Agricultural Irrigation	39.667,84 MWh
Commercial	429.822,93 MWh
Total	3.533.508,80 MWh

IV. RESIDENTIAL END-USE EFFICIENCY

The electricity consumption in residential sector is about one third of the total electricity consumption around the world. Although this rate is lower in Canakkale, as shown in Table 2, it can not be underestimated. For Canakkale, where the energy model is created through the ANSWER-TIMES interface, various scenarios will be created except for the main scenario created by using year 2016 data. One of these scenarios is end-use efficiency. In this study, some calculations were made to increase the end-use efficiency of the residential sector without entering the existing data to software.

By choosing LED bulbs which are known to be up to 90% more efficient than conventional bulbs and replacing existing electrical household appliances with more efficient ones can save significant amount of electricity. For example, when light bulbs are replaced by 50% more efficient ones and electrical household appliances are replaced by 20% more efficient ones, a total saving of 69.222 MWh could achieve. (Using the data in Table 2 and Table 3) According to the consumption data of Turkey in 2014, the average annual electricity consumption of a house is nearly 2339 KWh per year, a saving in this amount is approximately equal to yearly electricity consumption of 30 thousand houses.

TABLE III
PROPORTIONAL DISTRIBUTION OF ELECTRICITY CONSUMED IN A HOUSE [7]

Refrigerator	31,1
Air Conditioner	15,0
Washing Machine	8,5
Dish Washer	3,5
Drying Machine	3,2
Heaters	9,3
TV	6,7
Illumination	11,7
Others	10,9

Since the housing sector has a large share in electricity consumption, even increasing the end-use efficiency at home, can reduce the energy dependency.

Fig.4 Residential-Commercial Demand Technologies

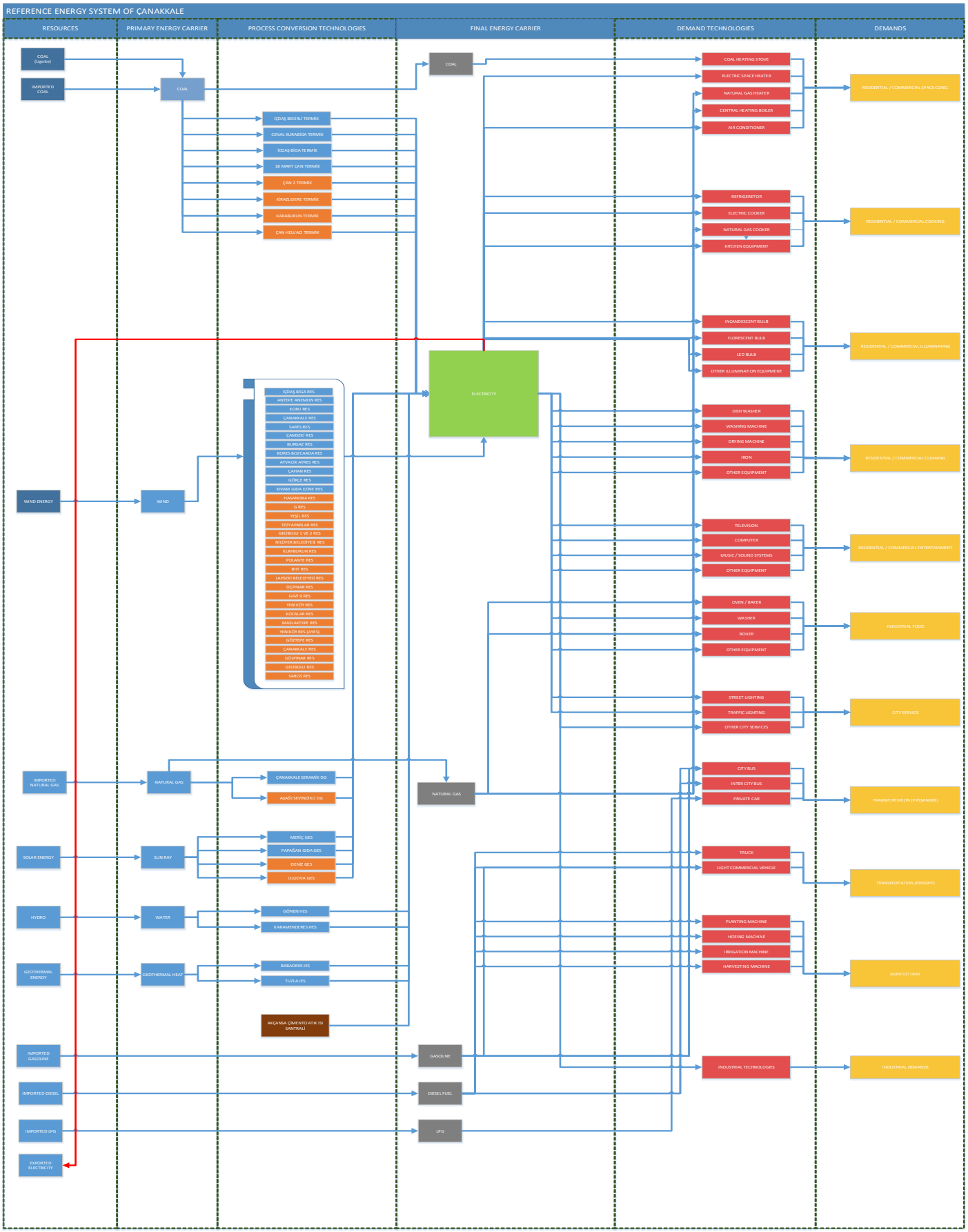

Fig.5 Reference Energy System (RES) of Çanakkale

V. CONCLUSION

The demand for electricity is rising rapidly, due to the evolving technologies, changes in social life and increasing population. But in today's conditions, it is unlikely to provide this supply/demand balance without distorting the natural equilibrium. Furthermore, it is obvious that energy efficiency has a significant role for transition to sustainable and clean energy. In this terms, the significant milestone is to develop technologies and policies that will take each sector separately and increase the overall productivity.

Efficient use of energy will enable the economy to strengthen, reduce fossil fuel consumption, increase the share of renewable energy resources, reduce carbon emissions and reduce health costs. As the energy sector and natural balance / quality of life are intricate, a small change in the parameters can lead to many positive or negative outcomes.

REFERENCES

[1] E. Jochem, «Energy End-Use Efficiency,» WORLD ENERGY ASSESSMENT: ENERGY AND THE CHALLENGE OF SUSTAINABILITY, New York, UNDP, 2000, p. 174.

[2] Renewable Energy Policy Network, «Renewables 2017 Global Status Report,» REN21, Paris, 2017.

[3] «Key Worl Energy Statistics,» IEA, 2017.

[4] M. S. T. U. Egemen Sulukan, «A Native Energy Decision Model for Turkey,» %1 içinde Towards 100% Renewable Energy, Springer, 2017, pp. 170-171.

[5] K. Noble, «ANSWER-TIMES Getting Started Manual,» Noble-Soft Systems Pty Ltd, 2014.

[6] «Elektrik Piyasası 2016 Yılı Piyasa Gelişim Raporu,» EPDK, Ankara, 2017.

[7] Ö. K. M. K. Mustafa Mutlu, «Elektrikli Ev Aletlerinin Enerji Etiketlemesinin İncelenmesi».

Reference Energy system Design for a Crude Oil Tanker

Mustafa Alper Yılmaz[1], Egemen Sulukan[2], Doğuş Özkan[3], and Tanay Sıdkı Uyar[4]

***Abstract*—**Maritime transportation has an increasing importance for humankind and expected to keep up with the trend in the future as a cost-effective transportation option. Taking effective measures in this sector has been necessary due to the increases in operating costs, fuel prices and the regulations brought by international organizations against the environmental pollution and climate change.

In this paper, every component of the energy system on a crude oil tanker, namely the fuel options, calculated demands and energy technologies onboard, are defined at the first step. Then, reference energy system, a detailed scheme indicating the interrelations and connections between the energy carriers, respective technologies, and the determined demands is established in energy system analysis concept.

***Keywords*—**Energy analysis, Reference energy system, Ship energy efficiency

I. INTRODUCTION

OVER the 80% of world trade by volume occur with marine transportation and by value is around 76% [1]. Also, the volume of maritime trade in 2016 increased by 2.6 percent compared to 2015, reaching 10.3 billion tons in volume [1]. In parallel with this growth, the world marine trade fleet also increased almost three-fold compared to 1987 and reached 171608800 dead weight tonnage (DWT) in 2016 [2]. Despite these developments, maritime transportation still faces some challenges, i.e. increasing operation cost due to rising fossil fuel prices. Reference [3] shows, the early of 70s the fuel cost was corresponding 13% in total cost but then increased to 43%-63% depending on ship type in 2008. Considering the growth in marine transportation, the demand for a marine bunker of 4.2 mboe/d (million barrels of oil equivalent per day) is expected to increase by 2 mboe/d in 2040 [4]. Therefore, fuel costs will increase depending on the diminishing fossil fuel resources.

Another challenge facing maritime transportation in recent decades is the international regulations designed to prevent environmental pollution arising from the use of fossil fuels. Currently, greenhouse gas (GHG) emission rate caused by the shipping sector is around 3% [5], but this ratio is expected to increase 50%-205% by the year 2050[6]. Therefore; International Maritime Organization (IMO), has taken some measures as the responsible institution for innovations and rules in the global maritime sector. For this purpose, the restriction of NO_x and SO_x was introduced by International Convention for the Prevention of Pollution from Ships (MARPOL) Annex VI and the emission control areas (ECA) were established to measure and reduce GHG emissions [7]. Also, energy efficiency design index (EEDI) was introduced to new-built ships and the ship energy management plan (SEEMO) for all ships in operation in the global merchant fleets [8]. In this way, it is aimed to reduce both fuel consumption and GHG emissions by increasing energy efficiency of the installed technologies onboard.

It is necessary to specify fuel types entering the energy system of the ship in order to improve energy efficiency on the vessels, where these types of fuels are used and how much energy is consumed to meet demands on the vessels. For this purpose, the *reference energy system (RES)*, which illustrates all steps and phases as an advanced energy network from resource to demand, was established in this study for a crude oil tanker [9].

II. BACKGROUND ON REFERENCE ENERGY SYSTEM CONCEPT

The reference energy system (RES) is a network diagram that includes all the steps and technologies which energy carrier is utilized and specifies the interactions from energy sources entering a system to the demand side met by the system. The general structure of a RES consists of five main components. In Fig. 1, these components are illustrated *as primary energy carriers (SRC), conversion technologies (CON)* from primary carrier to low-heat and electricity, *other processes (PRC), end-use technologies (or demand technologies) (DMD)* and finally *demands (DM)*, respectively [10].

Mustafa Alper Yılmaz[1] is a MSc student at the National Defense University, Barbaros Naval Science and Engineering Institute, Tuzla, 34940 Istanbul-TURKEY (Corresponding author's phone: +905398807726; mayilmaz@dho.edu.tr).

Egemen Sulukan[2], is a lecturer in Mechanical Engineering Department, Naval Academy, National Defense University, 34940 Tuzla-Istanbul/TURKEY (esulukan@dho.edu.tr).

Doğuş ÖZKAN[3] is a lecturer in Mechanical Engineering Department, Naval Academy, National Defense University, 34940 Tuzla-Istanbul/TURKEY (dozkan@dho.edu.tr).

Tanay Sıdkı Uyar[4] is a lecturer in Mechanical Engineering Department, Engineering Faculty, Marmara University, 34730 Göztepe-Istanbul/TURKEY (tanayuyar@marmara.edu.tr)

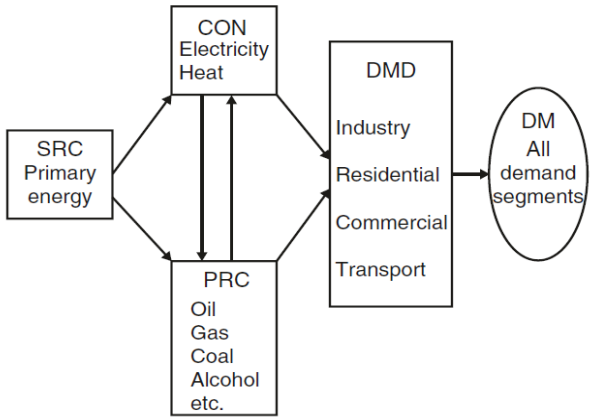

Fig. 1 Simplified Reference Energy System [11]

III. APPLICATION OF REFERENCE ENERGY SYSTEM FOR A CRUDE OIL TANKER

The proposed reference energy system of a crude oil tanker consists of six main blocks showing each step from resource to the demands and their connections; including conversion, process, and end-use technologies. RES for a crude oil tanker is shown Fig. 2, including the energy sources and flows as a whole.

Resource Technologies and Primary Energy Carriers

Ships do not include any energy resource in their structure internally, and all the required energy resources are imported. Marine vessels use various energy carriers according to their type, usage place, and purpose. For crude oil tanker; Heavy Fuel Oil (HFO), Marine Diesel Oil (MDO), Gasoline, Cylinder Oil and Lubrication Oil are introduced as primary energy carriers. These fuels are named primary energy carriers in the ship energy system and then stored in relevant tanks for convenient use. Fig. 3 shows the energy resources and primary energy carriers.

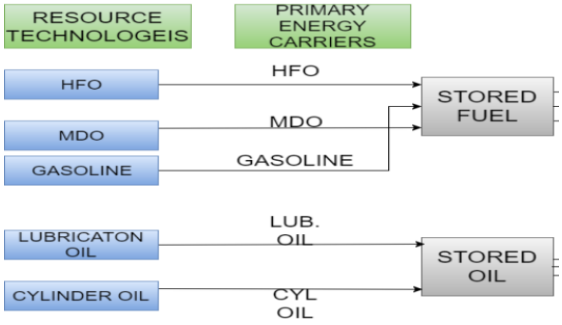

Fig. 3 Resource Technologies, Primary Energy Carriers and Fuel and Oil Storage

The Process, Conversion Technologies, and Final Energy Carriers

All the options for the primary energy carrier family are not suitable for direct use in onboard end-use technologies. Therefore, they are converted to final energy carriers by the conversion or process technologies. Respective conversion technology converts the primary energy carrier into low-temperature heat or electricity, namely the *final energy carriers*. The process technologies convert the energy carriers into different from and characters such as transforming from 440V/AC to 220V/AC electricity by transformers. Fig.4 shows the process, conversion technologies and the final energy carriers identified in RES.

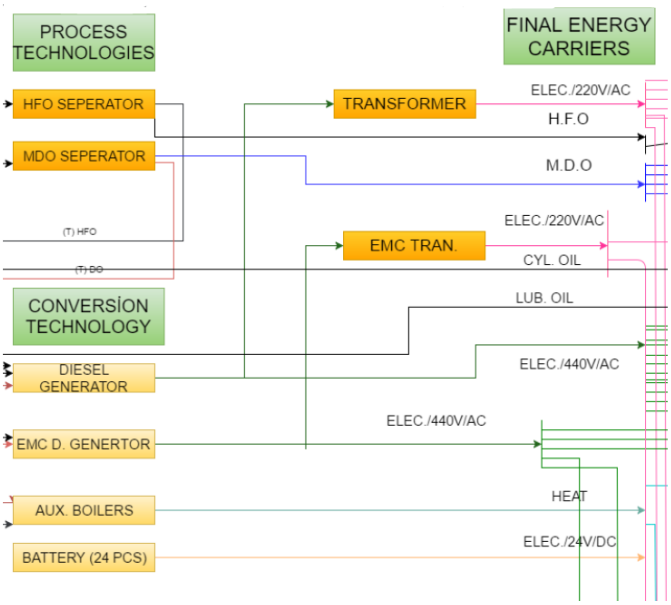

Fig. 4 Process, Conversion Technologies, and Final energy Carrier

End-Use Technology and Demands

End-use (demand) technologies are the technologies that meet demands by utilizing the final energy carriers in the energy system. For this reason, the demands and end-use technologies are determined according to requirements of the ship system and shown in Table I.

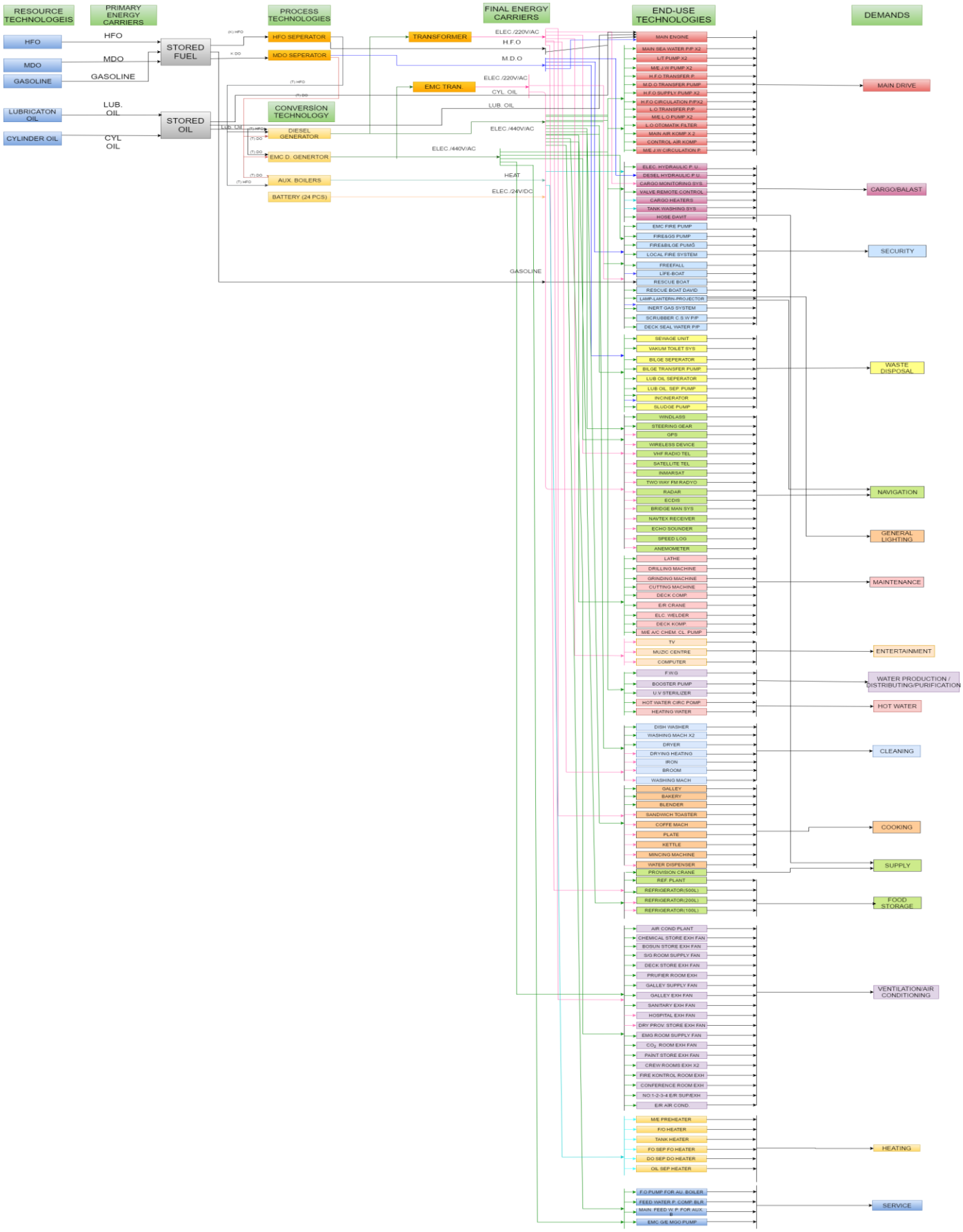

Fig. 2 Reference Energy System for a Crude Oil Tanker

TABLE I
END-USE TECHNOLOGIES AND DEMANDS ONBOARD

End-Use Technologies	Demands
Main Engine	MAIN ENGINE
L/T Pump x2	
M/E JW Pump x2	
HFO Transfer Pump	
MDO Transfer Pump.	
HFO Supply Pump x2	
LO Transfer P/P	
M/E LO Pump x2	
LO Automatic Filter	
Main Air Comp x2	
M/ JW Circulation P.	
Elec. Hydraulic P.Unit	CARGO/BALLAST
Diesel Hydraulic P.Unit	
Cargo Monitoring Sys.	
Valve Remote Control	
Cargo Heaters	
Tank Washing Sys.	
Hose Davit	
Emc Fire Pump	SECURITY
Fire & GS Pump	
Fire & Bilge Pump	
Local Fire Sys	
Freefall	
Life-boat	
Rescue Boat	
Rescue Boat Davit	
Lamp-Lantern-Projector	
Inert Gas System	
Scrubber CSW P/P	
Deck Seal Water P/P	
TV	ENTERTAINMENT
Music Centre	
Computer	
Fresh Water Generator	WATER PRODUCTION / DISTILLER / PRODUCTION
Booster Pump	
UV Sterilizer	
Dishwasher	CLEANING
Washing Machine x2	
Dryer	
Drying Heating	
Iron	
Washing Mach	
Hot Water Circ Pump	HOT WATER
Heating Water	
Hose Davit	SUPPLY
Provision Crane	
Lamp-Lantern-Projector	GENERAL LIGHTING
Sewage Unit	WASTE DISPOSAL
Vacuum Toilet Sys	
Bilge Separator	
Bilge Transfer Pump	
Lub. Oil Separator	
Lub. Oil Separator P.	
Incinerator	
Sludge Pump	
Windlass	NAVIGATION
Steering Gear	
GPS	
Wireless Device	
VHF Radio Tel	
Satellite Tel	
INMARSAT	
Two Way FM Radio	
RADAR	
ECDIS	

Bridge Man. Sys	
NAVTEX Receiver	
Echo Sounder	
Speed Log	
Anemometer	
Lathe	MAINTENANCE
Drilling Machine	
Grinding Machine	
Cutting Machine	
Deck Comp	
E/R Crane	
Elc. Welder	
M/E A/C Chem. Cl. P	
Galley	COOKING
Bakery	
Blender	
Sandwich Toaster	
Coffee Mach.	
Plate	
Mincing Machine	
Ref. Plant	FOOD STORAGE
Refrigerator (500L)	
Refrigerator (200L)	
Refrigerator (100L)	
M/E Preheater	HEATING
F/O Heater	
Tank Heater	
FO Sep Heater	
DO Sep Heater	
Oil Sep Heater	
F.O Pump For Boilers	SERVICE
Feed Water P. Boilers	
Main Feed. WP(AB)	
EMC G/E MGO Pup	
Air Cond Plant	VENTILATION / AIR CONDITIONING
Chemical Store Exh Fan	
Bosun Store Exh Fan	
Deck Store Exh Fan	
Purifier Room Exh Fan	
Galley Supply Fan	
Galley Exh Fan	
Sanitary Exh Fan	
Hospital Exh Fan	
Dry Prov Store Exh Fa	
Emc Room Supply Fan	
CO_2 Room Exh Fan	
Paint Store Exh Fan	
Crew Room Exh Fan	
Fire Control Room Exh	
Conference Room Exh	
No:1-2-3-4 E/R S/E Fans	
E/R Air Cond	

IV. RESULTS

In this paper, all the components in the energy system of a crude oil tanker and their interrelations are determined according to RES concept. Then, these components were examined thoroughly and the energy system of the ship which is a complex energy system is completely processed.

V. FUTURE WORK

At the first stage, the base scenario of the RES will be modeled with the real technical, economic and environmental parameters of a ship. Next, the current situation of the system will be analyzed under the name of base scenario. Finally, alternative scenarios; i.e. emission reduction, different technology applications for energy efficiency will be introduced and run against the base scenario and analyzed from the ecological, economical and technical point of view.

REFERENCES

[1] UNCTAD, "Review of Maritime Transport 2017," *United Nations Publication,* 2017

[2] Y. Ozer, "Rakamlarla Denizcilik Sektörü ve İstatistikler," *Deniz Ticareti,* ,Feb. 2017

[3] J. Kalli, T. Karvonen, T. Makkonen "Sulphur Content in Ships bunker fuel in 2015; A Study on the İmpacts of New IMO Regulations and Transportation Costs," *Ministry of Transport and Communications,* April 2009

[4] OPEC Secretariat, "Oil Demand and Transportation: an Overview," *OPEC Energy Review*, vol. 39, Dec 2015, pp. 349-375

[5] N. Olmer, B. Comer, B. Roy, X. Mao, D. Rutherford, “Greenhouse Gas Emissions From global Shipping*,” The International Council On Clean Transportation,* Oct. 2017
[6] IMO, “Third IMO Greenhouse Gas Study 2014,” *International Matitime Organization.,* 2015
[7] IMO, “International Convention for the Prevention of Pollution from Ships,” http://www.imo.org/en/About/Conventions/ListOfConventions/Pages/International-Convention-for-the-Prevention-of-Pollution-from-Ships-(MARPOL).aspx , March 10, 2018
[8] IMO, “ Guidelines for the Development of a Ship energy Efficiency Management Plan (SEEMP),” *Annex 9, Resolution MEPC.213(63),* 2012
[9] E. Sulukan, “Energy Modelling and Applications, Market Allocation (MARKAL),” *Lambert Academic Publishing,* 2016
[10] E. Sulukan, M. Sağlam, T, Sıtkı Uyar, “ A Native Energy Decision Model For Turkey” T, Sıtkı Uyar (Ed.), *Towards 100% Renewable EnergyvTechniques, Cost and regional Studies,* Springer, Switzerland, pp. 167-177, 2017
[11] R, Loulou, G, Goldstein, K, Noble,”Standart MARKAL User Manuel,” vol. 1, 2010

Developing the Business as Usual Scenario for TR-33 Region with EnergyPLAN

Utku Köker[1], Halil İbrahim Koruca[2], Egemen Sulukan[3]

***Abstract*—**Energy is one of the most important issues in contemporary world. Countries try to meet their various energy demands in a cost-effective way, while the fossil fuel costs are increasing day by day under the international regulations and policies. As the availability of the energy sources is still a debate issue, externalities which are left unanalyzed for long decades is also another important concern from the energy-economy perspective. Today, various approaches on calculation of these externalities are suggested and by adding these external parts into the operational costs, to obtain the "real" cost figures of energy items. It is so crucial for decision makers to determine the right energy resource or technology combinations for near future that gives the optimum energy costs in order to designate the acceptable public and investment policy. As a multidimensional topic, it does not only include cost perspective but it gets more complicated as emission and other factors are involved. The boom in renewable energy utilization in the last decades has seriously shifted the overall energy markets. As a result, almost all of the EU countries have gradually encompassed their routes to renewable energy from fossil fuels. From theoretical point of view, as the renewables have entered the energy mix lately, a need to modify the energy equations and calculations has occurred. As a result, new set of data of renewables has been added and had their places in optimum solutions. In this paper, EnergyPLAN software is briefly presented, and the "Business as Usual Scenario" for four cities in Uşak region, (called as "TR33 region" by the Ministry of Development of Turkey) was prepared and cost and emission outputs are obtained. BAU scenario is configured with and without external costs to prepare a basis for discussion.

***Keywords*—**Energy modelling, Business as Usual Scenario, Turkey, EnergyPLAN.

I. INTRODUCTION

Energy had a great importance since the invention of steam engine. The required form of energy changed over time and electricity has been the mostly utilized form of energy for the last decades. Energy has given the shape of modern industrial and post industrial societies' structure and dynamics. The affordable abundance of fossil fuels and energy has transformed every single sector in the last century. The biggest issue in the steady increase in average life expectancy of today's modern countries is adequate health care and secured food availability as well as the urbanization [1]. The middle and upper class urban people had the opportunity to have higher wages over time and this led to benefit from unprecedented variety of goods and services. Mobility of people is at an unbelievable level currently that just so few futurists may have guessed this overview fifty years ago. None of these transformations would be possible without the usage of fossil fuels. In the other hand, one of the biggest cons of the availability of this energy for rich countries is; the availability has elevated the economical levels of rich countries from the ones lack of them and this has led some significant controversies over time between these two camps. The threat of global warming has also recently been a topic of great interest and surpassed all the other cons of the fossil fuels in the last decade.

II. ENERGY PERSPECTIVE OF TR-33 REGION

Republic of Turkey has a population of 79.814.871 as of January 2017 [2]. Turkey is a natural bridge between Europe and Asia. With its fast growing economy, Turkey indicated a significant pace in terms of gross domestic product (GDP) among other OECD countries in the past decade with 820 billion dollars and ranking 17th biggest economy on the world [3] . Next to GDP, a great change has also happened in electricity market in Turkey in the same period. Fast growth in the electricity demand has reformed the Turkish electricity market between 2000 and 2012 [4]. Turkish electricity installed power capacity figures doubled in this period and almost tripled between 2000 and 2017 to meet the demand [5].

Turkey is a net energy importer and due to its insufficient primary resources, is buying from petroleum to natural gas from international energy market since the beginning of its industrialization era.

EU accession of Turkey has a long history dated back to "Agreement Creating an Association Between The Republic of Turkey and the European Economic Community", known as Ankara Agreement (1963). In the recent years, in 2006 as a part of this process, regional development agencies have been founded. The main purpose and the vision of these organizations were decreasing the inter-regional disparities and income differences all over the Turkey. Currently, there are 26 development agencies in Turkey and the Ministry of

Utku Köker[1] is a PhD candidate in Industrial Engineering Department, Institute of Natural and Applied Sciences, Süleyman Demirel University, 32260, East Campus, Isparta-TURKEY (utku.koker@afad.gov.tr).

Halil İbrahim Koruca[2] is a lecturer in Industrial Engineering Department, Engineering Faculty, Süleyman Demirel University, West Campus, Isparta/TURKEY (halilkoruca@sdu.edu.tr).

Egemen Sulukan[3], is a lecturer in Mechanical Engineering Department, Naval Academy, National Defense University, 34942 Tuzla-Istanbul/TURKEY (esulukan@dho.edu.tr).

Development is responsible for the coordination of these agencies. As the experiences of EU countries emphasizes, not a "top down"; but "bottom up" approach, models and structuring models parallel with regional development policy and practices of EU were chosen by Turkey policy makers [6].

Nomenclature of Units for Territorial Statistics (NUTS) is made in three levels in Turkey [7]:

1. NUTS-1 includes 12 regions,
2. NUTS-2 includes 26 sub-regions and
3. NUTS-3 includes 81 provinces.

With the establishment of NUTS-2;

1. Development of a national economic and social cohesion policy aimed at reducing regional disparities,
2. Adoption of the legal framework to facilitate the implementation of the acquits under this chapter,
3. Creation of a multi-annual budgeting procedures setting out priority criteria for public investment in the region,
4. Strengthening the administrative structures for managing regional development
5. Implementation of regional development plans was aimed.

TR-33 region is under the responsibility of ZAFER Development agency and covers four cities, Uşak, Manisa, Kütahya and Afyonkarahisar. The region with a population of 3 million people and area of 4.206.289 ha supplies 4 million dollars of exportation alone [8]. TR-33 that has 22 organized Industrial zones, 4 universities, 103 thousand university students, 78 thousand vocational high school students' ranks at the highest success levels in educational levels in Turkey. The four city region forms a natural connection between the major metropolis, trade centers and ports. It is located between the biggest cities of Turkey; i.e. Antalya, İstanbul, Ankara and İzmir. Since significant governmental incentives are applied in the region (such as land grant subsidies, customs duty exemptions, social security premium support -employers part-, reduced income/corporate tax rates, vat exemption and interest support), a number of industrial activities have gained power in the zone. TR-33 Region has an important weight in ceramics, mining, electronics, automotive, textile & leather, agricultural and culture-history-tourism sectors [8]. Almost one billion $ of ceramic exportation is done annually from Turkey and %43 of this export is from Kütahya-Eskişehir-Bilecik Ceramic Cluster with the production plants of popular trade marks in the zone. Uşak Province is also another powerful region in ceramic industry. Today %72 of world's total boron reserves (3 billion tons) is in Turkey. It is extracted in Kütahya-Emet. Marble is another important mining commodity and Afyonkarahisar acts an important role in Turkey with the important trade marks and their production fields. TR-33 has also important reserves of magnesite, silver, gold, titanium and uranium. Manisa Province is Turkey's pioneer in electronics and home appliances production. Vestel, Bosch, Indesit, Klimasan and many other brands are located in Manisa Organized Industrial Zone; an award winning zone that has many times rated as the best investment area by actors from economics and finance publications. Manisa Province is home to numerous automotive suppliers of automotive industry and quite optimal for a large scale main industry investment. Kütahya and other two cities in the region are also active in the sector. Automotive has a long history in Turkey. Annual production figures surpassed 1 million level and it is the 5th biggest automotive producer in Europe after Germany, France, Spain, England. Automotive industry statistics are collected and analyzed each year since it is one of the key sectors of Turkey. Furthermore, TR-33 cities produce the grossest value added in terms of agricultural activities from Gediz Basin, one of the most fertile agricultural regions. Olive, grape and raisins are the key agricultural fruits in the area. Textile and leather has always been a key product family in the region. Today, TR-33 is transforming itself with R&D activities and investments to be a key supplier in innovative garment sector. Design and fashion are also new focuses in TR-33 which has significant geographical advantages of closeness to European markets.

Turkey is one of the most visited countries in the world. Its historical background, as well as cultural mosaic and wonderful landscapes makes it a must visit country for travelers. Over 32.4 million people visited Turkey in 2017 [9]. TR-33 cities offer alternatives for the foreign and local travelers in health tourism with its extensive geothermal resources. Historical inheritances from Phrygian, Lydian, the Great Seljuk and Ottoman civilizations are also open to cultural tourism.

To be a key region in lots of different sectors TR-33 region needs extensive amount of energy. Change in energy consumption figures from 2004 to 2016 are given in Table 1

TABLE I
TR-33 ENERGY CONSUMPTION VALUES OF 2004 AND 2016

Cities	2004 (MWh)	2016 (MWh)	Increase In Consumption (%)
TR331 Manisa	1.805.105	4.293.169,12	137,83
TR332 Afyonkarahisar	697.510	1.615.010,15	131,54
TR333 Kütahya	654.493	1.483.817,29	126,71
TR334 Uşak	656.222	1.465.416,28	123,31
Total (MWh)	3.813.330	8.857.412,84	129,85

Electric consumption figures have already increased in the last decade and reached to 2.9 MWh in TR-33 Region in 2016. The highest consumption is determined to be in Uşak while the lowest figure belongs to Afyonkarahisar. Detailed information related to each city is given in Table 2. Table is configured by the help of TUIK and Energy Market Regulatory Authority data [7-10].

TABLE 2
TR-33 ELECTRIC CONSUMPTION PER CAPITA (2016) [5-10]

Consumption (MWh)	Electric Power Consumption per Capita	Total Electricity Consumption	TR-33 Region Ratio (%)
Afyonkarahisar	2,260263351	1.615.010,15	18,23%
Kütahya	2,586660827	1.483.817,29	16,75%
Manisa	3,073255654	4.293.169,12	48,47%
Uşak	4,084943468	1.465.416,28	16,54%
TR-33 Total	2,909941186	8.857.413	100,00%

Energy sources in TR-33 region are illustrated in Table 3. It is evaluated that Manisa and Kütahya cities have heavily invested on coal and more than the half of the installed capacity of TR-33 region belongs to those coal plants located in these two cities. The installed capacity of the renewable energy is found to be 35% of the grand total. It is found to be higher than the Turkey average ratio of renewables.

TABLE 3
POWER SUPPLIES OF TR-33 REGION [10]

Installed Power Capacities of TR-33 Region (MW)					
	Manisa	Kütahya	Afyonkarahisar	Uşak	Total
Solar	19,14	7,20	89,00	2,85	118,19
Wind	628,95	0,00	227,45	54,00	910,40
Geo	166,42	0,00	2,76	0,00	169,18
Biogas	0,00	0,00	16,22	1,20	17,42
Hydro	69,00	10,88	3,00	0,00	82,88
Nat Gas	274,99	23,36	0,00	22,75	321,10
Coal	1034,00	1020,57	0,00	0,00	2054,57
Other	0,00	0,00	12,80	3,72	16,52
Total	**2192,50**	**1062,01**	**351,23**	**84,52**	**3690,26**

Distribution of electricity generation in Turkey in 2016 is given in Table 4 [8].

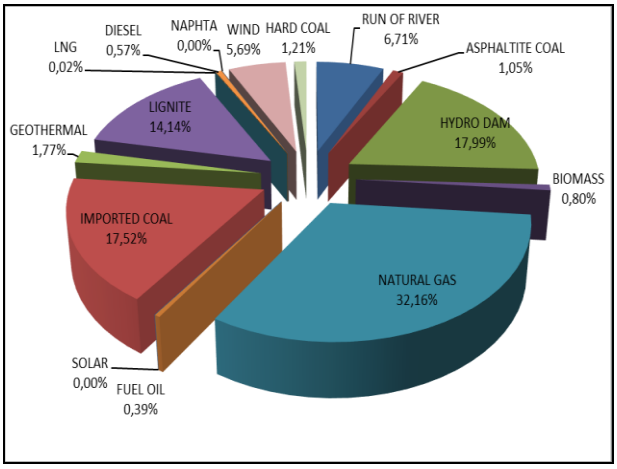

Fig. 1 Distribution of electricity generation in Turkey [10]

Energy Policy Models can be categorized under 4 titles:

1. Optimization Models
2. Simulation Models
3. Accounting Frameworks
4. Hybrids Models Combining Elements of Each Approach

Linear programming is the main element of optimization models. An optimization function is configured subject to various constraints and the best solution is found according to optimization procedure. Since the least cost/most profit is obtained at the end of the solution process, the output is mathematically optimal. MARKAL, EFOM, WASP are examples of the optimization models. On the other hand, the complex nature and the non-measurable factors that are hard to be put in equation forms are the biggest cons of these systems.

Simulation models balance the supply and demand under the given assumptions by using randomization processes. They do not optimize a given objective function and tends to be suitable for daily practices. Starting conditions can be very significant in terms of the outputs and the lack of mathematical optimization produces inferior results. ENPEP/BALANCE, Energy 20/20, EnergyPLAN, LEAP are examples for simulation softwares used in energy policy models.

Accounting frameworks are explicit accounts for outcomes of various scenarios rather than simulating decisions. They examine the implications of possible scenario under given assumptions. LEAP (can be used with simulation and accounting), MEDEE, MESAP are mostly used softwares in this category. This approach does not optimize or simulate but it does not dictate a perfect competition too. It is very helpful in capacity building applications.

Hybrid models combine elements of optimization and simulation as well as accounting (SEI). LEAP, NEMS (U.S. National Energy Modeling System).

A long list of energy tools classified as optimization, simulation and accounting framework (excluding hybrids) can be found in www.energycommunity.org website [11].

Categorization of energy tools is a popular subject and different categories appear in different sources [11-16].

There are a number of studies based on single energy tools in literature. EFOM [17], MARKAL [18-20], MOREHyS (based on BALMOREL) [21], Invert [22, 23] and UREM (University of Regina Energy Tool) [24] energy tools are studied from various point of views by the related authors. Reference [12] includes a more detailed analysis on energy policy softwares including 68 different softwares.

III. ENERGYPLAN

EnergyPLAN is a deterministic input/output simulation model [25] that can calculate various scenarios for the optimization of closed systems. Model is used to include renewable energy data from technical and financial point of view [26-28]. EnergyPLAN involves heat production from solar thermal, industrial CHP, CHP units, heat pumps, heat storage and boilers. It also includes electricity production from renewable energy. Inputs of the system are:

1- Annual heating and electricity consumption,
2- Solar and wind power capacity,
3- Capacities and operation efficiencies (boilers, CHP units, power stations, pumps),
4- Minimum power plant percentage needed to remain the grid stability,
5- Maximum heat pump percentage to achieve the specified efficiency of the heat pumps.

EnergyPLAN has been applied in 95, referred in 45 other and the model has been characterized in 40 different articles prior to 2015 [29].

TABLE 4
OCCURRENCE OF THE TERM "ENERGYPLAN" IN JOURNALS [29]

Category	Result of Article Survey
Irrelevant	7 publications prior to 2002
	14 Publications containing EnergyPLAN in URL
Duplicates	19 Publications
References to analysis	45 Publications
References to model characteristics etc	40 Publications
Application of EnergyPLAN	95 Publications between 2003-2015 2003-2010 (33 papers) 2011-2013 (34 papers) 2014-2015 (28 papers)

General overview of EnergyPLAN is given in Figure 2. Electricity and heat production with other processes are located on the figure at the right order.

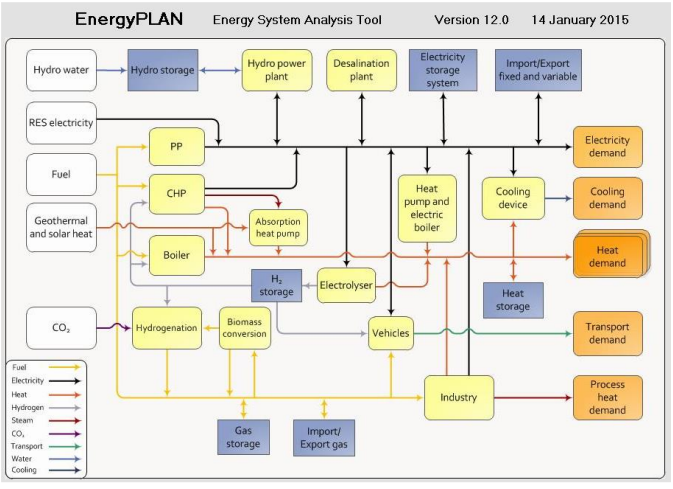

Fig. 2 Overview of EnergyPLAN [30]

A. Components of EnergyPLAN

I. Renewable Energy Sources

Wind power, offshore wind, photovoltaic, wave power, river hydro are defined in the system with their electric capacity and hourly distribution files. These files are prepared by the analysts or readily taken from EnergyPLAN website or program data files. Power generation from mainly five renewable resources have the highest priority to match the overall demand.

Hydro power, reversible hydro power and geothermal power have also various inputs to be entered to the program.

Solar thermal in district heating and in individual houses can also be defined in the program with different number of entry cells [30].

II. Waste Utilization and Conversion and Industrial Electricity and Heat Production for District Heating

Industrial CHP, industrial waste heat for district heating, waste incineration, waste CHP production, waste for biofuels for CHP and boilers and waste for biofuels for transport are entry field sets in EnergyPLAN requiring efficiency, hourly distribution and other inputs [30].

III. Nuclear Power

Electric capacity, efficiency, hourly distribution, variable operational costs, part load share are entered to EnergyPLAN [30].

IV. Power Plants, CHP units, heat pumps, electrolysers, heat storage and boilers for heat production

Boilers, CHP units, heat pumps, heat storage, electric boilers and electrolysers are defined in EnergyPLAN and numerous inputs (efficiency, capacity, cost etc.) are entered to the program [30]. Since these plants have last priority, plants counted here are utilized in the models after using renewable power plants.

V. Individual House Heating and Micro CHP

Coal boilers, oil boilers, natural gas boilers, biomass boilers, H2, natural gas and biomass micro CHP, heat pumps in individual houses, electric heating in individual houses data are entered to the program if they exist.

VI. Transport

JP (Jet Fuel) is defined for airplanes while petrol, diesel, natural gas and biofuels are defined for vehicles. Hydrogen, dump and smart charges are also available for battery electric vehicles.

VII. Electrolysers and Electricity Storage Systems

Electrolysers for hydrogen for transport and micro CHP, battery-hydro pump-hydrogen storages and Compressed Air Energy storages data are entered to EnergyPLAN if the availabilities exist.

VIII. Biomass Conversion Technologies

Data related to biogas, gasification, biodiesel and bioJP plants are required in EnergyPLAN if they will be in the model [30].

IX. Synthetic Gas and Liquid Fuel Production Plants

Data entries of hydrogenation from biogas, gasification gas and CO_2 as well as chemical synthesis are inputs of the program if required [30].

B. Externalities

It is known that electricity generation (especially) from fossil fuels, creates mostly negative impacts on third parties other than the producer and the consumer of the electricity [31]. These impacts are referred as externalities [31, 32] and described firstly in Pigou's work "The Economics of Welfare" [33]. Pigou addresses the right incentive to remove the divergence as "...by granting bounties and levying taxes, these uncompensated external benefits and costs could be internalized to those who create the externalities" [33].

Somehow, the calculation of this external cost needs a great amount of work to be carried by various parties. Numerous programs were carried out by related organizations to reach satisfactory data related to these externalities [34]. European Union initiated one of these programs, known as CASES, as a Coordination Action funded by the European Commission under the 6th Framework Programme, PRIORITY 6.1.3.2.5, Sustainable Energy Systems [35]. Objectives of CASES are:

1. To compile coherent and detailed estimates of both external and internal costs of energy production for different energy sources at the national level for the EU-27 Countries and for some non-EU Countries under energy scenarios to 2030;
2. To evaluate policy options for improving the efficiency of energy use, taking account of the full cost data (internalization of external costs);
3. To disseminate research findings to energy sector producers and users and to the policy making community.

In 2008 the project finalized its works and reports. Outputs of the project are as follows [35]:

1. Estimates of Private costs, External costs and full costs of electricity production are provided for a wide set of technologies at present in 2020 and 2030.
2. Reports on externalities of energy supply, electricity scenarios and social costs in China, Brazil, Bulgaria, India and Turkey and finally the full costs assessment of EU are reached.

This EU project covers the coal transport and power generation stages of Turkey. Since the power generation stage generally is viewed as the main externality source from fossil fuel based power generation, the final numbers are to some extent comparable with the other countries.

C. EnergyPLAN Application

TR-33 Region covers four cities. In this Business As Usual Model for 2016, the energy production and consumption figures of the cities are gathered and entered to the program (Figure 3). The inputs are gathered from various reports and websites [10],[36-46]. These figures consist of renewables such as the capacities of wind, PV etc and fossil fuels like coal, natural gas, fuels etc.

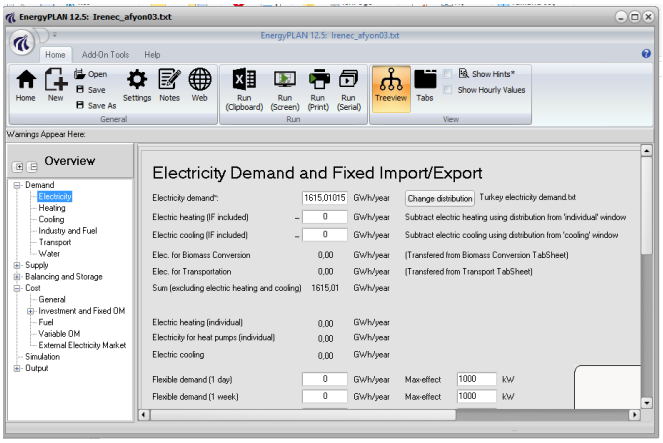

Fig. 3 Data Entry in EnergyPLAN

Cost information is available in Turkish Statistical Institute's website however for the information of externalities CASES project must be visited as described earlier. Since only two elements (lignite and hard coal was included in the project an approximation is needed to be done. It is shown that Poland is the EU country which has the nearest characteristics to Turkey when external cost calculations are done [45]. Electricity generation external costs according to CASES calculations are shown in Table 5.

TABLE 5
EXTERNAL COSTS [34]

Technology	eurocent/kWh
hydropower, run of river 10MW	0,0788
hydropower, run of river <100MW	0,0563
hydropower, run of river >100MW	0,0506
hydropower, dam (reservoir)	0,0984
hydropower, pump storage	0,0809
geothermal	1,6090
wind, off-shore	0,0774
solar PV, roof	0,9105
solar PV, open space	0,9215
solar thermal, parabolic trough	0,1292
nuclear power plant	0,1601
biogas	1,6090
heavy oil condensing power plant	3,6889
hard coal condensing power plant	3,8018
lignite condensing power plant	3,3832
natural gas combined cycle without CO_2 capture	1,6091
natural gas, gas turbine	2,5442

Two sets of EnergyPLAN models are built. In the first set, businesses as usual models are configured without external costs. These models use 415 TL/MWh cost for energy and also include the figures of energy items related to individual heating, transport and industrial activities (without coal usage in industry). EnergyPLAN models for each of the cities are built and reports are obtained.

In the second set of models external costs are included. Since the amount of sources of energy utilized in the first set of models were on hand, these data are used for external cost calculations. Average exchange rate of euro currency in 2016 is used in currency conversions [46].

IV. Results

After the proper excel calculations, electricity generation costs of TR-33 Region are found and given in Table 6:

TABLE 6
TR-33 ELECTRICITY COSTS

COSTS OF GENERATING ELECTRICITY (TL/MWh)				
	Uşak	**Afyonkarahisar**	**Kütahya**	**Manisa**
EXTERNAL COSTS	83,363	60,688	110,768	75,893
PRICE	415,000	415,000	415,000	415,000
TOTAL COST	498,363	475,688	525,768	490,893

CO_2 emissions are also given by EnergyPLAN at the end of the simulation. Values are presented in Table 7:

TABLE 7
TR-33 CO_2 NET EMISSION VALUES

CO_2 EMISSIONS (kt)				
	Uşak	**Afyonkarahisar**	**Kütahya**	**Manisa**
Coal	158,72	154,2	4650	6630
Oil	303,16	1151,38	640	1500
N.Gas	586,84	371,22	1060	1960
TOTAL	1048,72	1676,8	6350	10090

Since the overall produced electricity is known total amount of external cost calculations can be carried out. Table 8 shows the cost figures.

TABLE 8
TR-33 TOTAL EXTERNAL COSTS

	€ c	**TL**
Uşak	3.652.527.898,51	122.126.288,07
Afyonkarahisar	2.931.309.979,79	98.011.573,62
Kütahya	19.910.108.904,60	665.716.392,35
Manisa	20.042.376.590,84	670.138.907,93
TOTAL	46.536.323.373,75	1.555.993.161,96

Sorting, according to the emission rates in TR-33 region is shown in Figure 4 in ascending order. It will be concluded that Uşak has the least emission value. The amount of electricity produced in Uşak is so limited and it is importing %70 of its electricity demand from other cities. So its emission rates are fairly low. On the other hand, since Manisa and Kütahya are net energy exporters in this region, they supply more than their electricity demands and this surplus energy production causes more CO_2 emission in these two cities. In other words, they suffer the emission of the cities which import electricity from them like Uşak and Afyonkarahisar.

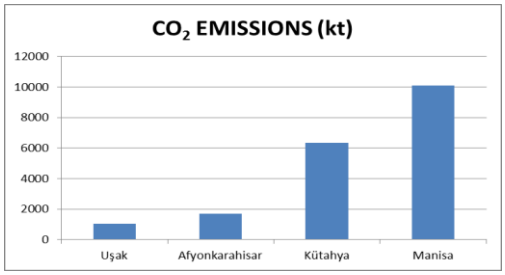

Fig. 4 CO_2 Emissions Sorted in Ascending Order

A similar analysis can be performed for external costs. The external cost (per MWh) data was given in Table 6. According to these data Kütahya had the worst external effects resulting with 525,768 TL of costs while Afyonkarahisar had the least costs of externalities only 50 TL lower than the high figures of Kütahya. Manisa and Kütahya had the high figures due to its excess electricity generation. Since Uşak buys about 70% of its electricity from these two cities its figures also resulted at high levels. Afyonkarahisar has higher amount of renewables with wind and geothermal plants. So its dependence on Kütahya and Manisa is lower than Uşak and this has caused better results by means of external costs per MWh. Ratios are shown on Figure 5.

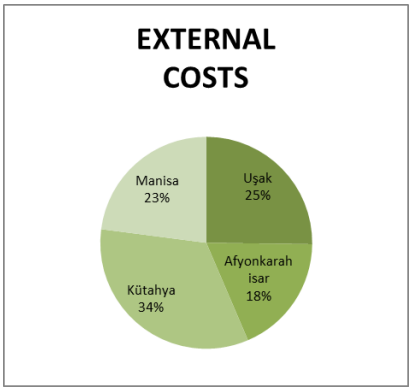

Fig. 5 External Costs of Power Generation per MWh

V. Future Work

Simulation of TR-33 Region with EnergyPLAN will be continued with the simulation of future periods. To prepare a healthy comparison base LEAP will also be applied to both BAU and future periods. After LEAP software application, the opportunity to compare the results of two different simulation packages will be available. After the simulation phase is over the optimization phase will take place and this process is planned to be held with ANSWER-TIMES optimization

package. And finally an algorithm will be applied onto the data to have outputs of the desired periods. By this way, 3 different approaches will be performed and outputs will be able to be compared for each different scenario. Business as Usual Scenario will be compared to the outputs of these approaches for each scenario and the best option will be chosen by means of technical and economical as well as environmental perspective.

REFERENCES

[1] V. Smil, *Energy - a beginners guide*, Oneworld Publications, pp. 85-90, 2006.

[2] Turkish Statistical Institute, 2017 Population of Turkey, http://www.tuik.gov.tr/ PreIstatistikTablo.do?istab_id =1590

[3] Department of State: Investment Climate Statement, June 2014 https://www.state.gov/documents/organization/229296.pdf

[4] M. Kılıç, E. Özdemir, "Long Term Energy Demand and Supply Projections for Turkey", In book: "Exergetic, Energetic and Environmental Dimensions", Edition: 1, Chapter: 1.7, Publisher: Elsevier, Editors: I. Dincer, C.O.Colpan, O.Kızılkan, pp.115-132.

[5] Turkish Statistical Institute, http://www.tuik.gov.tr/PreTablo.do?alt_id=1029

[6] Ö. Acar, "Avrupa Birliği NUTS Sisteminin Türkiye'de Uygulanması: İstatistiki Bölge Birimleri Sınıflaması (İBBS) Sisteminin Sınanması", Gazi Üniversitesi, 2008.

[7] Ü. Şengül, S. Eslemian, M. Eren, "Türkiye'de İstatistikî Bölge Birimleri Sınıflamasına Göre Düzey 2 Bölgelerinin Ekonomik Etkinliklerinin VZA Yöntemi ile Belirlenmesi ve Tobit Model Uygulaması", Yönetim Bilimleri Dergisi, vol. 11, no. 21, pp. 75-79, 2013.

[8] Official Site Of ZAFER Development Agency, About Link, http://www.zafer.org.tr/eng/about.html

[9] The General Directorate of Investment and Establishments, Turkish Border Statistics, http://yigm.kulturturizm.gov.tr/TR,9854/sinir-giris-cikis-istatistikleri.html

[10] Energy Market Regulatory Authority Electricity Market Development Report, 2016 http://www.epdk.org.tr/TR/Dokumanlar/Elektrik/YayinlarRaporlar/ElektrikPiyasasiGelisimRaporu

[11] Energy Modeling Tools in LEAP page of www.energycommunity.org, https://www.energycommunity.org/default.asp?action=tools

[12] D. Connolly, H. Lund, B.V. Mathiesen, M. Leahy , "A review of computer tools for analysing the integration of renewable energy into various energy systems" , Applied Energy vol, 87, pp. 1059-1082, April 2010.

[13] S. Jebaraj,S. Iniyan, "A review of energy models", Renewable and Sustainable Energy Reviews, vol. 10, pp. 281–311, 2006.

[14] H. Lund, Renewable Energy Systems, The Choice and Modeling of 100% Renewable Solutions, Elsevier, pp. 58, 2010

[15] R. Segurado, S. Pereira, A. Pipio, L. Alves, "Comparison between EMINENT and other energy technology assessment tools", Journal of Cleaner Production, vol. 17, pp.907–910, 2009

[16] H. Lund, Renewable Energy Systems, *The Choice and Modeling of 100% Renewable Solutions*, Elsevier, 2010

[17] C. Cormio, M. Dicorato, A. Minoia, M. Trovato, "A regional energy planning methodology including renewable energy sources and environmental constraints", Renewable Sustainable Energy Reviews, vol. 7, pp. 99-130, April 2003.

[18] R.M. Smekens, E.L. Koen, "Response from a MARKAL technology model to the EMF scenario assumptions", Energy Economics, vol. 26, pp.655– 674, 2004.

[19] F. Zonooz, M. Reza, Z.M. Nopiah, A.M. Yusof, K. Sopian, "A review of MARKAL energy modeling", European Journal of Scientific Research, vol. 26, no. 3, pp. 352-361, 2009

[20] A.J. Seebregts, G. Goldstein, K Smekens, 2001. Energy / Environmental Modelling Using the MARKAL Family of Models. In: P. Chamoni, et al., (Ed.), Operations Research Proceedings 2001—Selected Papers of the International Conference on Operations Research (OR2001) (Duisburg, Germany) Springer Verlag, Berlin, pp. 75–82, September 3–5, 2001. ISBN3-540-43344-9.

[21] M.Ball, M.Wietschel, O. Rentz, "Integration of a hydrogen economy into the German energy system: an optimising modelling approach. International Journal of Hydrogen Energy", vol. 32, no. 10-11, pp. 1355-1368, 2007.

[22] E. Tsioliaridou, G.C. Bakos, M. Stadler, "A new energy planning methodology for the penetration of renewable energy technologies in electricity sector application for the island of Crete", Energy Policy, vol.34, no. 18, pp. 3757–3564, 2006.

[23] L. Kranzl, C. Huber, "The Invert Simulation Tool", 20 Feb 2017, https://www.researchgate.net/publication/267558368.

[24] Y.P. Cai, G.H. Huang, Q.G. Lin., X.H. Nie, Q. Tan, "An optimization-model-based interactive decision support system for regional energy management systems planning under uncertainty", Expert Systems With Applications, vol.36, no. 2, part 2, pp. 3470–3482, March 2009.

[25] H. Lund, N. Duic, G. Krajacic, M.d.G. Carvalho., "Two energy system analysis models: a comparison of methodologies and results", Energy, vol. 32, no. 6, pp. 948–954, June 2007.

[26] H. Lund, E. Münster, "Management of surplus electricity-production from a fluctuating renewable-energy source", Applied Energy, vol. 76 no. 1-3, pp. 65–74, 2003.

[27] Lund H., "Large-scale integration of wind power into different energy systems", Energy, vol. 30, no. 13, pp. 2402–2412, October 2005.

[28] H. Lund, E. Munster, "Integrated energy systems and local energy markets", Energy Policy, vol. 34, no. 10, pp. 1152–1160, July 2006.

[29] P.A. Ostergaard, "Reviewing EnergyPLAN Simulations and Performance Indicator Applications in EnergyPLAN Simulations", Applied Energy, vol. 154, pp. 921-933, September 2015.

[30] H. Lund, EnergyPLAN, "Advanced Energy Systems Analysis Computer Model Documentation Version 13" September 2017

[31] A. Markandya, "Externalities From Electricity Generation and Renewable Energy. Methodology and Application in Europe and Spain", Cuadernos económicos de ICE, vol. 83, pp. 85-99, 2012.

[32] A. Longo, A. Markandya, M. Petrucci, "The internalization of externalities in the production of electricity: willingness to pay for the attributes of a policy for renewable energy". Ecological Economics, vol.67, pp. 140–152, 2008.

[33] A. Pigou, *The Economics of Welfare*, MacMillan, London, 1920, pp. 159-168.

[34] Official Site of EXTERNE, External Costs Of Energy Page, http://www.externe.info/externe_d7/?q=node/56

[35] Official website of Cost Assessment for Sustainable Energy Systems (CASES Consortium), http://www.feem-project.net/cases/

[36] Energy statistics page for Turkey, http://www.enerjiatlasi.com/

[37] Energy Market Regulatory Authority Turkish NG Market Report 2016 http://www.epdk.org.tr/TR/Dokumanlar/Dogalgaz/YayinlarRaporlar/Yillik

[38] Energy Market Regulatory Authority Turkish LPG Market Report 2016 http://www.epdk.org.tr/TR/Dokumanlar/LPG/YayinlarRaporlar/Yillik

[39] Energy Market Regulatory Authority Turkish Petroleum Market Report 2016http://www.epdk.org.tr/TR/Dokumanlar/Petrol/YayinlarRaporlar/Yillik

[40] 2016 Environmental Status Report of Uşak Provincial Directorate Of Ministry Of Environment and Urbanization, *webdosya.csb.gov.tr/db/ced/editordosya/Usak_icdr2016.pdf*

[41] 2016 Environmental Status Report of Manisa Provincial Directorate Of Ministry Of Environment and Urbanization, webdosya.csb.gov.tr/db/ced/editordosya/MANISA%20%202016%20ICDR.pdf

[42] 2016 Environmental Status Report of Kütahya Provincial Directorate Of Ministry Of Environment and Urbanization, *webdosya.csb.gov.tr/db/ced/editordosya/Kutahya_icdr2016.pdf*

[43] 2016 Environmental Status Report of Afyonkarahisar Provincial Directorate Of Ministry Of Environment and Urbanization, webdosya.csb.gov.tr/db/ced/editordosya/Afyonkarahisar_icdr2016.pdf

[44] EnergyPLAN Model of Turkey (2012-2020-2030) http://www.energyplan.eu/useful_resources/existingcountrymodels/

[45] E. DAL, The Analysis Of The Use Of Renewable Energy Sources in Electricity Generation Based on Technological, Political and Environmental Constraints in Turkey, Hacettepe University, 2017.

[46] Euro – TL Currency Conversion and Statistical Values http://paracevirici.com/doviz-arsiv/merkez-bankasi/gecmis-tarihli-doviz/2016/euro.

Design and Analysis of a 0.5 MW Grid-Connected Solar PV System in Karabuk University Using PVSYST Simulator

Abdurazaq Elbaz[1], Muhammet Tahir Güneşer[2]

Abstract - In this paper, PVSYST software was used to design and analysis 0.5 MW Grid-connected photovoltaic system for Karabuk University, Karabuk in Turkey. Detailed system configuration, system output and system losses were determined. Thanks to simulation results, the optimal size of the PV system was planned to supply the electricity to the university during the year. In the system, 1256 PV modules and five grid-connected inverters were offered as the optimal solutions for loading of the university. Totally 634.86 MWh electricity would be supplied to the grid in a year.

Additionally, the performance of the 0.5 MW grid-connected solar PV system was simulated over the guaranteed life of the system using PVSYST software. The project began with a broad database of meteorological data, including global daily horizontal solar irradiance and a database of various renewable energy system components from different manufacturers.

Keywords **-** PVSYST software, Grid-connected, photovoltaic system, meteorological data.

I. INTRODUCTION

Renewable energy sources can supply sustainable and clean energy for the world such as Sun and wind energy systems. Photovoltaic (PV) systems are one of the most important and promising technologies to supply electricity for demand of the whole globe. Since the last decade, the photovoltaic industry increases more than 40% per year beside of the decline in photovoltaic system costs. PV systems can be established in two different design, which are called as stand-alone and grid-connected PV systems. Grid-connected PV systems are connected to the grid whereas stand-alone system supply the load directly [1-2].

Turkey is known as dependent to others for energy resources, so 70 % of total energy consumption is supplied by importing. But according to researches and calculations, yearly renewable energy potential of Turkey is around 560 TWh and the potential of solar energy is greater than other renewable energy forms. Solar energy can be used to heat and cool buildings, hot water for domestic and industrial uses, generate electricity, and many more operations [3-4].

Abdurazaq Elbaz[1] Tripoli University / LIBYA
Muhammet Tahir Güneşer[2] Karabük University / TURKEY

In this paper, sizing and performance of output power of grid-connected photovoltaic system was designed and simulated for the Karabuk University, Karabuk, Turkey by using PVSYST 6.41 software analysis. The system is designed to supply the campus of the university with optimum power for all over the year.

B. Location Details and Meteorological Data For The Proposed Location

In PVSYST, the solar resource input can be determined the coordinates of the location. Based on position coordinates, data can be access from NASA website dealing with Meteorological data. The selected site at Karabuk University in Karabuk city, which lies on Lat.: 41.22º N, Long.: 32.65º E [5-6].
Karabuk, the city is a landlocked province in the northern part of central Turkey, located far away about 200 km north from Ankara and situated about 100 km south of the Black Sea coast as seen on Figure 1.

Figu 1. PV System Location

C. Solar PV Technology

The solar panel used in the system is Sunpower SPR-400. It composed of multi-crystalline 156mm by 156mm solar cells. Each panel has 128 cells and module dimensions are 2,067 × 1,046 × 54mm. The I-V curve of the module at Standard Test Condition (STC) with the total irradiance of 1000 W/m2 and cell temperature of u5 °C is shown in Figure 2. According to

the I-V curve, the maximum power point is 370.5 WDC. In addition, the electrical specifications of the module are present in Table 1 [5-7].

D.Inverter

In this section, the employed inverter and its specifications are introduced. A Green power PV100 inverter has been used here five inverters. The efficiency curve of the inverter is show in Figure 3 and the technical data are present in Table 2 [5-7].

Electrical specs	Value
Peak power watts-Pmax	400 W
Module Efficiency	18.5%
Maximum power current	5.49A
Maximum power voltage	72.9V
Short circuit current	5.74A
Open circuit voltage	85.3V
Maximum System Voltage	600V

Table 1. Module electrical data

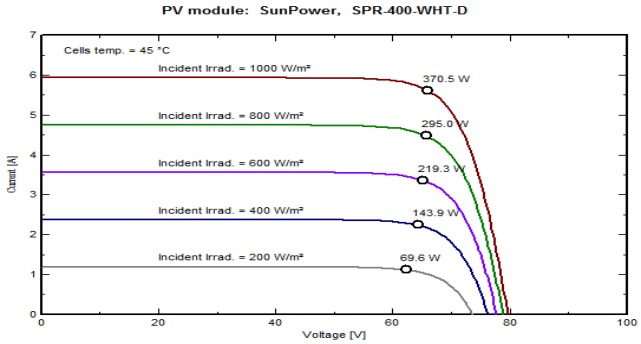

Fig. 2 Sunpower SPR-400 solar panel I-V curve at **STC.**

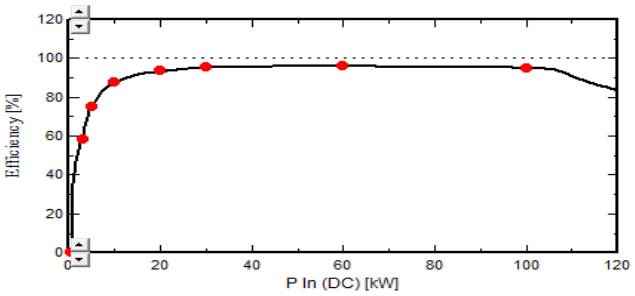

Fig. 3 Efficiency Curve of the inverter

Technical specs	Value
Voltage range (MPPT)	425-800 Vdc
Maximum input voltage	900 Vdc
Maximum current	250 A
Line voltage output	3x400 Vac
Nominal Power	100 kW
Maximum output current	173 A
Maximum efficiency	96 %
Size (mm)	1200x800x1800
Weight	10.20 kg

Table 2. Inverter Technical Data

II. DESIGN BASED ON SOFTWARE

Design and assess the results of 0.5 MW solar power plant by using PVSYST software version 6.49. It is probable to have prioritized and as well as post estimation test data for the feasible power generation. The total system performance and efficiency of each system of the plant are evaluated by entering the specifications of an individual design. Design the system through to the above specifications of all components [6- 8].

III. RESULTS AND DISCUSSIONS

All the parameters underlying this simulation: Geographical situation and Mateo data used, plane orientation, general information about shadings (horizon and near shadings), components used and array configuration, loss parameters, etc. Figure 4 shows sun path for the Karabuk University location [6-7].

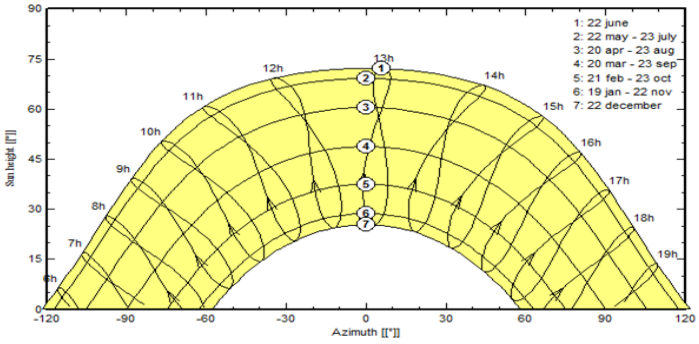

Fig. 4 Solar Paths at Karabuk (Lat. 41.220N, Long.32.650E, alt. 338m)

E. MAIN RESULTS

Produced energy: 635 MWh/year
Specific production: The produced energy divided by the Nominal power of the array (Pnom at STC).
This is an indicator of the potential of the system, taking into account irradiance conditions (orientation, site location, meteorological conditions).
Specific Production = (Produced energy/Nominal Power of the array).
Specific Production = 1270 kWh/kWp/year.
Performance ratio: 80% [6-8].

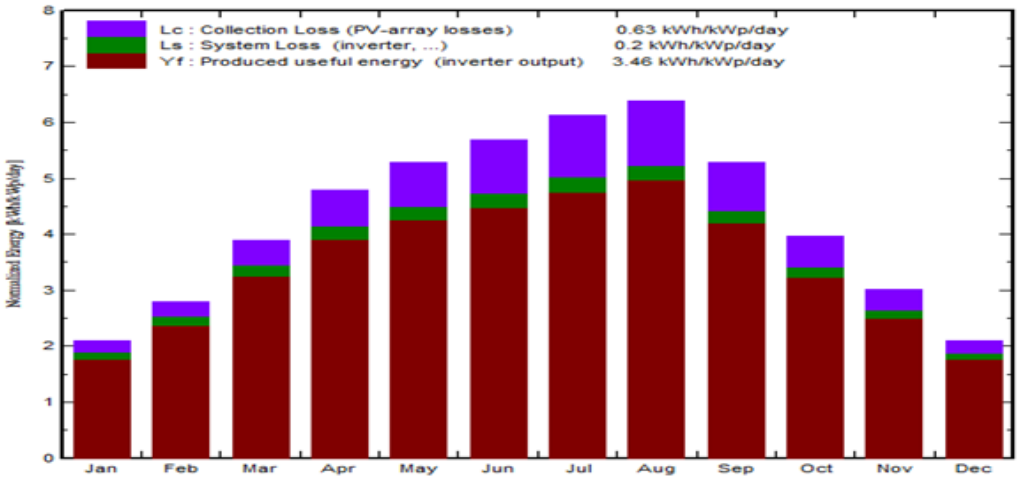

Fig. 5 Normalized Productions (per installed kWp)

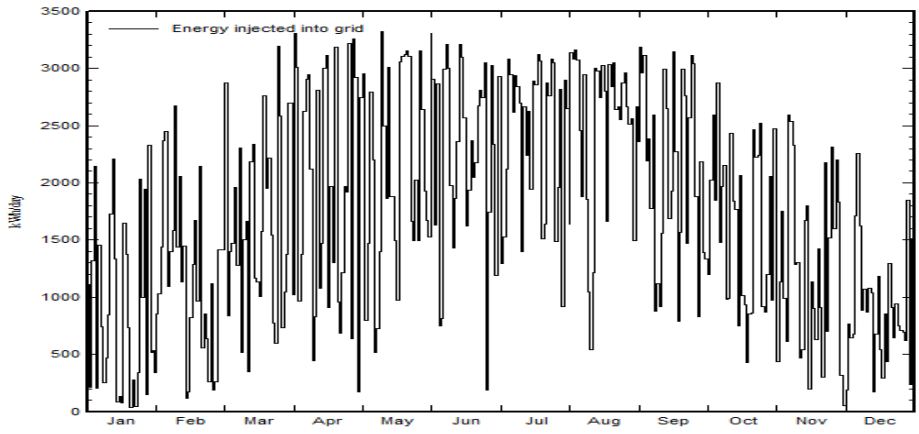

Fig. 6 Daily System Output Energy

The greatest power generation achieved was 3300kWh/day in the month of May. With the registered insulation, average module temperature, 310C, and 80 % respectively.
The decline in the energy generated during the January and December duration in figure 6 was mainly due to the higher plant downtime and number of cloudy days during that period. The deviation is clearly visible in figure 5.
System Losses: PV system is not able to convert 100% energy received from the solar radiation because of various losses. Figure 7 illustrate of detailed losses occur in the proposed grid- connected PV system. Firstly about 1402 kWh/m2 radiation is incident on the solar panels.

The Biggest losses had done during PV array electric production. Su-400 module has 15.25 % efficiency at the STC. By this, 765 units of the electricity will be produce in a year by the PV array. After that due to the PV panel losses, Inverter losses and wiring losses, about 635 units of electricity are available to the grid in a year.

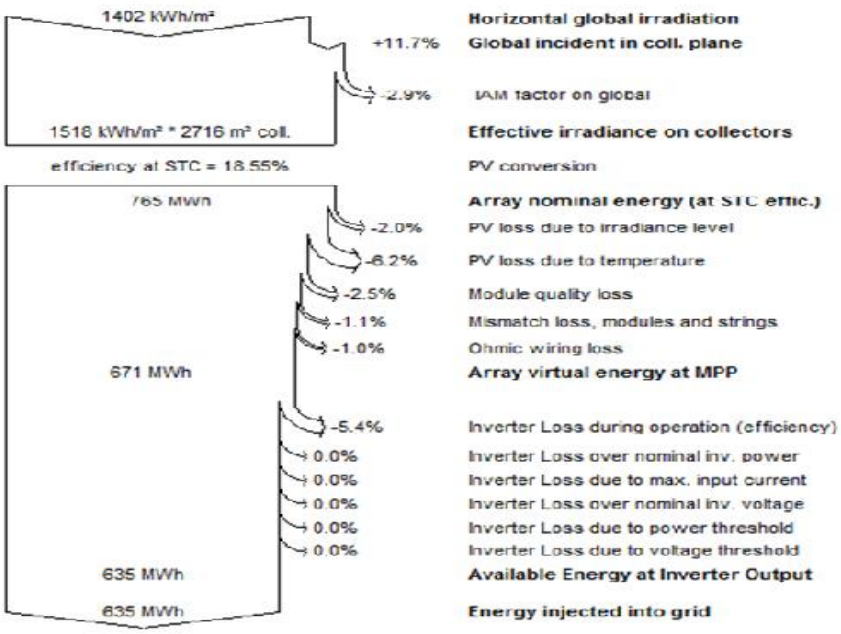

Figure 7 Detailed System Losses

IV. CONCLUSION

A grid-connected photovoltaic system was designed by using PVSYST V6.10 simulation software for the main campus of Karabuk University. By using the software, the energy yield analysis for 0.5 MW PV Solar power generation was performed for geographical position of Karabuk University, which is situated at a latitude of 41.22º N and longitude 32.65º E, and with the horizontal global irradiation of 1402 kWh/m2.

In this paper, we simulated an accurate sized of the grid-connected system with chosen suitable PV model and inverters. The system consisted of 1256 PV modules and five solar inverters with the power of 100 kW, which are the optimal solution for supplying the campus of Karabuk University during the year. With the proposed system, 634.862 MWh electrical energy will be generated in a year and the performance ratio of the system is calculated as 80.7%.

REFERENCES

[1] Rachit Srivastava, Vinod Kumar Giri, 2017. Design of Grid Connected PV System Using Pvsyst, African Journal of Basic & Applied Sciences, ISSN 2079-2034, doi: 10.5829/idosi.ajbas.2017.92.96, MMMUT, Gorakhpur, India.

[2] Ebenezer Nyarko Kumi, Abeeku Brew- Hammond. 2013. Design and Analysis of a 1MW Grid- Connected Solar PV System in Ghana. African Technology Policy Studies. Network, ATPS: ATPS WORKING PP No. 78.

[3] Renewables Global Status Report (Paris: REN21 Secretariat, Renewables 2017 Global status report, ISBN 978-3-9818107-6-9.

[4] Haci Sogukpinar, Ismail Bozkurt. An Economic Analysis Of Residential PV SYSTEM for Adiyaman, Turkey. 2015, Uludağ University Journal of The Faculty of Engineering, doi: 10.17482/uujfe.12093.

[5] Solar Server (2010), Solar Electricity: Grid-Connected Photovoltaic Systems, SolarServer Online Energy Portal to Solar Energy (Retrieved on April 17, 2011) http://www.solarserver. Com/knowledge/basic-knowledge/grid-connected-photovoltaic-systems.html.

[6] Vasanthkumar, Dr. S. Kumarappa, Dr. H. Naganagouda , 2017. Design and Development of 5MW Solar PV Grid Connected Power Plant Using PVsyst, International Research Journal of Engineering and Technology (IRJET) , e-ISSN: 2395-0056 , p-ISSN: 2395-0072.

[7] SolarEdge, "Application Note - How to Simulate a Solar Edge PV System in PVsyst", November 2016.

[8] PVSyst. PVSyst Photovoltaic Software. Satigny, Switzerland: PVSyst SA. Available online at http://www.pvsyst.com/en/).

A review of perylene diimides for solar cell application

Tonderai Linah Ruwa[1]

***Abstract*—**Solar energy has gone past the era of pleading for attention both in research and development as well as in use. Organic materials such as polymers and small molecules are gaining much ground as seen from the exponential rise in publications. This study aims to focus on reviewing the use of polymer materials in photovoltaic applications, in particular, perylene diimides (PDIs) and their derivatives. A number of reviews have been presented previously, this review serves to give an updated look at recent developments and also bring out evidence of the effect of different functional groups at different positions on the material's chemical and electronic properties. With a clear review of the current synthesized PDIs, a research direction can be mapped to select the PDIs with the highest potential to produce efficient bulk heterojunction BHJ solar cells as well as any existing gaps in the current knowledge base.

***Keywords*—** Perylene diimides, bulk heterojunction organic solar cells

I. INTRODUCTION

THE year 2017 saw the world's highest installation of solar power to date [1], [2]. The most prevalent material in solar photovoltaic technology is Silicon [3]. Organic materials such as polymers and small molecules are gaining much ground as seen from the exponential rise in publications [4]-[11], only to mention a few. Their main selling points are easy processing, mechanical flexibility and low fabrication cost [12]-[17]. This study aims to focus on reviewing the use of polymer materials in photovoltaic applications, in particular, perylene diimides and their derivatives. This group of compounds is most interesting because of the wide range of derivatives that can come from the main Perylene-3,4,9,10-perylene tetracarboxylic acid diimide (PDI) backbone. By functionalizing the PDI on different positions, namely imide and bay positions, the chemical and electronic properties can be tailored.

II. ORGANIC PHOTOVOLTAICS

Electron orbital hybridization in certain small molecules and polymers ensures the availability of delocalized electrons which are readily polarizable [18]. In lieu of the valence and conduction band, OPV materials contain the highest occupied molecular orbital (HOMO) and lowest unoccupied molecular orbital (LUMO) [19]. The basic device structure consists of the active layer containing organic semiconductor material sandwiched between two electrodes [20]. The active layer consists of a donor (D); a p-type semiconductor and acceptor (A); an n-type semiconductor material [21]. The configuration of the active layer evolved from single layer to multiple layer and now most commonly used is the bulk heterojunction (BHJ) [22]. The BHJ is considered most successful as it offers a wider donor-acceptor interface for the improved electron-hole separation [23].

Fig. 1 shows a schematic of the organic solar cell structure. Electropositive metals such as Aluminum and Calcium are used for the cathode and Indium tin oxide is normally used as the anode [24]. A hole-collecting layer is used to interface between active layer and anode, most commonly PEDOT:PSS [25].

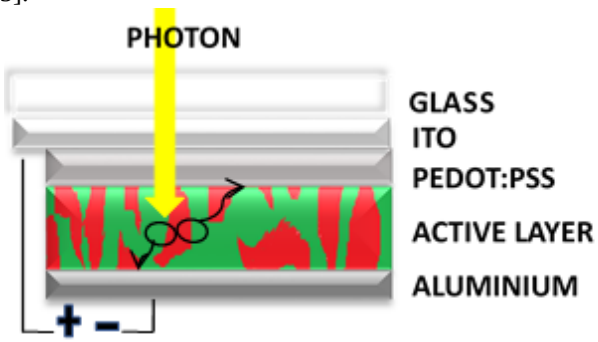

Fig. 1 Schematic of bulk heterojunction solar cell

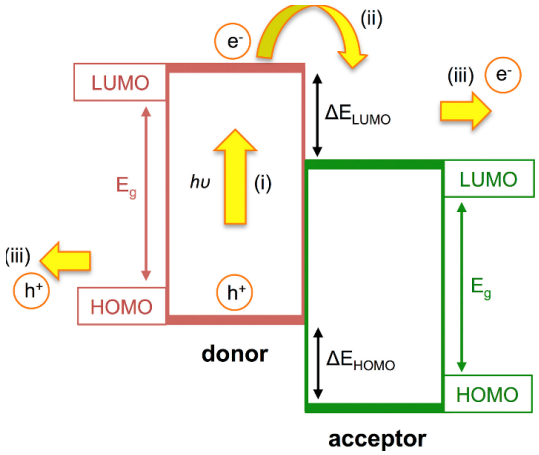

Tonderai Linah Ruwa[1], Energy Systems Engineering, Institute of Graduate Studies and Research, Lot 7/9 Chicago plots, Kwekwe, ZIMBABWE (+90 392 671 1111-2466 / +905338846522 ; truwa@ciu.edu.tr)

Fig. 2 adapted from [26] shows the energy levels and the movement of electrons due to photo excitation to produce current in the external circuit.

Fig. 2 Schematic diagram showing the HOMO and LUMO energy levels of the donor and acceptor. (i) Photon hυ > Eg when absorbed causes promotion of electron from HOMO to LUMO of donor (ii) charge transfer at donor-acceptor interface (iii) charge transport to electrodes [26].

Organic photovoltaic materials (OPVs) offer a potential to produce cheaper, more environmentally PV panels through cheaper fabrication processes e.g. roll-to-roll printing on more flexible substrates that can be integrated on any surface or material e.g. in buildings or clothing [27]. Conjugated polymers have been widely used as donor materials whilst fullerenes have been used as acceptor materials. Where polymers are used as both donor and acceptor materials the devices are called "all polymer" solar cells [6], [28]-[32].

Acceptor materials should have a high electron affinity. Fullerene derivatives such as phenyl-C61-butyric acid methyl ester (PCBM) have been well researched and applied in bulk heterojunction solar cells [33]-[35]. The good electron mobility, sufficient band gap and compatibility with donor materials of fullerenes has favored them for use as n-type materials in OPV devices that recorded good PCEs. Upcoming acceptor materials, not based on fullerene, with demonstrated high electron mobility have been reviewed. When used in OPV devices, relatively low PCEs where obtained [26]-[32]. However, this is not a deterrent as the other advantages of the acceptor materials such as high absorptivity and tunable band gaps still provide motivation to researchers [27]-[31].

III. PERYLENE DIIMIDES

Perylene diimides (PDIs) is the name given to the derivatives of Perylene-3,4,9,10-perylene tetracarboxylic acid diimides. This compound is a very versatile compound discovered in the early 1900s and used as dyes and pigments [36]. It has also been used in many other applications including biochemical and electronic functions [37], [38]. The structure of the PDI is of great interest as it presents so many functionalization options. Fig. 3 adapted from [36] shows the imide and bay positions that are of interest to this review. Much research is going into trying different groups to different positions so as to manipulate the energy levels and enhance the electronic, optical and chemical properties of the PDIs for use in BHJ solar cells.

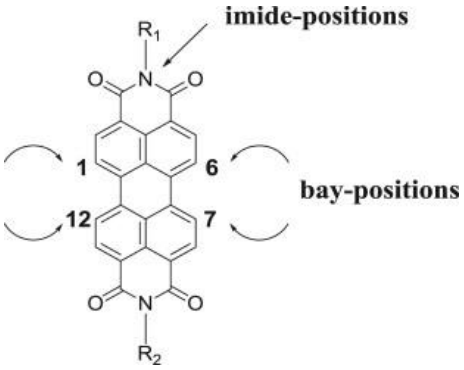

Fig. 3 Structure of perylene diimides [36].

Reference [36] is a comprehensive review conducted in 2013 of 78 PDI based materials for organic solar cells, 56 of which have actually been tested in cells. The best performance recorded were 2.23% PCE for polymer acceptors containing PDI and 3.88% for single PDI molecule acceptor. The authors state that imide position substitutions on the PDI molecule influence solubility, with branched long alkyl chains giving high solubility. Imide substitutions also influences the solid state aggregation of PDI. In addition, bay position substitutions are said to influence electronic properties of the PDI molecule. The type of the substituent groups influences the imposed structural and electronic effect. Highly electron donating groups lower the energy gap by lowering the HOMO energy level. In conclusion, the authors list the main areas from which improvement of PDIs for solar cells should emanate; (i) focus of chemical design on improving processability and solid state aggregation properties for ease of device fabrication and industrial scale-up efforts; (ii) energy level tailoring to enhance optical absorption, charge separation and transport; (iii) continuous search for better donor materials to match with the synthesized acceptors; (iv) examining the other issues surrounding efficient device fabrication such as device architecture process optimization.

IV. RECENT ADVANCES

There have been many recent developments in PDIs applied in BHJ solar cells. Although the efficiency has still not reached levels to compete with silicon solar cells. Unfortunately, there has also been some erroneous results that have been published purporting to have high efficiencies [39]. Advances have been made in both polymer containing PDI as well as small molecule PDIs.

A. PDI small molecules

The small molecules of perylene diimides tailored for use in organic solar cells have to strike a balance between limiting π stacking and maintaining enough orbital overlap for electron transport [40]. For this review, only best results from the different references are reported. Solar cell performance figures are given in Table 1. Reference 41 gives the star linked small molecules shown in Fig. 4. The results show that the S and Se annulated PDIs performed better than the PDI.

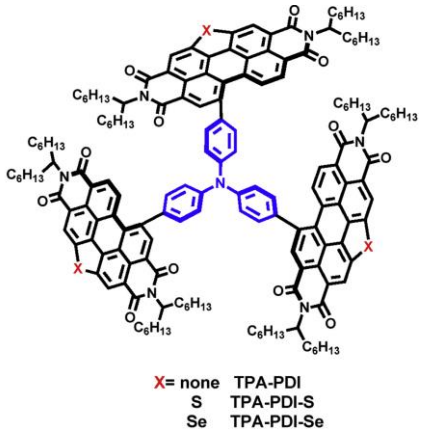

Fig. 4 Three star linked small molecule PDIs synthesized and tested in OSCs in [41]

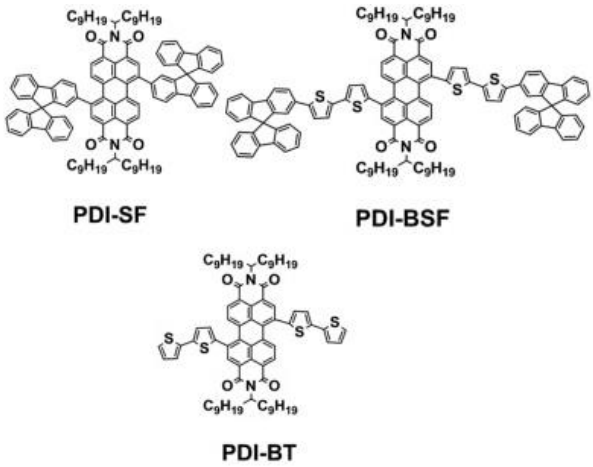

Fig. 5 Three Donor-Acceptor-Donor perylene diimide (PDI) molecules, substituted in bay positions synthesized and tested as electron-acceptor materials in solar cells in [42]

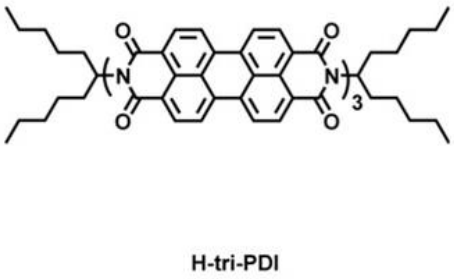

Fig. 6 Trimer of PDI was synthesized and tested in [43]

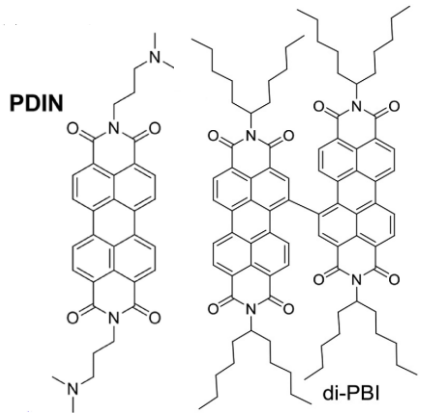

Fig. 7 PDIN is the imide substituted PDI synthesized and tested in [44] and di-PBI is the dimer reported in [45]

Comparison similar PDIs synthesized in [44] showed that the alkyl chain length and branching point affects drastically solubility and film formation.

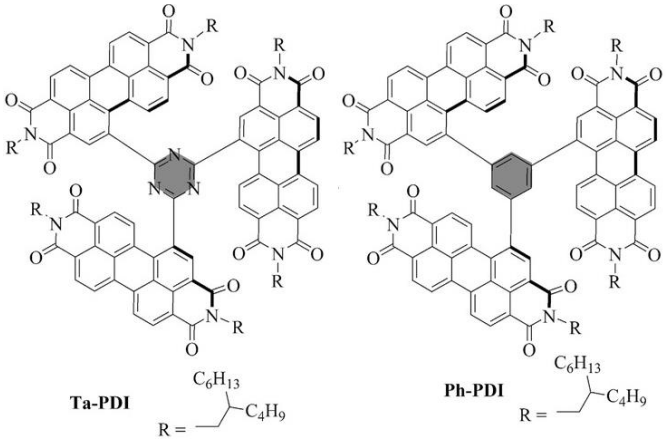

Fig. 8 shows two star linked small molecule PDIs synthesized and tested in [46].

TABLE I
SOLAR CELL PERFOMANCE OF SMALL MOLECULE PDIS

PDI	V_{OC} (V)	J_{SC} (mA cm^{-2})	FF	PCE %	Ref.
TPA-PDI	0.942	9.80	0.47	4.42	41
TPA-PDI-S	0.999	9.42	0.59	5.60	41
TPA-PDI-Se	0.999	10.24	0.58	6.10	41
PDI-SF	0.77	3.61	0.57	1.58	42
PDI-BSF	0.71	3.11	0.53	1.18	42
PDI-BT	0.52	3.05	0.51	0.81	42
H-tri-PDI	0.732	16.52	0.60	7.25	43
PDIN	0.75	8.09	0.53	3.21	44
di-PBI	0.80	11.98	0.59	5.90	45
Ph-PDI	0.85	11.91	0.549	5.57	46
Ta-PDI	0.78	17.10	0.685	9.15	46

The central cores of 2,4,6-trichloro-1,3,5-triazine and 1,3,5-tribromobenzene of the Ta-PDI and the Ph-PDI respectively, significantly affected the properties of the molecules. Ta-PDI ultimately showed better results due to stronger and wider absorption and greater π–π stacking and thus higher charge transport mobility [46].

It would seem that the small molecules that have achieved success contain more than one perylene core.

B. PDI Polymers

The ultimate goal in developing organic materials for solar cells is to end up with materials that can be easily processed in solution for the purpose of large scale production. In this regard, polymers have proved to be superior to small molecules [48]-[51]. Their disadvantage on the other hand is the active layer morphology commonly characterized by large domain sizes which hinder charge separation and transport and thus limit PCEs [50]. Bay linked conjugated polymers of PDI have shown good performance in OSCs with PCEs of 8% and above [50]-[51]. The pioneering conjugated polymers of perylene diimides bridge by electron rich dithienothiophene (DTT) and DTT oligomers to create alternating donor and acceptor moieties. These have been well documented in previous reviews [52], [53].

A novel polymer of vinylene bridged PDI units was synthesized with the intention to reduce steric hindrance in the bay area of the polymer backbone and subsequently enhance electron transport [47]. The structure is shown in fig. 9. This polymer is highly notable because it was air processed and had no post treatment or processing additives. This is of great advantage when it comes to up-scaling production for commercial purposes as it reduces processing costs.

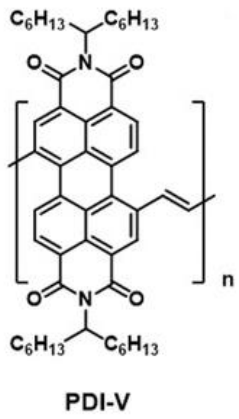

Fig. 9 PDI-V polymer synthesized and tested in OSCs in [47]

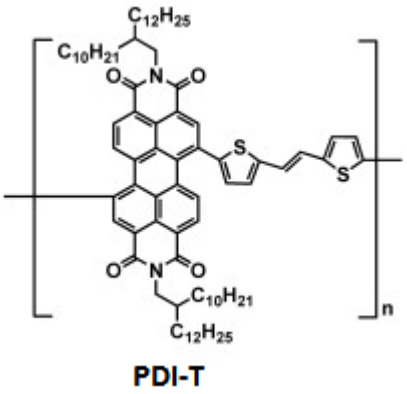

Fig. 10 PDI polymer synthesized in [54]

The polymer presented in [54] performed better than a small molecule dimer of PDI linked with the same thiophene group and this is attributed to improved network morphology and balanced hole and electron mobilities of the blended films.

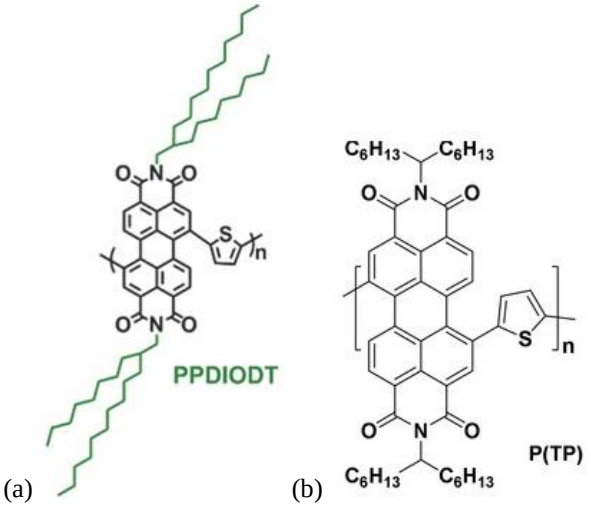

Fig. 11(a) PPDIODT polymer synthesized and tested in conventional as well as inverted solar cells in [55]. Fig. 11(b) P(TP) perylene diimide based polymer synthesized in [56].

The long alkyl chains produce high solubility in the polymer. The molecular design also limits recombination and produces higher carrier collection efficiency [55]. Reference [56] states that a side-chain engineering approach using polystyrene allows for the manipulation of phase separation domain size and enhances all-polymer solar cell performance. This is proved to influence the current density and ultimately the efficiency in a positive way.

TABLE 2
SOLAR CELL PERFOMANCE OF POLYMERIC PDIs

PDI	V_{OC} (V)	J_{SC} (mA cm^{-2})	FF	PCE %	Ref.
PDI-V	0.75	16.1	0.64	7.57	47
PDI-T	0.76	3.29	0.40	1.00	54
PPDIODT	0.76	15.72	0.55	6.58	55
P(TP)	1.05	9.16	0.47	4.31	56

V. Conclusion

PDI polymer as well as small molecules are making reasonable progress in terms of power conversion efficiency of bulk heterojunction solar cells. Even though fullerene remains higher in efficiency, the market and industry will soon have to make way for non-fullerene acceptors and particularly PDIs. The review looked at the small molecules and polymers reported from 2014. Most other publications include those reported earlier and have since been reported multiple times. It appears as if more progress is being made in small molecules than in polymers. In terms of effect of substituent groups, there is a consensus that imide groups generally influence the chemical properties, mainly solubility and bay groups influence electronic properties. However, the effects of other major factors such as solvents and device architecture cannot be ignored.

Acknowledgment

The author would like to acknowledge Associate Professsor Dr. Mustafa Dağbaşı for the financial and moral support given towards this paper.

References

[1] Kaushika N.D., Mishra A., Rai A.K. (2018) Introduction to Solar Photovoltaic Power. In: Solar Photovoltaics. Springer, Cham pp 3-14
[2] REN21. 2017. Renewables 2017 Global Status Report (Paris: REN21 Secretariat) pp 63-65
[3] Parida, B., Iniyan, S. and Goic, R., 2011. A review of solar photovoltaic technologies. Renewable and sustainable energy reviews, 15(3), pp.1625-1636.
[4] Li, S., Ye, L., Zhao, W., Zhang, S., Mukherjee, S., Ade, H. and Hou, J., 2016. Energy-Level Modulation of Small-Molecule Electron Acceptors to Achieve over 12% Efficiency in Polymer Solar Cells. Advanced Materials, 28(42), pp.9423-9429.
[5] Yao, H., Chen, Y., Qin, Y., Yu, R., Cui, Y., Yang, B., Li, S., Zhang, K. and Hou, J., 2016. Design and synthesis of a low bandgap small molecule acceptor for efficient polymer solar cells. Advanced Materials, 28(37), pp.8283-8287.
[6] Gao, L., Zhang, Z.G., Xue, L., Min, J., Zhang, J., Wei, Z. and Li, Y., 2016. All-Polymer Solar Cells Based on Absorption-Complementary Polymer Donor and Acceptor with High Power Conversion Efficiency of 8.27%. Advanced materials, 28(9), pp.1884-1890.
[7] Yang, L., Zhang, S., He, C., Zhang, J., Yao, H., Yang, Y., Zhang, Y., Zhao, W. and Hou, J., 2017. New wide band gap donor for efficient fullerene-free all-small-molecule organic solar cells. Journal of the American Chemical Society, 139(5), pp.1958-1966.
[8] Zhang, G., Zhang, K., Yin, Q., Jiang, X.F., Wang, Z., Xin, J., Ma, W., Yan, H., Huang, F. and Cao, Y., 2017. High-performance ternary organic solar cell enabled by a thick active layer containing a liquid crystalline small molecule donor. Journal of the American Chemical Society, 139(6), pp.2387-2395.
[9] Zhao, W., Li, S., Yao, H., Zhang, S., Zhang, Y., Yang, B. and Hou, J., 2017. Molecular optimization enables over 13% efficiency in organic solar cells. Journal of the American Chemical Society, 139(21), pp.7148-7151.
[10] Bin, H., Yang, Y., Zhang, Z.G., Ye, L., Ghasemi, M., Chen, S., Zhang, Y., Zhang, C., Sun, C., Xue, L. and Yang, C., 2017. 9.73% Efficiency nonfullerene all organic small molecule solar cells with absorption-complementary donor and acceptor. Journal of the American Chemical Society, 139(14), pp.5085-5094.
[11] Hou, J., Inganäs, O., Friend, R.H. and Gao, F., 2018. Organic solar cells based on non-fullerene acceptors. Nature materials, 17(2), p.119.
[12] Elumalai, N.K. and Uddin, A., 2016. Open circuit voltage of organic solar cells: an in-depth review. Energy & Environmental Science, 9(2), pp.391-410.
[13] Yang, X. and Uddin, A., 2014. Effect of thermal annealing on P3HT: PCBM bulk-heterojunction organic solar cells: A critical review. Renewable and Sustainable Energy Reviews, 30(C), pp.324-336.
[14] Chen, S., Liu, Y., Zhang, L., Chow, P.C., Wang, Z., Zhang, G., Ma, W. and Yan, H., 2017. A wide-bandgap donor polymer for highly efficient non-fullerene organic solar cells with a small voltage loss. Journal of the American Chemical Society, 139(18), pp.6298-6301.
[15] Ameri, T., Khoram, P., Min, J. and Brabec, C.J., 2013. Organic ternary solar cells: a review. Advanced Materials, 25(31), pp.4245-4266.
[16] Ameri, T., Li, N. and Brabec, C.J., 2013. Highly efficient organic tandem solar cells: a follow up review. Energy & Environmental Science, 6(8), pp.2390-2413.
[17] Li, G., Zhu, R. and Yang, Y., 2012. Polymer solar cells. Nature photonics, 6(3), p.153.
[18] Hoppe, H. and Sariciftci, N.S., 2004. Organic solar cells: An overview. J. Mater. Res, 19(7), pp.1924-1945.
[19] H. Spanggaard and F. C. Krebs, A 2004. Brief History of the Development of Organic and Polymeric Photovoltaics. Solar Energy Materials and Solar Cells, Vol. 83, No. 2-3, pp. 125-146.
[20] Kippelen, B. and Brédas, J.L., 2009. Organic photovoltaics. Energy & Environmental Science, 2(3), pp.251-261.
[21] Yu, G., Gao, J., Hummelen, J.C., Wudl, F. and Heeger, A.J., 1995. Polymer photovoltiac cells: Enhanced efficiencies via a network of internal donor-acceptor heterojunctions. Science, 270(5243), p.1789.
[22] Brabec, C.J., Sariciftci, N.S. and Hummelen, J.C., 2001. Plastic solar cells. Advanced functional materials, 11(1), pp.15-26.
[23] Mayer, A.C., Scully, S.R., Hardin, B.E., Rowell, M.W. and McGehee, M.D., 2007. Polymer-based solar cells. Materials today, 10(11), pp.28-33.
[24] Sun, S., Fan, Z., Wang, Y. and Haliburton, J., 2005. Organic solar cell optimizations. Journal of materials science, 40(6), pp.1429-1443.
[25] Park, S.H., Roy, A., Beaupré, S., Cho, S., Coates, N., Moon, J.S., Moses, D., Leclerc, M., Lee, K. and Heeger, A.J., 2009. Bulk heterojunction solar cells with internal quantum efficiency approaching 100%. Nature photonics, 3(5), pp.297-302.
[26] Holliday, S., Li, Y. and Luscombe, C., 2017. Recent Advances in High Performance Donor-Acceptor Polymers for Organic Photovoltaics. Progress in Polymer Science.
[27] Spyropoulos, G.D., Kubis, P., Li, N., Baran, D., Lucera, L., Salvador, M., Ameri, T., Voigt, M.M., Krebs, F.C. and Brabec, C.J., 2014. Flexible organic tandem solar modules with 6% efficiency: combining roll-to-roll compatible processing with high geometric fill factors. Energy & Environmental Science, 7(10), pp.3284-3290
[28] Facchetti, A., 2013. Polymer donor–polymer acceptor (all-polymer) solar cells. Materials Today, 16(4), pp.123-132.
[29] Zhou, E., Cong, J., Wei, Q., Tajima, K., Yang, C. and Hashimoto, K., 2011. All-Polymer Solar Cells from Perylene Diimide Based Copolymers: Material Design and Phase Separation Control. Angewandte Chemie International Edition, 50(12), pp.2799-2803.
[30] Earmme, T., Hwang, Y.J., Murari, N.M., Subramaniyan, S. and Jenekhe, S.A., 2013. All-polymer solar cells with 3.3% efficiency based on naphthalene diimide-selenophene copolymer acceptor. Journal of the American Chemical Society, 135(40), pp.14960-14963.

[31] Hwang, Y.J., Courtright, B.A., Ferreira, A.S., Tolbert, S.H. and Jenekhe, S.A., 2015. 7.7% Efficient All-Polymer Solar Cells. Advanced materials, 27(31), pp.4578-4584.
[32] Kim, T., Kim, J.H., Kang, T.E., Lee, C., Kang, H., Shin, M., Wang, C., Ma, B., Jeong, U., Kim, T.S. and Kim, B.J., 2015. Flexible, highly efficient all-polymer solar cells. Nature communications, 6, p.8547.
[33] Brabec, C.J., Gowrisanker, S., Halls, J.J., Laird, D., Jia, S. and Williams, S.P., 2010. Polymer–fullerene bulk-heterojunction solar cells. Advanced Materials, 22(34), pp.3839-3856.
[34] Deibel, C. and Dyakonov, V., 2010. Polymer–fullerene bulk heterojunction solar cells. Reports on Progress in Physics, 73(9), p.096401.
[35] He, Y. and Li, Y., 2011. Fullerene derivative acceptors for high performance polymer solar cells. Physical chemistry chemical physics, 13(6), pp.1970-1983.
[36] Kozma, E. and Catellani, M., 2013. Perylene diimides based materials for organic solar cells. Dyes and Pigments, 98(1), pp.160-179.
[37] Chesterfield, R.J., McKeen, J.C., Newman, C.R., Ewbank, P.C., da Silva Filho, D.A., Brédas, J.L., Miller, L.L., Mann, K.R. and Frisbie, C.D., 2004. Organic thin film transistors based on N-alkyl perylene diimides: charge transport kinetics as a function of gate voltage and temperature. The Journal of Physical Chemistry B, 108(50), pp.19281-19292.
[38] Dubey, R.K., Niemi, M., Kaunisto, K., Stranius, K., Efimov, A., Tkachenko, N.V. and Lemmetyinen, H., 2013. Excited-State Interaction of Red and Green Perylene Diimides with Luminescent Ru (II) Polypyridine Complex. Inorganic chemistry, 52(17), pp.9761-9773.
[39] Zimmermann, E., Ehrenreich, P., Pfadler, T., Dorman, J.A., Weickert, J. and Schmidt-Mende, L., 2014. Erroneous efficiency reports harm organic solar cell research. Nature Photonics, 8(9), p.669.
[40] Yan, C., Barlow, S., Wang, Z., Yan, H., Jen, A.K.Y., Marder, S.R. and Zhan, X., 2018. Non-fullerene acceptors for organic solar cells. Nature Reviews Materials, 3, p.18003.
[41] Luo, Z., Xiong, W., Liu, T., Cheng, W., Wu, K., Sun, Y. and Yang, C., 2017. Triphenylamine-cored star-shape compounds as non-fullerene acceptor for high-efficiency organic solar cells: Tuning the optoelectronic properties by S/Se-annulated perylene diimide. Organic Electronics, 41, pp.166-172.
[42] Kotowski, D., Luzzati, S., Scavia, G., Cavazzini, M., Bossi, A., Catellani, M. and Kozma, E., 2015. The effect of perylene diimides chemical structure on the photovoltaic performance of P3HT/perylene diimides solar cells. Dyes and Pigments, 120, pp.57-64.
[43] Liang, N., Sun, K., Zheng, Z., Yao, H., Gao, G., Meng, X., Wang, Z., Ma, W. and Hou, J., 2016. Perylene diimide trimers based bulk heterojunction organic solar cells with efficiency over 7%. Advanced Energy Materials, 6(11).
[44] Sun, J.P., Hendsbee, A.D., Dobson, A.J., Welch, G.C. and Hill, I.G., 2016. Perylene diimide based all small-molecule organic solar cells: Impact of branched-alkyl side chains on solubility, photophysics, self-assembly, and photovoltaic parameters. Organic Electronics, 35, pp.151-157.
[45] Zang, Y., Li, C.Z., Chueh, C.C., Williams, S.T., Jiang, W., Wang, Z.H., Yu, J.S. and Jen, A.K.Y., 2014. Integrated Molecular, Interfacial, and Device Engineering towards High-Performance Non-Fullerene Based Organic Solar Cells. Advanced Materials, 26(32), pp.5708-5714.
[46] Duan, Y., Xu, X., Yan, H., Wu, W., Li, Z. and Peng, Q., 2017. Pronounced Effects of a Triazine Core on Photovoltaic Performance–Efficient Organic Solar Cells Enabled by a PDI Trimer-Based Small Molecular Acceptor. Advanced Materials, 29(7).
[47] Guo, Y., Li, Y., Awartani, O., Zhao, J., Han, H., Ade, H., Zhao, D. and Yan, H., 2016. A Vinylene-Bridged Perylenediimide-Based Polymeric Acceptor Enabling Efficient All-Polymer Solar Cells Processed under Ambient Conditions. Advanced Materials, 28(38), pp.8483-8489.
[48] Hwang, Y.J., Earmme, T., Courtright, B.A., Eberle, F.N. and Jenekhe, S.A., 2015. n-Type semiconducting naphthalene diimide-perylene diimide copolymers: controlling crystallinity, blend morphology, and compatibility toward high-performance all-polymer solar cells. Journal of the American Chemical Society, 137(13), pp.4424-4434.
[49] Lee, C., Kang, H., Lee, W., Kim, T., Kim, K.H., Woo, H.Y., Wang, C. and Kim, B.J., 2015. High-Performance All-Polymer Solar Cells Via Side-Chain Engineering of the Polymer Acceptor: The Importance of the Polymer Packing Structure and the Nanoscale Blend Morphology. Advanced materials, 27(15), pp.2466-2471.
[50] Zhan, X., Tan, Z.A., Domercq, B., An, Z., Zhang, X., Barlow, S., Li, Y., Zhu, D., Kippelen, B. and Marder, S.R., 2007. A high-mobility electron-transport polymer with broad absorption and its use in field-effect transistors and all-polymer solar cells. Journal of the American Chemical Society, 129(23), pp.7246-7247.
[51] Zhan, X. et al. Copolymers of perylene diimide with dithienothiophene and dithienopyrrole as electrontransport materials for all-polymer solar cells and field-effect transistors. J. Mater. Chem. 19, 5794–5803 (2009).
[52] Kozma, E. and Catellani, M., 2013. Perylene diimides based materials for organic solar cells. Dyes and Pigments, 98(1), pp.160-179.
[53] Günes, S., Neugebauer, H. and Sariciftci, N.S., 2007. Conjugated polymer-based organic solar cells. Chemical reviews, 107(4), pp.1324-1338.
[54] Dai, S., Lin, Y., Cheng, P., Wang, Y., Zhao, X., Ling, Q. and Zhan, X., 2015. Perylene diimide–thienylenevinylene-based small molecule and polymer acceptors for solution-processed fullerene-free organic solar cells. Dyes and Pigments, 114, pp.283-289.
[55] Li, S., Zhang, H., Zhao, W., Ye, L., Yao, H., Yang, B., Zhang, S. and Hou, J., 2016. Green-Solvent-Processed All-Polymer Solar Cells Containing a Perylene Diimide-Based Acceptor with an Efficiency over 6.5%. Advanced Energy Materials, 6(5).
[56] Zhou, Y., Kurosawa, T., Ma, W., Guo, Y., Fang, L., Vandewal, K., Diao, Y., Wang, C., Yan, Q., Reinspach, J. and Mei, J., 2014. High performance all-polymer solar cell via polymer side-chain engineering. Advanced materials, 26(22), pp.3767-3772.
[57] Hwang, Y.J., Earmme, T., Courtright, B.A., Eberle, F.N. and Jenekhe, S.A., 2015. n-Type semiconducting naphthalene diimide-perylene diimide copolymers: controlling crystallinity, blend morphology, and compatibility toward high-performance all-polymer solar cells. Journal of the American Chemical Society, 137(13), pp.4424-4434.

Energy and Exergy Analysis of Combined Cooling System with Parabolic Solar Collector Using Phase Change Material

Sercan Gulce Gungor[1], Ahmet Kabul[2], Mehmet Esen[3]

***Abstract*—**In this study, it is aimed to operate the cooling system by using the heat obtained from the parabolic solar collector. The Organic Rankine Cycle was run with heat energy from the parabolic collector. The energy obtained in the Organic Rankine Cycle turbine is used in the compressor of the vapor compression refrigeration cycle. At this point, unlike conventional cooling systems, the electrical energy required for the refrigeration cycle is provided by solar energy. When the solar energy cannot be used, the heat storage was done in order to maintain the system continuity. Thanks to this system, which uses phase change material, cooling process can be continued for a while. Energy and exergy analysis was made with the designed system values.

***Keywords*—**Renewable energy, Parabolic solar collector, Combined cooling system, Energy and exergy analysis, Thermal energy storage

I. INTRODUCTION

THE Industrial Revolution, there has been an increase in energy use to meet high production needs. This energy requirement is met by fossil sources. As a result of the use of fossil fuels, greenhouse gas emissions have increased and have started to damage the ozone layer and face environmental threats such as global warming [1]. Renewable energy has become increasingly important as a result of the use of fossil resources that have been exposed to environmental impacts at serious levels over the past decades [2]. Today, rather than fossil fuels, renewable sources are becoming a necessity in favor of creating a clean and sustainable energy sector [3].

Solar energy in renewable energy sources promises to meet clean energy demand [2]. It reduces greenhouse gas emissions and does not create pollutants or waste. Most sources of renewable energy are either directly or indirectly solarized.

Sercan Gülce Güngör[1] is now with the Department of Energy Systems Engineering, Faculty of Technology, Fırat University, Elazig, 23119, TURKEY (corresponding author's phone: +90 424 237 0000/7656; e-mail: sggungor@firat.edu.tr).

Ahmet Kabul[2] is now with the Department of Energy Systems Engineering, Faculty of Technology, Süleyman Demirel University, Isparta, 32260, TURKEY (e-mail: ahmetkabul@sdu.edu.tr).

Mehmet Esen[3] is now with the Department of Energy Systems Engineering, Faculty of Technology, Fırat University, Elazig, 23119, TURKEY (e-mail: mesen@firat.edu.tr).

Because of this feature, the sun is expressed as the energy of the future [1]. As a promising renewable resource, solar energy, parabolic, or condensation systems are used to generate thermal energy, which can be converted to electricity by the steam turbine. Systems that generate energy using parabolic solar collectors have been established and commercialized around the world in recent years [3].

Alzahrani and Dincer designed the parabolic solar power plant in 2018. They used CO_2 as a fluid in the power plant. The parabolic solar collector energy and emaciation values were calculated as 66.35% and 38.51%, respectively [4]. Al-Sulaiman in 2014 studied the parabolic solar collector and steam Rankine Cycle and Organic Rankine Cycle. Seven different fluids for Organic Rankine Cycle have been examined in terms of exergy efficiency. These fluids are R134a, R152a, R290, R407c, R600 and R600a. The exergy efficiency of the R134a fluid was 26% higher than the other fluids [5]. Toghyani et al., In their study in 2016, integrated the steam Rankine power cycle into the parabolic solar collector system and used a thermal energy storage system. The storage system is planned to be used to protect system performance in the absence of sun. They performed thermodynamic analysis with different nano-fluids to the solar collector system. They determined the best performing nano-fluid [6]. Li has conducted studies in 2015 to study the energy and exergy of latent heat storage in an effort to improve system performance. It examines parameters such as heat transfer fluid, mass flow rate, phase change material (PCM) melting temperature, heat exchanger surface increase and sensible heat affecting system performance. Among these parameters, the most important is to optimize the PCM melting point [7].

II. SYSTEM DESCRIPTION

In this study, a new combined cooling system design was made. The system includes a parabolic solar collector, a heat storage unit, an Organic Rankine Cycle, a vapor compression refrigeration cycle and a cooling tower. The Organic Rankine Cycle is operated with heat energy obtained from the parabolic solar collector. The energy required for the compressor of the vapor compression refrigeration cycle is derived from the

organic Rankine cycle turbine. Moreover, energy required for the vapor compression refrigeration cycle compressor is obtained from the sun as opposed to conventional systems. It is also aimed to increase the working time of the system by storing a quantity of heat from solar renewable energy source. The designed system is shown in Figure 1.

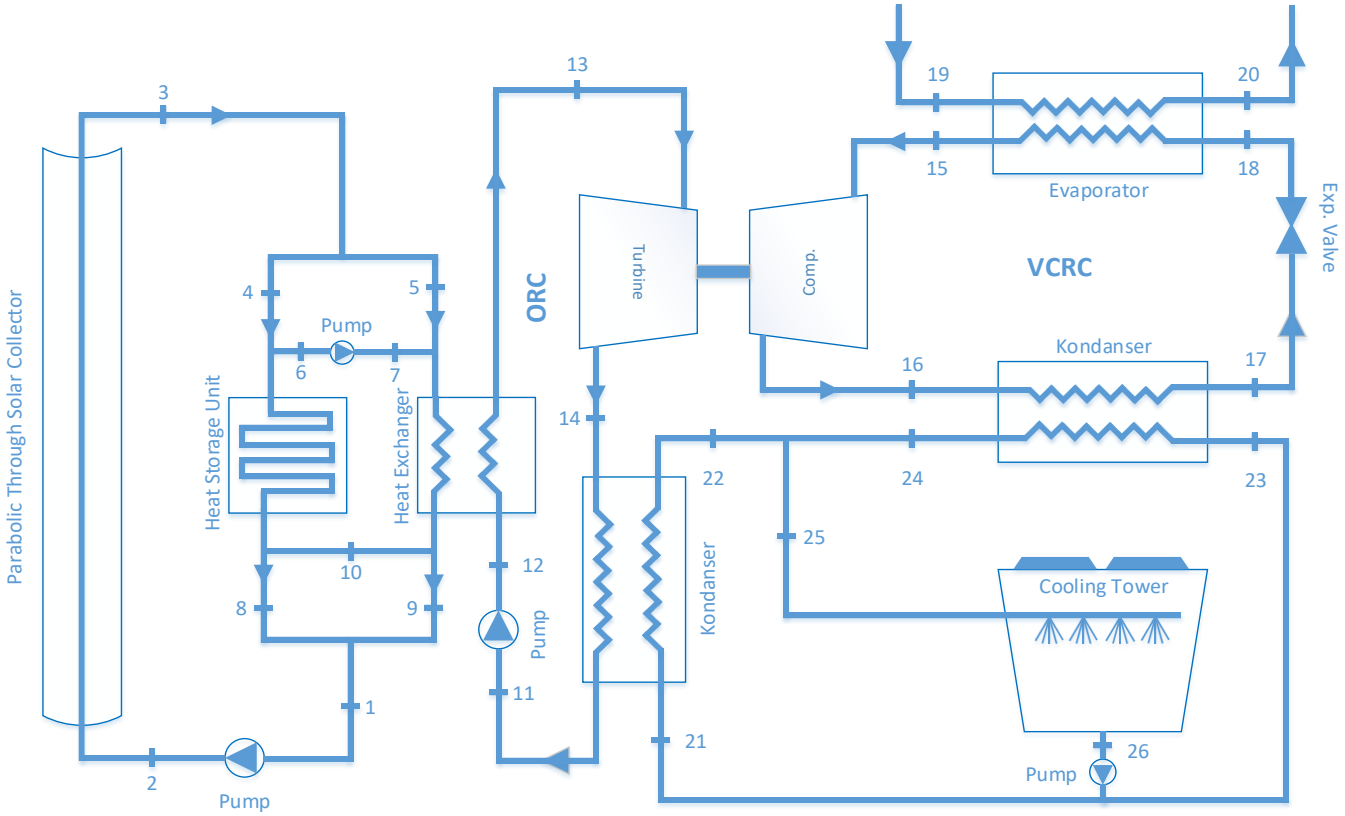

Fig. 8 Schematic view of parabolic collector power-refrigeration system

A. Parabolic Trough Solar Collector

Parabolic solar collectors play an important role for achieving high temperatures from solar energy. In these systems heat transfer fluid is usually used. In this point, Therminol-VP1 heat transfer fluid is used in the parabolic solar collector system. In Table 1, the characteristics of Therminol-VP1 are given.

TABLE 1
THERMINOL-VP1 PROPERTIES [9].

Appearance	Clear, water white liquid
Composition	Biphenyl/diphenyl oxide (DPO)
Bulk temperature (max.)	400°C
Film temperature (max.)	430°C
Boiling point	257°C
Flashpoint	124°C
Kinematic viscosity (100°C)	0.99 mm^2/s
Kinematic viscosity (40°C)	2.48 mm^2/s
Liquid density (25°C)	1060 kg/m^3

B. Heat Storage Unit

Some of the heat energy from the parabolic solar collector is stored as latent heat in the heat storage unit. The remaining part of heat is sent to the Organic Rankine Cycle evaporator. KNO_3 was used as a phase change material in the heat storage unit. In terms of the designed system, this material is one of the important parameters having a phase change temperature of 330 ºC and a latent heat capacity of 266 kJ/kg [8].

C. Organic Rankine Cycle(ORC)

The heat obtained in the parabolic solar collector is used in the ideal Organic Rankine Cycle evaporator. This heat is transferred to the R134a fluid. R134a fluid is one of the commonly used fluids in the organic Rankine cycle.

D. Vapor Compression Refrigeration Cycle(VCRC)

The high energy requirement of the compressor in the vapor compression refrigeration cycle has led to the development of this system. This energy required at this point is provided by the solar. The cooling capacity of the system is set at 50 kW. R134a is used as the work fluid in the system.

E. Cooling Tower

The cooling tower was used to heat the atmosphere produced in the ORC and VCRC condenser. For this reason, in a system where water is used as a working fluid, water is continuously delivered to the condensers at a temperature of 15 ° C.

III. Thermodynamic Analysis

Thermodynamic analysis was performed to evaluate system performance. The first law of thermodynamics expresses the

conservation of energy. The second law of thermodynamics expresses the importance of quality besides the quantity of energy. Analysis of the first and second laws of thermodynamics were used to evaluate the system condition.

A. Energy Analysis

Thermodynamic equations were used in the analysis of the system. While thermodynamic analysis is carried out on the continuous flow open system, mass and energy basic equilibrium equations are used. For a system with a stable control volume, the mass balance is expressed with Equation (1).

$$\sum \dot{m}in = \sum \dot{m}out \tag{1}$$

Here ṁ represents the mass flow.

The energy balance which is the first law of thermodynamics, can be written with Equation (2).

$$\sum \dot{E}in = \sum \dot{E}out \tag{2}$$

Where Ein is energy input to the system, Eout is the energy output from the system. The first law of thermodynamics analyzes the conservation of energy. The energy conservation equation on the system is given below at Equation (3).

$$\dot{Q} + \sum (\dot{m}h)in = \dot{W} + \sum (\dot{m}h)out \tag{3}$$

Here; Q is the energy of the heat, W is the energy of the work, and ṁh is the energy entering and exiting with the mass flow. The efficiency calculation of the first law of thermodynamics was made using the Equation (4).

$$\eta_{energy} = (\text{energy obtained}) / (\text{spent energy}) \tag{4}$$

B. Exergy Analysis

Exergy is expressed as the quality of energy. It is also expressed as the maximum work that can be achieved when the balance is reached with a reference environment. Exergy analysis is a set of calculations in terms of logical and meaningful evaluation based on the second law of thermodynamics used to compare systems. A system helps to find the optimum working conditions. For this purpose, the aim is to investigate the causes of minimum exergy destruction and irreversibility in the system. At this point, the energy of the work is equal to the exergy, and the exergy of the heat is calculated according to the ambient temperature.

Exergy analysis ignores kinetic, potential and chemical exergy in all elements, and exergy balance for a continuous flow open system is written in Equation (5).

$$ExQ - ExW = \sum (\dot{m}\varepsilon)out - \sum (\dot{m}\varepsilon)in + T0 * Sgen \tag{5}$$

Equation ExQ is the exergy of heat, ExW is exergy of work, ṁ is mass flow rate and ε is flow exergy which is expressed as thermomechanical exergy. These expressions are given in Equations (6), (7) and (8).

$$\dot{E}x_Q = Q\left(\frac{T - T_0}{T}\right) \tag{6}$$

$$\dot{E}x_W = \dot{W} \tag{7}$$

$$\varepsilon = (h - h_0) - T_0(s - s_0) \tag{8}$$

Here, Q is the heat, W is the work, and 0 is the enthalpy (h), entropy (s) and temperature (T) values in the reference conditions.

Exergy efficiency is seen as a definite criterion for evaluating system performance. Because different types of energy can be taken into account directly from exergy point of view.

$$\eta_{exergy} = (\text{recovered exergy}) / (\text{provided exergy}) \tag{9}$$

IV. Results and Discussion

As a result of the energy and exergy analysis made with the study data, the values in Table 1 were obtained. Energy and exergy analysis was conducted in the Engineering Equations Solver (EES) program [11]. Parabolic solar collector energy efficiency was calculated as 36% for 59% exergy efficiency. Organic Rankine Cycle energy efficiency is 6% and exergy efficiency is 3%. The COP value of the vapor compression refrigeration cycle was calculated to be 3.506.

TABLE I
COMBINED COOLING SYSTEM ANALYSIS DATA

Point	Fluid	T(ºC)	P(kPa)	h(kj/kg)	ṁ(kg/sn)
1	Therminol-VP1	260	220	464.5	10.12
2	Therminol-VP1	260	220.5	464.5	10.12
3	Therminol-VP1	300	320	555	10.12
4	Therminol-VP1	300	320	555	5.062
5	Therminol-VP1	300	320	555	5.062
6	Therminol-VP1	300	300	554.9	1.001
7	Therminol-VP1	301	301.2	557.3	1.001
8	Therminol-VP1	281	200.5	511.4	5.062
9	Therminol-VP1	281	200.5	511.4	5.062
10	Therminol-VP1	200	200	336.7	1.001
11	R134a	77.54	2500	169.6	1.163
12	R134a	79.94	4000	171.2	1.163
13	R134a	150	4000	361	1.163
14	R134a	127.4	2500	348.7	1.163
15	R134a	-15	164	241.5	0.3753
16	R134a	47.38	1017	279.5	0.3753
17	R134a	40	1017	108.3	0.3753
18	R134a	-15	164	108.3	0.3753
19	Water	15	101.325	63.01	2
20	Water	20.98	101.325	88.01	2
21	Water	15	101.325	63.01	4
22	Water	27.44	101.325	115.1	4
23	Water	15	101.325	63.01	2
24	Water	22.68	101.325	95.15	2
25	Water	25.85	101.325	108.4	6
26	Water	15	101.325	63.01	6

V. Conclusions

In this study, a combined cooling system was designed and investigated in terms of thermodynamics. The amount of energy needed by the cooling systems is met by solar energy. The system constructed for this purpose consists of the parabolic collector, ORC, VCRC and cooling tower. In addition, heat storage has been performed to keep system performance in balance and ensure system continuity. Energy and exergy analysis were done considering system data. Given the results of the analysis and the designed system, it is clear that renewable energy sources will become more and more useful nowadays.

References

[1] M. Chafie, M. F. B. Aissa, A. Guizani, "Energetic end exergetic performance of a parabolic trough collector receiver: An experimental study", Journal of Cleaner Production, vol. 171, 2018, pp. 285-296.

[2] S. Toghyani, E. Baniasadi, E. Afshari, "Thermodynamic analysis and optimization of an integrated Rankine power cycle and nano-fluid based parabolic trough solar collector", Energy Conversion and Management, vol. 121, 2016, pp. 93-104.

[3] S. K. Sansaniwal, V. Sharma, J. Mathur, "Energy and exergy analyses of various typical solar energy applications: A comprehensive review", Renewable and Sustainable Energy Reviews, vol. 82, 2018, pp. 1576–1601.

[4] A.A. AlZahrani, I. Dincer, "Energy and exergy analyses of a parabolic trough solar power plant using carbon dioxide power cycle", Energy Conversion and Management, vol. 158, 2018, pp. 476-488.

[5] F.A. Al-Sulaiman, Exergy analysis of parabolic trough solar collectors integrated with combined steam and organic Rankine cycles", Energy Conversion and Management, vol. 77, 2014, pp. 441-449.

[6] S. Tonghyani, E. Baniasadi, E. Afshari, "Thermodynamic analysis and optimization of an integrated Rankine power cycle and nano-fluid based

[7] parabolic trough solar collector", Energy Conversion and Management, vol. 121, 2016, pp. 93-104.

[8] G. Li, "Energy and exergy performance assessments for latent heat thermal energy storage systems", Renewable and Sustainable Energy Reviews, vol. 51, 2015, pp. 926-954.

[9] A. Vasu, F.Y. Hagos, M.M. Noor, R. Mamat, W.H. Azmi, A.A. Abdullah et al. "Corrosion effect of phase change materials in solar thermal energy storage application", Renewable and Sustainable Energy Reviews, vol. 76, 2017, pp. 19-33.

[10] Therminol Heat Transfer Fluids by Eastman Inc. Therminol-VP-1, https://www.therminol.com/products/Therminol-VP1, Access date; 29.04.2018.

[11] F-Chart Software, Engineering Equation Solver (EES), http://www.fchart.com/ees/, Access date; 01.05.2018.

An Investigation of the Environmental Impacts on the Efficiency of Photovoltaic Panel in Adıyaman, Malatya, Şanlıurfa Region

Yasin İçel[1], M. Salih Mamiş[2], Abdulcelil Buğutekin[3], Seydi Vakkas Üstün[4]

Abstract—The efficiency of a solar cell is defined as the rate of power output to the power of solar radiation that falls on the photovoltaic cell. One of the main factors affecting the efficiency of photovoltaic batteries is the temperature. There is an inverse relationship between PV module power output and module temperature. The module temperature varies depending on ambient temperature, nausea and wind quantity. In this study, energy efficiency of the three provinces is compared by measuring the parameters (temperature, humidity, solar radiation, wind, altitude) and voltage, current data and centering them on GSM in solar energy systems. In this work the level of efficiency to be achieved by considering the environmental effects in a solar power plant to be installed in these regions is aimed. For the measurement of environmental factors and other electrical values in the installed measuring stations and for collecting the data coming from the stations in the center, a data logging card was designed and a software for the cards was realized. As a result of the measurements made between 14-20 August 2017 in the study, it was seen that in terms of efficiency, the cities were ordered as Adıyaman-Malatya-Şanlıurfa. In a future study, the system will be modeled and packaged using artificial neural network algorithms using the theoretical information on the energy efficiency effects of environmental factors in solar energy systems and annual data from the measuring stations. Then, when temperature, humidity, wind, solar radiation, altitude values belonging to specific region will be used to estimate the energy to be to be obtained at that region.

***Keywords*—**Efficiency, Environmental Factors, Photovoltaics, Renewable Energy, Solar Radition.

I. INTRODUCTION

BECAUSE of the increase in population and industrilisation, demand for electric power is increasing rapidly day by day. But, due to the fact that majority of the power is obtained from such fossil fuels as petroleum, natural gas and coal, it also results in environmental problems. In addition, the fact that these fuels will run out soon has revealed the need for energy resources which are non-detrimental to the environment and also infinite and renewable. The solar power, one of the renewable energy recourses, contributes to the formation of other energy resources, as well. In addition, the clearity and easy-usage of the solar power makes is more effective among other renewable forms [1],[2].

Energy can be obtained from solar power through direct and indirect methods. Solar cells, the smallest units of Photovoltaic (PV) system, which are one of these methods, directly turns the energy into DC voltage. By means of serial or parallel connections, solar cells forms PV modules, and through these serial or parallel connections desired current, voltage and power values can be attained [3]. PV panels, depending on the semi-conductive material on its structure transforms the solar power into electrical energy with %6-%22 efficiency. There are many factors effecting the efficacy of the PV panels with low-efficiency, and these are panel tilt angle, ghostling, temperature, the magnitude of solar radiation, PV temperature, speed of wind, moisture and other losses [4],[5]. Among these factors, the magnitude of solar radiation, temperature, speed of wind and moisture are the most important parameters affecting the efficacy of the panel. Through the day, change of atmospheric conditions like the magnitude of solar radiation and temperature affects significantly the efficacy of the panel. Thus, it is important to know the effect of the environmental factors on the efficacy of the panel depending on the changing atmospheric conditions. The values indicated on PV panels, as a result of tests carried out on laboratories, gives the electrical values of the panel which are called Standardised Test Conditions (STC) in which the magnitude of radiation is 1000 W/m², cell temperature is 25 ºC, air-mass rate is A.M. 1,5. Electrical values of the PV panel for non-STC values are unknown. [6]-[8]. For the accurate annual performance evaluation of PV systems, inclusion of environmental factors for the determination of correct method is necessary [9], [10].

Through the literature survey carried out over the subject, in his “Structural Features and Characteristics of Photovoltaic Solar Cells” named research Altaş has studied how output voltage and current on load change depending on temperature and light intensity, and then he determined that photovoltaic

Yasin İçel[1] Electrical and Energy Department, Technical Vocational School, Adıyaman University, Altınşehir Mah. 3005 Sok. No:13 02040 Adıyaman, Turkey. (04162233800-3628, yicel@adiyaman.edu.tr).

M.Salih Mamiş[2], Electrical and Electronics Engineering Department, Engineering Faculty, İnönü University, İnönü University Central Campus, 44280 Malatya, Turkey. (mehmet.mamis@inonu.edu.tr).

Abdulcelil Buğutekin[3] Mechanical Engineering Department, Engineering Faculty, Adıyaman University, Altınşehir Mah. 3005 Sok. No:13 02040 Adıyaman, Turkey. (abugutekin@adiyaman.edu.tr).

Seydi Vakkas Üstün[4] Electrical and Electronics Engineering Department, Engineering Faculty, Adıyaman University, Altınşehir Mah. 3005 Sok. No:13 02040 Adıyaman, Turkey. (svustun@adiyaman.edu.tr).

This research was supported by the Scientific Research Project Unit of Adıyaman University with the project numbered MÜFMAP/2015-0011.

cells are adversely affected by heat. That is, the output voltage and output power of photovoltaic cells decline as the heat increases [11].

As a result of the research, carried out by Yılmaz et al., it has been indicated that efficiency of the modules has decreased as the ambient temperature increases. The power produced in the temperature zone that the photovoltaic cells are exposed to isn't linear. Photovoltaic cells are exposed to the sunlight and they absorbs infrared rays emitted by the sun and thus get warmer. Meanwhile, the modules are dark in color and their temperatures can get at values as high as 80°C when there is no wind-blow [12].

A simulation, especially by taking cloudy weather conditions into account, has been carried out in the research conducted by Fesharaki et al. and as a result of this simulation, it has been well established that the efficiency of photovoltaic panels decreases as the temperature increases [13].

Omubo-Pepple et al, have investigated the effects of temperature, sun light intensity and relative humidity on photovoltaic panels. They have stated that ambient temperature doesn't affect directly the efficiency of the panel but rather the temperature of the panel and the relative humidity affect it [14]. Skoplaki and Palyvos have examined the relevance of electrical performances of photovoltaic panels with temperature in their article. They have concluded that panel running temperature is the most important factor in the process of photovoltaic transformation. In addition, it has been stated that the effect of the temperature changes in accordance with not only the pattern of panel construction but also the places they are used [15], [16].

A. Electrical Equivalent Circuit Model of PV Cells

PV cell produces a very low voltage with a high intensity of current. Therefore, PV element is a source of current. Under standart conditions, which is a radiation of 1 kW/m^2 and crystal temperature of 25°C, typical elektrical values are I_{sc}=30-40 mA/cm^2 for short-circuit current and V_{oc}=0,5-0,6 V as open circuit voltage [10]. Electrical Equivalent Circuit of PV cell is seen on Fig. 1 [17].

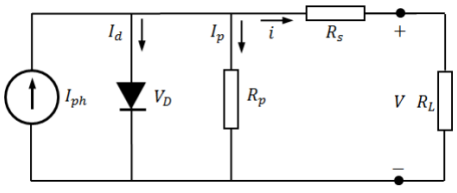

Fig. 1 Electrical equivalent circuit of PV cell [14]

There are serial and parallel internal resistances in electrical equivalent circuit of PV cell, so the output current equation of the PV cell can be stated as it is in equation (1):

$$i = I_{pv} - I_0 \left\{ e^{\frac{q(V+iR_s)}{nkT}} - 1 \right\} - \frac{V + iR_s}{R_p} \qquad (1)$$

where;
i: photovoltaic output current,
I_0: reverse diode saturation current,
V: photovoltaic output voltage,
n: diode quality factor,
q: electron load (1.60217646 e-19 C),
k: Boltzmann constant (1.3806503 e-23 J/K),
T: Temperature in Kelvin at the p-n connection point [18].

There is a linear correlation between Ipv, the light current produced by the photovoltaic cell, and the temperature. This connection is given through the equation (2):

$$I_{pv} = \left(I_{pvn} + k\Delta T\right) {}^{G}/_{G_n} \qquad (2)$$

where;
I_{pvn}: the light current produced under standart conditions (1000 W/m^2 and 25°C),
G: the surface sun radiation of PV (W/m^2),
G_n: the nominal solar radiation [18].

ΔT=T-Tn , T and Tn (Kelvin) are the real and nominal temperatures.

When the power-voltage characteristics of photovoltaic cells are examined, power is seen to increase primarily in proportion to the cell voltage. The sharp decrease occuring after the maximum power point causes output voltage to decrease. (Fig. 2) [19].

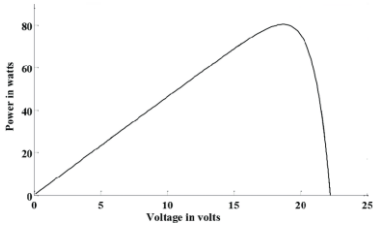

Fig. 2 Power-voltage characteristics of photovoltaic cell [16]

Efficiency of a photovoltaic cell, η, is defined as the ratio of the power of the solar radiation falling onto the photovoltaic cell over the power that can be attained from that same cell (equation 3).

$$\eta = (P_{out} \times I_{mp}) / (V_{in} \times I_{sc}) = (V_{oc} \times I_{sc} \times FF) \qquad (3)$$

where;
V_{oc}: open current voltage,
I_{sc}: short-cut voltage,
V_{mp}: the positive maximum voltage on I-V curve,
I_{mp}: the positive maximum current on I-V curve [20].

B. Ambient Factors Affecting PV Cells

1. Effect of Solar Radiation

Total quantity of energy directly coming from sun to the world is 174 petawatt, 10 PW of which is reflected back from the atmosphere, 35 PW is through clouds and another 7 PW is reflected back by the surface of the earth. The amount absorbed by the atmosphere is 33 PW, while the amount absorbed by lands and seas is about 89 PW [10].

Solar radiation in PV systems has the maximum impact on power output. Amplitude of photo-current (PV short circuit current) changes in accordance with solar radiation. Efficiency of photo-transformation in the PV cell's practical working range isn't affected much by the changes in solar radiation. But this doesn't necessarily mean the same amount of energy will be obtained, because as the energy input decreases so will the output power be as there will be less energy input in a cloudy day [10]. Furthermore, the current produced at the panel will increase along with the sunlight intensity and radiation. Though, a significant change in radiation changes the current significantly, the voltage almost virtualy remains constant (Fig. 3) [21].

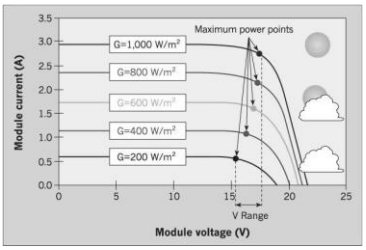

Fig. 3 The effect of solar radiation on PV Cells [21]

Our country, in view of its solar power capacity owing to its geographical position, is in a more adventageous state compared to many countries (Fig. 4,5).

Fig. 4 Map of capacity of solar power of cities in Turkey (GEPA) [22]

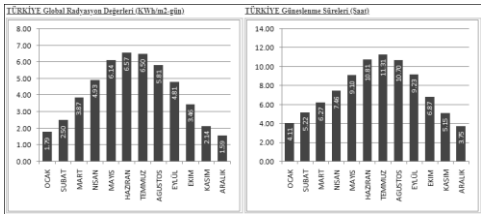

Fig. 5 Global radiation values and ınsolation periods for Turkey (GEPA) [22]

Solar radiation reaching to the earth is regarded as approximately 1000 W/m^2. As Turkey is located between the latitudes 36° and 42° in the north hemisphere, its solar energy potential is very high. Turkey's annual solar energy potential is equal to 1,3 billion ton petroleum. In Turkey, the yearly total of average insolation period is determined to be 2640 hours and the daily total solar radiation quantity was detected to be 3,6 kWh/m²-day [22].

2. Effect of Temperature and Humidity

Running temperatures for photovoltaic cells has a wide range depending on the usage areas. Thus, the effect of temperature on the efficiency of photovoltaic cell is necessary to be known. As the temperature increases, a small increase over the short-cut circuit current is observed. This is due to the fact that as the temperature increases, semi-conductor forbidden band gap gets narrower and as a result an accumulation occurs in the amount of absorption of radiation [16]. Since the change in temperatures mostly affect open-circuit voltage, high running temperatures affect adversely power and efficiency of PV systems. Efficiency of the cell shows a decrease with the increasing temperature. In Figure 6, the effect of temperature on the current-voltage (I-V) curve of photovoltaic modules with crystal silicon cells is clearly seen. Every 1°C increase in the temperature decreases the power obtained in a rate of % 0.5 [10]. Extra water vapour in atmosphere leads to the shadowing of the radiation. When the water vapour in the air condenses into rain and snow, the atmosphere becomes more transparent and thus, shadowing of the radiation minimizes [23].

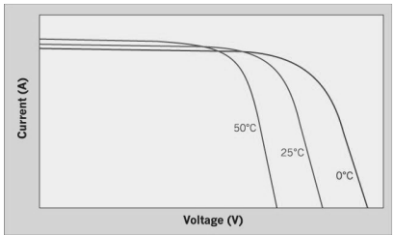

Fig. 6 The effect of temperature on PV cells [10]

3. Effect of Speed of Wind

Weather conditions affects the power output in energy production. Heat of the module is affected by the ambient heat, the structure of the cloud, the speed of wind and the position of the PC system. As the speed of the wind will decrease the temperature of the PV panel, PV cell temperature is depends significantly on the speed of wind while its direction affects it insignificantly [24].

II. Installation Of Measurement Stations

In order to investigate the parameters affecting the efficiency of solar energy systems;

By means of picking measurements in Adıyaman-Malatya-Şanlıurfa region, the design of the measurement systems were

completed. These terminals measure all the values, namely temperature, humidity, wind, solar radiation, output current and voltage of the panel, and then send these values through GSM as a short message to the main terminal located in Vocational High School in Adıyaman University and then these data is processed after being stored into an SD card.

In order to process the data coming from sensors, in the design of the cards, DSPIC 33F processors were used. Data obtained form reginal terminals are transmitted to the main terminal by using SIM900 module. Regional measurement terminals consist of 120 W monocrystal panel, 100Ah Jel accumulator, 10 A - 12 V MPPT charge control device, 4 resistive loads to discharge the energy obtained from the panels, sensors of temperature, humidity, wind, current, voltage; card designed for measurement and the panel to keep the equipment enclosed.

Main terminal provides first the storage of the data measured every 5 minutes and coming from regional terminals via short message service to the SD card and the processing of the data on the SD card by computerising them. In regional terminals, in order to measure temperature and humidity values, external area humidiometer and thermometer probe with radiation protection cover and analog voltage output is being used. An anemometer with an analog voltage output that can make measurements in 0,28-50 m/sec range, with an error range of 0,02 m/sec has been used to detect the speed of wind. A piranometer probe with an anaolg voltage outupt which can detect values in the range of 0-2000 W/m^2 to measure the solar radiation was used. The energy produced by 120 W monocrystal panel is chagerd to the acumulator through the charge control device with MPPT controllor, and then the energy is being spent through the resistive load and by the way the production efficiency of the panel is examined in comparison with the ambient conditions. Schematic diagrams and application images of terminal measurement stations established in Adıyaman-Malatya-Şanlıurfa regions are given in figure 7,8.

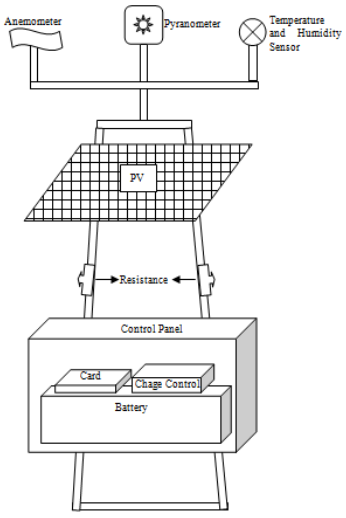

Fig. 7 Schematic diagrams of terminal measurement stations

Fig. 8 Application images of terminal measurement stations

A. Measurement

By means of using the values, namely temperature, humidity, wind, solar radiation, panel temperature, current and voltage obtained through panel, the effect of ambient factors on PV panel power has been displayed on the following graphs. Hourly average values read from the terminal measurement stations from 14th to 20th of August 2017 were utilised in the graphs. In view of the fact that the data is obtained in August, values of the time period of 06:00-20:00 were used.

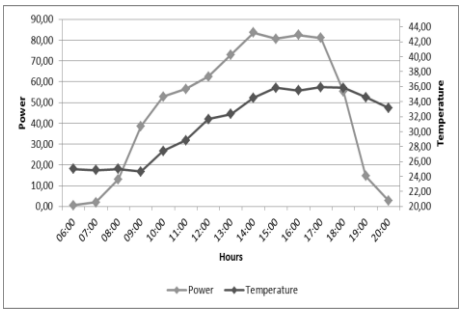

Fig. 9 Temperature-power relation in Adıyaman

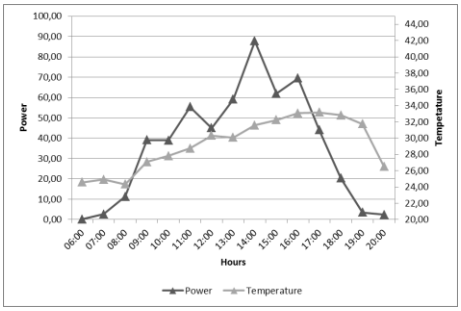

Fig. 10 Temperature-power relation in Malatya

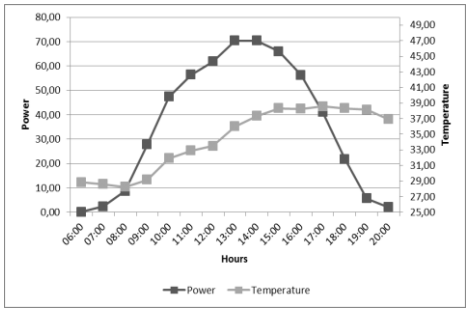

Fig. 11 Temperature-power relation in Şanlıurfa

When the graphics are examined, Şanlıurfa district is seen to be the hottest and also the power obtained from the panel in this district is seen to be the lowest. During midday hours, a decline in the produced power, though not as much as the one in Şanlıurfa, is also seen. The reason why the effect of temperature is not seen on graphics is that the period chosen for solar radiation measurement is the highest period of the year, so there is no significant change in the power of the produced energy (Fig. 9,10,11).

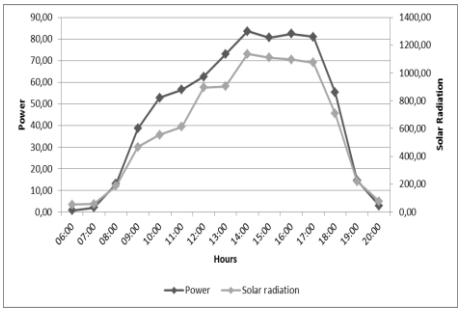

Fig. 12 Solar radition-power relation in Adıyaman

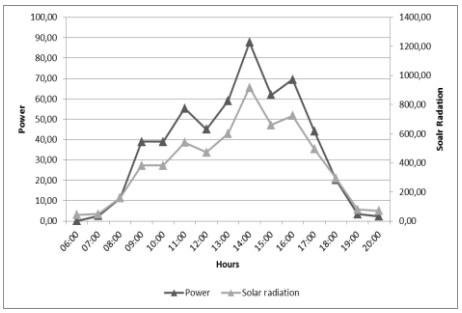

Fig. 13 Solar radition-power relation in Malatya

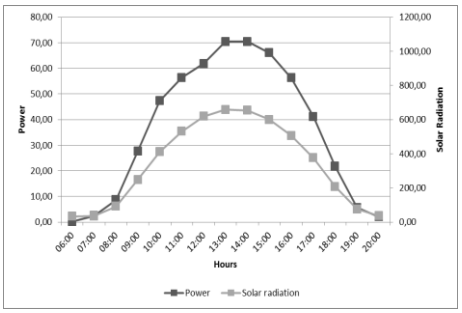

Fig. 14 Solar radition-power relation in Şanlıurfa

When solar radiation-power graphics are examined, it is seen that in accordance with changes in solar radiation magnitude, the power produced changes in parallel. This shows us that solar radiation is the most important factor on the power produced by PV panels. When regions are compared, City of Adıyaman is seen to be the most efficient region in terms of both solar radiation magnitude and power produced (Fig. 12,13,14).

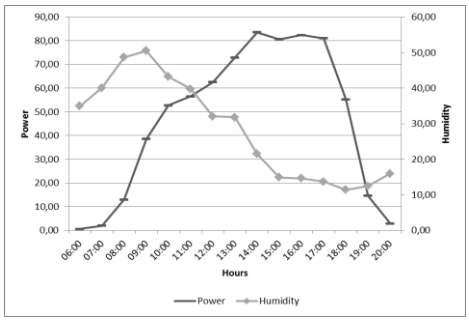

Fig. 15 Humidity-power relation in Adıyaman

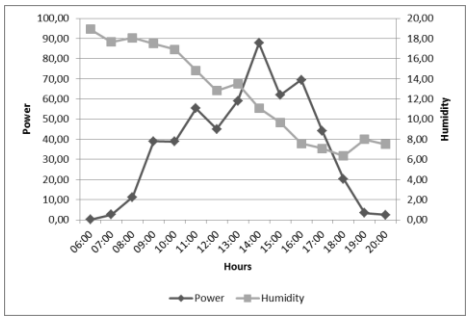

Fig. 16 Humidity-power relation in Malatya

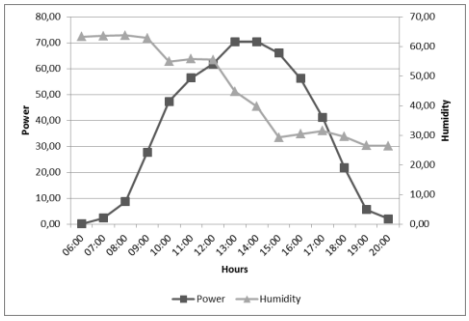

Fig. 17 Humidity-power relation in Şanlıurfa

When the humidity-power graphics of the regions were examined, power produced trhough PV panels and humididty were detected to be inversely proportional. As the humidity descreases, especially at noon when humidity is minimum, power produced was seen to rise up to the maximum value (Fig. 15, 16, 17).

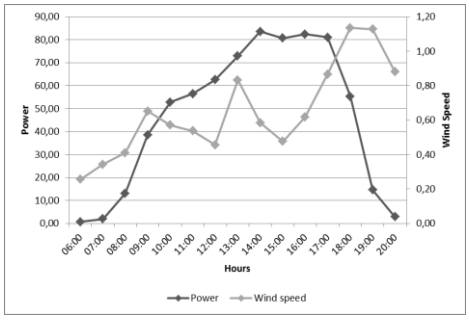

Fig. 18 Wind speed-power relation in Adıyaman

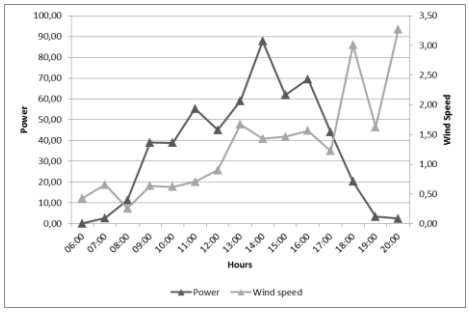

Fig. 19 Wind speed-power relation in Malatya

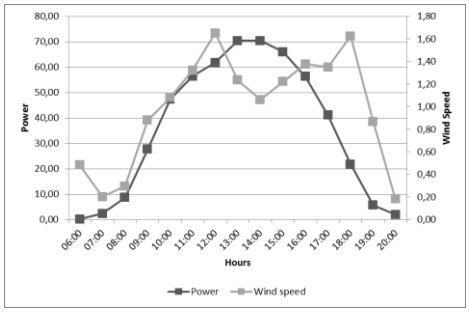

Fig. 20 Wind speed-power relation in Şanlıurfa

When wind speed-power graphics were examined, it has been seen that power changes show a paralellism with the wind speed. It is also seen that as the wind speed decreases the temperatures of the panels, even if partially, it has a positive effect on the power produced. As the measurement period was in summer, the wind speed was measured in minimal values (Fig. 18, 19, 20).

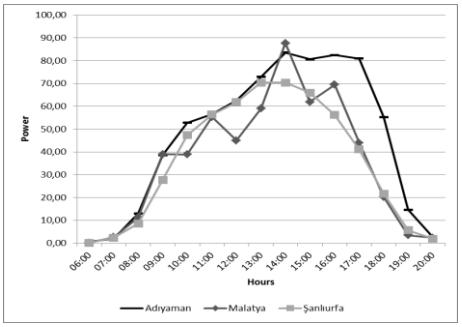

Fig. 21 Power comparison of cities Adıyaman, Malatya and Şanlıurfa

When the power graphics of the cities where the measurements were taken were compared Adıyaman is seen to be more efficient than Malatya and Şanlıurfa. In terms of solar radiation Adıyaman has higher values than the other two cities, too. In addition, power obtained from solar panels in this city is higher than that of the other regions (Fig. 21).

III. Conclusion

In the study conducted measurements made between 14th and 20th August 2017, the cities were seen to be lined up as Adıyaman, Malatya and Şanlıurfa in terms of power obtained from PV panels and the solar radiation. Ambient factors like solar radiaiton, temperature, humidity and wind were detected to be effective on the power produced through the PV panels. The magnitude of the solar radiation was seen to be the most effective factor on PV panel output power. Measurement and assessment work is still continuing. In a different study, by using effects of ambient factors on solar energy systems about energy efficiency, theoritical data and annual data obtained from measurement stations and by utilising (ANN) Artificial Neural Networks algorithms, the model of the system will be constructed and a package software will be produced. Afterwards, when temperature, humidity, wind, altitude and solar radiation values for different regions will be given to the application, possible power that will be produced by a system-to-be installed and its possible efficiency will be estimated through this application.

References

[1] S.S. Inamdar, and A.P. Vaidya, "Performance analysis of solar photovoltaic module for multiple varying factors in MATLAB/Simulink", *Smart Technologies and Management for Computing, Communication, Controls, Energy and Materials (ICSTM), 2015 IEEE Int. Conf.*, pp. 562-567.

[2] S. Rustemli, and F. Dincer, "Modeling of photovoltaic panel and examining effects of temperature in Matlab/Simulink", *Elektronika ir Elektrotechnika*, vol. 109, no. 3, pp. 35-40, 2011.

[3] M. Almaktar, H. A. Rahman, and M. Y. Hassan, "Effect of losses resistances, module temperature variation, and partial shading on PV output power", *Power and Energy (PECon), 2012 IEEE Int. Conf.,* pp. 360-365.

[4] M. Irwanto, Y. M. Irwan, I. Safwati, W. Z. Leow, and N. Gomesh, "Analysis simulation of the photovoltaic output performance", *Power Engineering and Optimization Conf. (PEOCO), 2014 IEEE 8th International*, pp. 477-481.

[5] R. Bhol, A. Pradhan, R. Dash, S. M. Ali, "Environmental effect assessment on performance of solar PV panel", *Circuit, Power and Computing Technologies (ICCPCT), 2015 IEEE Int. Conf.*, pp. 1-5.

[6] M. Islam, M. Z. Rahman, and S. M. Mominuzzaman, "The effect of irradiation on different parameters of monocrystalline photovoltaic solar cell", *Developments in Renewable Energy Technology (ICDRET), 2014 3rd IEEE Int. Conf.*, pp. 1-6.

[7] N. Besli, M. A. Aktacir, and B. Yesilata, "Testing and Characterization of Photovoltaic Panels Under Real Field Conditions", *Engineer & the Machinery Magazine*, vol. 51, no. 601, pp. 21-28, 2010.

[8] A. Karanfil, H. Özbay, M. Kesler, "Simulation Analysis of Temperature and Solar Radiation Changes on the Photovoltaic Panel Power", *Electrical-Electronics and Computer Symposium,* May 2016.

[9] S. Ghazi , K. Ip, "The effect of weather conditions on the efficiency of PV panels in the southeast of UK," *Renewable Energy*, vol. 69, pp. 50-59, Sep. 2014.
[10] E. Köse, and E. Zengin, "Evaluation of the significant factors that affect energy conversion quality of solar batteries", emo.org.tr.
[11] İ. H. Altaş, "Photovoltaic Solar Cells: Structural Properties and Characteristics", in *Energy*, *Electricity*, *Electromechanics*, 3rd ed. vol. 47, İstanbul:Bileşim Publishing, 1998, pp.66-71.
[12] U. Yılmaz, A. Demirören, and H. L. Zeynelgil, "Investigation of the Potential for Electrical Energy Production with Renewable Energy Sources in Gökçeada", *Journal of Polytechnic*, vol. 13, no. 3, pp. 215-223, 2010.
[13] V. J. Fesharaki, M. Dehghani, J. J. Fesharaki, and H. Tavasoli, "The effect of temperature on photovoltaic cell efficiency", *Proceedings of the1st International Conference on Emerging Trends in Energy Conservation – ETEC,* Nov. 2011.
[14] V. B. O. Pepple, C. I. Cookey, and g. I. Alaminokuma, "Effects of temperature, solar flux and relative humidity on the efficient conversion of solar energy to electricity", *European Journal of Scientific Research*, Vol. 35 No. 2, pp. 173-180, 2009.
[15] E. Skoplaki, and J. A. Palyvos, "On the temperature dependence of photovoltaic modüle electrical performance: A review of efficiency/power correlations", *Solar Energy*, Vol. 83, no: 5, pp. 614–624, May 2009.
[16] M. Bilgin, "*Analyzing the effect of surface temperature on the efficiency of photovoltaic panels*", Master's Thesis, İstanbul: Marmara University, 2013
[17] K. Başaran, N.S. Çetin, and H. Çelik, " Wind-solar hybrid power system design and implementation ", *6 th International Advanced Technologies Symposium (IATS'11)*, pp. 114-119, May 2011.
[18] M.G. Villava, J.R. Gazoli, and E.R. Filho, "Modeling and Circuit-Based Simulation of Photovoltaic Arrays", *10th Power Electronics Conf. (COBEP),* 2009.
[19] J. Imhoff, F. G. Rodrigues, J. R. Pinheiro, and H. L. Hey, "A Stand Alone Photovoltaic System Based On Dc-Dc Converters In A Multi String Configuration". *Power Electronics And Applications, European Conf. Control Research Group*, pp. 1-10, Sept. 2007.
[20] M. E. Meral, and F. Dinçer, "A review of the factors affecting operation and efficiency of photovoltaic based electricity generation systems", *Renewable and Sustainable Energy Reviews*, vol. 15, no. 5, pp. 2176-2184, June 2011.
[21] R. Mayfield, "The Highs and Lows of Photovoltaic System Calculations", *Renewable Energy Consultants Electrical Construction and Maintenance*, 2012.
[22] http://www.eie.gov.tr/mycalculator/default.aspx, 13.03.2018.
[23] K. M. Aksungur, M. Kurban, and Ü. B. Filik, "Solar radiation data analysis and evaluation in different regions of Turkey", 5th Energy Efficiency and Quality Symposium, 2013.
[24] J. K. Kaldellis, M. Kapsali, and K. A. Kavadias, "Temperature and wind speed impact on the efficiency of PV installations. Experience obtained from outdoor measurements in Greece", *Renewable Energy*, vol. 66, pp. 612-624, June 2014.

Energy and Exergy Analysis of a Hospital Trigeneration System

Mehmet Burak Özgöztaşi[1], Ayşegül Abuşoğlu[2]

***Abstract*—** Developing countries like Turkey have a growing need for energy in a wide variety of areas. In addition, existing energy sources must be used in the most efficient way. Since trigeneration systems are both electricity generating and heating and cooling effects producing systems, they clearly reduce operating costs with less fuel consumption than systems that produce them separately. Besides, in these systems, greenhouse effect can be avoided by using environmentally friendly refrigerants or refrigerant pairs. Trigeneration systems can be thought of as a system that basically includes chiller units that have been added to a cogeneration system and operate with waste heat energy. Trigeneration systems are the most effective solutions to reduce the electricity consumption in summer, especially due to the cooling requirement, as well as being a system that clearly reduces operating costs. Given all these features, the trigeneration systems offer a unique solution for medium and large-scale businesses such as hospitals, university campuses, hotels, shopping malls for electricity generation, heating and cooling effects.

The trigeneration system discussed in this study is an actual natural gas internal combustion engine powered trigeneration system in a research hospital campus. This system is designed to have 2000 kWh electricity, 2155 kWh heating and 1350 kWh cooling load capacities. First, the process flow diagram of this system will be presented to explain the basic operating principles and then a detailed energy and exergy analysis of all the sub-units of the system will be presented. In thermodynamic analysis, the actual operating data of the system will be used. Thus, the reasons of the exergy destructions occurred in the sub-units will be discussed; specific improvement methods and solution proposals will be presented.

***Keywords*—** Natural Gas Engine Powered Trigeneration, Energy, Exergy, Exergy Destruction

I. INTRODUCTION

Trigeneration systems, which means “combined cooling, heating and power systems”, are not only the production of heat and electricity but also the production of cooling effect using the hot water by the exhaust gas of a cogeneration system. Therefore, trigeneration systems are a cooling system addition to cogeneration systems.

In recent years, consumption of electricity, heating and cooling demands are increased. For these increasing demands and efficiency of energy and exergy, trigeneration systems are broadly used as a solution especially in hospitals, university campuses and many facilities. E. Santo [1] performed an energy and exergy analyses of a high efficiency engine trigeneration system for a hospital. In this paper, the energy demand of a Brazilian university hospital was assessed. F. Calise, M. Dentice d’Accadia, L. Libertini, E. Quiriti and M. Vicidomini [2] studied thermoeconomic analysis and optimization of a trigeneration system in a hospital located in Italy. In this case, it was aimed to minimize the plant costs and maximized the performance of the system with comparing three different operating strategies on different time bases. D. Ziher and A. Poredos [3] evaluated the economics of a trigeneration system in a hospital in Slovenia. In this paper, there was not an optimization of the whole trigeneration system, but they focused on economics. P. Arcurui, G. Florio, and P. Fragiacomo [4] presented a mixed integer programming model to solve the optimal strategy of a combined cooling, heating and power system occurred from a cogeneration system developed with compression and absorption heat pumps to meet the variable and complex energy demands of a hospital. M. İmal, T. Kısakesen and A. Kaya [5] compared cogeneration and tri-generation systems depending on the principle of energy efficiency and economic analysis in a research hospital in Kahramanmaraş named KSU Health Application Research Hospital. D. Ekinci [6] studied the feasibility of a trigeneration system in a campus hospital in Erzurum. In this feasibility, they researched applicability of the trigeneration system by using economic analyses and simulations. Pagliarini, C. Corradi and S. Rainieri [7] presented an optimization of combined cooling, heating and power system for a hospital existing in Parma in Italy by using building energy simulation tool. In this paper, natural gas fired boiler was used in mentioned hospital system, cause of electrical and hot water demands, the management of hospital decided to develop the hospital energy and hot water production. B. Taseli and B. Kilkis [8] studied on site biogas fueled trigeneration retrofit in a university hospital in Malatya. In this paper, they compared two scenarios, first scenario was base scenario, three trigeneration engines with natural gas, total capacity was 5,65 MW. A. Cumbul, H. Tavman and A. Ezan [9] studied thermodynamic analysis of a trigeneration system in hospital application. In this paper, case study hospital is in Ankara. The capacity of trigeneration system is 17,2 MW.

II. SYSTEM DESCRIPTION

The schematic of hospital trigeneration system plant is shown in Fig. 1. This plant has a total installed electricity 4

Mehmet Burak Özgöztaşı[1] is with Dr. Lütfi Kırdar Research and Practice Hospital/ Energy Division, Kartal, Istanbul, 34865 Turkey (e-mail: bozgoztasi@kalyongrup.com)

Ayşegül ABUŞOĞLU[2] is with Department of Mechanical Engineering/ Energy Division/ Gaziantep University Gaziantep, 27310 Turkey (e-mail: ayabusoglu@gantep.edu.tr).

MW, respectively. The electricity will be generated by two, natural gas engine sets each having one turbocharger. Each natural gas engine–generator set in the plant produces 2 MW electricity. The schematic diagram of this plant for one engine set is shown in Figure 1. The engine is 20 cylinders in a V configuration. Natural gas is used as the fuel.

As a description of schematic shown in Fig. 8.1, In state 1, natural gas is used for engine. After reaction, exhaust gas goes directly to the waste heat boiler as state 2. In state 3, water gets heat from waste heat water boiler and goes to the absorption chiller's generator state 4. In generator, the temperature of the water decreases as state 5 and the temperature of the LiBr/H2O increases. As state 5 the water is used as hospital's hot water. In state 6 the pressure of the hot water increases with two pumps. Pressured water goes the heat exchanger as state 7.

In state 8, 9 and 10 %35 ethylene glycol and water are used with pump as high temperature circulation. In state 11,12 and 13 %35 ethylene glycol and water are used with pump as low temperature circulation and the temperature decreases with dry cooler.

For absorption chiller, cooling tower is used in state 14, 15, 16 and 17. Saturated vapor goes condenser to give its heat to the condenser in state 20, condensed vapor is pressurized in state 21 and goes to the evaporator as state 22. In state 22, h hospital's cold water is produced, and vapor produced. Vapor goes to the absorber and in state 23 and in absorber LiBr-H2O mix is used for heat transfer in state 24, 25, 26, 27, 28, 29

The reference (i.e. dead state) temperature is taken as the actual ambient conditions (25°C and 101 kPa). Other assumptions include:

a. The KLKTRH trigeneration system operation is in the steady-state.

b. The ideal gas principles are applied to exhaust gases.

c. The combustion reaction in natural gas engine is complete.

d. The kinetic and potential energy changes are negligible.

e. Because the state of water in the exhaust is generally vapor in internal combustion engines, the lower heating value (LHV) of the fuel is used.

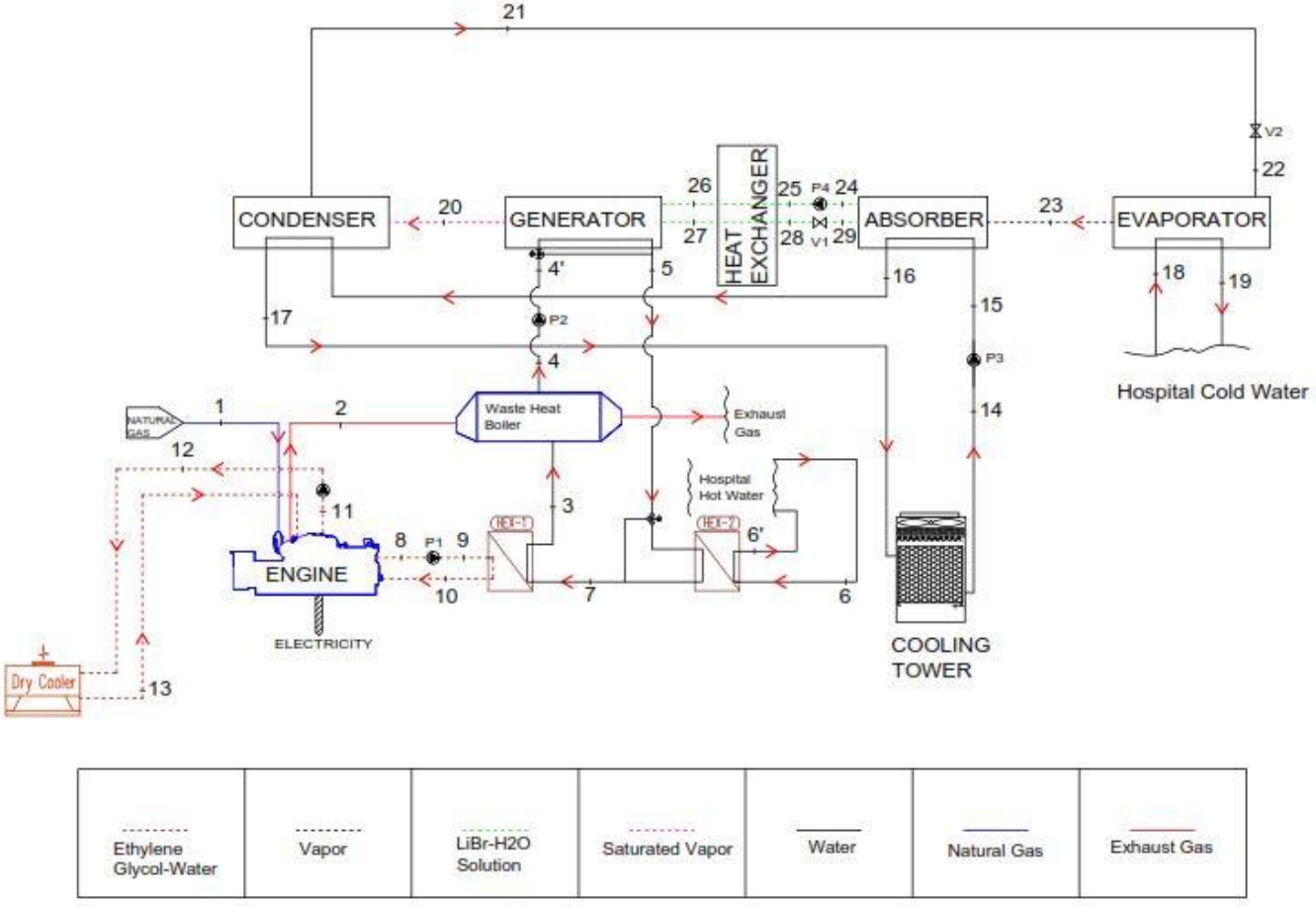

Fig. 1 Schematic of Trigeneration System

III. THERMODYNAMIC ANALYSIS OF SYSTEM

B. Energy Analysis

Energy conversation is expressed by energy balances and together with corresponding mass balances they are widely use in the modeling and analysis of energy conversion systems.

In steady flow systems, in a control volume the total amount of mass does not change with time. Therefore, due to the conservation of mass principle, the total amount of mass entering in a control volume equal to the total amount of mass leaving a control volume. In the rate form it is expressed as

$$\sum \dot{m}_{\mathrm{i}} - \sum \dot{m}_{\mathrm{e}} = \frac{dm_{\mathrm{system}}}{dt} \tag{1}$$

Where i refers to inlet and e refers to exit states of the any control system. For a general steady-flow system with multiple inlets and exits, the conservation of mass principle can be expressed in the rate form as

$$\sum \dot{m}_{\mathrm{i}} = \sum \dot{m}_{\mathrm{e}} \tag{2}$$

Also, energy balance can be expressed in the rate form as

$$\dot{E}_{\mathrm{in}} - \dot{E}_{\mathrm{out}} = \Delta \dot{E}_{\mathrm{system}} \tag{3}$$

Then the rate form of the general energy balance reduces for a steady-flow process to

$$\dot{E}_{\mathrm{in}} = \dot{E}_{\mathrm{out}} \tag{4}$$

Exergy Analysis

The total exergy of a system can be divided into four components: Physical exergy, kinetic exergy, potential exergy and chemical exergy. Then the total exergy of a system is given by

$$E_{\mathrm{sys}} = E_{\mathrm{sys}}^{\mathrm{PH}} + E^{\mathrm{KN}} + E^{\mathrm{PT}} + E^{\mathrm{CH}} \tag{5}$$

The total specific exergy is given by

$$e_{\mathrm{sys}} = e_{\mathrm{sys}}^{\mathrm{PH}} + e^{\mathrm{KN}} + e^{\mathrm{PT}} + e^{\mathrm{CH}} \tag{6}$$

The rate of physical exergy with a material stream is

$$\dot{E}^{\mathrm{PH}} = (H - H_0) - T_0(S - S_0) \tag{7}$$

The exergy destruction in the overall system is equal to the sum of the exergy destruction in all system components:

$$\dot{E}_{\mathrm{D,total}} = \sum_{\mathrm{k}=1}^{\mathrm{n_k}} \dot{E}_{\mathrm{D,k}} \tag{8}$$

The rate of exergy destruction in the component of a system is given by

$$\dot{E}_{\mathrm{D,k}} = \dot{E}_{\mathrm{F,k}} - \dot{E}_{\mathrm{P,k}} - \dot{E}_{\mathrm{L,k}} \tag{9}$$

Where, $\dot{E}_{F,k}$ and $\dot{E}_{P,k}$ are called fuel and exergetic product, respectively, and $\dot{E}_{L,k}$ represents the exergy rate loss in the component, which is usually zero when the component boundaries are at T_0. For an overall system, $\dot{E}_{L,total}$ includes the exergy flow rates of all non-useful streams rejected by this system to the surroundings.

The total exergy destruction value is also obtained from the exergy balance written for the overall system.

$$\dot{E}_{\mathrm{D,total}} = \dot{E}_{\mathrm{F,total}} - \dot{E}_{\mathrm{P,total}} - \dot{E}_{\mathrm{L,total}} \tag{10}$$

Exergetic Efficiency

The exergetic efficiency of the component is defined as the ratio between product and fuel. The exergy rates of product and the fuel are defined by considering the desired result produced by the component, and the exergetic resources expended to generate this result, respectively:

$$\varepsilon_{\mathrm{k}} = \frac{\dot{E}_{\mathrm{P,k}}}{\dot{E}_{\mathrm{F,k}}} = 1 - \frac{\dot{E}_{\mathrm{D,k}} + \dot{E}_{\mathrm{L,k}}}{\dot{E}_{\mathrm{F,k}}} \tag{11}$$

Exergy Destruction Ratio and Exergy Loss Ratio

In addition to the exergy destruction and the exergetic efficiencies, the exergy destruction ratio is used in the thermodynamic evaluation of a component. This ratio compares the exergy destruction in the component with the total fuel exergy supplied to the overall system.

$$y_{\mathrm{D,k}} = \frac{\dot{E}_{\mathrm{D,k}}}{\dot{E}_{\mathrm{F,total}}} \tag{12}$$

Also, the exergy destruction rate of the component can be compared to the total exergy destruction rate.

$$y^{*}_{\mathrm{D,k}} = \frac{\dot{E}_{\mathrm{D,k}}}{\dot{E}_{\mathrm{D,total}}} \tag{13}$$

The exergy loss ratio is defined similarly to equation 12, by comparing the exergy loss to the total fuel exergy supplied to the overall system.

$$y_{L,total} = \frac{\dot{E}_{L,total}}{\dot{E}_{F,total}} \quad (14)$$

The difference between the exergy destruction ratio and the exergetic efficiency is that in the former the exergy destruction within a component is related to the fuel exergy supplied to the overall system, whereas the latter refers the same exergy destruction to the fuel exergy supplied to the component. The exergy destruction ratio expresses the percentage of the decrease of the exergetic efficiency for the overall system caused by the exergy destruction in the component.

$$\varepsilon_{total} = \frac{\dot{E}_{P,total}}{\dot{E}_{F,total}} = 1 - \frac{\dot{E}_{D,total} + \dot{E}_{L,total}}{\dot{E}_{F,total}} = 1 - y_{D,total} - y_{L,total} \quad (15)$$

IV. RESULTS

The hospital plant is divided into fifteen components/subsystems as shown in Fig.1. the temperature, pressure and mass flow rate data and certain exergy evaluations of the plant to the nomenclature shown in Fig.1 and presented in Table I. The energy and exergy calculations are done using commercial software with built-in thermodynamic property functions for a variety of substances. In defining the exergy flow through the subsystems, fuel and product terms must be identified. The product represents the desired result produced by the component whereas the fuel represents the resources expended to generate the product. Both the product and the fuel are expressed in terms of exergy and definitions of the exergies of the fuels and the exergies of products for the components of the plant.

TABLE I (A)
PLANT DATA, THERMODYNAMIC PROPERTIES AND EXERGIES

State No	Fluid	Pressure P (kpa)	Temperature T (°C)	Mass flowrate ṁ (kg/s)	Enthalpy h (kJ/kg)	Entropy s (kJ/kg°C)	Specific exergy ψ (kJ/kg)	Exergy rate, Ė (kW)
1	Natural Gas	15,00	25,00	17,53	-4666,99	11,60	51,38	900,74
2	Exhaust Gas		414,00	3,01	699,47	2,55	145,60	438,93
3	Saturated Water	196,00	86,10	27,19	360,48	1,15	23,18	630,23
4	Saturated Water	201,00	95,00	27,19	398,09	1,25	29,93	813,90
4'	Saturated Water	245,00	95,00	27,19	398,09	1,25	29,93	813,90
5	Saturated Water	245,00	77,00	27,19	327,14	1,05	17,81	484,22
5'	Saturated Water	217,00	95,00	27,19	398,09	1,25	29,93	813,90
6	Saturated Water	135,00	60,00	23,01	251,18	0,83	7,98	183,59
6'	Saturated Water	135,00	80,00	23,01	335,02	1,08	18,98	436,74
7	Saturated Water	196,00	77,00	27,19	327,14	1,05	17,81	484,22
8	Saturated Water	403,00	93,00	16,58	389,67	1,23	28,37	470,40
9	Saturated Water	403,00	93,00	16,58	389,67	1,23	28,37	470,40
10	Saturated Water	403,00	80,00	16,58	335,02	1,08	18,98	314,70
11	Ethylene glycol+ water	124,00	44,20	11,05	185,09	0,63	2,50	27,65
12	Ethylene glycol+ water	257,00	44,20	11,05	185,09	0,63	2,50	27,65
13	Ethylene glycol+ water	124,00	40,00	11,05	167,53	0,57	1,52	16,79
14	Saturated Water	117,00	28,00	104,05	117,38	0,41	0,11	11,77
15	Saturated Water	248,00	28,00	104,05	117,38	0,41	0,11	11,77
16	Saturated Water	240,00	30,00	104,05	125,74	0,44	0,16	16,52
17	Saturated Water	238	33	104,05	138,28	0,48	0,5	52,49

TABLE I (B)
PLANT DATA, THERMODYNAMIC PROPERTIES AND EXERGIES

State No	*Fluid*	*Pressure* *P (kpa)*	*Temperature* *T (°C)*	*Mass flowrate* *ṁ (kg/s)*	*Enthalpy* *h (kJ/kg)*	*Entropy* *s (kJ/kg°C)*	*Specific exergy* *Ψ (kJ/kg)*	*Exergy rate,* *Ė (kW)*
18	Saturated Water	155,00	12,00	58,23	50,41	0,18	1,27	73,98
19	Saturated Water	150,00	7,00	58,23	29,42	0,11	2,41	140,21
20	Hot Vapor	8,00	95,00	0,53	2667,60	7,42	308,68	162,67
21	Saturated Water	7,30	45,80	0,53	191,78	0,65	2,94	1,55
22	Saturated Water	0,87	5,00	0,53	191,83	0,69	-9,33	-4,92
23	Water Vapor	0,87	5,00	0,53	2510,60	9,03	-175,64	-92,56
24	Solution	0,80	40,00	5,27	97,38	0,21	14,00	73,79
25	Solution	8,00	40,00	5,27	97,38	0,21	14,00	73,79
26	Solution	8,00	70,00	5,27	140,40	0,39	1,57	8,26
27	Solution	8,00	95,00	4,75	201,14	0,49	33,09	157,17
28	Solution	8,00	50,00	4,75	153,70	0,29	44,09	209,41
29	Solution	0,80	45,00	4,75	149,36	0,30	37,66	178,88

TABLE II
ENERGETIC AND EXERGETIC ANALYSES

	Q (kW)	W (kW)	E_F (kW)	E_P (kW)	E_D (kW)	y* (%)	y (%)	ε (%)
Engine		2000	1301,32	1040,25	21,07	31,08	0,04	79,94
Dry Cooler	194,04		27,65	16,79	10,86	1,88	0,24	60,72
HEX-1	906,10		954,62	944,92	9,70	1,68	0,21	98,98
WHB	1022,72		1069,16	813,90	255,26	44,10	5,61	76,13
HEX-2	1929,16		997,49	920,97	76,52	13,22	1,68	92,33
Generator	1929,13		822,16	804,07	18,09	3,13	0,40	97,80
Condenser	2037,75		188,47	83,52	104,96	18,13	2,31	44,31
Evaporator	1221,97		69,06	47,65	21,41	3,70	0,47	69,00
Absorber	1359,15		104,70	99,59	5,11	0,88	0,11	95,12
Heat Exchanger	225,34		230,96	217,66	13,30	2,30	0,29	94,24
Cooling Tower	3396,90		81,97	18,39	63,58	10,99	1,40	22,43
Pump 1		5,50	470,40	469,58	0,82	0,14	0,02	99,83
Pump 2		15,00	813,90	810,13	3,78	0,65	0,08	99,54
Pump 3		75,00	11,77	5,88	5,89	1,02	0,13	49,95
Pump 4		3,00	10,81	9,76	1,05	0,18	0,02	90,31

The rates of exergy destructions of the components of the plant as compared with total fuel exergy input are given in Table II. We note the followings from these results:

The exergetic efficiency of the Engine is %79,94, Dry Cooler is %60,72, HEX-1 is %98,98, Waste Heat Boiler is %76,13, HEX-2 is %92,33.

The exergetic efficiency of Absorption Chiller's Generator is %97,80, Condenser is %44,31, Evaporator is %69, Absorber is %95,12, Heat Exchanger is %94,24 and the exergetic efficiency of Cooling Tower is %22,43.

According to the exergetic analyses, healing the exergetic efficiency of cooling tower, makes the system exergetic efficiency better.

ACKNOWLEDGMENT

I would like to thank to Dr. Lütfi Kırdar Research and Practice Hospital staff, Borusan Power Systems staff for helping me to get the right data in time and also, I would like to thank to my company Kalyon Construction Industry and Trade Corp.

REFERENCES

[1] E. Santo "An energy and exergy analysis of a high efficiency engine trigeneration system for a hospital: A case study methodology based on annual energy demand profiles" Energy and Buildings 7 (2014) 185-198

[2] F. Calise, M. Dentice d'Accadia, L. Libertini, E. Quiriti and M. Vicidomini "A novel tool for thermoeconomic analysis and optimization of trigeneration systems: A case study for a hospital building in Italy", Energy 126 (2017) 64-87

[3] D. Ziher and A. Poredos, "Economics of a trigeneration system in a hospital" Applied Thermal Engineering 26 (2006) 680-687

[4] P. Arcurui, G. Florio, and P. Fragiacomo, "A mixed integer programming model for optimal design of trigeneration in a hospital complex" Energy 32 (2007) 430-1447.

[5] M. İmal, T. Kısakesen and A. Kaya "A Comparative Analysis of Heating and Cooling Capacities for Technologies of Cogeneration and Trigeneration from Perspective of Energy Economy: The Case of KSU Health Application and Research Hospital" KSU Journal of Engineering Sciences, 19(2) 2016

[6] D. Ekinci, "The feasibility of trigeneration system applied on Erzurum Campus Hospital". PhD Thesis 2013

[7] F. Pagliarini, C. Corradi and S. Rainieri "Hospital CHCP system optimization assisted by TRNSYS building energy simulation tool" Applied Thermal Engineering 44 (2012) 150-158.

[8] B. Taseli and B. Kilkis "Ecological sanitation, organic animal farm and cogeneration: Closing the loop in achieving sustainable development-A concept study with onsite biogas fueled trigeneration retrofit in a 900-bed university hospital" Energy and Buildings 129 (2016) 102-119

[9] A. Cumbul, H. Tavman and A. Ezan "Thermodynamic Analysis of a Trigeneration System in Hospital Application" in *2017 ULIBTK 21. National Heat Science and Technic Congress.*

Effect of Variation in Heat Supply to the Performance of a Biomass-fired Combined Power and Refrigeration Cycle – Utilization of Kalina Cycle Heat in an Ejector Refrigeration Cycle

Candeniz SECKIN[1]

***Abstract*—**In this study, a novel combined cycle of power and refrigeration production is proposed which is a combination of Kalina cycle and ejector refrigeration cycle. In the proposed configuration of the combined cycle, an ejector refrigeration cycle is inserted into the Kalina cycle to generate refrigeration by utilizing the high energy content of one working fluid stream in Kalina cycle which does not directly contribute to the power production of the Kalina cycle. Supplied heat to the proposed combined cycle is derived from biomass which is a renewable energy source and is regarded as a promising alternative to fossil fuel consumption in energy generation processes. A parametric analysis is performed to determine the effect of variation in the rate of heat supplied to the combined cycle and the amount of biomass consumed in heat generation on selected performance parameters of the combined cycle: thermal efficiency, power production and refrigeration generation. A computational program is developed to simulate the combined cycle and details of the applied mathematical model are reported in the study. It is determined that increasing heat supply to the combined cycle results in increase in net power production of the cycle. Refrigeration capacity is not influenced by the heat supply and thermal efficiency follows a decreasing trend as supplied heat to the combined cycle increases.

***Keywords*—** Biomass-fired combined cycle, Ejector refrigeration cycle, Kalina cycle.

I. INTRODUCTION

Rapidly increasing population and increasing energy demand of world leads to pose a rising trend in fossil fuel use predictions over the long term future of the World. As a result, renewable energy utilization and energy efficient technology development have become the focus of interest for many researchers in an attempt to meet the increasing energy demand of the World with minimum degradation and/or depletion of fossil fuel sources and to overcome the environmental and social problems which emerge from fossil fuel use in energy generation (such as: climate change due to greenhouse gas emissions, pollution of air and water sources, energy crisis and resource scarcity). As a result, introducing new ways for the use of renewable energy sources instead fossil fuels in energy generation and developing new technologies for efficient utilization of non-renewable energy resources have become the crucial concerns for a sustainable future [1,2].

Biomass is a renewable energy form that causes less environmental damage and can be directly utilized in energy generation processes instead non-renewable fuels (fossil fuels). Every year, millions of tons of organic waste is produced which can be used as source of biomass instead being disposed to nature (landfilling) which causes harmful results to human health and environment. Incineration of waste is a process which enables to produce energy by heat generation, providing cost effectiveness and minimizing the mass and volume of final waste disposal [1]. Therefore, in this study, organic fraction of municipal solid waste (MSW) undergoes incineration process to produce heat and then, produced heat is supplied to the analyzed combined cycle to produce power and refrigeration, simultaneously. As a result, in this study, considered power/refrigeration cycle is driven by biomass which is a renewable energy source.

In recent years, to enhance the efficiency of energy generation processes, the concept of combined power and cooling cycles using binary mixtures as the working fluid have gained considerable attention. Binary mixtures, which is widely used as working fluid in power and refrigeration cycles to decrease the irreversibilities via providing a better temperature match in heat exchangers of the cycle (including boiler, evaporator and condenser). Binary fluids have variable boiling/condensation temperatures at constant pressure (while one-component fluids boil and condense at constant temperatures), which supplies a better thermal match between the working fluid and the heat source, i.e., less irreversibility production during heat transfer processes causes increased energy and exergy efficiency of the cycle [3,4]. Ammonia–water is the most commonly used binary mixture in power and/or combined power and cooling cycles. It is reported in many studies that, compared to conventional Rankine cycle with steam as a working fluid, ammonia–water mixture using cycles can provide higher thermal efficiencies in different thermal boundary conditions [5]. As a result, ammonia–water is used as the working fluid to construct combined cooling and power cycles with improved overall energy efficiency. In the early 1980s, Kalina [6,7] introduced a power cycle (Kalina cycle) using a binary mixture as working fluid to produce power from heat. The configuration of Kalina cycle can be viewed as

Candeniz SECKIN[1] (corresponding author) is with the Department of Mechanical Engineering, Faculty of Engineering, Marmara University, Goztepe Campus, Istanbul 34722, Turkey (corresponding author's phone: 00902613480292; e-mail: candeniz.seckin@marmara.edu.tr).

further development of Rankine cycle and absorption power cycle which also takes the advantages of binary mixture use as the working fluid (details can be seen in [8,9]).

In an ejector refrigeration cycle (ERC), ejector is used instead the compressor in the vapor compression refrigeration system which serves as a compression agent for the low pressure fluid (comes from the evaporator) and as an expansion agent for the high temperature fluid (comes from the boiler) [10]. The low-grade energy sources can be used as the necessary energy supply to the ERC in contrast to electrical energy that powers the conventional vapor compression refrigeration cycles. As a result, in the absence of compressor, total energy consumption of the refrigeration cycle gets lower and hence, energy efficiency (COP) gets higher. Since the use of ejector also provides several additional advantages such as [11,12]: simplicity of conception, low installation and operational costs (due to the absence of moving parts except the pumps in ERC), operation with a wide range of refrigerants, in an attempt to develop and promote energy efficient technologies, ejector use in refrigeration systems has become the focus of interest for many researchers.

The objective of this study is to present a new design for a power/refrigeration combined cycle (combination of Kalina cycle and ERC) and to determine the effect of variation in energy input to the selected performance parameters (energy efficiency, power production and refrigeration capacity) by means of a performed parametric analysis. In the configuration of the combined cycle, refrigeration is produced by an ejector refrigeration cycle (ERC) which is inserted into the Kalina cycle. ERC is driven by heat transferred from one stream of Kalina cycle working fluid (at high temperature/pressure) which does not directly contribute to the power production of the Kalina cycle. Supplied heat to the proposed combined cycle is obtained by combustion of biomass (organic waste). The analysis is performed by simulation of the combined cycle and details of the applied mathematical model are extensively reported in the paper.

II. SYSTEM DESCRIPTION

Schematic overview of the considered combined power/refrigeration cycle is presented in Fig. 1. The Kalina cycle has the similar schematic diagram to the illustrated schematic in Fig. 1. When the ejector refrigeration cycle (dashed box in Fig. 1) is not inserted into the Kalina cycle, state-points 3 and 4 become the identical points. Hence, Kalina cycle has the same form with Fig.1 at the absence of the ERC. As seen in the Fig. 1, Kalina cycle is made up of the following components: a heat exchanger (HE I), a separator, a turbine, a high temperature recuperator (HTR), a low-temperature recuperator (LTR), a condenser (condenser I), a pump (pump I) and a valve (valve I). Heat which is derived from combustion of biogas is transferred to the Kalina cycle in the heat exchanger I (HE I). Extensive details of the operational mechanism and technical details for Kalina cycle [13] and the analyzed combined power/refrigeration cycle (Fig. 1) are extensively provided in earlier studies [8]. As a result, duplication is avoided here.

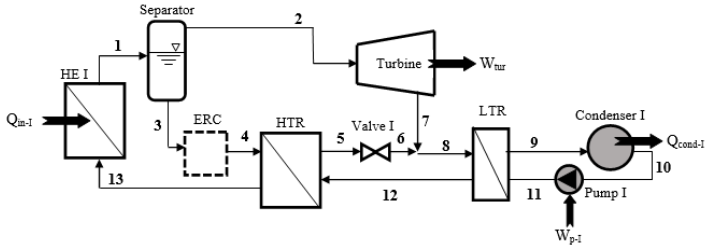

Fig. 1 Schematic representation of Kalina sub-cycle.

Schematic overview of the ejector refrigeration cycle (ERC) is shown in Fig. 2. As seen in Fig. 2, ERC consists of an ejector, a heat exchanger (HE II), an evaporator, a condenser (condenser II), an expansion valve (valve II), and a pump (pump II). Schematic of the ejector (with the names of the ejector parts) is presented in Fig. 3. Details of the ERC flows and operational mechanism of ERC and the ejector are extensively available in [8,11,14,15].

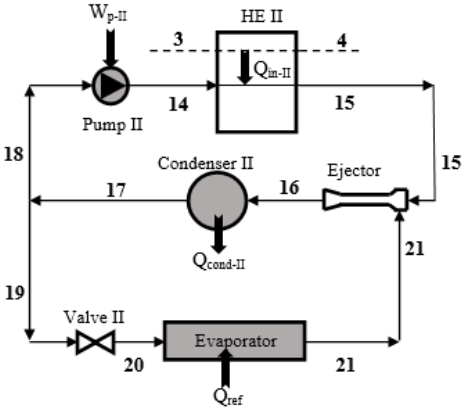

Fig. 2 Schematic representation of ERC.

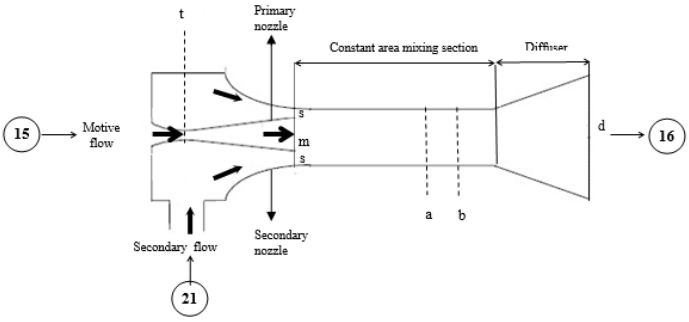

Fig. 3 Schematic representation of the ejector.

III. COMPUTATIONAL PROCEDURE

In the analysis, each component of the combined power/refrigeration cycle is regarded as a control volume. Extensive details of the applied computational procedure, mathematical model and applied assumptions are provided in some earlier studies by the same author [8,11]. Conservation of mass, energy and momentum equations are successively applied to each component of the cycle and the mathematical expressions for the equations are summarized below. In the equations, $\dot{m}$ is the mass flow rate of the working fluid, $\dot{Q}$ is the rate of heat transfer, $\dot{W}$ is power, h is specific enthalpy, x is the concentration of ammonia-water mixture (ammonia mass fraction), η is efficiency and V is the velocity of the fluid. In subscripts: "is" is isentropic, "in" is input flow and "out" is output flow.

The mass balance, ammonia mass balance and conservation of energy principle equations for the separator are given in Eqs. (1-3).

$$\dot{m}_{in} = \dot{m}_{out,1} + \dot{m}_{out,2} \tag{1}$$

$$\dot{m}_{in}\, x_{in} = \dot{m}_{out,1}\, x_{out,1} + \dot{m}_{out,2}\, x_{out,2} \tag{2}$$

$$\dot{m}_{in}\, h_{in} = \dot{m}_{out,1}\, h_{out,1} + \dot{m}_{out,2}\, h_{out,2} \tag{3}$$

Conservation of mass principle is applied to the heat exchangers (HE I, HE II, HTR, LTR, condensers and evaporator) by the following equation:

$$\sum \dot{m}_{in} = \sum \dot{m}_{out} \tag{4}$$

Conservation of energy principle is applied to the HE II, HTR and LTR by the following:

$$\dot{m}_{in,1}\, h_{in,1} + \dot{m}_{in,2}\, h_{in,2} = \dot{m}_{out,1}\, h_{out,1} + \dot{m}_{out,2}\, h_{out,2} \tag{5}$$

Conservation of energy principle is applied to the condensers, the evaporator and HE I by the following:

$$\dot{m}_{in,1}\, h_{in,1} + \dot{Q}_{in} = \dot{m}_{out,1}\, h_{out,1} + \dot{Q}_{out} \tag{6}$$

Applying the conservation of energy equation to the turbine, turbine power generation ($\dot{W}_{tur}$) is computed as follows:

$$\dot{W}_{tur} = \dot{m}_2\, (h_2 - h_7) \tag{7}$$

Mass and energy balance principles are applied to the mixing process of ammonia rich solution (state 7) and ammonia weak solution (state 6) as presented below:

$$\dot{m}_{out} = \dot{m}_{in,1} + \dot{m}_{in,2} \tag{8}$$

$$\dot{m}_{out}\, h_{out} = \dot{m}_{in,1}\, h_{in,1} + \dot{m}_{in,2}\, h_{in,2} \tag{9}$$

Power consumption of the pumps ($\dot{W}_p$) is determined by the following:

$$\dot{W}_p = \dot{m}_{in}\, (h_{out} - h_{in}) \tag{10}$$

To determine the thermodynamic properties of the refrigerant flow in ejector, derived equations for different ejector parts are given below. At the exit of each ejector nozzle, velocity of the refrigerant flow (V_{out}) is determined by applying the conservation of energy principle as presented in the following equation:

$$V_{out} = \sqrt{2\, (h_{in} - h_{out})} \tag{11}$$

In the constant area mixing section, conservation of momentum and energy equations are applied as seen in the below equations to determine the properties of the mixed refrigerant flow (cross section a in Fig. 3). φ is the coefficient of frictional loss, subscript "tot" is total.

$$P_a\, A_a + \dot{m}_{tot}\, V_a = \varphi \left(P_{in,1}\, A_{in,1} + \dot{m}_{in,1}\, V_{in,1} + P_{in,2}\, A_{in,2} + \dot{m}_{in,2}\, V_{in,2} \right) \tag{12}$$

$$\dot{m}_{tot} \left[h_a + \frac{V_a^2}{2} \right] = \dot{m}_{in,1} \left[h_{in,1} + \frac{V_{in,1}^2}{2} \right] + \dot{m}_{in,2} \left[h_{in,2} + \frac{V_{in,2}^2}{2} \right] \tag{13}$$

The isentropic efficiency for pumps (η_p), turbine (η_{tur}), nozzles in the ejector (η_n), diffuser part of the ejector (η_d) are defined in Eqs. (14-17), respectively.

$$\eta_p = \frac{\dot{W}_{p,\,is}}{\dot{W}_p} = \frac{h_{out,is} - h_{in}}{h_{out} - h_{in}} \tag{14}$$

$$\eta_{tur} = \frac{h_{in} - h_{out}}{h_{in} - h_{out,is}} \tag{15}$$

$$\eta_n = \frac{h_{in} - h_{out}}{h_{in} - h_{out,is}} \tag{16}$$

$$\eta_d = \frac{h_{out,is} - h_{in}}{h_{out} - h_{in}} \tag{17}$$

In this study, thermal efficiency (energy efficiency, η_{th}), net power production ($\dot{W}_{net}$) and refrigeration capacity ($\dot{Q}_{ref}$) are selected system parameters to evaluate the combined cycle performance. The thermal efficiency is defined as the ratio of

the produced energy output of the system to the energy input from the heat source in HE I. Mathematical definitions of the net power output ($\dot{W}_{net}$) and combined cycle thermal efficiency (η_{th}) are presented in Eqs. (18-19) where $\dot{Q}_{in\text{-}I}$ is the amount of heat transferred to the Kalina cycle working fluid in HE I.

$$\dot{W}_{net} = \dot{W}_{tur} - \dot{W}_{p-I} - \dot{W}_{p-II} \tag{18}$$

$$\eta_{th} = \frac{\dot{W}_{net} + \dot{Q}_{ref}}{\dot{Q}_{in\text{-}I}} \tag{19}$$

Heat generated by combustion of municipal solid waste organic fraction (biomass) is the heat source of the combined cycle. Chemical composition of biomass and properties of the combustion process are given in Table I. For the combustion process, energy balance equation is:

$$\dot{Q}_{in-I} = \dot{m}_{bio}\, LHV_{bio}\, \eta_B = \dot{m}_K\, (h_1 - h_{13}) \tag{20}$$

where $\dot{Q}_{in\text{-}I}$ is the amount of heat transferred to the Kalina cycle working fluid in HE I, $\dot{m}_{bio}$ is the mass flow rate of the biomass which is combusted in the biomass boiler, LHV_{bio} is the low heating value of biomass, η_B is the boiler efficiency (defined over LHV_{bio}), $\dot{m}_K$ is the mass flow rate of the Kalina cycle working fluid, h is the specific enthalpy of the Kalina cycle working fluid at subscripted states in Fig. 1. Eq. (20) is LHV basis because organic waste undergoes a drying process before combustion in the boiler.

TABLE I
ULTIMATE ANALYSIS OF BIOMASS (ORGANIC WASTE) [16].

C/H/O/N/S/ash (%wt., wet basis)	47.8/6.4/37.6/2.6/0.4/5
HHV_{bio}/LHV_{bio} (MJ/kg) (wet basis)	18.95/17.55
Boiler efficiency (η_B)	0.85

In Table I, HHV_{bio} is the high heating value of as received (wet basis) biomass sample (MJ/kg) calculated by Eq. (21) [17]. In Eq. (21), C, H, O, N and S are weight percent of carbon, hydrogen, oxygen, nitrogen and sulphur in the composition of biomass which are seen in Table I.

$$HHV_{bio}\ (MJ/kg) = \left[33.5(C) + 142.3(H) - 15.4(O) - 14.5(N)\right] \times 10^{-2} \tag{21}$$

LHV_{bio} is calculated via Eq. (22) [18]:

$$LHV_{bio}\ (MJ/kg) = HHV - 8.94\, X_H\, h_{fg} \tag{22}$$

X_H is the mass friction of hydrogen in the sample (in as received (wet) composition) 0.064 for organic waste (see Table I), h_{fg} (2.4423 MJ/kg) is the enthalpy of evaporation of water at standard environmental conditions (25°C and 1 atm) [18].

In this current work, combined cycle of Kalina and ERC is simulated using Engineering Equation Solver (EES) Software. The ejector operates at critical mode, i.e., the ejector is designed in such a manner so that the primary and secondary flows are both chocked, hence, entrainment ratio is constant in the ejector [15]. Ideal gas assumption based Rankine–Hugoniot equations are used to determine the properties of flow at the cross section b in Fig. 3. Details of the Rankine–Hugoniot equations are extensively given in [8]. Secondary flow of the ejector performs the critical flow at the nozzle exit [15] and thermodynamic properties of the fluid at critical conditions are determined by Henry and Fauske method. Details and use of Henry and Fauske method are extensively discussed in [8].

IV. RESULTS AND DISCUSSION

A parametric analysis is performed by applying the above presented mathematical model to the analyzed power/refrigeration cycle which has a novel design of Kalina cycle and ejector refrigeration cycle combination. In the analysis, the effect of variation in energy input ($\dot{Q}_{in\text{-}I}$) on selected performance parameters of the combined cycle (thermal efficiency, net power production, refrigeration capacity) is investigated. An extensive discussion of the physical mechanism behind the determined results is also presented. Additionally, since the heat which is supplied to the combined cycle ($\dot{Q}_{in\text{-}I}$) is obtained from a renewable energy source (organic waste, biomass), the necessary amount of biomass to generate the supplied heat to the combined cycle is also determined. The boundary conditions and simulation parameters for Kalina cycle and ERC are reported in Table II.

TABLE II
OPERATIONAL PARAMETERS OF THE COMBINED CYCLE.

Rate of heat transfer to the combined cycle - $\dot{Q}_{in\text{-}I}$ (kW)	500 - 1500
Pressure at turbine inlet - P_2 (kPa)	3250
Temperature at condenser I exit - T_{10} (C)	25
Concentration of NH_3-H_2O basic solution - x_1 (%)	70
Isentropic efficiency of pumps ($\eta_{p\text{-}I}$, $\eta_{p\text{-}II}$) (%)	60
Isentropic efficiency of turbine and ejector parts (η_{tur}, η_n, η_d) (%)	80
Mass flow rate of the Kalina cycle working fluid - $\dot{m}_1$ (kg/s)	0.98

As presented in Table II, the parametric analysis of the considered combined cycle is conducted with variable heat input rate ($\dot{Q}_{in\text{-}I}$) to the cycle. Hence, mass flow rate of the organic waste supplied to the cycle is not constant and computed by inserting the organic waste and biomass boiler properties (given in Table I) into the Eq. (20). Computed amount of biomass supplied to the boiler is presented in Fig. 4 with the corresponding amount of heat which is transferred to the Kalina cycle working fluid through the HE I.

Applying the computational procedure presented in Section 3, effect of increasing heat supply to the combined cycle in HE I ($\dot{Q}_{in\text{-}I}$) on combined cycle net power production ($\dot{W}_{net}$) and refrigeration capacity ($\dot{Q}_{ref}$) is determined and is shown in Fig.

4. As presented in Table II, operational pressure through the HE I (which is identical to the pressure of the working fluid at the turbine inlet) is constant during the operation. It is very predictable that, increasing $\dot{Q}_{in\text{-}I}$ results in the rise of working fluid specific enthalpy (and hence, temperature) at the exit of the HE I, based on Eq. (6). Since the temperature at the HE I exit (state point 1) and at the turbine inlet (state point 2) are identical, it can be concluded that, temperature of the working fluid at the turbine inlet rises as $\dot{Q}_{in\text{-}I}$ increases. It is determined that as the turbine inlet temperature (T_2) increases, the magnitude of specific enthalpy difference of the ammonia rich solution across the turbine (h_2-h_7) increases. Based on Eq. (7), it can be concluded that increasing $\dot{Q}_{in\text{-}I}$ with increasing T_2 results in increase in $\dot{W}_{tur}$ of the considered power/refrigeration combined cycle.

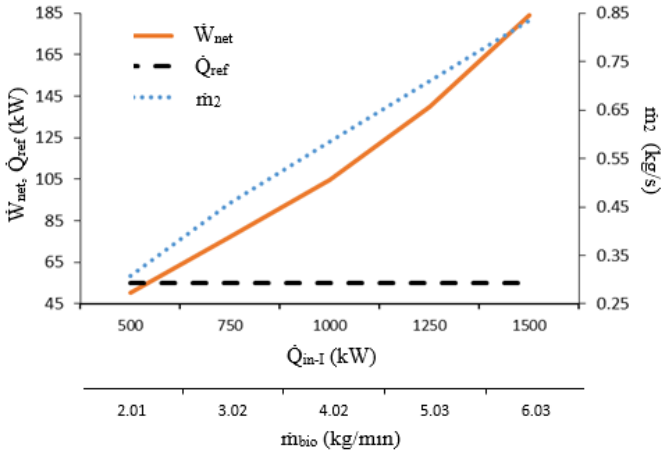

Fig. 4 Variation of $\dot{W}_{net}$, $\dot{Q}_{ref}$, $\dot{m}_2$ and $\dot{m}_{bio}$ with respect to $\dot{Q}_{in\text{-}I}$.

On the other hand, above explained temperature rise of the working fluid at the HE I exit (i.e. at the turbine inlet, state point 2 in Fig. 1) with increasing $\dot{Q}_{in\text{-}I}$ causes increasing mass flow rate of the saturated rich ammonia water vapor (mass flow rate of the working fluid passing through the turbine, $\dot{m}_2$). Phase diagram of ammonia-water solution is presented in [9]. It is easily seen that for constant concentration of ammonia water solution (as it is in this parametric analysis), fraction of saturated ammonia vapor gets higher in ammonia water solution with the rise of ammonia-water solution temperature. Hence, as $\dot{Q}_{in\text{-}I}$ increases, the rate of saturated ammonia vapor production gets higher. Since the ammonia-water basic solution in two-phase region is separated into the saturated rich ammonia-water vapor (state point 2 in Fig. 1) and the saturated weak ammonia-water liquid (state point 3 in Fig. 1) in the separator and ammonia rich vapor is transferred to the turbine, the mass flow rate of the working fluid passing through the turbine ($\dot{m}_2$) rises with increasing $\dot{Q}_{in\text{-}I}$. Since, based on Eq. (7), $\dot{W}_{tur}$ and $\dot{m}_2$ are directly proportional, $\dot{W}_{tur}$ results of the combined cycle gets higher with increasing $\dot{Q}_{in\text{-}I}$. As a result, due to the combined effect of growing enthalpy difference of the ammonia water solution through the turbine (h_2-h_7) and increasing $\dot{m}_2$, power production by the turbine ($\dot{W}_{tur}$) considerably rises as the heat supply to the combined cycle ($\dot{Q}_{in\text{-}I}$) increases, based on Eq. (7). It must be stated that, $\dot{W}_{tur}$ is by far the largest constituent of the net power production ($\dot{W}_{net}$) of the combined cycle, i.e., magnitude of power consumption by pump I ($\dot{W}_{p\text{-}I}$) and pump II ($\dot{W}_{p\text{-}II}$) is negligible relative to that of $\dot{W}_{tur}$. Hence, $\dot{W}_{tur}$ determines the $\dot{W}_{net}$ characteristics of the cycle. As a result, increasing $\dot{Q}_{in\text{-}I}$ results in increasing $\dot{W}_{tur}$ (and hence $\dot{W}_{net}$) which is presented in Fig. 4.

On the cooling capacity ($\dot{Q}_{ref}$) side of the issue, due to the constant operational parameters of ERC (condenser II pressure/temperature, evaporator pressure/temperature, HE II pressure, etc.), constant flow properties of the refrigerant are determined at the HE II inlet (state-point 14 in Fig. 2). At the exit of the HE II (state-point 15 in Fig. 2), the state of the refrigerant (R134a) is saturated vapor and the properties of the refrigerant is a function of HE II pressure which is constant. Hence, based on Eq. (5), $\dot{Q}_{in\text{-}II}$ is not affected by the Kalina cycle operational parameters including heat supply to the combined cycle ($\dot{Q}_{in\text{-}I}$). As a result, $\dot{Q}_{ref}$ of the combined cycle is constant as $\dot{Q}_{in\text{-}I}$ increases which is seen in Fig. 4.

In Fig. 5, variation of thermal efficiency (η_{th}) as a function of supplied heat to the combined cycle in HE I ($\dot{Q}_{in\text{-}I}$) is presented. It is determined that as $\dot{Q}_{in\text{-}I}$ increases, there is a concurrent increase in $\dot{W}_{net}$ but the rate of increase in $\dot{Q}_{in\text{-}I}$ is higher than that of $\dot{W}_{net}$. Hence, based on Eq. (19), thermal efficiency (η_{th}) of the combined cycle follows a decreasing trend with increasing $\dot{Q}_{in\text{-}I}$ as presented in Fig. 5. It must be stated that, determinative influence of $\dot{W}_{net}$ and $\dot{Q}_{in\text{-}I}$ on thermal efficiency (η_{th}) is supported by constant $\dot{Q}_{ref}$ as presented in Fig 4.

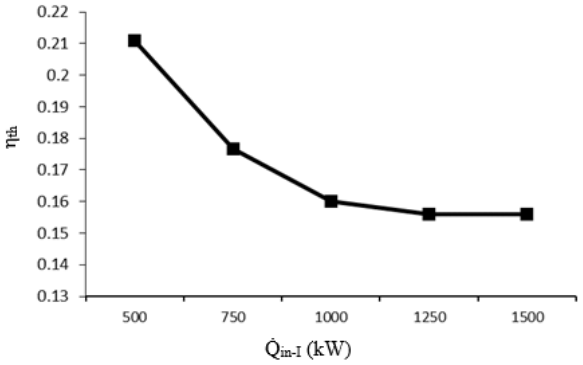

Fig.5 Variation of η_{th} with respect to $\dot{Q}_{in\text{-}I}$.

V. CONCLUSION

In this study, a novel combined cycle -which produces power and refrigeration simultaneously- is analyzed. The combined cycle is designed as the combination of Kalina cycle and ejector refrigeration cycle (ERC). In the configuration, the ERC is placed at the exit of the separator to absorb heat from the ammonia poor solution stream (working fluid of the Kalina

cycle) which leaves the separator at high temperature/pressure. The extracted heat from the ammonia poor solution is utilized in the ERC which is a thermal energy powered refrigeration cycle. Working fluid of Kalina cycle and ERC are ammonia-water solution and R134a, respectively. The results of a performed parametric analysis of the cycle are presented which show the effect of variation in rate of supplied heat to the cycle ($\dot{Q}_{in-I}$) and the necessary amount of biomass to generate the supplied heat ($\dot{m}_{bio}$) on selected performance parameters of the combined cycle: thermal efficiency (η_{th}), power production ($\dot{W}_{net}$) and refrigeration capacity ($\dot{Q}_{ref}$). The parametric analysis is performed by means of a developed simulation program.

The main findings of this study are summarized as follows: To supply the necessary heat to the combined cycle in the selected variation range of 500 – 1500 kW, biomass must be supplied to the boiler in the range of 2.01-6.03 kg/min. As $\dot{Q}_{in-I}$ rises, both of the mass flow rate of the working fluid transferred to the turbine ($\dot{m}_2$) and enthalpy difference of the ammonia water solution through the turbine (h_2-h_7) increase. As a result, based on Eq. (7), $\dot{W}_{tur}$ (hence, $\dot{W}_{net}$) rises as $\dot{Q}_{in-I}$ increases. Thermal efficiency (η_{th}) of the combined cycle follows a decreasing trend with increasing $\dot{Q}_{in-I}$. $\dot{Q}_{ref}$ is constant as $\dot{Q}_{in-I}$ increases due to the constant operational conditions of ERC.

REFERENCES

[1] A. Smith, K. Brown, S. Ogilvie, K. Rushton and J. Bates, "Waste Management Options and Climate Change: Final Report". *European Commission*, 2001[Online]. Available:: http://ec.europa.eu/environment/waste/studies/pdf/climate_change.pdf.

[2] A. Moharamian, S. Soltani, M. A. Rosen, S. M.. S. Mahmoudi and T. Morosuk, "A comparative thermoeconomic evaluation of three biomass and biomass-natural gas fired combined cycles using organic Rankine cycles,". *Journal of Cleaner Production,* vol. 161, pp. 524-544, 2017.

[3] D. S. Ayou, J. C. Bruno, R. Saravanan, and A. Coronas, "An overview of combined absorption power and cooling cycles,". *Renew Sustain Energy Rev*, vol. 21, pp. 728–48, 2013.

[4] O. M. Ibrahim and S. A. Klein, "Absorption power cycles," *Energy*, vol. 21, pp. 21–27, 1996.

[5] C. H. Marston and M. Hyre, "Gas turbine bottoming cycles: triple-pressure steam versus Kalina," *J. Eng. Gas Turbines Power,* vol. 117, pp. 10-15, 1995.

[6] A. I. Kalina, "Combined cycle and waste-heat recovery power systems based on a novel thermodynamic energy cycle utilizing low-temperature heat for power generation," in *Proc. of the 1983 Joint Power Generation Conference*, 1983, ASME Paper No. 83-JPGC-GT-3.

[7] A. I. Kalina, "Combined cycle system with novel bottoming cycle," *ASME J. Eng. Gas Turbines Power*, vol. 106, pp. 737–742, 1984.

[8] C. Seckin, "Thermodynamic analysis of a combined power/refrigeration cycle: Combination of Kalina cycle and ejector refrigeration cycle," *Energy Convers Manage.*, vol. 157, pp. 631–643, 2018.

[9] E. Wang and Z. Yu, "A numerical analysis of a composition-adjustable Kalina cycle power plant for power generation from low-temperature geothermal sources," *Appl Energy.*, vol. 180, pp. 834–848, 2016.

[10] K. Ameur, Z. Aidoun, and M. Ouzzane, "Modeling and Numerical Approach for the Design and Operation of Two-phase Ejectors," *Applied Thermal Engineering,* vol. 109, pp. 809-818, 2016.

[11] C. Seckin, "Parametric analysis and comparison of ejector expansion refrigeration cycles with constant area and constant pressure ejectors," *J Energy Res Technol – Trans ASME*, vol. 139, pp. 042005-1–042005-10, 2017.

[12] L. Boumaraf and A. Lallemand, "Modeling of an ejector refrigerating system operating in dimensioning and off-dimensioning conditions with the working fluids R142b and R600a," *Appl Therm Eng.*, vol. 29, pp. 265-274, 2009.

[13] X. Zhang, M. He and Y. Zhang, "A review of research on the Kalina cycle," *Renew Sust Energy Rev.*, vol. 16, pp. 5309-5318, 2012.

[14] R. Yapıcı and H. K. Ersoy, "Performance characteristics of the ejector refrigeration system based on the constant area ejector flow model," *Energy Convers Manage.*, vol. 46, pp. 3117–3135, 2005.

[15] A. Khalil, M. Fatouh and E. Elgendy, "Ejector design and theoretical study of R134a ejector refrigeration cycle," *Int. J. Refrig.*, vol. 34, pp. 1684–1698, 2011.

[16] R. Chandrappa and D. B. Das, *Waste Quantities and Characteristics, in: Solid Waste Management Principles and Practice,* 1st ed., Berlin, Germany: Springer-Verlag, 2012.

[17] S. Bilgen, K. Kaygusuz and A. Sari, "Second Law Analysis of Various Types of Coal and Woody Biomass in Turkey," *Energy Sources*, vol. 26, pp. 1083–1094, 2004.

[18] I. S. Ertesvag, Energy and exergy in moist fuels, 2000. [Online]. Available: http://folk.ntnu.no/ivarse /energi/moistfuel.pdf.

Utilization of Low Cost Sensor Networks for Energy and Indoor Environmental Quality Assessment

Mustafa Cem Çelik[1], Barbaros Batur[2], Muammer Akgün[3]

***Abstract*—**Indoor environmental quality (IEQ) and indoor air quality (IAQ) directly affect public health, occupancy well being and energy performance of a building. Ventilation rate should be optimized according to the comfort conditions. On the other hand, the energy consumption and the pollutant concentrations in the indoor air should also be considered. Most of the existing building stock in Turkey is using natural ventilation. Regular measurements on, indoor and outdoor air temperature, humidity and pollutant concentrations are necessary to maintain a satisfactory IEQ levels. The aim of this work is to introduce a low cost wireless sensor network to determine the IEQ parameters continuously to support control systems. The IEQ measurements with a set of the low cost sensors and some solution strategies for a better indoor environment and energy efficiency are also presented.

***Keywords*—**Indoor air quality, indoor environmental quality, low cost sensors, sensor networks

I. Introduction

The human activities are more and more taking place in indoors. Industrialized nations spend considerable energy to sustain the quality of the indoor life. Household energy usage consists of 25.4 % of the total energy consumption in EU-28 in 2015 (EUROSTAT). The efficient use of this significant portion of energy depends upon the quality of the indoor environment. Additionally, the health, well being, labor and academic performance of dwellers are also subjected to the IEQ [1] [2].

The urbanization rate in Turkey was increased from %32 in 1960 to %74 in 2016 [3]. The majority of the Turkish people living in city and town centers are exposed to the air pollution. Due to the innumerable construction sites in big cities, the particulate matter (PM) has become one of the major pollutants. Table 1 demonstrates that, the annual average PM10 values in largest cities are higher than EU exposure limit 40 $\mu g/m^3$ per year [4] [5].The external air pollution has enormous effect on IEQ and human health. Besides, in some cases IEQ parameters may become worse in the inside because of the indoors pollutant sources [6] [7] [8].

Mustafa Cem Çelik[1] is with the Mechanical Engineering Department, Engineering Faculty, Marmara University, 34722, Istanbul, Turkey (corresponding author's phone: +90 5325919227 ; e-mail: cem@marmara.edu.tr).

Barbaros Batur[2], is with the Mechanical Engineering Department, Yildiz Technical University, Istanbul, Turkey (e-mail: batur@yildiz.edu.tr).

Muammer Akgün[3] is with the Chimney Producers & Installers Association, Istanbul, Turkey (e-mail: infoakgun@gmail.com).

TABLE I.
THE AVERAGE ANNUAL PM10 CONCENTRATIONS IN CITIES FROM 2015 TO 2017 [5]

	2015	2016	2017	Data
	$\mu g/m^3$	$\mu g/m^3$	$\mu g/m^3$	%
Kadikoy / Istanbul	53.38	52.12	48.13	91
Esenkent / Istanbul	114.12	74.34	76.42	94
Sihhiye / Ankara	66.91	71.81	85.32	96
Gaziemir / Izmir	33.42	51.32	59.56	96

The indoor environment quality is characterized by numerous factors. The thermal comfort conditions (temperature, relative humidity and their perception), indoor air quality, illumination, noise levels, ergonomics and their effects on people are the main scope of IEQ research. There is an important demand for better IEQ both in existing and new buildings. In conventional sense only the heating and cooling demand in a dwelling was considered. Consecutively, in some mechanically ventilated buildings, fresh air and humidity was also taken into account. On the other hand some ventilation systems provided poor performance and even caused adverse health effects in time. The heating and ventilation is still an important problem, even for modern, smart high rise buildings. Developments in Internet of things (IoT) and the affordable sensor technologies provide new possibilities on determining and improving IEQ.

The constant monitoring and the feedback from occupants are necessary for a better IEQ. The sensors and equipment for IEQ measurements was costly and required a large space. The emerging new technologies in open source platforms and cheaper sensors help us to develop custom made, affordable and considerably small devices for IEQ measurements. The long time monitoring, data storage and real time access to the data enable us develop better control strategies and even learning systems that consider occupants behaviors.

II. THE OPEN SOURCE PLATFORM AND THE LOW COST SENSORS

The main motive of this study is the devise a low cost, open platform system to monitor IEQ from multiple sensors. Besides, the long term data collection while ensuring data quality is another important aim. The low cost sensors are small, easy to use, consume low power and their quality is increased considerably in recent years. The combination of such platforms and sensors has been used successfully in various research areas. There are various number of brands

and models of temperature & relative humidity (T&RH) and particulate matter (PM) sensors are The wide application possibilities of low cost sensors with the open source platforms (OSP) are drawing considerable attention in the scientific community. There are approximately 160,000 research and review articles about the "Low Cost Sensors" search in ScienceDirect.com [9].

Arduino boards are easy to learn program and use, all platform compatible, mini computers. The knowledge about the open source software and hardware has been accumulating. Arduino Uno is the main, robust board. It is based on 8 bit, 16 MHz ATmega328P microcontroller [10]. Arduino pro mini 3.3V runs the same controller at 8MHz in order to reduce the power consumption. pro mini is suitable for battery powered long terms data generation. The boards are easy to program for data acquisition (6 analog inputs, 14 digital inputs/outputs) and data storage to an SD card. The sensor modules, clock module, SD card module and Wi-Fi module are controlled by the boards. Controller and the sensors cost less than $100 as demonstrated in table 2.

TABLE II.
THE COMPONENTS AND COSTS OF THE SYSTEM COMPONENTS

Function	Device	Price
Controllers	Arduino Uno R3	$6.11
	Arduino Pro Mini	$2.30
T&RH Sensors	DHT11	$0.87
	DHT 22	$2.87
	BMP 280	$1.28
PM10 Sensors	Nova SDS011	$19.5
	GP2Y1010AU0F	$7.65
	PPD 42NS	$4.15
Light Intensity Sensors	BH 1750	$1.09
	TSL2561	$3.12
CO_2 Sensor	MH Z19B	$22.00
Data Storage Module	SD Card Module	$0.99
Memory Card	16 GB	$7.50
Clock Module	DS3231	$1.06
Wi-Fi Module	Esp8266	$1.65
	Total	$82.14

The sensor network consists of a main hub and two main nodes. The Arduino Uno board controls the main hub, which is powered by a 12V, 1A power supply. Battery powered Arduino Pro Mini 3.3V boards are used in nodes. There are sensors at both main hub and the nodes according to the current they draw. The technical characteristics of the sensors are indicated in table 3. The proposed set of sensors are selected in order to determine the indoor air quality, fresh air requirement in a room, lighting level and to control an air purifier.

TABLE III.
THE TECHNICAL CHARACTERISTICS OF THE LOW COST SENSORS

Sensor	Sensor	Range	Accuracy	Current
T&RH	DHT11	RH 20-80% T. 0-50ºC	RH 5% T. ±2ºC	Active 3.6mA Sleep 0.15µA
T&RH	DHT22	RH 0-100% T. -40-80ºC	RH 2.5% T. ±0.5ºC	Active 1.5mA Sleep 0.05µA
T&RH	BMP 280	RH 0-100% T. -40-85ºC	RH 3% T. ±0.5ºC	Active 3.6µA Sleep 0.10µA
PM10	Nova SDS011	0–1,000 µg/m^3	±10 µg/m^3	Active 70mA Sleep 2mA
PM10	GP2Y10 10AU0F	0–500 µg/m^3	±50 µg/m^3	Active 20mA Sleep 11mA
PM10	PPD 42NS	0–600 µg/m^3	±50 µg/m^3	Active 90mA Sleep NA
Light Intensity	BH 1750	0.11-100.000 lx	4 lx	Active 0.19mA Sleep 1µA
Light Intensity	TSL 2561	0.1-40.000 lx	NA	Active 0.5mA Sleep 3.2µA
CO_2	MH Z19B	0-5,000 ppm	%3	Active 150 mA Sleep 60 mA

III. THE SENSOR NETWORK SYSTEM

Various network topologies are proposed in scientific literature. Due to the scale and simplicity of the application, the sensor network structure is formed as a data logging base unit and two sensor nodes [11] [12]. The base unit has the biggest share in terms of power due to the high power consumption of PM sensors and continuous power need of the data logging and broadcasting. Thus, the base unit is powered by a 12V-1A power supply. On the other hand the nodes are powered by 3.7V - 2mAh batteries and waiting most of the time in the sleep mode. The base unit, sensor nodes and modules are demonstrated in figure 1.

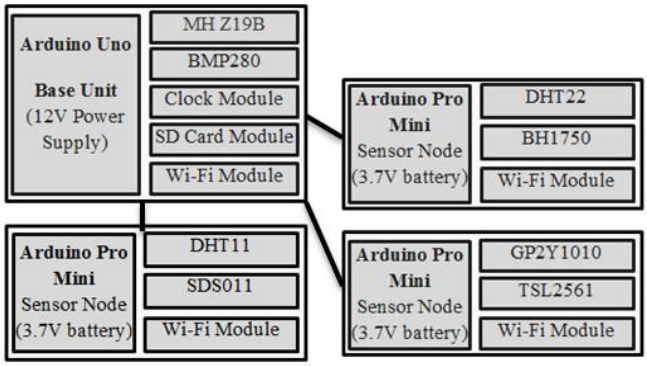

Fig. 1. The topology of wireless sensor network

The low cost sensors generally have low signal to noise ratio. Noise filtering provides better results especially in low concentrations. The reason for utilizing several different types of sensors for the same measurement is to ensure the data quality and calibration. Besides, high precision but low accuracy is another common drawback of the low cost sensors. Although, the sensor manufacturers or users generally supply calibration curves, field calibration is a viable option for better data quality [13] [14].

IV. DATA QUALITY AND SENSOR CALIBRATION

Determination of the amount of fresh air supply into en indoor environment is necessary. Hence, it directly affects IEQ and energy consumption for heating or cooling. The characteristics of the outer air directly affect the indoor air. Tracer gas decay method is a very commonly utilized method to evaluate air change rate (ACH) of a room [15]. ACH is the amount of air volume supplied to a room in a time interval (mostly, in an hour). CO_2 can be used as a tracer gas in ACH calculations. ACH calculation is demonstrated in (1), where I is ACH, t is time in hours, C_0 is the initial concentration of the tracer gas and C is the concentration of the tracer gas in time t.

$$I = \left(\frac{1}{t}\right)\ln\left(\frac{C_0}{C}\right). \quad (1)$$

Data Quality Objective (DQO) of EU is described explicitly by the European Air Quality Directive [4]. According to the Directive 2008/50/EC, minimum of 90% data has to be captured and allowed uncertainty for PM10 is 25% (5 μg/m^3 of the 40 μg/m^3 yearly limit). On the other hand EU directive EN12341 states that the reference measuring methodology for PM10 is sampling with filter on a regulated flow device and gravimetric mass analysis. The reference method requires very costly equipment, experienced operators and time for the evaluations. On the other hand, the directive also describes the factors for an equivalence candidate instrument and measurement method [4].

Most of the sensors are claimed to be delivered as factory calibrated. In both the scientific and the open software – hardware environment, calibration functions for the LCSs are presented. Linear regression, multivariate linear regression and artificial neural network are the most common calibration methodology for candidate sensors. The applications and the correction coefficients for various conditions are published. On the other hand, some sensors don't have enough calibration data. In some cases LCSs may produce inaccurate signals due to sensor heating period or simply may be broken due to long period of inactivity.

Linear regression is the most basic method for sensor calibration, assuming the low cost sensors' signal is a linear variation of a reference sensor [14]. The linear function $Y=a\cdot X+b$ is used, where Y is the sensor readings, X is reference measurements. The coefficients a and b are calculated using the least square of residuals. The inverse function (2) of the linear function is used for calibration in sensor readings Y into corrected value X_C. Also, the residual sum of squares (RSS) can be calculated as in (3).

$$X_C = \left(\frac{Y-b}{a}\right). \quad (2)$$

$$RSS = \sum_{i=1}^{n}\left(y_i - a - b\cdot x_i\right)^2 \quad (3)$$

Simple linear regression produces mostly satisfying results with the low cost sensors. Yet, the measurements close to the limits of sensor range generally demonstrate a nonlinear behavior. A higher order polynomial or a more advanced form of calibration should be utilized at such occasions [13].

V. CONCLUSIONS

Low cost sensors are important help to measure the IEQ parameters, in spite of the current drawbacks. Most LCVs generally provide high precision but low accuracy results and currently can not satisfy EU directives monitoring standards, due to strict rules. Yet, LCS network applications are proven to be useful in terms of collecting huge amount of data from various locations. Such applications reveal promising results in monitoring and controlling parameters that have direct effect on public health and domestic energy consumption. The LCSs provide low cost do it yourself solutions, LCSs are better in identifying the relative increase or decrease in the concentration. In order to achieve better solutions, statistical methods, field calibration and noise reduction techniques must be utilized. Main factors and long term performances of LCSs must be analyzed to maintain data quality.

The proposed sensor network model can be utilized to contribute the improvements in, IEQ, energy efficiency, health and wellbeing of the household in a smart home application. Such networks may also contribute real time environment and energy monitoring as an integrated part of a wider networks in smart city applications.

REFERENCES

[1] Turunen M. et. al., 2014. Indoor environmental quality in school buildings, and the health and wellbeing of students. International Journal of Hygiene and Environmental Health Volume 217, Issue 7, September 2014, Pages 733-739

[2] Habibi S. Smart innovation systems for indoor environmental quality (IEQ). Journal of Building Engineering Volume 8, December 2016, Pages 1-13

[3] The World Bank. [accessed 2018 Mar 15]. Urban population (% of total). The United Nations Population Division's World Urbanization Prospects. https://data.worldbank.org.

[4] EN 14907:2005. Ambient air quality – standard gravimetric measurement method for the determination of the PM2.5 mass fraction of suspended particulate matter. European Committee for Standardization (CEN), Brussels, Belgium (2005)

[5] T.C. Cevre ve Sehircilik Bakanligi Hava Izleme Istasyonlari Web Sitesi. [accessed 2018 Mar 15]. Istasyon Raporu. http://www.havaizleme.gov.tr/

[6] Bi D. et. al., 2018. Seasonal characteristics of indoor and outdoor fine particles and their metallic compositions in Nanjing, China. Building and Environment. In Press, Accepted Manuscript.

[7] Spiru P., Simona P. L. 2017. A review on interactions between energy performance of the buildings, outdoor air pollution and the indoor air quality. Energy Procedia 128 (2017) 179–186

[8] Li Y. et. al. 2018. Indoor/outdoor relationships, sources and cancer risk assessment of NPAHs and OPAHs in PM2.5 at urban and suburban hotels in Jinan, China. Atmospheric Environment. Volume 182, June 2018, Pages 325–334

[9] Sciencedirect. [accessed 2018 Mar 15]. Search results"Low Cost Sensors" https://www.sciencedirect.com.

[10] Arduino. [accessed 2018 Mar 15]. ARDUINO UNO REV3 https://www.arduino.cc/

[11] Yu T. et. al. 2013. Wireless sensor networks for indoor air quality monitoring. Medical Engineering & Physics. Volume 35, Issue 2,

February 2013, Pages 231-235
[12] Dener M."WiSeN: A new sensor node for smart applications with wireless sensor networks". Computers & Electrical Engineering. Volume 64, November 2017, Pages 380-394
[13] Rai A. C. et. al. End-user perspective of low-cost sensors for outdoor air pollution monitoring. Science of The Total Environment. Volumes 607–608, 31 December 2017, Pages 691-705
[14] Spinelle L. Field calibration of a cluster of low-cost available sensors for air quality monitoring. Part A: Ozone and nitrogen dioxide. Sensors and Actuators B: Chemical. Volume 215, August 2015, Pages 249-257
[15] Kiwan et al. Air exchange rate measurements in naturally ventilated dairy buildings using the tracer gas decay method with 85Kr, compared to CO2 mass balance and discharge coefficient methods. Biosystems Engineering 116 (2013) 286 -296

Application and Comparison of Exergetic Cost Theory and Wonergy Methods to a Biogas Engine Powered Cogeneration

Derya Haydargil[1], Ayşegül Abuşoğlu[2]

***Abstract*—**This study presents the application and comparison of the two exergoeconomic cost accounting methodologies, exergetic cost theory and wonergy methods, to a simple biogas engine powered cogeneration system. Exergetic cost theory is one of the most remarkable exergoeconomic methods, based on a solid mathematical background; in this respect, it is one of the leading approaches in the field of thermoeconomic. In this method, exergetic cost of the inner flows are determined with the help of an incidence matrix. This matrix shows the inlet and outlets of the subcomponents of the system. By implementing the exergetic costs to known initial investment costs and operating and maintaining costs as well as other system economic data, exergy-based costs of all flows and components are calculated.

Wonergy method takes its name from the worth of energy. This approach is simply based on the division of the system in three parts: work producing and/or consuming components, heat producing and/or consuming components and both heat and work producing and/or consuming components. With this way, for each flow, the time-consuming calculations may be eliminated. Exergoeconomic costs can be determined by defining three wonergetic constants for each component in the system. Although these two methodological approaches have their own and different implementation principles, their common points are, in essence, to combine exergy and economic principles. In this study, the application of these two methods to a cogeneration system will be presented and the results obtained will be discussed within the framework of thermoeconomic system parameters.

***Keywords*—** Exergetic cost theory, Wonergy, Biogas engine powered cogeneration, Thermoeconomics.

I. INTRODUCTION

ENERGY saving gains importance due to restricted resources in recent years. Although exergetic analysis on power plants gives hints about irreversibilities and efficiencies of the system it does not deal with the economics. It is more reasonable to combine the exergetic and economic analyses to investigate the systems in detail. In this aspect, thermoeconomics is a science which deals with the exergetic applications linked to economics. Exergetic cost theory (ECT) is one of the thermoeconomic cost accounting methodologies developed by Lozano [1] and the methodology introduces a new term as ‘‘exergetic cost’’. Valero [2] defined an incidence matrix which represents a system and interconnects the subsystems with flows in this system. The two main routes for calculating costs are identified and criticized in the light of the cost hexagon method. Vieira [3], made an analysis of a thermal power plant with the primary objectives of knowing its actual operating condition and evaluating the costs of internal flows. A new thermoeconomic methodology, wonergy, [4] is suggested for energy systems in the fields of cost allocation, cost optimization, and cost analysis by Kim. Exergetic balances in the components are tabulated and both work and heat costs are obtained.

This study aims to compare and show the differences of application rules of two thermoeconomic cost accounting methodologies, ECT and wonergy, on a biogas based powered cogeneration system (BPCS).

Derya Haydargil[1], is with the Graduate School of Natural and Applied Sciences, Mechanical Engineering Division, Gaziantep University, Gaziantep, 27310 Turkey (e-mail: derya.haydargil@mail2.gantep.edu.tr).

Ayşegül Abuşoğlu[2], is with the Department of Mechanical Engineering, Energy Division, Gaziantep University, Gaziantep, 27310 Turkey (e-mail: ayabusoglu@gantep.edu.tr)

II. SYSTEM DESCRIPTION

BPCS has five components; compressor, turbine, intercooler, gas engine, exhaust gas heat exchanger. Its fuel is biogas having a mass flowrate of 0.129 kg/sn and cogeneration produces 1000 kW work. Air-fuel mixture is compressed and cooled before entering the gas engine to prevent corrosions. Exhaust gas is used to produce work in turbine and this work is the fuel of the compressor. Exhaust gas heat exchanger provides heat from the exhaust gas to the water. Flow diagram of the system is shown in Fig. 1 and state properties according to Fig. 1 is tabulated in Table I.

III. EXERGETIC AND ECONOMIC DEFINITIONS

Before the application of the methods, necessary definitions should be given. These definitions help to examine the system more obviously.

Fuel-Product; for any component or system both fuel and product are expressed in terms of exergy as $\dot{E}x_F$ or $\dot{E}x_P$. They can be a single exergy or difference or sum of two either more exergetic flows. Table II shows the fuel-product definitions for BPCS.

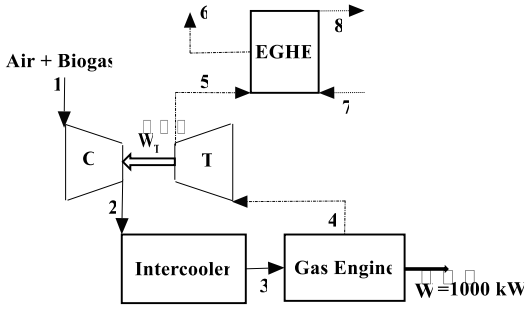

Fig. 1 Flow diagram of BPCS

Incidence matrix; A(n×m), is the presentation of the connection between the n subsystems with m flows through the system. According to incidence matrix, fuel and product matrices are formed and represented in Fig. 2a, 2b and 2c. It also helps to find the destroyed exergy. In a given state, exergy of a flow, $\dot{E}x$, and destroyed exergy, $\dot{E}x_{dest}$, corresponds to each component can be related with the help of the incidence matrix,

$$\vec{A} \times \vec{\dot{E}x} = \vec{\dot{E}x}_{dest} \quad (1)$$

It is obvious from Fig. 2, $\vec{A} = \vec{A}_F - \vec{A}_P$ hence fuel and product exergies of the components are calculated as,

$$\vec{\dot{E}x}_F = \vec{A}_F \times \vec{\dot{E}x} \quad (2)$$

$$\vec{\dot{E}x}_P = \vec{A}_P \times \vec{\dot{E}x} \quad (3)$$

Exergetic cost; It is specified as, $\dot{E}x^*$, amount of exergy per unit time required to produce a flow. $\dot{E}x^*$ like $\dot{E}x$ is a thermodynamic function. Exergetic cost of flows are determined according to the limits of the system hence it is not possible to define an absolute exergetic cost of a flow. Whether a flow pass the limits of a system, its exergetic cost equals to its exergy since no exergy has so far consumed to obtain it. For a defined subsystem, exergetic cost of fuel is equal to exergetic cost of product; $\dot{E}x^*_{F,i} = \dot{E}x^*_{P,i}$. Exergetic costs of the flows are obtained by using incidence matrices formed for the system,

$$\vec{A} \times \vec{\dot{E}x}^* = 0 \quad (4)$$

$$\vec{\dot{E}x}^*_F = \vec{A}_F \times \vec{\dot{E}x}^* \quad (5)$$

$$\vec{\dot{E}x}^*_P = \vec{A}_P \times \vec{\dot{E}x}^* \quad (6)$$

$\vec{\dot{E}x}^*$ is the exergetic cost vector of dimension m, which is the number of flows through the system.

Unit exergetic cost; κ^*, a flow's unit exergetic cost is defined as, $\kappa^* = \dot{E}x^* / \dot{E}x$. Its value demonstrates the inefficiency of the production process therefore greater unit exergetic cost emphasizes the more destroyed exergy to produce the flow. All the components in the system have two unit exergetic costs, one is for fuel $\kappa_F^* = \dot{E}x_F^* / \dot{E}x$, other is for product $\kappa_P^* = \dot{E}x_P^* / \dot{E}x$.

Thermoeconomic cost; $\dot{C}$, of a flow is the number of monetary units per second, required to obtain this flow.
Unit thermoeconomic cost; c^*, of a flow is the cost of each unit of exergy consumed in producing this flow and related with thermoeconomic cost as, $\dot{C} = c^* . \dot{E}x^*$.
Unit exergoeconomic cost; c, of a flow is the cost of each unit of exergy concerned with this flow. It is related with thermoeconomic cost as, $\dot{C} = c . \dot{E}x$.
After defining useful parameters, last step for thermoeconomic analysis is forming the thermoeconomic cost balance in (7),

$$\vec{A} \times \vec{\dot{C}} + \vec{\dot{Z}} = 0 \quad (7)$$

$\dot{Z}$ is the cost of maintenance and operation of the production system. Calculated *Z* values for BPCS is given in [5]. After calculating the exergetic costs, thermoeconomic costs in the system are determined by the application of the (8), (9) and (10).

$$\dot{C}_P = \dot{C}_F + \dot{Z} \quad (8)$$

$$\dot{C}_P = c^*_P . \dot{E}x^*_P = (c^*_P . \kappa^*_P) . \dot{E}x_P = c_P . \dot{E}x_P \quad (9)$$

$$\dot{C}_F = c^*_F . \dot{E}x^*_F = (c^*_F . \kappa^*_F) . \dot{E}x^*_F = c_F . \dot{E}x^*_F \quad (10)$$

IV. EXERGETIC COST THEORY

Exergetic cost theory is developed by Lozano [1]. This theory forms its specific rules and application of these rules gives hints for the calculations.

Rule 1: Fuel or product exergy of a component should be positive, $\dot{E}x_F^*, \dot{E}x_P^* > 0$.

Rule 2: In a component, unit exergetic cost of each fuel is greater than or equal to one, $\kappa_F^* > \dot{E}x_F^* / \dot{E}x_F \geq 1$, also the currents which make up the fuel has the same unit exergetic cost.

Rule 3: If a component has more than one product, all the products have the same unit exergetic cost in the absence of external exergetic application.

Rule 4: Residue or loss must appear explicitly as products in a subsytem. However, exergetic cost of any loss or residue is equal to zero, $\dot{E}x_L^* = 0$.

TABLE I
STATE PROPERTIES OF FLOWS IN FIG. 1

State No	Fluid	Pressure *P* (bar)	Temperature *T* (°C)	Mass flowrate, $\dot{m}$ (kg/sn)	Enthalpy *h* (kJ/kg)	Entropy *s* (kJ/kg)	Energy rate, $\dot{E}$ (kW)	Exergy rate, $\dot{E}x$ (kW)
0	Air	1.00	25.00	-	298.60	5.699	0.00	0.00
0’	Water	1.00	25.00	-	104.20	0.3648	0.00	0.00
0’’	Biogas	1.00	25.00	-	-4650	11.62	---	---
1	Air-fuel	1.00	25.00	1.50	298.60*	5.699*	0.00	4046.40
2	Air-fuel	1.90	116.9	1.50	391.20*	5.786*	155.21	4154.13
3	Air-fuel	1.90	51.00	1.50	324.70*	5.599*	43.474	4136.31
4	Exhaust gas	2.40	460.0	1.50	749.40	6.375	676.20	374.30
5	Exhaust gas	1.17	360.6	1.50	642.90	6.425	516.50	192.25
6	Exhaust gas	1.00	65.00	1.50	338.80	5.826	60.340	3.692
7	Water	6.10	82.80	20.8	347.10	1.108	5071.70	447.30
8	Water	3.40	88.00	20.8	368.70	1.169	5522.70	518.70

[a]This values correspond to air not the air-fuel mixture, during analyses air state properties and biogas state properties are calculated separately and summation of them are used.

This situation results the exergetic cost equality for fuel and product which is valid for any component, $\dot{E}x^*_F = \dot{E}x^*_P$.

TABLE II
FUEL AND PRODUCT DEFINITIONS FOR FIG. 1

Component No	Component	Fuel	Product
1	Compressor	$\dot{W}_T$	2-1
2	Intercooler	2	3
3	Gas Engine	3	$\dot{W}$
4	Turbine	5-6	$\dot{W}_T$
5	EGHE	5-6	8-7
	BPCS	1	$\dot{W}$ + (8-7)

By implementing these rules, (11) is determined.

$$\dot{E}x^*_8 / \dot{E}x^*_8 = \dot{E}x^*_7 / \dot{E}x_7 \rightarrow \dot{E}x^*_8 - x_5\,\dot{E}x^*_7 = 0 \qquad (11)$$

where $x_5 = \dot{E}x_8 / \dot{E}x_7$. Table 3 shows the obtained exergetic cost results of flows in BPCS. Thermoeconomic costs of flows and components are determined with the help of related equations. These values are illustrated in Table 4 and Table 5. Flow 1 is air-fuel mixture and its exergetic cost is equal to its exergy because air has no exergetic cost. Thermoeconomic cost of fuel, $\dot{C}_0$, is known before it is 92.55 $/h. Work flow from gas engine is the most expensive thermoeconomic flow through the system as expected. It is obvious from Table 3, thermoeconomic costs of the flows are directly related to the exergetic costs and the costs of equipments where they are consumed or produced.

Component	1	2	3	4	5	6	7	8	$\dot{W}_T$	$\dot{W}$	← Flow
1	1	-1	0	0	0	0	0	0	1	0	
2	0	1	-1	0	0	0	0	0	0	0	
3	0	0	1	-1	0	0	0	0	0	-1	$\vec{A}$
4	0	0	0	1	-1	0	0	0	0	0	
5	0	0	0	0	1	-1	1	-1	0	0	
BPCS	1						1	-1		-1	

Fig. 2a Incidence matrix of BPCS

Component	1	2	3	4	5	6	7	8	$\dot{W}_T$	$\dot{W}$	← Flow
1									1		
2		1									
3			1								$\vec{A}_F$
4				1	-1						
5						1	-1				
BPCS	1										

Fig. 2b Fuel matrix of BPCS

Component	1	2	3	4	5	6	7	8	$\dot{W}_T$	$\dot{W}$	← Flow
1	1	-1									
2			-1								
3										-1	$\vec{A}_P$
4									-1		
5							-1	1			
BPCS							-1	1		-1	

Fig. 2c Product matrix of BPCS

TABLE III
OBTAINED COST RESULTS FOR BPCS FLOWS

Flow No	Exergy Ėx (kW)	Exergetic cost, Ėx* (kW)	Unit exergetic cost, κ*	Unit exergoeconomic cost, c ($/GJ)	Unit thermoeconomic cost, c* ($/GJ)	Thermoeconomic cost, Ċ ($/h)
1	4046.4	4046.4	1	6.35	6.35c	92.55
2	4154.13	4228.36	1.017	7.234	7.107	108.186
3	4136.23	4228.36	1.02	7.271	7.113	108.277
4	374.3	374.3b	1	23.516	23.516c	31.688
5	192.25	192.25b	1	23.698	23.698	16.402
6	3.692	3.692b	1	34.985	34.985c	0.469
7	447.3	670.958c	1.500	39.065	26.044c	62.907
8	518.7	859.516	1.657	42.275	25.521	78.942
Ẇ	1000	4228.36	4.228	30.685	7.257	110.466
$\dot{W}_T$	159.75	181.96	1.139	26.927	23.640c	15.486

[b]In exhaust gas line,4-5-6, exergetic values are equal to their exergetic costs since no more exergy is spent to obtain this line. [c]These values are calculated before, in Phd thesis of the writer.

TABLE IV
FUEL COST RESULTS FOR BPCS COMPONENTS ACCORDING TO ECT

Flow No	Exergy Ėx (kW)	Exergetic cost, Ėx* (kW)	Unit exergetic cost, κ*	Unit exergoeconomic cost, c ($/GJ)	Unit thermoeconomic cost, c* ($/GJ)	Thermoeconomic cost, Ċ ($/h)
1	159.75	181.96	1.139	26.927	23.640	15.486
2	4154.13	4228.36	1.017	7.234	7.107	108.186
3	4136.23	4228.36	1.022	7.271	7.113	108.277
4	182.05	182.05	1	23.323	23.323	15.286
5	188.558	188.558	1	23.471	23.471	15.933

TABLE V
PRODUCT COST RESULTS FOR BPCS COMPONENTS ACCORDING TO ECT

Flow No	Exergy Ėx (kW)	Exergetic cost, Ėx* (kW)	Unit exergetic cost, κ*	Unit exergoeconomic cost, c ($/GJ)	Unit thermoeconomic cost, c* ($/GJ)	Thermoeconomic cost, Ċ ($/h)
1	107.73	181.96	1.689	40.316	23.869	15.636
2	4136.23	4228.36	1.022	7.271	7.113	108.277
3	1000d	4228.36	4.228	30.685	7.257	110.466
4	159.75	182.96	1.139	26.927	23.640	15.486
5	71.4	188.558	2.640	62.383	23.622	16.035

[d]In the gas engine only product is mechanical work,1000kW, flow 4 is byproduct therefore cost of produced work is considered only, in gas engine calculations. However, flow 4 is valuated in the turbine to produce **turbine work, 159.75, so it takes exergetic cost in turbine calculations.**

It is interesting to see the highest calculated unit thermoeconomic cost is belonging to flow 6 even having the least exergy. This situation can be explained as; it becomes quite expensive to take nearly all the exergy from flow 5 to flow 6 to heat the water in the exhaust gas.
Components 1, 4 and 5 are installed in this cogeneration system to utilize the byproduct from gas engine so they have higher unit thermoeconomic costs both in Table 4 and Table 5. Unit exergetic costs also thermoeconomic costs of gas engine have the highest values compared to others in because it is in charge of producing the main product.

V. WONERGY METHOD

In this method various energies combining enthalpy and exergy is integrated with ‘’wonergy’’, fusing of worth and energy. Wonergy is detected as an energy that can equally appraise the worth of each product.
Thermodynamic first law emphasizes the energy balance equation for the i-th component, and overall system,

$$\dot{W}_i + \dot{E}_{Q,i} = \dot{E}_{F,i} - \dot{E}_{P,i} - \dot{E}_{L,i} \tag{12}$$

$$\dot{W} + \dot{E}_Q = \dot{E}^{CHE} - \dot{E}_L \tag{13}$$

$\dot{E}_{F,i}$ is energetic fuel inlet, $\dot{E}_{P,i}$ is product energy output and is the lost heat energy to the environment for the i-th component. $\dot{E}^{CHE}$ denotes the amount of chemical energy input of fuel $\dot{W}$ and $\dot{E}_Q$ and are the quantity of work and heat as the desirable final products for a cogeneration system. The tabulated values of energy balance equations of the components are listed in Table 6.
Wonergy method states the exergy balance equation for the i-th component and overall system as,

$$\dot{W}_i + \dot{E}x_{Q,i} = \dot{E}x_{F,i} - \dot{E}x_{P,i} - \dot{E}x_{L,i} \tag{14}$$

$$\dot{W} + \dot{E}x_Q = \dot{E}x_F^{CHE} - \dot{E}x_L \tag{15}$$

$\dot{E}x_F^{CHE}$ demonstrates chemical exergy input of fuel and $\dot{W}$ and $\dot{E}x_Q$ are the exergetic quantity of work and heat. Table 7 shows the exergy balance equations for the components. Combining energy and exergy as wonergy and modifying the symbols of $\dot{E}$ and $\dot{E}x$ with $\dot{K}$ the wonergy balance equations are written.

$$\dot{W}_i + \dot{K}_{Q,i} = \dot{K}_{F,i} - \dot{K}_{P,i} - \dot{K}_{L,i} \tag{16}$$

$$\dot{W} + \dot{K}_Q = \dot{K}_F - \dot{K}_L \tag{17}$$

Cost balance equation requires that the sum of the output costs must be equal to the sum of the input costs in the whole system.

$$c_W \dot{W} + c_Q \dot{E}_Q = \dot{C}_0 + \sum \dot{Z} \tag{18}$$

Where c_W and c_Q are the unit exergoeconomic cost of work and heat produced by the system.

Wonergy method divides the system into three components; the common components [ς], associated to both work and heat production, the work only components [W], associated to work production, and the heat only components [Q], associated to heat production. According to these classifications; gas engine and turbine are work only, EGHE is heat only, compressor and intercooler are common components in BPCS.
It is obvious from wonergy equations and Table 6 and Table 7 the summation of $\dot{K}_{F,i}$ and $\dot{K}_{P,i}$ for all components is exactly zero. Thus, multiplying (19)

$$\dot{K}_\varsigma + \dot{K}_W + \dot{K}_Q = \sum \dot{K}_{F,i} + \sum \dot{K}_{P,i} \tag{19}$$

by the wonergetic unit cost and adding the term to (16), wonergetic cost balance equation is formed. Kc

$$c_W \dot{W} + c_Q \dot{E}_Q = \dot{C}_0 + \dot{Z}_W + \dot{Z}_Q + c_K \left(\dot{K}_\varsigma + \dot{K}_W + \dot{K}_Q \right) \tag{20}$$

Equation (20) is divided into to (22) for [ς] components, (23) for [W] components, and (24) for [Q] components.

$$\dot{K}_\varsigma + \dot{K}_W + \dot{K}_Q = 0 \tag{21}$$

$$0 = \dot{C}_0 + c_K \dot{K}_\varsigma \tag{22}$$

$$c_W \dot{W} = \dot{Z}_W + c_K \dot{K}_W \tag{23}$$

$$c_Q \dot{E}_Q = \dot{Z}_Q + c_Q \dot{K}_Q \tag{24}$$

where each value of $\dot{K}_W$ and $\dot{K}_Q$ is positive and $\dot{K}_\varsigma$ is negative. The sign of these values can be checked from the values $\dot{E}_F$, $\dot{E}_P$, $\dot{E}x_F$, $\dot{E}x_P$ and Tables 6 and 7.
If the above equations are rearranged, exergoeconomic cost of work, c_W, exergoeconomic cost of heat, c_Q, cost flow rate of work, $\dot{C}_W$, and cost flow rate of heat, $\dot{C}_Q$ are determined.

$$c_W = k_W \cdot \frac{\dot{C}_0}{k_W \dot{W} + k_Q \dot{Q}} + \frac{\dot{Z}_W}{\dot{W}} \tag{25}$$

$$\dot{C}_W = c_W \dot{W} = \dot{K}_W \frac{\dot{C}_0}{\dot{K}_W + \dot{K}_Q} + \dot{Z}_W \tag{26}$$

$$c_Q = k_Q \cdot \frac{\dot{C}_0}{k_W \dot{W} + k_Q \dot{Q}} + \frac{\dot{Z}_Q}{\dot{Q}} \tag{27}$$

Where $k_W = \dot{K}_W / \dot{W}$ and $k_Q = \dot{K}_Q / \dot{Q}$. $\dot{K}$ is the wonergy input and k is the wonergy input ratio. The key point of the wonergy method is to obtain the ratio of wonergy input for each product. This methodology suggests that cost flow of the

$$\dot{C}_Q = c_Q \dot{Q} = \dot{K}_Q \frac{\dot{C}_0}{\dot{K}_W + \dot{K}_Q} + \dot{Z}_Q \qquad (28)$$

product is proportional to the amount of wonergy input. Cost of components are calculated and results are shown in Table 8.

TABLE VI
THE ENERGY BALANCE OF BPCS ACCORDING TO WONERGY METHOD

Component	Ẇ (kW)	$\dot{E}_Q$ (kW)	$\dot{E}x_F^{CHE}$ (kW)	$\dot{E}_F$ (kW)	$\dot{E}_P$ (kW)	$\dot{E}_L$ (kW)
Compressor	-155.21	-	-	-	-155.21	-
Intercooler	-	-	-	155.21	-43.474	-111.736
Gas Engine	1000	-	2308.06	43.474	- 676.2	-675.334
Turbine	159.7	-	-	159.7	-	-
EGHE	-	451	-	456.16	-	-5.16
BPCS	1004.4	451	2308.06	814.54	-874.884	-792.23

TABLE VI
THE EXERGY BALANCE OF BPCS ACCORDING TO WONERGY METHOD

Component	Ẇ (kW)	$\dot{E}_Q$ (kW)	$\dot{E}x_F^{CHE}$ (kW)	$\dot{E}_F$ (kW)	$\dot{E}_P$ (kW)	$\dot{E}_L$ (kW)
Compressor	-155.21	-	-	-	-107.73	-47.48
Intercooler	-	-	-	4154.13	-4136.231	-17.899
Gas Engine	1000	-	4046.4	89.83	-374.3	-2761.93
Turbine	159.7	-	-	182.05	-	-22.35
EGHE	-	71.4	-	188.558	-	-117.158
BPCS	1004.49	71.4	4046.4	4614.568	4618.261	-2966.817

TABLE VIII
COST ALLOCATIONS FOR BPCS ACCORDING TO WONERGY METHOD

Component	$\dot{K}$ (kW)	$\dot{W}$, $\dot{E}x_Q$ (kW)	k%	$\dot{C}_0$ ($/h)	$\dot{Z}$ ($/h)	c ($/GJ)	$\dot{C}$ ($/h)
Common [ς]	-88	-	92.451	0.29135	291.827	-	-88
Work only [W]	-100.558	1004.49	10.01	-	2.394	28.552	103.25
Heat only [Q]	188.558	451	41.80	-	0.10237	122.063	198.182

TABLE IX
COSTS OF WORK PRODUCED BY BIOGAS ENGINE

Method	Unit exergoeconomic cost, c_W ($/GJ)	Thermoeconomic cost, $\dot{C}_W$ ($/h)
ECT	30.685	110.466
Wonergy	28.552	103.25

VI. RESULTS AND CONCLUSIONS

Two cost accounting thermoeconomic methods are applied to a simple cogeneration system and two different thermooeconomic costs are obtained for the same work production. These costs are illustrated in Table 9.

ECT begins the analyses by forming an incidence matrix which shows the flows through the components through the system. This method introduces a new approach, exergetic cost, giving information of exergetic consumption. Incidence matrix leads to determine exergetic costs of flows. Related to exergetic costs unit exergetic costs are determined which help to understand the destructions for flows and components in the system. Specific ECT rules require auxiliary equations which direct us to reach unit exergoeconomic and thermoeconomic costs. Combination of known economic parameters with the obtained unit costs, results the thermoeconomic costs both for flows and components. Although detailed calculations, ECT injects destruction costs to flows and components. This situation causes to obtain high cost results.

A new method is generated by composing energy and exergy in a term, wonergy. Wonergy method classifies the components according to their processes. It is important to form true energy and exergy balances in this theorem. These equations guide us to generate wonergetic balance equations. With the help of the cost equations and defined wonergetic terms, costs for components are determined. It must be noticed that in ECT unit exergoeconomic and thermoeconomic costs are obtained for all flows and components however in wonergy method these parameters are determined only specified components. Wonergy shares the costs to work production and heat production explicitly therefore it classifies the components according to their processes. Finally, less unit exergoeconomic cost also thermoeconomic cost are obtained for work flow as seen in Table 9.

REFERENCES

[1] M.A. Lozano, A. Valero, ‘’Theory of the exergetic cost,’’ Energy, vol. 18, no. 9, pp. 939-60, 1993.

[2] A. Valero, M.A. Lozano, M. Munoz, ‘’A general theory of exergy saving. I. On the exergetic cost,’’ Computer Aided Engineering Energy Systems,vol. 2, no. 3, pp. 1-8, 1986.

[3] G. Tsatsaronis, M. Winhold, ‘’Exergoeconomic analysis and evaluation of energy conversion plants,’’ Energy Int. J., vol. 10, pp. 69-94, 1985.

[4] D.J. Kim, ‘’A new thermoeconomic methodology for energy systems,’’ Energy, vol. 35, pp. 410–422, 2010.

[5] A. Abusoglu, S. Demir, M. Kanoglu, ‘’ Thermoeconomic analysis of a biogas engine powered cogeneratıon system,’’ Journal of Thermal Science and Technology, vol. 33, no. 2, pp. 9-21, 2013.

Author Index